METABOLIC ACTIVITY CONTROL OF THE L-LYSINE FERMENTATION BY RESTRAINED GROWTH FED-BATCH STRATEGIES

by

Robert D. Kiss

B.S. Chemical Engineering
University of California, Davis
(1984)

M.S. Chemical Engineering Practice
Massachusetts Institute of Technology
(1987)

Submitted to the Department of
Chemical Engineering in Partial Fulfillment of
the Requirements for the
Degree of

DOCTOR OF PHILOSOPHY
IN CHEMICAL ENGINEERING

at the

MASSACHUSETTS INSTITUTE OF TECHNOLOGY
September, 1991

Signature of the Author _____
Department of Chemical Engineering
August 23, 1991

Certified by _____
Gregory N. Stephanopoulos
Professor of Chemical Engineering
Thesis Supervisor

Accepted by _____
William M. Deen
Chairman, Departmental Committee on Graduate Students
Chemical Engineering

METABOLIC ACTIVITY CONTROL OF THE L-LYSINE FERMENTATION BY RESTRAINED GROWTH FED-BATCH STRATEGIES

by

Robert D. Kiss

Submitted to the Department of Chemical Engineering
on August 23, 1991 in partial fulfillment of the
requirements for the Degree of Doctor of Philosophy in
Chemical Engineering

ABSTRACT

Control of the microbial environment, through reactor feed control strategy, has been demonstrated as an effective means of manipulating a microbe's metabolism to favor amino acid overproduction. Batch and continuous culture experiments were conducted with the L-lysine producer *Corynebacterium glutamicum* to characterize fermentation yields and rates as well as the relationship between biomass catalytic activity toward L-lysine production and on-line respiratory measurements. Batch fermentations revealed an interesting culture dynamic behavior when grown in the L-threonine limited medium necessary to bypass L-lysine regulation and achieve L-lysine overproduction. The batch fermentation performance indicators, specific L-lysine productivity and instantaneous L-lysine yield from glucose, were shown to be suboptimal during most of the cultivation. Furthermore, the decay in time of the specific productivity and yield were shown to be correlated to decays in on-line respiratory measurements. These results indicated that the growth limitation by L-threonine in batch culture results in a general decay of metabolic activity including a gradual deterioration in L-lysine producing capacity.

To complement the batch culture dynamic characterization, continuous culture studies were performed to elucidate the effect of culture specific growth rate on metabolic efficiency in producing L-lysine. In addition to establishing the specific growth rate dependence of specific rates and yields, the intrinsic yields of L-lysine from glucose and from ammonia were determined to be approximately 0.41 and 0.40 mol/mol, respectively. The continuous culture data also provided sufficient information for the estimation of intracellular carbon fluxes and carbon partitioning at key locations within the metabolic network, providing both an understanding of the underlying causes of the low observed yields and rational directives for future strain manipulations.

The continuous culture work also identified a culture instability which could result in the takeover of both continuous and extended-length fed-batch fermentations by unproductive (revertant) cells. A deterministic mathematical model satisfactorily described the dynamics of the reversion and competition phenomena. The model also predicted the ability to control the growth and subsequent takeover

by revertant cells through proper medium design with respect to the second growth-limiting nutrient (L-leucine). Such a stabilizing role was verified by using medium manipulation to successfully stabilize the performance of an extended fed-batch fermentation.

The experimental correlations from the batch and continuous culture characterizations suggested that improved fermentation performance could be expected by cultivating the organism under conditions of controlled, or restrained, growth. Furthermore, the results indicated that this restrained growth could be achieved in a fed-batch operation using on-line respiratory measurements as a metabolic activity indicator for feed rate control. Following the successful verification of this hypothesis by constant feed rate fed-batch experiments, two different restrained growth control strategies were developed, both heuristic in nature, for maximization of the fermentation yield and maximization of the fermentation productivity. The algorithms take appropriate control actions based on an evaluation of the trends in time of the on-line respiratory measurements.

Both restrained growth fed-batch strategies were successful in maintaining high yield and specific productivity for extended times, resulting in significant improvements in the overall fermentation yield, volumetric productivity and L-lysine titer. Thus, this thesis work presents a complete picture of a novel method of biocatalyst activity control which requires only qualitative relationships between performance variables and on-line respiratory measurements and also includes a design criterion for insuring the culture integrity for extended length fed-batch fermentations.

Thesis Supervisor: Dr. Gregory N. Stephanopoulos

Title: J. R. Mares Professor of Chemical Engineering

Acknowledgements

I want to thank my advisor, Greg Stephanopoulos, for providing just the right amount of support and guidance in pursuit of the goals of this thesis. I appreciate his confidence in my abilities and even thank him for giving me the freedom to occasionally find my own dead ends. I also would like to thank the members of my thesis committee, Charlie Cooney, Larry Evans, Arnie Demain, and Tony Sinskey for their time and efforts on behalf of this project. Their interesting and important viewpoints on various aspects of this work helped to keep me moving in the right direction.

Much thanks must go out to the members of the Stephanopoulos research group: Joe Vallino, for all of his contributions to this work including his posing as plumber, mechanic, and electrician in the setup of the MBR fermentor, his guidance in the use of the flux estimation techniques, and for teaching me not to be hesitant about breakin' it down, fixin' it up, and throwin' it back together (Joe, you're in the wrong business!); John Chung, for his unique perspectives on just about everything and for finally "seeing it from the other side" (he knows what this means); Mark Applegate and Craig Ekpuz, for commiserating with me on the employment outlook and "spicing up" group events, particularly Thursday seminars; Sung Park, for providing his own perspectives on this fermentation and the numerous discussions about the promises of biotechnology; and Grace Colón, for asking the right questions and forcing me to analyze my own perspectives on the L-lysine fermentation in greater depth and for being persistent about getting us interested in musicals. Thanks also to all the other members of the group for making seminars interesting

and enjoyable and to all the BPEC and BEAM folks for providing constructive analyses and criticisms of this work during the many presentations.

Thanks also go to Max Follettie and John Archer of the MIT Biology Department for their help in the development of the threonine assay and for their assistance on the biological side of this fermentation. Thanks for being willing to listen to an engineer's viewpoint on fermentation of *Corynebacteria*. In addition, I would like to thank Hugo Guterman and Urs Saner for their help in the digital filter design and analysis. Finally, thanks to UROP students Steve Buonopane and John Freeman for their work with the development of the FERMCON program.

I also need to thank all the residents of the Windsor palace, Chuck, Tim, Russ, Pete, and Steve for providing a great place to live when not at the lab. Mike Barrera is also to be acknowledged for getting me wrapped up in intramural sports, one of my more important outlets.

Thanks, of course, go to my parents for supporting me throughout all of my escapades. All I can say at this point is "I'm done yet!" Also, I want to thank my in-laws, the Bastons, for providing still more support and encouragement in this past year.

Most sincere thanks and love go to my wife, Linda, for being my best friend and faithful late night lab assistant these past few years. Her love and support have made these last few grueling weeks (almost) bearable. To you, Linda, I am happy to say, "You can have your husband back, now!"

Finally, financial support from the National Science Foundation through my advisor's PYI Grant and through the MIT Biotechnology Process Engineering Center and the donation of the MBR bioreactor by Sulzer Bros., Inc. are acknowledged.

Table of Contents

List of Figures

List of Tables

Chapter 1

Introduction

1.1 Motivation

The bulk of L-lysine production throughout the world depends on direct fermentation of carbohydrates by auxotrophic and regulatory mutants of *Corynebacteria* and *Brevibacteria* species in batch culture [Nakayama, 1985]. For fermentation processes intensive in raw material use (such as amino acids, organic acids and ethanol), process yield (product produced/substrate consumed), in addition to productivity, is a critical measure of performance and economic viability.

While industrial L-lysine titers can reach quite high levels (60 - 100 g/l), the overall process yields are somewhat low at 0.2 - 0.3 grams L-lysine·HCl per gram of glucose (L-lysine is typically isolated as the hydrochloride salt; this 0.2 - 0.3 g/g yield corresponds to about 0.2 - 0.3 molar yield as well). Although the maximum theoretical yield cannot be calculated unequivocally due to uncertainties regarding the exact biochemistry of L-lysine biosynthesis, a 75% molar yield (0.757 g/g, see Section 2.4.3) is accepted as the most likely maximum yield compatible with the current understanding of L-lysine biosynthesis.

Previous efforts to improve the performance of the L-lysine fermentation have focused primarily on strain manipulation by mutation and selection for auxotrophic and regulatory mutant development [Tosaka *et al.*, 1978; Nakayama, 1985; Beppu, 1986; Yokata and Shiio, 1988]. More recently, recombinant genetic technology has

been employed for the amplification of key enzymes [Nakayama, 1985; Beppu, 1986; Sano *et al.*, 1987; Menkel *et al.*, 1989; Cremer *et al.*, 1991]. Although these approaches have produced mutants exhibiting increased rates of product formation, they do not necessarily improve the fermentation yield. Increasing fermentation yield presents additional difficulties for it requires re-directing the cellular metabolism in favor of the desired product as opposed to biomass or other side product formation.

Previous attempts to improve L-lysine fermentation performance by process manipulation have examined the effects of environmental and process variables such as dissolved oxygen concentration [Akashi *et al.*, 1979; Hilliger and Hanel, 1981], redox potential [Radjai *et al.*, 1984], and power input and aeration rates [Hilliger *et al.*, 1984] in batch cultures; sugar concentration [Hadj *et al.*, 1988] or the optimal constant feed rate [Rutkov, 1984] in fed-batch cultures; and sugar concentration, agitation rate, and oxygen enrichment [Hirao *et al.*, 1989], and aeration rate and dilution rate [Michalski *et al.*, 1984], in continuous cultures. Such studies typically aim to determine the most appropriate set points for the various bioreactor environmental variables. Controls are then implemented to regulate the culture at this desired state, which reflects the operator's assessment of optimality. These controls, however, are not the only answer to the pursuit of fermentation performance improvement. Since the optimal fermentation set points may, in fact, vary with time, performance improvement may be more effectively improved by attempting to maintain the biocatalyst, or metabolic, activity of the culture, rather than the abiotic environmental variables, at an optimal state.

Such controls of metabolic activity would thus control the microbial environment, in response to a "measurement of metabolic activity," as a means of

manipulating the microbe's metabolism to favor the production of L-lysine. This type of strategy would obviously require some form of on-line measurement or evaluation of the culture's metabolic state as input for determining the appropriate control action.

1.2 Thesis Objectives

Motivated by the desire to demonstrate the benefits of controlling biological activity through control of the microbial environment and its effects on microbial metabolism, the primary objectives of this thesis work are stated as:

(1) Characterize the production of L-lysine by *Corynebacterium glutamicum* in terms of yields and rates with special emphasis on the elucidation of relationships between on-line fermentation measurements and the culture metabolic activity.

(2) Use the on-line measurement/metabolic activity relationships to develop and demonstrate strategies for the control of culture metabolic activity which improve fermentation performance.

1.3 Method of Approach and Scope

In meeting the thesis objectives outlined above, the method of approach shown in Figure 1.1 was followed.

In addressing objective (1), both batch and continuous fermentations were performed and extensively characterized. The information obtained from these fundamental kinetic studies was synthesized into a working hypothesis identifying the proper operating mode (batch, fed-batch, or continuous) and control strategies for

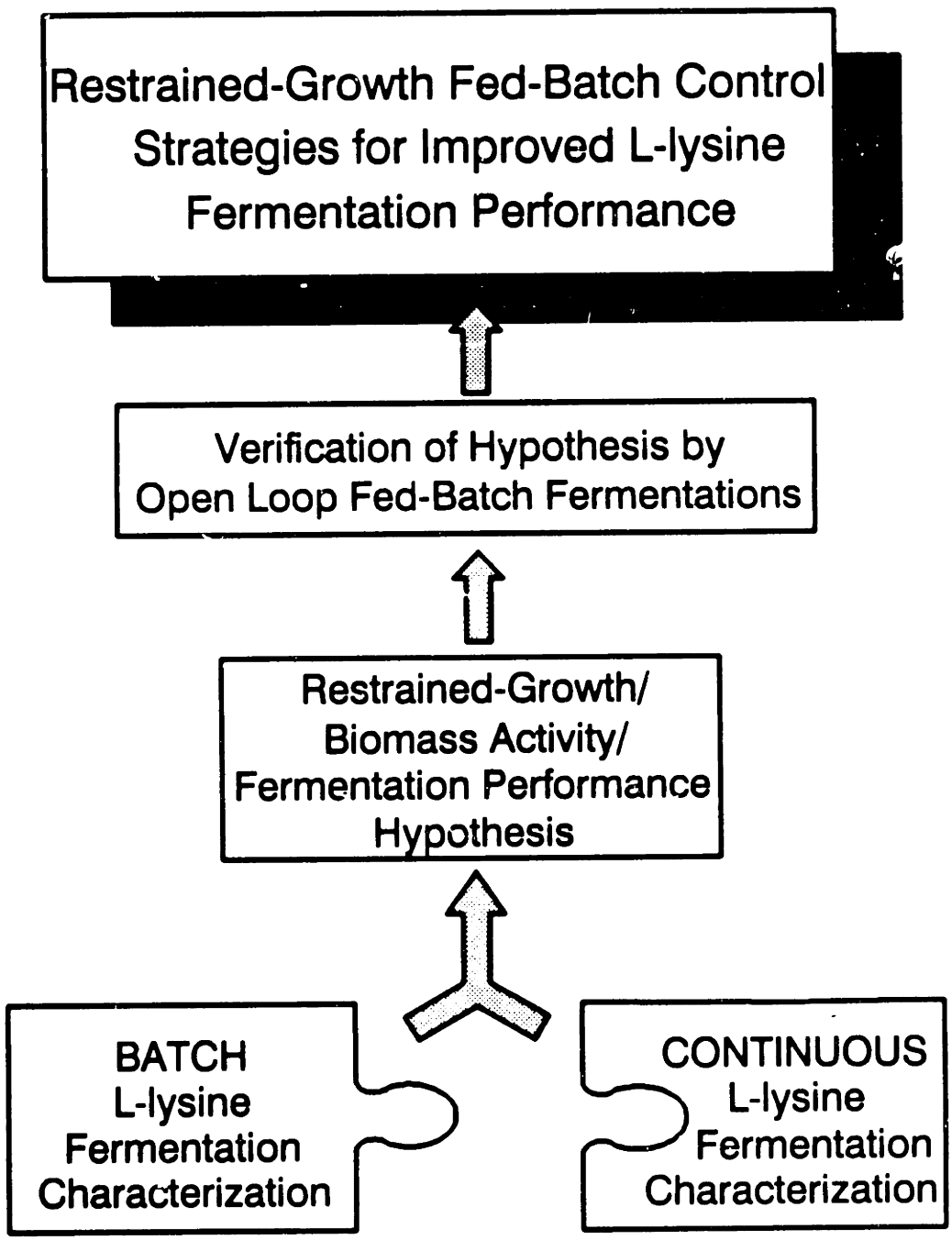

Figure 1.1. Thesis method of approach.

manipulating the culture activity and improving fermentation performance.

Objective (2) was addressed by first verifying the validity of the performance improvement working hypothesis. Following the successful hypothesis verification, relationships developed between on-line respiratory measurements and fermentation performance indicators (yield and specific productivity) were used to formuiate the restrained growth fed-batch feed control strategies. The utility of these metabolic activity control strategies was then demonstrated through a set of feedback-controlled fed-batch fermentations.

In the course of the characterization work, a number of fundamental issues concerning the microbial production of L-lysine were investigated. The batch culture dynamics were analyzed and explained in terms of the type of growth limitation required for the overproduction of L-lysine. The steady-state continuous culture data were used not only to study the metabolic efficiency of the organism over a range of growth rate, but also to estimate the intrinsic conversion efficiencies of carbon and nitrogen to L-lysine. The steady-state fluxes were also utilized to estimate intracellular carbon fluxes and carbon partitioning at key locations within the metabolic network, providing both an understanding of the underlying causes of the low observed yields and rational directives for future strain manipulations.

A culture instability which affected both long-term continuous cultures and extended-length fed-batch fermentations was also studied in detail. A theoretical modeling effort was applied to predict the appropriate steps necessary to reduce instability problems. The theoretical predictions were tested experimentally and verified the importance and utility of proper medium formulation in insuring the maintenance of a productive culture.

The efforts of this work combine to present a complete picture of a method of biocatalyst activity control which manipulates a microbial metabolism through control of the microbial environment.

Chapter 2

Production of Amino Acids

2.1 The Beginning of the Amino Acid Industry

In 1908, a Japanese researcher identified the taste-enhancing properties of *konbu*, a kelp-like seaweed long used as a traditional seasoning source in Japan, as being due to L-glutamic acid [Ikeda, 1908]. Based on this discovery, the industrial production of monosodium L-glutamate (MSG) was initiated by Ajinomoto Co. in 1909 [Hirose and Okada, 1979]. Up until the 1950's, MSG was exclusively produced by isolation from acid-hydrolyzed natural proteins such as wheat gluten or soybean protein.

Fifty years after Ikeda's discovery, it was reported that considerable quantities of L-glutamic acid could be accumulated in cultures of what are now collectively referred to as glutamic acid bacteria [Kinoshita *et al.*, 1957]. This discovery of the production of L-glutamic acid by fermentation stimulated a tremendous amount of research aimed at isolating productive wild strains and developing genetic mutants which could accumulate large quantities of primary metabolites, such as amino acids.

2.2 Glutamic Acid Bacteria in Amino Acid Production

Amino acids are used in many different applications. The major uses are for human food products, animal feeds, medicines, cosmetics, polymers, and synthetic

leathers [Hirose and Okada, 1979]. The most well-known human food products are the flavor enhancers MSG, L-alanine, and glycine and the artificial sweetener aspartame (methyl ester of the L-phenylalanine - L-aspartate dimer). L-lysine, L-threonine, and L-methionine are used to improve the nutritional quality of plant protein materials used as livestock feed. Medical infusions typically contain both essential and non-essential amino acids. L-arginine, L-cysteine, L-glutamine, and L-histidine are all used therapeutically. L-alanine is used in the production of poly-alanine fibers and L-lysine is used for lysine-isocynate resins. Poly-γ-methyl glutamate is used in the manufacture of synthetic leather.

A variety of different methods have been used in producing amino acids on an industrial scale. These include isolation from protein hydrolysates, chemical synthesis, and microbiological methods such as enzymatic bioconversion and direct fermentative production from carbon sources such as glucose. In most cases, the most efficient production method is via the fermentative route from cheap carbon sources, given that an appropriate production strain can be developed. Table 2.1 lists production and pricing information for a number of amino acids. Although the L-lysine production figure is for 1989, Greer *et al.* (1983) have estimated annual demand increases of 3.3-5.8 percent in the U.S. and 3-4 percent in Japan. Those rates of increase predict worldwide demand for L-lysine to currently be 120 to 130 thousand metric tons per year. It should be mentioned that as of late 1990, Archer-Daniels-Midland (ADM; Decatur, IL) was planning to begin operation of a 125-million lb/yr (57,000 metric tons/yr) L-lysine plant (the world's largest) based on a fermentation process licensed from Eastman Kodak. L-lysine prices have thus been falling in the past year as competitors compete for sales in preparation for ADM's

Table 2.1 - Production and pricing information for several amino acids

Amino Acid	Worldwide Annual Production (metric tons)[a]	Major Production Method[b]	Price ($/kg)[c]
L-lysine	113,000[d]	DF	2.97-3.19 (feed grade)
DL-methionine	70,000	CS	3.63-3.70 (feed grade) 6.50 (USP)
L-threonine	100	DF,CS	11.50-13.00 (feed grade) 45-50 (USP)
L-phenylalanine	7900[e]	DF,CS	20-35 (food grade)[f] 84 (USP)
L-tryptophan	200[g]	CS,ES	68 (feed grade)
L-glutamic acid	320,000	DF	6-7 (food grade)

[a] Production figures are for 1981 unless otherwise noted [Crueger and Crueger, 1984].
[b] As of 1981. DF=Direct Fermentation from carbohydrates; CS=Chemical Synthesis; ES=Enzymatic or Immobilized Cell Synthesis [Crueger and Crueger, 1984].
[c] Prices are for June 28, 1991 [*Chemical Marketing Reporter*] unless otherwise noted. food grade=human consumption; feed grade=livestock consumption; USP=United States Pharma Copeia.
[d] 1989 worldwide production [Greer, 1991].
[e] Estimated 1990 production based on 1985 demand and projected increases in demand [Klausner, 1985].
[f] Price on June 24, 1985 [*Chemical Marketing Reporter*].
[g] Japanese 1981 capacity only [Greer *et al.*, 1983].

entrance into the market [Hunter and Morris, 1990].

Most industrial amino acid fermentations are carried out in batch mode or batch mode with periodic addition of large amounts of the carbon source and can run anywhere from two to four days. The nitrogen source is typically supplied by adding gaseous ammonia as the pH controlling agent. Organic nitrogen requirements, such

as for auxotrophic mutants, are typically met by the use of inexpensive hydrolyzed protein material [Crueger and Crueger, 1984]. There have been few reports of continuous industrial amino acid fermentations, although some extensive work had been done on development of a continuous glutamic acid process [Ueda, 1972].

The major bacterial amino acid producers are the coryneform or glutamic acid bacteria, namely *Corynebacteria* and *Brevibacteria*. Most of the available literature deals with the producers *C. glutamicum*, *B. flavum*, and *B. lactofermentum*. Some taxonomical studies have concluded that many, if not most, of the glutamic acid bacteria should be considered strains of *C. glutamicum* [Abe *et al.*, 1967].

Glutamic acid bacteria are gram-positive, non-sporulating, and non-motile ellipsoidal spheres or short rods (from 1 to a few microns in length). Without exception, they require biotin (vitamin H) for growth, and some strains also require thiamine (vitamin B_1) [Kinoshita, 1985]. The natural biotin requirement renders the organism biotin-deficient in a low biotin environment. Because biotin is necessary in fatty acid synthesis, an altered plasma membrane is made under biotin deficiency. This altered membrane is incapable of retaining high concentrations of glutamate (produced due to a natural shunt towards glutamate) and thus glutamate is excreted into the medium. When biotin is supplied in amounts optimal for growth [> (10-30) μg/l], the permeability barrier is effective and glutamate stops its own synthesis when it reaches an internal level of 25 to 50 milligrams per gram of dry cell weight [Demain, 1972]. This barrier against glutamate excretion may be extremely beneficial to the overproduction of other amino acids since the nitrogen of all the amino acids is derived from glutamate by transamination. Therefore, maintaining a sufficient supply of intracellular glutamate would be of importance in the efficient

overproduction of other amino acids.

In biosynthetic pathways leading to primary metabolites, such as amino acids, the main regulation is through either feedback inhibition of an early biosynthetic enzyme or feedback repression of one or more of the biosynthetic enzymes by the final product or its derivative [Demain, 1972]. These pathways are normally regulated so rigidly that wild type organisms rarely excrete more than a few milligrams per liter of any primary metabolite, the exception being the large number of natural L-glutamate producers and a few producers of L-valine and L-alanine. To increase the production of a given metabolite, the feedback regulation must be bypassed. Usually this is done by mutation and subsequent isolation of auxotrophic mutants or selection of regulatory mutants. It should be mentioned that in coliform bacteria, such as *E. coli*, the use of isoenzymes at the entrance to a pathway is the principle mode of control. In glutamic acid bacteria, isoenzymes are not typically found and the principle control is through the concerted action of two end products on the initial pathway enzymes [Dattas *et al.*, 1973]. This second mode of control is much simpler to bypass than the first mode by the use of auxotrophic or regulatory mutants. Thus, microbial production of amino acids has been pursued almost exclusively with glutamic acid bacteria.

Auxotrophic mutants avoid feedback inhibition or repression because of their inability to produce the effector metabolite (usually the end product or a derivative of the end product of one of the branches of the pathway). Since the mutant cannot synthesize the effector, but it is required for growth, the effector must be supplied in the fermentation medium. When grown on a limiting supply of the effector, the auxotrophic mutant can overproduce and excrete a related metabolite whose

biosynthesis has been released from normal regulation by the removal of the effector. This is the principle by which many amino acids have been overproduced using glutamic acid bacteria, including L-lysine [Kinoshita, 1958; Crueger and Crueger, 1984].

Regulatory mutants avoid feedback regulation because of either an altered structure of an enzyme subject to inhibition or a modified regulatory gene such that the expression of an enzyme is no longer repressible. These modifications are performed by mutating cells and selecting for mutants which resist the toxic effects of an analogue of the desired product. Such mutants are insensitive to feedback regulation by the desired product [Demain, 1972]. There are many examples of regulatory mutants of glutamic acid bacteria being used successfully in the overproduction of amino acids, including L-lysine [Nakayama *et al.*, 1973; Crueger and Crueger, 1984].

It should be mentioned here that recent work with amino acid production by glutamic acid bacteria has utilized recombinant DNA technology in what is now known as "Metabolic Engineering" [Beppu, 1986; Follettie *et al.*, 1991; Cremer *et al.*, 1991; Stephanopoulos and Vallino, 1991; Bailey, 1991]. More will be said about recombinant genetic modifications of glutamic acid bacteria in Section 3.2.2.

2.3 L-lysine Biosynthesis

This section discusses the biochemical pathways involved in the biosynthesis of L-lysine as well as the metabolic regulation of those pathways. Similar information will also be presented concerning several common side products in the L-lysine

fermentation.

2.3.1 Biochemical Pathways and Regulation

In glutamic acid bacteria growing on glucose, the standard glycolytic pathway and TCA cycle are operative in conjunction with the carboxylation of phosphoenol pyruvate, PEP, to form oxaloacetate, OAA (discussed in detail in Section 2.4.2). OAA is transaminated to form L-aspartate which is the starting point for the aspartate amino acid family, of which L-lysine is a member.

Studies with L-lysine producing strains of glutamic acid bacteria determined that L-lysine biosynthesis occurs via the diaminopimelate (DAP) pathway [Nakayama and Kinoshita, 1961a,b] shown in Figure 2.1. The figure gives the detailed steps between L-aspartate and L-lysine. Note that the figure shows two routes from L-2-amino-6-ketopimelate to meso-DAP. The one-step conversion (catalyzed by meso-DAP dehydrogenase, enzyme 11 in the figure) was found to be present in glutamic acid bacteria by Misono *et al.* (1979) and further work by Ishino *et al.* (1984) showed that both routes exist at approximately equal levels.

The metabolic regulation of the aspartate family of amino acids in glutamic acid bacteria is shown in Figure 2.2. The main obstacle to L-lysine accumulation is feedback inhibition of the first enzyme, aspartate kinase, via the concerted effect of L-lysine plus L-threonine [Nakayama *et al.*, 1966; Miyajima *et al.*, 1968; Shiio and Miyajima, 1969; Shiio *et al.*, 1970]. By mutating the enzyme leading to homoserine from the ASA branch point, homoserine dehydrogenase, an auxotrophic mutant is obtained which cannot grow unless homoserine (or L-threonine plus L-methionine)

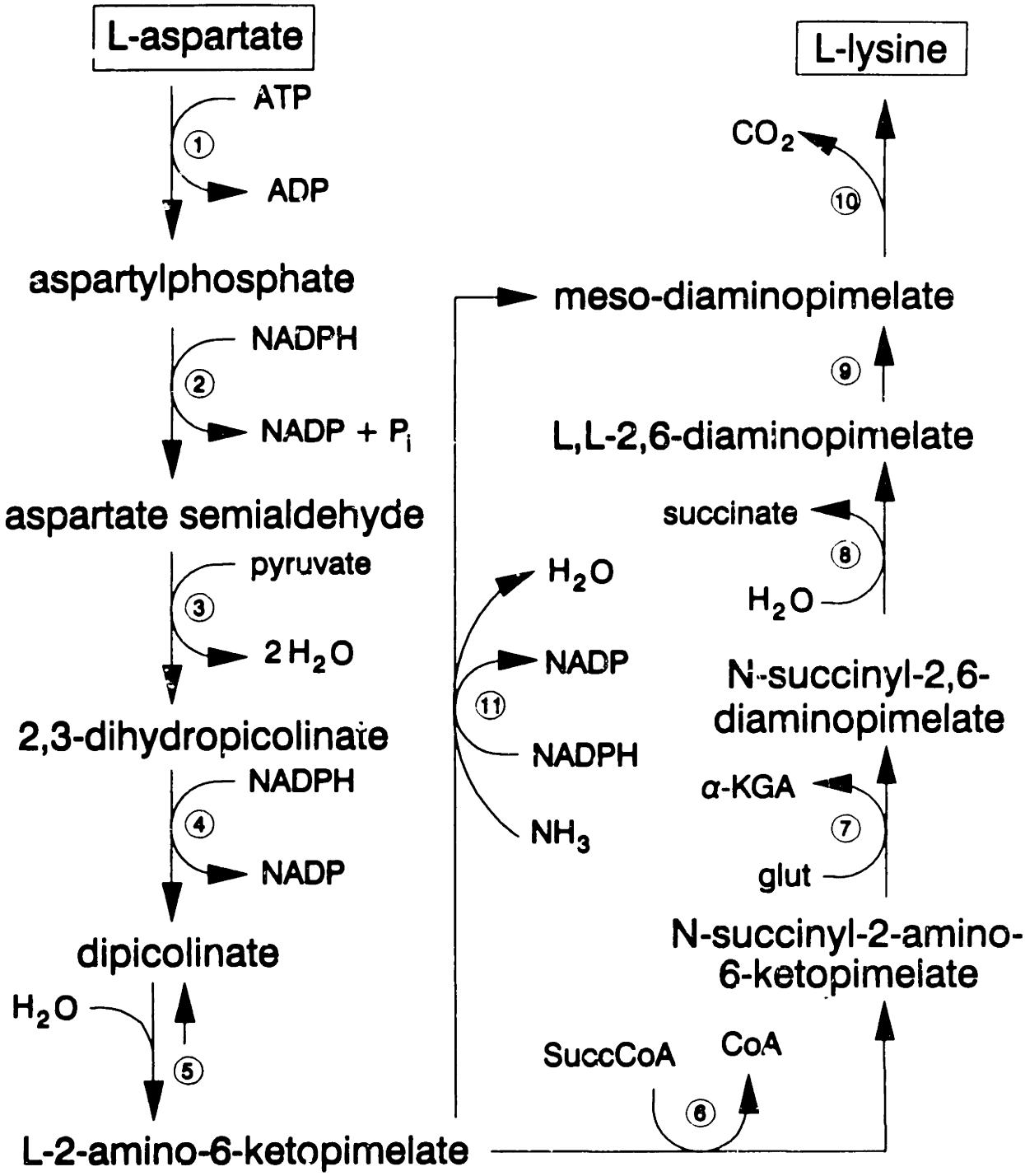

Figure 2.1. Detailed biochemical reaction sequence from L-aspartate to L-lysine. Enzymes are: 1) aspartate kinase 2) aspartic-β-semialdehyde dehydrogenase 3) dihydrodipicolinate synthase 4) dihydrodipicolinate reductase 5) ring-opening step, enzyme unknown 6) N-succinyl-2-6-ketopimelate synthase 7) N-succinyl-aminoketopimelate:glutamate aminotransferase 8) N-succinyl diaminopimelate desuccinylase 9) diaminopimelate epimerase 10) diaminopimelate decarboxylase 11) meso-α,ϵ-diaminopimelate D-dehydrogenase (alternate pathway).

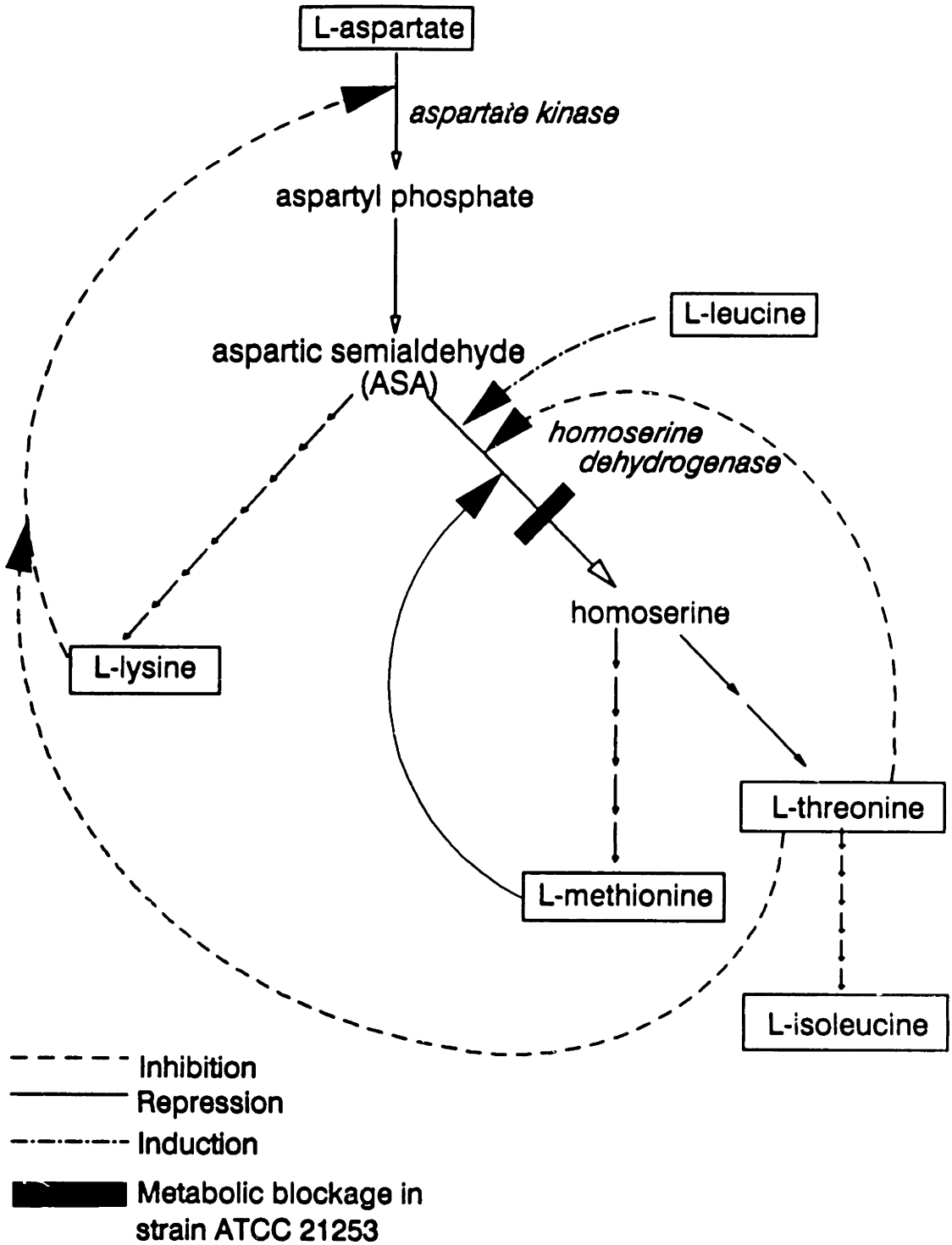

Figure 2.2. Biosynthesis and feedback regulation of the Aspartate family of amino acids in *C. glutamicum.*

is supplied in the medium. The intracellular L-threonine concentration is then dependent on the extracellular concentration of L-threonine (or homoserine). Therefore, as long as the extracellular L-threonine concentration is low enough, the concerted feedback inhibition of aspartate kinase cannot occur. Consequently, metabolic intermediates, which cannot travel down the homoserine branch, are shunted toward the L-lysine branch at increased rates due to the defeat of the natural regulation. As discussed further in Section 4.1, this is the principle by which the strain used in this work accumulates L-lysine.

Although homoserine dehydrogenase is dysfunctional in our working strain, it is of interest to discuss its regulation. It is strongly inhibited by L-threonine and repressed by L-methionine [Miyajima and Shiio, 1970; Follettie *et al.*, 1988; Cremer *et al.*, 1988; Kiss *et al.*, 1990; Follettie *et al.*, 1991]. One report [Cremer *et al.*, 1988] demonstrated that L-leucine induces the synthesis of homoserine dehydrogenase in *C. glutamicum.*

There appears to be very little regulation of the chain of reactions from ASA to L-lysine. Although one study [Cremer *et al.*, 1988] reported a repressive effect of L-lysine on *C. glutamicum* DAP decarboxylase, the last enzyme in the chain, that claim was later retracted [Cremer *et al.*, 1991]. Tosaka *et al.* (1978c) reported the repression of dihydrodipicolinate (DDP) synthetase (the first step from ASA toward L-lysine) by L-leucine in *B. lactofermentum*, but those results could not be duplicated in *C. glutamicum* [Cremer *et al.*, 1988]. The observed negative effect of L-leucine on L-lysine overproduction seen in the results of Tosaka *et al.* (1978c) may have been due to L-leucine inducing increased levels of homoserine dehydrogenase and thus drawing off ASA towards homoserine rather than L-lysine.

Relatively little work has been done to investigate L-lysine transport and excretion. One study [Luntz *et al.*, 1986] proposed that L-lysine excretion occurs via active transport through L-lysine specific channels (pores). These hypothetical channels would open in response to increases in intracellular L-lysine concentration.

2.3.2 Side Product Formation

Several side products are commonly formed during the fermentative production of L-lysine: the disaccharide trehalose and the amino acids L-alanine and L-valine.

Trehalose is a disaccharide of two α-α linked glucose residues. It is typically synthesized as an intracellular carbohydrate storage compound by yeast in the presence of high concentrations of glucose [D'Amore *et al.*, 1991] and in bacteria under nitrogen growth limitation [Wilkinson and Munro, 1967]. It has been observed to accumulate extracellularly in the L-lysine fermentation [Inbar *et al.*, 1985]. If the trehalose which is excreted is not recovered, or reutilized, as a carbon source, then its formation effectively decreases the fermentation yield by wasting glucose.

L-alanine can also be excreted during the L-lysine fermentation. It is formed in one step by the transamination of pyruvate. Since pyruvate is a precursor for L-lysine, the conversion of pyruvate to L-alanine and subsequent excretion reduces the amount of pyruvate available for L-lysine production. More glucose would be needed to replenish the pyruvate "wasted" as L-alanine, and the fermentation yield would be decreased. It is also possible that, if enough pyruvate were diverted for side products, such as L-alanine and L-valine, the rate of pyruvate formation could limit

the rate of L-lysine formation.

L-valine is also formed from pyruvate and can also be excreted during production of L-lysine. A comprehensive work on the pathways and regulation (in gram-negative bacteria) of the branched-chain amino acid family, of which L-valine is a member, was published by Umbarger (1969). The pathway in *Brevibacteria* [Tsuchida and Momose, 1975] has been determined to be very similar to that in the gram-negative bacteria. Figure 2.3 shows the detailed pathway from pyruvate to L-valine and L-leucine. Note that the production of L-valine requires the oxidation of one NADPH. Thus, any L-valine produced during the L-lysine fermentation takes not only pyruvate away from use for L-lysine formation, but also NADPH.

Figure 2.4 shows the regulation of the branched-chain amino acid family in glutamic acid bacteria [Tsuchida and Momose, 1975]. Note that the sequences of reactions forming L-valine and L-isoleucine are shown to run in parallel and are mediated by a common set of enzymes. For example, the enzymes condensing pyruvate with acetaldehyde and α-ketobutyrate with acetaldehyde are collectively referred to as acetohydroxyacid (AHA) synthetase. The key regulatory locations are at threonine dehydratase, which is feedback inhibited by L-isoleucine; α-isopropylmalate synthetase, which is both inhibited and repressed by L-leucine; and AHA synthetase which is weakly inhibited by each of L-isoleucine, L-valine and L-leucine and strongly repressed by the simultaneous presence of L-isoleucine, L-valine, and L-leucine (multivalent repression).

2.4 Theoretical L-lysine Fermentation Yield

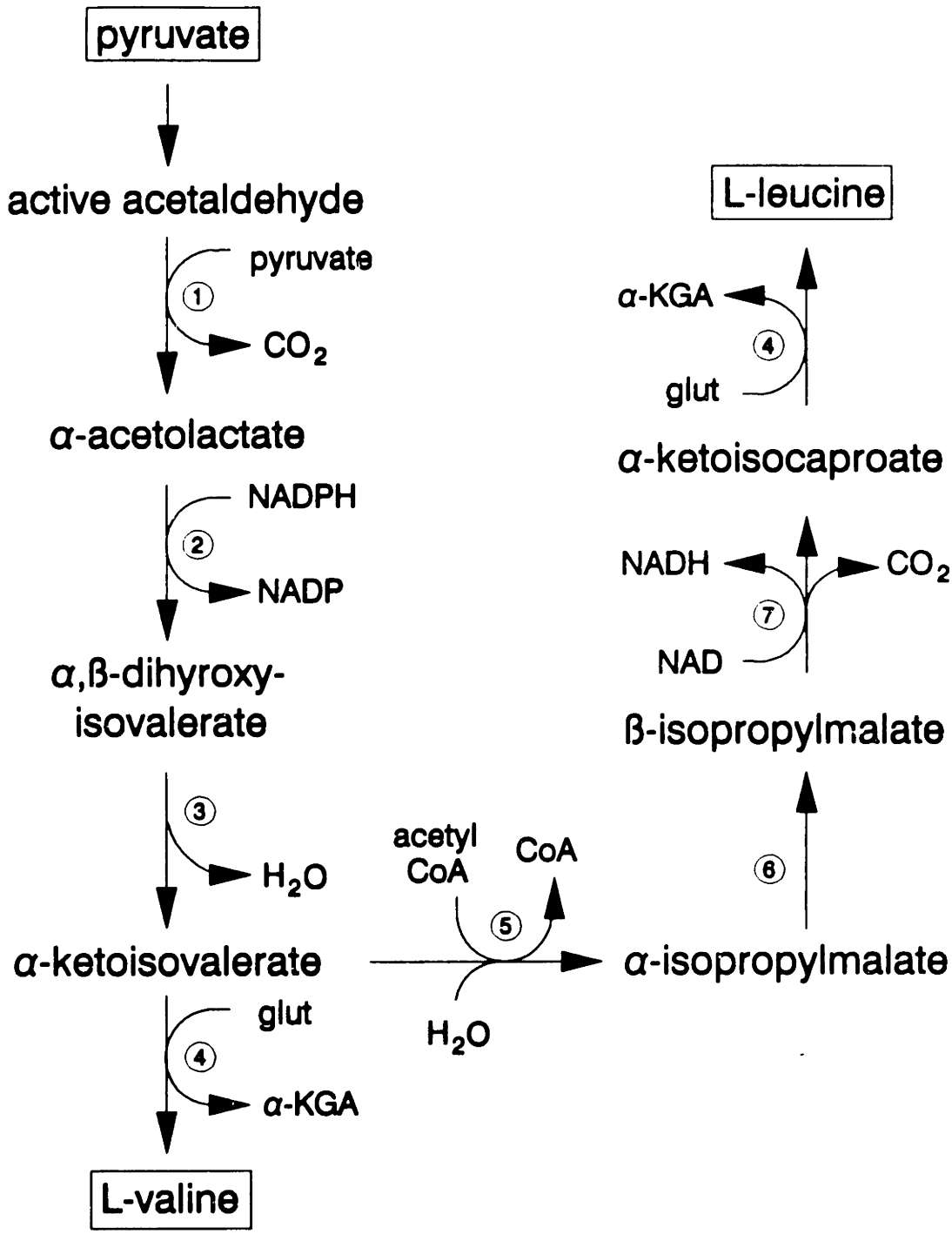

Figure 2.3. Detailed biochemical reaction sequence from pyruvate to L-valine and L-leucine. Enzymes are: 1) acetolactate synthetase (or acetohydroxyacid synthetase) 2) dihydroxy-isovalerate reducto-isomerase (or dihydroxy-acid reducto-isomerase) 3) dihydroxy-isovalerate dehydratase (or dihydroxy-acid dehydratase) 4) branched-chain amino acid transaminase 5) α-isopropylmalate synthetase 6) α-isopropylmalate isomerase 7) β-isopropylmalate dehydrogenase.

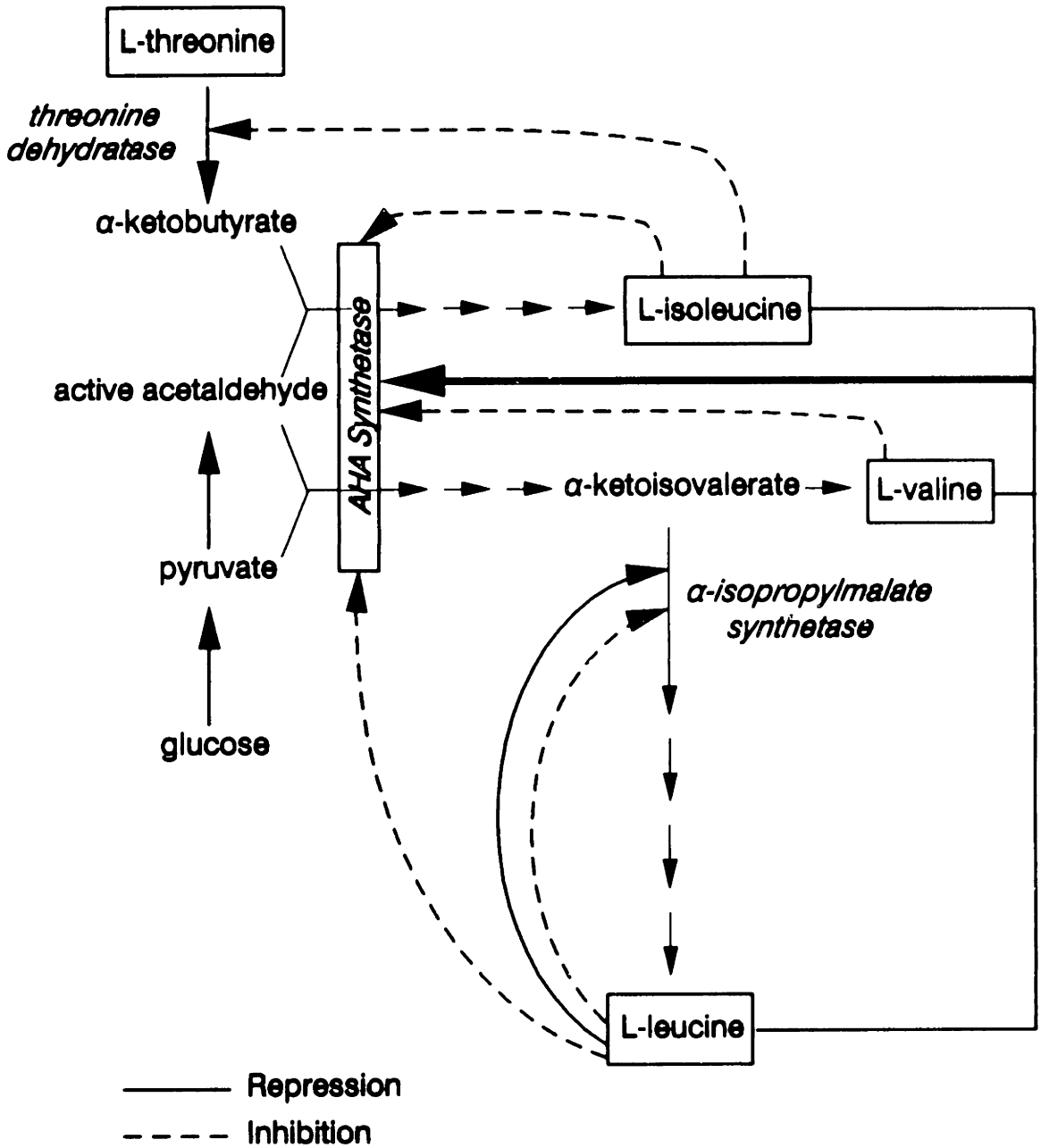

Figure 2.4. Feedback regulation of the family of branched amino acids in *C. glutamicum.*

To gauge the efficiency of any chemical process, a knowledge of the best possible, or theoretical, outcome is helpful. There are two approaches to calculating theoretical efficiencies: the stoichiometric or lumped approach using elemental balances and the detailed reaction scheme (or metabolic pathway in the case of microbial transformations) approach. Examples of the metabolic pathway approach have been presented in the literature for one of the several L-lysine biosynthetic scenarios [Simon *et al.*, 1984; Shvinka *et al.*, 1980] and for the synthesis of penicillin [Cooney and Acevedo, 1977]. Both the stoichiometric and pathway approaches have been used in this work to estimate the theoretical maximum yield (L-lysine produced/glucose consumed) for the L-lysine fermentation.

2.4.1 Stoichiometric Approach

The stoichiometric approach to determining the maximum theoretical yield assumes that the synthesis of the desired product from glucose, oxygen, and ammonia can be represented by a lumped elemental balance as given in equation 2.1:

$$a\,C_6H_{12}O_6 + b\,O_2 + c\,NH_3 \rightarrow d\,C_\alpha H_\beta O_\gamma N_\delta + e\,CO_2 + f\,H_2O \qquad 2.1$$

The desired yield coefficient, Y^{MAX}, is given by the ratio of the stoichiometric coefficients d and a (*i.e.*, d/a). Equation 2.1 has 6 unknowns, a - f. Four elemental balances for C, H, N, and O can be constructed (note the degree of reductance balance is a linear combination of the 4 elemental balances and so cannot offer any new information). Without any loss of generality, the coefficient d can be set equal to 1 (all other coefficients are then normalized per mole of product). That leaves 5

unknowns but only 4 equations with which to solve for the unknowns. There is, therefore, 1 degree of freedom which cannot be specified for this system. Choosing to leave the oxygen stoichiometric coefficient, b, unspecified, it can be shown that the lumped product synthesis equation becomes:

$$\left(\frac{r_p + 4b}{24}\right) C_6H_{12}O_6 + b\,O_2 + \delta\,NH_3 \rightarrow$$
$$C_\alpha H_\beta O_\gamma N_\delta + \left(\frac{4b + r_p - 4\alpha}{4}\right) CO_2 + \left(\frac{r_p - 2\beta + 6\delta}{4}\right) H_2O \qquad 2.2$$

and the maximum yield is given by:

$$Y^{MAX} = \frac{24}{r_p + 4b} \qquad 2.3$$

where r_p is the degree of reduction [Erickson *et al.*, 1979] of the product molecule and is equal to $4\alpha + \beta - 2\gamma - 3\delta$. Equation 2.3 gives the maximum yield as a function of the ratio of moles of oxygen consumed to moles of product formed. For L-lysine ($C_6H_{14}O_2N_2$), $r_p = 28$, and in the limit of no oxygen consumption, Y^{MAX} is equal to 24/28 or 0.857 mol/mol.

The theoretical maximum yield as a function of oxygen consumption is shown in Figure 2.5A. The respiratory quotient, RQ (CO_2 production/O_2 consumption), for the L-lysine biosynthesis reaction is plotted as a function of theoretical maximum

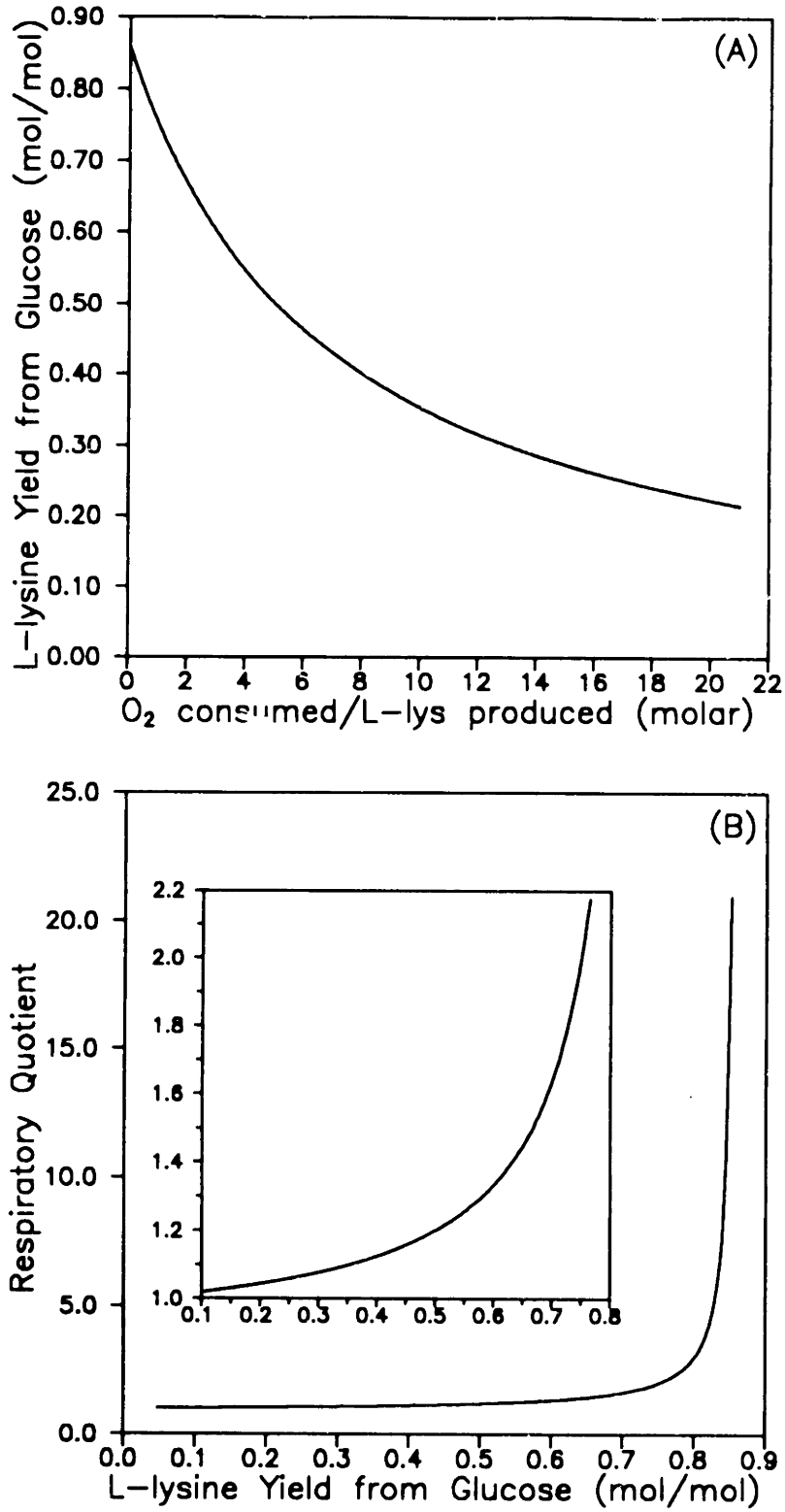

Figure 2.5. Theoretical calculations based on stoichiometric balance for pure product synthesis. (A) Maximum yield vs. degree of oxygen utilization. (B) Respiratory quotient vs. maximum yield.

yield of L-lysine on glucose, Y^{MAX}, in Figure 2.5B.

Table 2.2 gives the theoretical maximum yield for several discrete values of oxygen to L-lysine ratios along with the calculated RQ from the L-lysine biosynthesis reaction. Note that the respiration associated with the biosynthesis of L-lysine simply contributes to the overall respiration of a cell, which may be growing and producing other products or side-products as well. It should be mentioned that the maximum yields calculated by this method are unlikely to be achievable in practice (even with zero growth rate) due to a variety of factors such as futile cycles and less than complete recycling of intermediates, even though Equation 2.2 may be thermodynamically favored. In fact, an equilibrium calculation based on free energies of formation [L-lysine free energy of formation estimated to be -359 kJ/mol by the method of Mavrovouniotis (1990)] shows Equation 2.2 to be highly thermodynamically favorable for all the values of b investigated above.

Table 2.2 - Y^{MAX} and RQ as a function of b/d for pure product synthesis.

b/d (mol O_2/mol lys)	Y^{MAX} (mol lys/mol gluc, g/g)	RQ
0	0.857, 0.696	∞
1	0.750, 0.609	2.00
2	0.667, 0.542	1.50
3	0.600, 0.487	1.33
4	0.545, 0.443	1.25
5	0.500, 0.406	1.20

The limiting theoretical yield value of 0.857 corresponds to an infinite value for the RQ. A biochemical explanation for the infinite RQ will be offered in the

discussion of the detailed metabolic pathway approach. The fact that the maximum theoretical yield changes with the degree of oxygen utilization (which is observed via the change in the L-lysine biosynthesis equation's contribution to the culture respiratory quotient) is of interest. In a fermentation system, the synthesis of product is generally accompanied by synthesis of biomass. For synthesis of biomass on glucose, the respiratory quotient should be very close to 1.0 [Grosz *et al.*, 1984] since the degree of reduction of biomass is generally very close to the degree of reduction of glucose (24 or 4.0 on a per carbon basis). From the stoichiometric balance results, for lysine synthesis in the absence of biomass formation, the RQ will always be greater than 1.0, the exact value depending on the true oxygen demand for lysine synthesis. To determine the true oxygen demand requires knowledge of the exact metabolic pathway leading to lysine synthesis, as will be discussed subsequently. If, for example, the RQ for lysine synthesis is 2.0, when lysine synthesis becomes significant compared to biomass synthesis, the observed respiratory quotient of the fermentation should deviate significantly upward from 1.0. To predict the observed culture respiratory quotient as a function of the observed yield of L-lysine from glucose requires the use of a stoichiometric equation for biomass synthesis. Such an equation can be approximated given an analysis of the biomass elemental composition and a value of the biomass yield on glucose. Using a *C. glutamicum* biomass elemental composition of $C_{3.97}H_{6.46}O_{1.94}N_{0.845}$ [Vallino, 1991] and a biomass yield of 0.60 g/g (see Section 5.3.3), the calculated observed RQ as a function of observed L-lysine yield is shown in Figure 2.6. Included in the figure are data from several of the L-lysine fermentations carried out during this work. This type of analysis points out the utility of the respiratory quotient measurement as an on-line

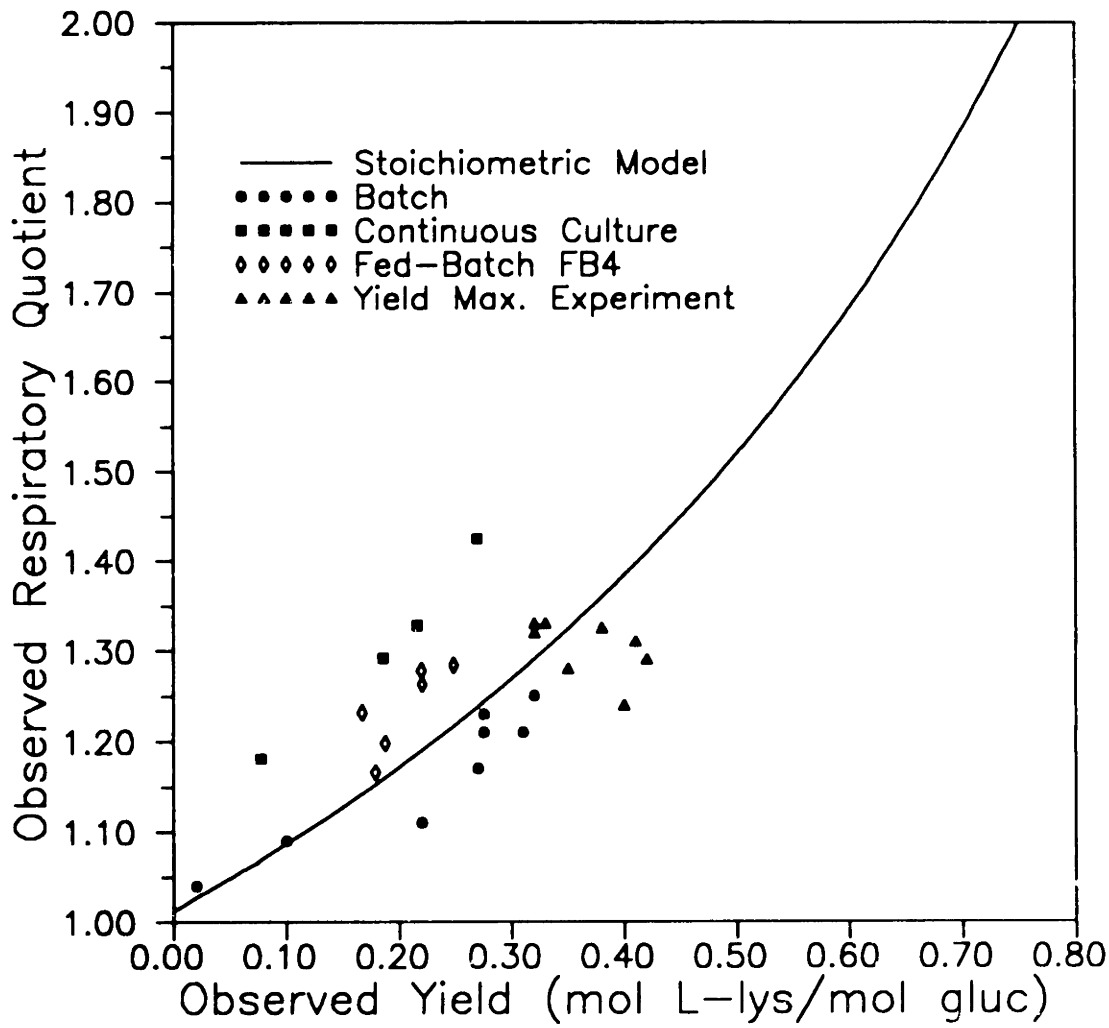

Figure 2.6. Theoretical (from stoichiometric balances) and experimental observed respiratory quotient vs. observed yield.

predictor of lysine overproduction.

In a general sense, this type of approach not only provides a quick means to place reasonable bounds on the maximum yield but also provides a simple way (requires no knowledge of biochemical pathways) to predict the utility of the RQ measurement as a monitor of fermentation performance. In particular, this could be extremely useful to amino acid production since the flux of carbon to product is generally of the same order of magnitude as the carbon flux to biomass. Predicted relationships between observed RQ and observed yield, as in Figure 2.6, for other amino acid fermentations are given in Section 5.6.5 in the discussion of the application of the techniques developed in this work to other fermentations.

2.4.2 Detailed Metabolic Pathway Approach

The maximum theoretical yield can also be calculated by accounting for all individual reactions in the conversion of substrates to product. This approach offers the advantage of obtaining a unique solution for the yield for a specified reaction pathway (recall that the lumped stoichiometric approach, in many cases, and for all amino acid products, gives the yield as a function of an unspecified coefficient). The disadvantage to this approach is that one must know the stoichiometry of all individual reactions involved. For a microbial synthesis, this requires knowledge of the biochemical pathways used in synthesizing the product.

For *C. glutamicum*, many of the metabolic pathways have been well characterized and mapped out. Figure 2.7 is a simplified version of the primary metabolism. In calculating the theoretical maximum yield, one must first specify the

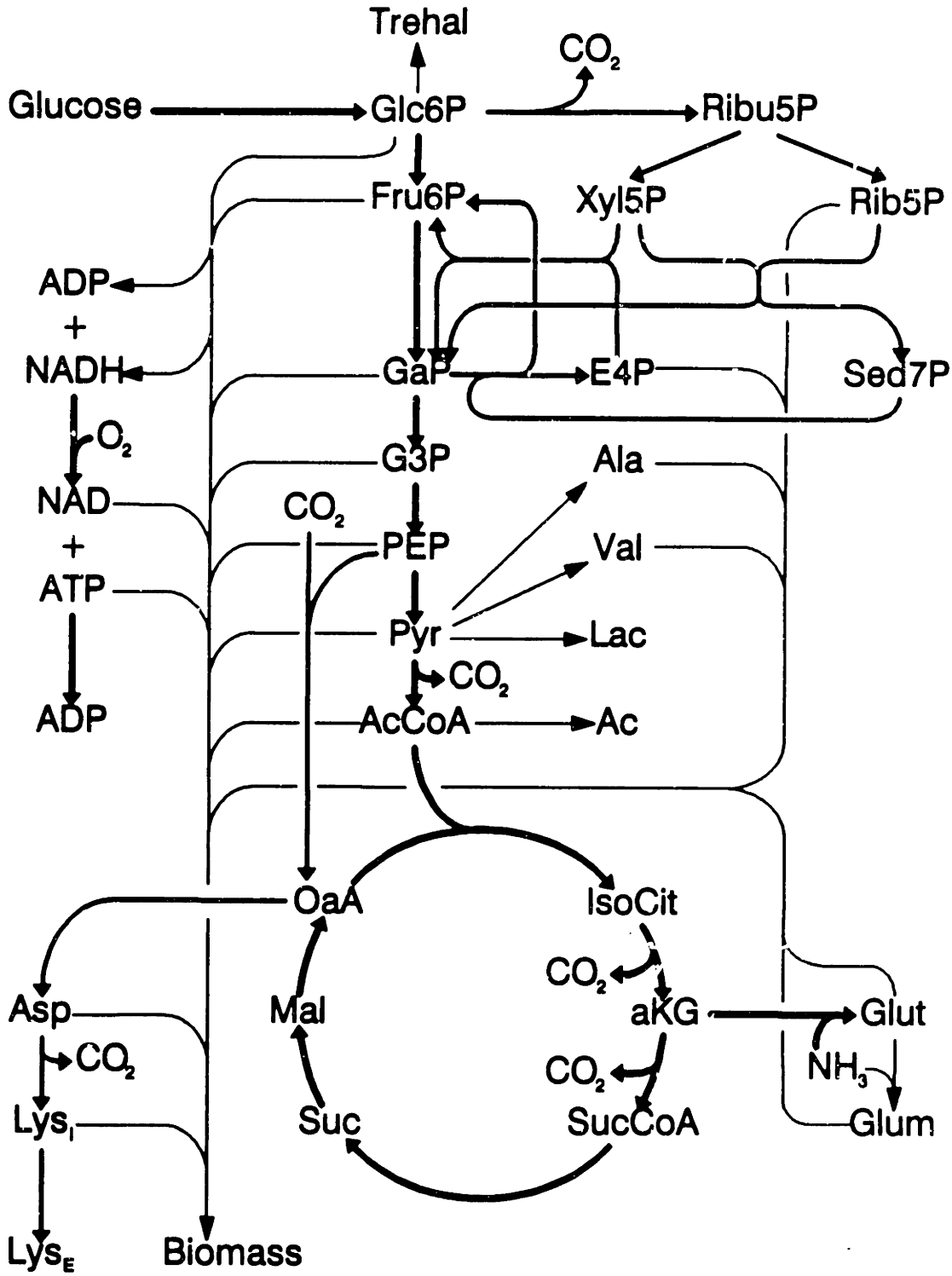

Figure 2.7. Simplified representation of *C. glutamicum* primary metabolism [adapted from Vallino (1991)].

exact pathway for the synthesis of L-lysine. The detailed steps from L-aspartate (ASP) to L-lysine were shown in Figure 2.1.

The most direct route to L-lysine is by use of phosphoenolpyruvate carboxylase (PPC) to carboxylate PEP, which is synthesized in the glycolytic pathway, directly to OAA, avoiding the TCA cycle. Summing all of the reactions in this pathway, the synthesis equation becomes:

$$\begin{aligned} &\text{glucose} + 2\text{NAD} + \text{ATP} + 4\text{NADPH} + 2\text{NH}_3 \rightarrow \\ &\text{L-lysine} + 2\text{NADH} + \text{ADP} + 4\text{NADP} + 2\text{H}_2\text{O} \end{aligned} \qquad 2.4$$

It should be noted that recycling of biosynthetic intermediates, such as α-KGA, L-glutamate, and succinylCoA, has been assumed to be one hundred percent efficient. To proceed further, some assumptions about reducing power and energy generation must be made. First, assume that the efficiency of oxidative phosphorylation (for oxidation of NADH back to NAD and concomitant production of ATP) is 2 [Gottschalk, 1986]:

$$2\text{NADH} + \text{O}_2 + 4\text{ADP} \rightarrow 2\text{NAD} + 4\text{ATP} + 2\text{H}_2\text{O} \qquad 2.5$$

Then assume that 12 NADPH can be generated per glucose by way of the pentose phosphate cycle [Mandelstam *et al.*, 1982]:

$$\text{Glucose} + \text{ATP} + 12\text{NADP} + 6\text{H}_2\text{O} \rightarrow 6\text{CO}_2 + \text{ADP} + 12\text{NADPH} \quad 2.6$$

Additionally, the glucose requirement for ATP production must be accounted for [Gottschalk, 1986]:

$$\text{Glucose} + 6\text{O}_2 + 26\text{ADP} \rightarrow 6\text{CO}_2 + 26\text{ATP} + 6\text{H}_2\text{O} \quad 2.7$$

The last assumption needed to proceed is whether or not NADH and NADPH are to be considered energetically equivalent (freely interconvertible). This would require the presence of dinucleotide transhydrogenases to perform such a conversion. If NADH and NADPH are considered equivalent, then the use of the pentose phosphate pathway is not necessary to regenerate NADPH. For the case of equivalence between NADH and NADPH, the final result is then:

$$(\text{NADH} = \text{NADPH}): \frac{7}{6}\text{Glucose} + 2\text{NH}_3 \rightarrow \text{L-lysine} + \text{CO}_2 + \text{H}_2\text{O} \quad 2.8$$

and thus Y^{MAX} = 6/7 or 0.857 mol L-lysine/mol glucose. This agrees closely with the value of 0.850 mol/mol calculated by Shvinka *et al.* (1980) for the same overall pathway with a few minor differences in detail. Note that this result predicts no net oxygen consumption and that the yield value is equivalent to that obtained from the stoichiometric balance with the b coefficient equal to zero. For the case of no interconversion of NADH and NADPH, the final result is:

$$(\text{NADH} \neq \text{NADPH}):\ \frac{4}{3}\text{Glucose} + O_2 + 2NH_3 + \frac{8}{3}\text{ADP} \rightarrow$$
$$\text{L-lysine} + 2CO_2 + \frac{8}{3}\text{ATP} + \frac{5}{3}H_2O \qquad 2.9$$

and thus Y^{MAX} = 3/4 or 0.750. This theoretical value has been reported previously by Simon *et al.* (1984). Note that this yield value is equivalent to that obtained from the stoichiometric balance with the b coefficient equal to one. Also, this pathway calculation predicts a net production of 2 moles of ATP per mole of glucose converted to L-lysine.

It should be noted that these calculations have assumed that glucose is brought into the cell and directly converted to glucose-6-phosphate via a glucokinase enzyme. Recently, work by Mori and Shiio (1987) suggests that the majority of glucose is actually transported into the cell and phosphorylated via the phosphoenolpyruvate:glucose phosphotransferase system (PTS). This system results in the conversion of one PEP to pyruvate for each glucose transported in and phosphorylated. If the PTS is used for glucose uptake, the theoretical maximum is reduced to 0.64 mol/mol due to the inability to convert some of the pyruvate back to PEP (the reaction catalyzed by pyruvate kinase, which converts PEP to pyruvate, is irreversible). However, Vallino (1991) measured *in vitro* activity of PEP synthetase (converts pyruvate to PEP) in *C. glutamicum* cultured on glucose. Therefore, the maximum yield may not actually be constrained due to the use of the PTS for glucose uptake.

To calculate the maximum theoretical yield for synthesis through the TCA cycle, the glyoxylate bypass [Shiio, 1961] must be assumed to be functioning (modified

TCA cycle is then the terminology). This is because if OAA is drawn off of the standard TCA cycle into the lysine synthesis pathway, there must be an anaplerotic (from the Greek for 'filling up') reaction to replace that OAA or the cycle can't continue to function. This is accomplished by means of the glyoxylate shunt. This shunt converts isocitrate to glyoxylate plus succinate, and the glyoxylate condenses with acetyl coenzyme A to form malate. It should be mentioned that Shvinka *et al.* (1980) published some calculations for the L-lysine theoretical yield from glucose via the TCA cycle, without the use of the glyoxylate shunt. Due to the above reasoning, their calculations were obviously in error.

Summing up all the appropriate reactions for this modified TCA cycle bioreaction scheme, the synthesis equation can be shown to be:

$$\frac{3}{2}\text{Glucose} + 7\text{NAD} + \text{FAD} + \text{ADP} + 4\text{NADPH} + 2\text{NH}_3 \rightarrow \text{L-lysine} + 7\text{NADH} + \text{FADH} + \text{ATP} + 4\text{NADP} + 3\text{CO}_2 \qquad 2.10$$

The efficiency of oxidative phosphorylation with respect to FAD is assumed to be 1 [Gottschalk, 1986]:

$$2\text{FADH} + \text{O}_2 + 2\text{ADP} \rightarrow 2\text{FAD} + 2\text{ATP} + 2\text{H}_2\text{O} \qquad 2.11$$

Then, for the case of interconversion between NADH and NADPH:

$$\text{(NADH = NADPH):}\quad \frac{3}{2}\text{Glucose} + 2O_2 + 2NH_3 + 8\text{ADP} \rightarrow \text{L-lysine} + 3CO_2 + 8\text{ATP} + 5H_2O \qquad 2.12$$

and thus Y^{MAX} = 2/3 or 0.667. Note that this yield value is equivalent to that obtained from the stoichiometric balance with the b coefficient equal to 2.

For the case of no interconversion of NADH and NADPH, the synthesis equation becomes:

$$\text{(NADH} \neq \text{NADPH):}\quad \frac{11}{6}\text{Glucose} + 4O_2 + 2NH_3 + \frac{47}{3}\text{ADP} \rightarrow \text{L-lysine} + 5CO_2 + \frac{47}{3}\text{ATP} + \frac{20}{3}H_2O \qquad 2.13$$

and thus Y^{MAX} = 6/11 or 0.545. This yield value is equivalent to that obtained from the stoichiometric balance with the b coefficient equal to 4.

2.4.3 Connection Between the Two Approaches

How does one know which value of the theoretical maximum yield is correct and should be used as a measure of comparison for the actual fermentation efficiency? Table 2.3 compares the results of the stoichiometric and metabolic pathway yield calculations. The stoichiometric approach gives a spectrum of yield values as a function of oxygen requirements while the pathway approach gives a unique yield value for each pathway, which happen to correspond to some of the "discrete b values" from the stoichiometric approach.

Table 2.3 - Comparison of stoichiometric and pathway approaches to calculating maximum theoretical yield for pure product synthesis.

Y^{MAX} (mol lys/mol gluc)	RQ	b/d Stoichiometric	Detailed Pathway
0.857	∞	0	PEP Carboxylation NADPH = NADH
0.750	2.0	1	PEP Carboxylation NADPH ≠ NADH
0.667	1.5	2	Modified TCA NADPH = NADH
0.600	1.33	3	-
0.545	1.25	4	Modified TCA NADPH ≠ NADH
0.500	1.20	5	-

The maximum calculated value (0.857) is shown by the pathway approach to come about only if the cell can freely interconvert NADPH and NADH. There have been no reports of dinucleotide transhydrogenases (enzymes catalyzing the conversion) in glutamic acid bacteria and the contribution to the observed respiratory quotient of such a conversion pathway would likely produce a much larger increase in RQ than has been observed experimentally.

The question as to whether lysine production from glucose proceeds through carboxylation of PEP to OAA or through the glyoxylate shunt was answered by Vallino (1991), who showed that the glyoxylate shunt is not active in *C. glutamicum* ATCC 21253 grown on glucose, but is induced when grown on acetate as the carbon source.

This information, along with the measurement of PEP synthetase activity [Vallino, 1991], suggests that the theoretical maximum yield of L-lysine from glucose as the carbon source is that predicted by the stoichiometric balance with b equal to 1 and by the metabolic pathway balance for direct carboxylation of PEP to OAA, 0.750 mol/mol.

2.5 Theoretical L-lysine Fermentation Productivity

Calculating a theoretical value for the productivity of a given fermentation system, based solely on knowledge of the biochemical reactions and metabolic regulation of the product of interest, is not as straightforward as calculating a theoretical yield. To do so would require knowledge of the rates of the biochemical reactions involved in the formation of the product as opposed to simply knowing the stoichiometry of those reactions for the yield calculation. Given a detailed model of the metabolism, including kinetic rate and saturation constants for the many enzymatic steps and some good estimates for the intracellular concentrations of the many metabolites involved in the product's biosynthesis, such a calculation of theoretical fermentation productivity could presumably be performed. That type of calculation is beyond the scope of this work. Rather, two semi-empirical calculations will be discussed which, together, put an upper and lower bound on realistic productivities in the L-lysine fermentation.

The volumetric productivity (the amount of product produced per unit time per unit volume), Q_p, is of primary concern in amino acid fermentations. This term can be broken down into the product of the specific productivity (product per unit

biomass per unit time), q_p, and the biomass concentration (biomass per unit volume), X:

$$Q_p = q_p \cdot X \qquad 2.14$$

Clearly, volumetric productivity can be increased by either increasing specific productivity or increasing biomass concentration. This work will focus on determining the maximum theoretical specific productivity as that is the more fundamental biological question at hand. There are many proven engineering approaches to increasing biomass concentration, with the limit usually determined by the ability to supply enough oxygen to the culture.

For a product formed from glucose, the specific productivity can be further broken down into the product of the specific glucose uptake rate (glucose per unit time per unit biomass), q_{glc}, and the yield of product from glucose (product per unit glucose),Y. Then the maximum specific productivity is given by:

$$q_p^{MAX} = q_{glc}^{MAX} \cdot Y^{MAX} \qquad 2.15$$

For the L-lysine fermentation, Y^{MAX} was previously calculated to be 0.75 mol L-lysine/mol glucose. In the continuous culture characterization work (Section 5.3.2), the specific glucose uptake rate was measured as a function of specific growth rate. The largest specific glucose uptake rate measured was about 0.5 g glucose/g biomass·hr. Taken together, these two pieces of information predict a maximum L-lysine specific productivity of:

$$q_p^{MAX} = 0.379 \frac{\text{g L-lysine·HCl}}{\text{g DCW·hr}} \qquad 2.16$$

The second approach to calculating theoretical specific L-lysine productivity follows from the work of Liao (1989), which looked at the theoretical specific productivity of L-tryptophan from *E. coli*. That approach utilized the known growth requirements of bacterial cells (as determined by an experimental quantitation of many of the building blocks of a dry cell weight sample) to estimate the existing flux capacities of the different metabolic steps required in the biosynthesis of L-tryptophan.

If the L-lysine requirement for cell growth is 0.047 g L-lysine·HCl/g DCW (as determined by amino acid analysis of hydrolyzed dry cell mass [Kimura, 1963]), the existing maximum flux of the biochemical step from meso-diaminopimelate (DAP) to L-lysine is equal to $0.047\mu_m$ (g Lys·HCl/g DCW·hr). This means that even if the cell were not growing ($\mu = 0$), the machinery exists for the cell to be producing L-lysine at a rate given by $0.047\mu_m$. If the cell is growing at a specific growth rate μ, then the amount of L-lysine available for excretion into the medium is at most $0.047\cdot(\mu_m - \mu)$. For the *C. glutamicum* strain used in this work, the maximum specific growth rate measured in a defined glucose medium approached 0.7 hr^{-1}. Therefore, the maximum existing capacity of the DAP to L-lysine step (for normal growth conditions) is about 0.033 g L-lysine·HCl/g DCW·hr. It should be mentioned that these calculations were done for each biochemical step involved in the biosynthesis of L-lysine and, as should be the case, all other existing flux capacities were found to be greater than or equal to the existing capacity of the DAP to L-lysine step.

A caveat must be mentioned in regards to this second type of productivity estimation. As alluded to above, these calculations are based upon the growth requirements under normal growth conditions. Clearly, economical amino acid fermentations utilize microbial strains in which the normal regulation of the product's biosynthesis is somehow defeated or bypassed. Therefore, existing flux capacities based on growth requirements should be looked at only as a lower bound on what could be expected to be achieved with a given microbe.

Chapter 3

Fermentation Performance Improvement

As mentioned previously, typical industrial L-lysine fermentations are carried out in either batch mode or batch mode with periodic addition of the carbon source. Nitrogen is typically supplied by ammonium salts or urea and the use of concentrated ammonium hydroxide for control of the pH at near neutral conditions. L-lysine titers can reach quite high levels of 60-100 g/l (as L-lysine·HCl) or higher, but the overall process yields are somewhat low at 0.2-0.3 grams L-lysine·HCl per gram of glucose (or glucose equivalent). This yield value is not very impressive compared to the theoretical maximum of 0.757 g/g, In addition, the processes reaching the highest titers may run for as much as 100 hours, indicating considerable room for improvement in the rate of L-lysine accumulation, or the average volumetric productivity.

3.1 Common Problems in Amino Acid Fermentations

Significant literature exists in regards to efforts to improve many different amino acid fermentations. The ultimate goal in all of these works is to achieve increases in the fermentation performance (product titer, productivity, and yield).

Some of the most common obstacles to meeting fermentation performance goals include intrinsically low specific productivities and instantaneous yields, strain instability, side product formation, improper medium design, non-optimal process

parameters such as dissolved oxygen concentration or feed rate, and decay of metabolic activity. Efforts to combat these obstacles can be divided into two categories: strain manipulations and environmental manipulations. The next two sections outline many of these efforts applied to amino acid fermentations in general and the L-lysine fermentation in particular.

3.2 Strain Manipulations

Up until the last ten years, the term "strain manipulation" would be interpreted to imply the use of classical mutagenesis techniques to isolate or select for desired phenotypic characteristics. The category now includes the use of recombinant DNA technologies to manipulate the genetics of amino acid producers. This section will treat the two types of manipulation separately and then conclude with a discussion of difficulties encountered with strain instability and the selection of stable producers.

3.2.1 Classical Manipulations

Although many of the different varieties of amino acid producers are considered under the broad category "glutamic acid bacteria," this discussion deals separately with each of three producers, *C. glutamicum*, *B. flavum*, and *B. lactofermentum* so as to illustrate the chain of events in the development of efficient production strains.

Work with *C. glutamicum* began with the isolation of mutants auxotrophic for homoserine (or L-threonine plus L-methionine) which produced 28-30 g/l of

L-lysine·HCl (ATCC 13287; U.S. Patent 2,979,439). Further mutagenic treatment added an auxotrophic requirement for L-leucine, resulting in a production of about 34 g/l (ATCC 21253, the strain utilized in this work; U.S. Patent 3,708,395). Mutating ATCC 21253 further resulted in the successful selection of regulatory mutants resistant to the L-lysine analog S-(β-aminoethyl)cysteine (AEC; ATCC 21526; U.S. Patent 3,708,395), the L-threonine analog α-amino-β-hydroxyvaleric acid (AHV; ATCC 21527, U.S. Patent 3,708,395), or the L-isoleucine analog 2-amino-3-methylthiobutyric acid (AMTB; ATCC 21544; U.S. Patent 3,708,395), all of which produced 38-40 g/l. Unfortunately, most of the work with *C. glutamicum* is in the form of patent literature and few further details were provided such as productivities or yields.

C. glutamicum has also been manipulated to a L-lysine producing state without the use of auxotrophic mutations. Simple deregulation of aspartate kinase by mutation and subsequent selection of AEC resistant mutants has been reported [Cremer *et al.*, 1988] with titers in the 7-9 g/l range. It should be noted that biomass concentration was not reported (nor in the patent literature) so it is impossible to compare the strain of Cremer *et al.* with the strains discussed above. This is a common problem with much of the amino acid fermentation literature which renders it difficult to compare different researcher's results with each other.

Work with *B. flavum* has also pursued homoserine auxotrophs [Sano and Shiio, 1967] and AEC resistant mutants [Sano and Shiio, 1970] which produced L-lysine at titers of ca. 30 g/l with yields of 25-30 molar percent (note that the absolute values given for small scale shake flask culture yields are somewhat unreliable in that they are based on initial glucose charges and final L-lysine·HCl concentrations without

necessarily accounting for factors such as liquid evaporation during the course of the 48-60 hours of fermentation). Further attempts to improve yield began to focus on alterations of the primary metabolism in an effort to provide more adequate supplies of L-lysine precursors, such as aspartate, PEP, pyruvate, and NADPH. An AEC resistant mutant derived from a mutant possessing low citrate synthase activity (and thus reduced TCA flux) produced 41 g/l [Ozaki and Shiio, 1983]. This strain was further treated to select mutants sensitive to fluoropyruvate (FP), since FP sensitive strains usually have attenuated activity of pyruvate dehydrogenase (PDH). Two mutants were selected which accumulated 51 g/l L-lysine·HCl from 100 g/l glucose. It was found, however, that these strains, and the parent they were derived from, actually contained mutations which were not selected for, such as reduced inhibition of PPC by aspartate and reduced pyruvate kinase activity [Ozaki and Shiio, 1983]. Therefore, these results were very difficult to interpret. Further work isolated a mutant with reduced PDH activity and amplified PPC activity with reduced PPC sensitivity to aspartate inhibition which accumulated 55 g/l L-lysine·HCl from 100 g/l glucose [Shiio *et al.*, 1984]. It was concluded that attenuating PDH in L-lysine producing strains and desensitizing PPC to inhibition by aspartate can increase L-lysine productivity and yield.

Work with *B. lactofermentum* also initially focused on homoserine auxotrophs and AEC resistant mutants. As discussed in Section 2.3.1, it was reported that L-leucine represses dihydrodipicolinate (DDP) synthetase and then shown that leucine auxotrophs of AEC resistant mutants accumulated more L-lysine (41 g/l vs. 18 g/l) than the parent AEC resistant strain [Tosaka *et al.*, 1978b]. However, in experiments with AEC resistant mutants of *C. glutamicum* (DDP synthetase not

repressed by L-leucine), the same study showed that L-leucine auxotrophy also improved L-lysine production. These findings suggest that the positive effect of L-leucine auxotrophy is most likely due to either increased pyruvate availability or less activation of homoserine dehydrogenase due to lower intracellular L-leucine levels. In further work by this group, L-alanine auxotrophs of AEC resistant *B. lactofermentum* showed increased L-lysine production (39 g/l vs. 20 g/l) [Tosaka *et al.*, 1978d]. This was presumably due to increased pyruvate availability. Further work with the AEC resistant alanine auxotrophs yielded a FP sensitive mutant which produced 70 g/l at a reported yield of 50 percent [Tosaka *et al.*, 1985].

The above works clearly demonstrated the benefits of reducing inhibition of aspartate kinase upon L-lysine production. The results also addressed the need for modification of the primary metabolism as well for further improvement of L-lysine production.

3.2.2 Recombinant Genetic Manipulations

There has been a great deal of work in the past several years in tailoring recombinant DNA techniques for use in glutamic acid bacteria [Yoshihama *et al.*, 1985; Archer *et al.*, 1989; Follettie *et al.*, 1991]. Much of this work has dealt with cloning and determining the organization of genetic elements within *C. glutamicum*. Consequently, there have been few reports of the effects of recombinant genetic manipulations on the performance of amino acid fermentations.

In one study, L-phenylalanine biosynthetic genes of *C. glutamicum* were cloned and reintroduced into *C. glutamicum* with a subsequent doubling of L-phenylalanine

titer over the non-recombinant parent [Ozaki *et al.*, 1985]. In another study, *B. lactofermentum* PPC was cloned and reintroduced into *B. lactofermentum* to improve the availability of oxaloacetate. Improvements were obtained for the production of L-proline and L-threonine [Sano *et al.*, 1987].

In an extensive study of the control of L-lysine biosynthesis, seven enzymes (PPC plus six of the enzymes in the DAP pathway) were cloned and overexpressed in *C. glutamicum* [Cremer *et al.*, 1991]. Overexpression of a feedback-resistant aspartate kinase enzyme in a wild strain (ATCC 13032) was found sufficient to cause L-lysine overproduction (6.9 g/l). Also, overexpression of wild-type DDP synthetase in the wild strain also enabled L-lysine overproduction, but at lower levels (2 g/l). Simultaneous overexpression of both the feedback-resistant aspartate kinase and the wild-type DDP synthetase in the wild strain resulted in a L-lysine titer of 8.2 g/l while simultaneous overexpression of both enzymes in an AEC resistant strain yielded 12.4 g/l of L-lysine·HCl. Overexpression of wild-type PPC in the wild strain did not result in L-lysine overproduction, but overexpression of wild-type PPC in the AEC resistant strain resulted in an increased level of L-lysine production (8.9 g/l vs. 7.3 g/l). Although the authors expressed surprise at some of their results, all of their results could be anticipated based on existing knowledge of *C. glutamicum* metabolic regulation. Unfortunately, the authors do not report any yield or specific rate data, which again makes comparison with other work all but impossible. Nonetheless, this type of work takes the right approach by studying the effect of well characterized metabolic perturbations on amino acid production.

3.2.3 Strain Instabilities

Mutation and degeneration, or strain instability, can be a severe problem for amino acid fermentations (much more so than for fermentations producing cell mass or energy-related metabolites). First, amino acid processes may depend on some circumvention of normal control mechanisms in the cell [Pirt, 1967], requiring stressful environmental conditions in the culture. Second, amino acid formation is an anabolic process yielding no benefit to overproducing cells, as opposed to the energy-producing catabolic processes of ethanol and organic acid formation. When an auxotrophic strain reverts to the prototrophic type by back (or reverse) mutation, also known as reversion, the ability to overproduce an amino acid is usually lost [Nakayama, 1972]. These revertant cells in an amino acid culture are likely to grow faster than the parent cells and will easily take over the reactor. Amino acid producing strains should be contrasted to cell-mass producing cultures which typically operate at as high a dilution (growth) rate as possible for which mutations leading to faster growing cells are beneficial to the process. Stain instability can affect batch, fed-batch, or continuous processes, with the risk generally being greatest for continuous cultures.

An interesting example of an instability in batch culturing and repetitive subculturing concerned the appearance of revertants in a L-leucine fermentation [Azuma *et al.*, 1987]. In that work, the L-leucine productivity was found to decrease rapidly due to the appearance of revertants with little or no ability to overproduce L-leucine (L-leucine auxotrophs were even isolated). The stability problem was attributed to the depletion of the intracellular L-valine pools by the large diversion

of flow to L-leucine. In further work, the addition of L-valine to the fermentation medium was found to stabilize the culture against reversion [Azuma *et al.*, 1988a]. Turning then to genetic manipulation, the researchers were also able to stabilize the culture by enhancing the strain's ability to synthesize L-valine in the presence of L-leucine overproduction (*i.e.* L-valine was expressed as a side product) [Azuma and Nakanishi, 1988a]. Further analysis revealed the biochemical mechanism by which the enhancement of L-leucine overproduction induced the depletion of L-valine pools and subsequently resulted in the reversion problems [Azuma and Nakanishi, 1988b]. This work pointed out the benefit of tailoring the metabolism to support overproduction of the desired product while still providing adequate fluxes for production of other necessary r :tabolites.

In a report dealing with continuous production of L-arginine [Azuma *et al.*, 1988b], it was shown that a L-arginine hyperproducing *Corynebacterium acetoacidophilum* mutant exhibited instability with respect to L-arginine overproduction during continuous cultivation over about 150 hours. By examining strains from various time points during a continuous culture, the researchers were able to isolate a strain which was stable for over 250 hours of continuous culture.

Instability in a continuous L-lysine fermentation was encountered with a homoserine auxotroph of *C. glutamicum* species grown in a complex medium over a time course of about 120 hours. This instability was caused by the appearance of prototrophic cells no longer requiring homoserine for growth. The authors were unsuccessful in stabilizing this culture [Slezak *et al.*, 1969].

In another study of L-lysine production by continuous culture, a mutant resistant to AEC, rifampicin, streptomycin, and 6-azauracil was found to be stable for

at least 380 hours of continuous culture. Apparently, the stability of the selected strain was fortuitous [Hirao *et al.*, 1989].

The presence of multiple auxotrophic mutations has been described as preventing the reversion of L-lysine producers to a non-producing state [Woodruff and Jackson, 1970]. These workers observed a stabilization of L-lysine producing cultures by the addition of second auxotrophic requirement (L-threonine, L-methionine, or L-isoleucine) in addition to a homoserine requirement. A biochemical mechanism was not presented to explain this stabilizing effect. As will be described in detail in Section 5.4.3, it is likely that the stabilization due to the presence of multiple auxotrophic markers results from the inability of revertants (in one of the auxotrophic mutations) to grow any faster than the multiple auxotrophs because of the remaining growth requirements. Thus the medium composition becomes of extreme importance in controlling the propagation of revertants.

With the application of recombinant technology to the overexpression of biosynthetic genes and subsequent overproduction of amino acids, the stability of recombinant production strains must be considered. In two studies addressing the issue, one found a definite segregational instability under non-selective conditions [Archer *et al.*, 1989], and the other found evidence of a structural instability in a plasmid containing a cloned gene for an AEC resistant aspartate kinase [Cremer *et al.*, 1991].

3.3 Environmental Manipulations

A tremendous amount of literature exists concerning the use of environmental

manipulations of all kinds in the improvement of processes for the production of amino acids. This section will attempt to touch briefly on a number of different techniques useful in this regard.

3.3.1 Media Optimization

Many different studies have detailed the effect of media composition on the production of amino acids. The medium was optimized with respect to pH, temperature, ammonium sulfate, potassium phosphate, and biotin concentrations for an auxotrophic mutant of *B. lactofermentum* which produces L-leucine [Tsuchida *et al.*, 1975]. The effect of medium composition was also investigated with respect to different sources of carbon and nitrogen and sucrose concentration for an auxotrophic mutant of *Corynebacteria* which produces L-valine [Plachy, 1979]. Another study examined the effect of different carbon sources on the production of L-glutamic acid and L-phenylalanine [Shiio *et al.*, 1990]. In addition, many studies with auxotrophic mutants investigate the effect of different levels of the required amino acids. Two groups have investigated appropriate means of insuring proper iron availability for *C. glutamicum* [Nakayama *et al.*, 1964a,b; von der Osten *et al.*, 1989].

With respect to the L-lysine fermentation, many initial studies with homoserine auxotrophs attempted to determine optimum levels of L-threonine and L-methionine. Unfortunately, most of these studies reported different optimum concentrations for these two amino acids. It is felt that the reason for the discrepancies is the general disregard for establishment of the growth-limiting nutrient in these systems. If the culture is not growth-limited by the effector molecule for all values of the other

(varied) metabolite concentrations, then it is inappropriate to compare the effect of the other nutrient concentrations on product formation. In addition, if growth becomes limited by something other than the required amino acids, conclusions based on varying the amino acid concentrations are clearly inappropriate. Daoust and Stoudt (1961) determined optimum L-threonine and L-methionine concentrations for L-lysine production of 300 and 100 mg/l, respectively. However, many of their experimental results showing negative effects of various metabolite concentrations can be interpreted simply in terms of a switch in growth-limiting nutrient, resulting in excess L-threonine which then inhibited aspartate kinase. Their ratio of optimal L-threonine to L-methionine concentrations (3/1) corresponds approximately to the ratio of the corresponding biomass yield values (mg amino acid/g biomass) obtained in this work (Section 5.1.2), indicating that their "optimal culture" was approximately equally growth limited by L-threonine and L-methionine. One would then expect that scaling up their "optimal medium composition" (keeping the ratio of L-threonine to L-methionine constant) would produce higher L-lysine titers (their criterion of optimality), assuming that growth limitation by another nutrient was not encountered.

Biotin concentration, above the critical lower level necessary to avoid L-glutamate excretion, has been found to stimulate L-lysine concentration in *B. lactofermentum*, but not in *C. glutamicum* or *B. flavum* [Tosaka *et al.*, 1979]. This improvement has been attributed to an increase in pyruvate carboxylase (PC) activity, as PC requires biotin as a cofactor. Neither *C. glutamicum* nor *B. flavum* have been found to contain PC activity.

3.3.2 Fermentation Operating Parameters Optimization

Previous attempts to improve amino acid fermentation performance by process manipulation have examined the effects of environmental and process variables such as dissolved oxygen concentration [Akashi *et al.*, 1979; Hilliger and Hanel, 1981], redox potential [Radjai *et al.*, 1984], and power input and aeration rates [Hilliger *et al.*, 1984] in batch cultures; sugar concentration [Hadj *et al.*, 1988] or the optimal constant feed rate [Rutkov, 1984] in fed-batch cultures; and sugar concentration, agitation rate, and oxygen enrichment [Hirao *et al.*, 1989], and aeration rate and dilution rate [Michalski *et al.*, 1984], in continuous cultures.

The most informative study of the effect of dissolved oxygen concentration on L-lysine production reported a slight decrease in final L-lysine titer for dissolved oxygen level less than 0.01 atm and no effect for levels between 0.01 and 0.1 atm. This minimum critical dissolved oxygen level corresponded to a culture redox potential of -170 mv [Akashi *et al.*, 1979]. This agrees reasonably well with another study which determined -220 mv as the optimal redox potential for L-lysine yield (g/g) [Radjai *et al.*, 1984]. It should be noted that the effect of low levels of dissolved oxygen on L-lysine fermentation is much less than the effect on fermentative production of amino acids such as L-proline, L-glutamine, and L-arginine which all require L-glutamic acid as a precursor.

In a study of fed-batch cultivation of a *C. glutamicum* homoserine auxotroph at constant feed rates (complex medium), the yield of L-lysine from glucose was found to increase with decreasing nutrient mass addition rate [Rutkov, 1984]. Assuming that higher mass rates of nutrient addition imply higher specific growth

rates, those results agree well with the results obtained in this work for the effect of specific growth rate on yield from glucose (see Section 5.3.2). In another report of fed-batch operation at constant feed rates with an AEC resistant *C. glutamicum* strain, the use of high glucose concentrations (between 90 and 140 g/l) appeared to improve L-lysine titer and yield, although the work was very poorly documented and difficult to interpret [Hadj *et al.*, 1988].

The continuous culture work discussed previously (Section 3.1.3) with the AEC resistant *C. glutamicum* strain demonstrated the importance of dissolved oxygen concentration on continuous culture performance and determined optimal dilution rates for L-lysine concentration and yield (0.02 hr^{-1}, 105 g/l, 0.38 molar yield) and L-lysine productivity (0.16 hr^{-1}, 5.6 g/l·hr). Unfortunately, the work does not report biomass densities, so it is difficult to interpret the results in terms of specific rates.

These types of studies typically aim to determine the most appropriate set points for the various bioreactor environmental variables and then attempt to regulate the culture at this desired state. This type of approach usually reflects the operator's assessment of optimality. Truly optimal fermentation set points may, in fact, vary with time during the course of the fermentation.

3.3.3 Dynamic Optimization

Optimal control theory has been applied to predict optimal feed rate profiles during fed-batch L-lysine fermentation. One study [Ohno and Nakanishi, 1976] applied Green's theorem to the maximization of L-lysine mass productivity (product/time). This methodology found that the optimal feed rate profile depended

on the ratio of final to initial reactor liquid volume. However, this work relied on overly simplistic empirical relationships between process variables (for example, the specific growth rate - substrate concentration relationship was based upon experimental measurement of specific growth rate as a function of *initial* concentration of a complex substrate). Furthermore, no experimental tests of the calculated feed profiles were performed.

Another study [Modak *et al.*, 1986] determined general characteristics of optimal feed rate profiles for a variety of fed-batch processes. The case described of a monotonic increase in specific growth rate with increasing substrate concentration and a nonmonotonic relationship between specific productivity and substrate concentration (high substrate concentrations inhibit product formation) corresponds well to the production of L-lysine in a L-threonine limited medium. The most interesting solution for this case is for a large initial substrate (L-threonine) concentration. For maximization of product, the optimal solution requires initial batch operation until the substrate concentration is reduced to non-inhibitory levels, followed by a period of singular control in which the feed rate is continually increased until the fermentor is full. Unfortunately, experimental verification of such optimal control strategies was not attempted (and are difficult to find in general in the literature). However, this is very similar to the feed rate profile which was experimentally determined to maximize L-lysine productivity using an on-line feedback metabolic activity control strategy (requiring no mathematical model) in this work (Section 5.6.2).

It should be mentioned that dynamic optimization approaches depend critically on the quality of the mathematical models used to describe the fermentation

dynamics. In addition, the open-loop structure of most optimal control structures is usually inadequate for biological processes due to the large variability in inoculum quality, nature of the medium, and even bioreactor operation. Formulation of the optimization problem with a feedback structure would address such inherent problems associated with open-loop control, but would likely require extensive on-line bioreactor measurements, such as biomass, substrate, and product concentrations, for which on-line probes are still largely unavailable. Estimation algorithms can reduce the number of required measurements, but can be quite complex and subject to sensitivity and error propagation problems [Grosz *et al.*, 1984].

3.3.4 Controls of Metabolic Activity

The environmental manipulations discussed to this point are not the only answer to the pursuit of fermentation performance improvement. As mentioned previously, optimal set points may indeed vary with time. Thus, performance may be more effectively improved by attempting to maintain the metabolic activity of the culture, rather than the abiotic environmental variables, at an optimal state. This type of strategy would obviously require some measurement or evaluation of a culture's metabolic state as input for determining appropriate control action.

The most representative example of controls of metabolic activity is the fed-batch baker's yeast fermentation. In that fermentation, overfeeding of sugars results in ethanol formation and poor biomass yield, even under aerobic conditions (Crabtree effect). At the same time, underfeeding causes cell starvation and specific growth rate deterioration, leading to low volumetric productivities. These opposing effects

are optimally balanced by regulating the sugar feed rate to maintain the sugar concentration at a value optimal for growth. In one example of metabolic activity control, the respiratory quotient was used as an indirect measure of metabolic activity towards ethanol production [Wang *et al.*, 1977; Spruytenberg *et al.*, 1979]. In another strategy, the ethanol production rate was monitored by on-line measurement of the exhaust gas ethanol concentration and was used as a direct indicator of metabolic activity [Dairaku *et al.*, 1983].

The yeast fermentation is an example of the use of metabolic activity control to maximize biomass productivity or biomass yield while minimizing side product (ethanol) formation. In the L-lysine fermentation, the general objective is the maximization of L-lysine production while allowing biomass formation just sufficient to meet the L-lysine goal specifications. A metabolic activity control strategy must balance the two opposing uses of substrate for biomass formation and L-lysine overproduction in order to meet the fermentation performance goals regarding yield and productivity.

There has been no previous work in developing controls of metabolic activity to improve amino acid fermentation performance. In this work, performance improvement is achieved by manipulating the metabolism to favor the desired pathway through control of the microbial environment. As will be described in detail, the control strategies aim to provide an environment which maximizes the L-lysine yield and specific productivity (our measures of metabolic activity towards L-lysine overproduction) and maintains them at their maxima for extended fermentation times.

Chapter 4

Materials and Methods

4.1 L-lysine Producing Strain

4.1.1 Strain Description

The strain utilized in this work was *Corynebacterium glutamicum* ATCC 21253 (U.S. Patent 3,708,395), obtained from the American Type Culture Collection (Rockville, MD). This strain is auxotrophic for biotin and both L-homoserine (or L-threonine plus L-methionine) and L-leucine. The L-homoserine auxotrophy results in overproduction of L-lysine in cultures with low levels of L-threonine due to the bypass of concerted aspartate kinase inhibition by L-threonine plus L-lysine (recall Figure 2.2).

The original parent strain for development of 21253 and many other strains is *C. glutamicum* ATCC 13032, a strain which produces large quantities of glutamic acid when cultured under low levels of biotin. Strain 13032 was originally isolated from sewage by researchers at Kyowa Hakko Kogyo Company in Tokyo, Japan (U.S. Patent 3,002,889). Treatment of strain 13032 with ultraviolet (UV) light resulted in the generation of mutants auxotrophic for homoserine (or L-threonine plus L-methionine) which could accumulate L-lysine in the medium when cultured under low levels of L-threonine (ATCC 13287, U.S. Patent 2,979,439). Further treatment of strain 13287 with UV light resulted in the generation of mutants with an additional

auxotrophic requirement for L-leucine, ATCC 21253, the strain used in this work. The patent literature does not discuss the reasons for seeking the L-leucine auxotroph, but it is likely that the researchers believed that L-leucine could negatively affect the production of L-lysine, as discussed previously in Sections 2.3.1 and 3.2.1. It should be mentioned that strain 21253 was further mutagenized (Kyowa Hakko Kogyo) by treatment with nitrosoguanadine, resulting in the selection of strains resistant to either AEC (ATCC 21526), AHV (ATCC 21527), or AMTB (ATCC 21544), as discussed previously in Section 3.2.1.

4.1.2 Strain Maintenance

The strain used in this work, ATCC 21253, was maintained on LB5G (described in Section 4.2.1) complex medium plates at 4°C. Plate cultures were transferred monthly by re-streaking and growing at 30°C for 24 hours. Long-term culture storage was done at -70°C in 80% (v/v) LB5G medium, 20% glycerol.

4.2 Fermentation Details

4.2.1 Fermentation Media

Complex medium used in this work was modified Luria-Bertani (LB) broth, designated LB5G medium: 10 g Tryptone, 5 g Yeast Extract, 10 g NaCl, 18 g Agar (plates only) and 5 g D-glucose per liter of distilled water. This medium was used for strain maintenance, total viable cell plate counts, and for initial seed cultures for fermentations. Bacto® Tryptone, Yeast Extract, and Agar were from Difco Laboratories (Detroit, MI).

Defined, L-threonine growth limiting medium was used for all inoculum steps (except the initial seed culture, which was in LB5G medium), shake flask experiments, reactor initial charges, and reactor feed streams. Slight variations in the recipe were made for different types of cultures, primarily for reasons such as support of higher biomass levels or stronger buffering capacity in shake flask cultures. The different variations are listed below, with a description of the cultures for which the particular medium was used. It should be pointed out, as will be obvious when comparing the recipes, that the variations are fairly minor. All of the defined media are similar to the medium developed by von der Osten *et al.* (1989). In that work, they developed a medium for growth of *C. glutamicum* prototrophs, and investigated the importance of medium design in facilitating iron uptake. Our media must, of course, also include appropriate amounts of the amino acids required for growth by our strain. Experimentally determined cell mass yields (g dry cell weight/mg amino acid) were employed in determining the necessary amino acid composition (those experiments are discussed in Section 5.1.2).

The medium described in Table 4.1 (designated CGM1) was used for small scale shake flask cultures and for inoculum used to inoculate the batch and fed-batch fermentations. All of these small-scale and inoculum cultures were performed without the use of pH control. Note the increased potassium phosphate concentration and ratio (dibasic to monobasic), as compared to the other media, which increase the buffering capacity and initial pH, respectively, thus helping to decrease the rate of pH decline during growth. This medium is capable of supporting about 5 g/l dry cell weight (DCW), given that the pH does not drop to growth-inhibiting levels (< 5) and that oxygen limitation does not occur.

Table 4.1 - CGM1 growth medium for cultures without pH control.

Component	Concentration†	
Portion A:		
D-Glucose	20	g/l
Na_3·Citrate·$2H_2O$	1.14	g/l
$MgSO_4$·$7H_2O$	200	mg/l
$Na_2EDTA·2H_2O$	75	mg/l
$FeSO_4·7H_2O$	25	mg/l
$CaCl_2·2H_2O$	50	mg/l
NaCl	1	g/l
100x Mineral Salts	10	ml/l
pH adjusted to 5.0		
Portion B:		
K_2HPO_4	8	g/l
KH_2PO_4	1	g/l
L-Threonine	150	mg/l
L-Methionine	80	mg/l
L-Leucine	100	mg/l
Biotin	1	mg/l
Thiamine·HCl	1	mg/l
Portion C:		
$(NH_4)_2SO_4$	5	g/l
100x Salts Solution:		
$MnSO_4$	200	mg/l
$Na_2B_4O_7·10H_2O$	20	mg/l
$(NH_4)_6Mo_7O_{24}·4H_2O$	10	mg/l
$FeCl_3·6H_2O$	200	mg/l
$ZnSO_4·7H_2O$	50	mg/l
$CuCl_2·2H_2O$	20	mg/l
pH ~2 w/ HCl (to avoid precipitation)		

† Concentrations listed for Portions A, B, and C are component concentrations per liter of final medium volume (after mixing A, B, and C). Concentrations for 100x Salts Solution are component concentrations per liter of the 100x Salts Solution. All solutions prepared in distilled water.

To minimize browning and to achieve an initial pH (after autoclaving) as near to 7.0 as possible, the following steps were carried out. Portions A, B, and C were each autoclaved in separate vessels and aseptically mixed after cooling (the reason for the separation of the ammonium sulfate lies in the fact that autoclaving the ammonium sulfate with portion B resulted in a lower than desired initial pH for MCG1. It was found that, using the separate portions B and C, the initial pH was close to 7.0). Autoclaving is at 121°C for 30 minutes. Even with the high phosphate concentration, however, the pH drops rapidly and $CaCO_3$ (20 g/l) should be used to be able to reach the full 5 g/l DCW that this medium is capable of supporting. This medium was also used in preparing selective plates, such as for the scoring of revertant cells (discussed in Section 5.4.1). In that case, 18 g/l Agar was used and the glucose and ammonium sulfate concentrations were reduced to 5 and 2 g/l, respectively.

Medium CGM2, described in Table 4.2, was used for the continuous culture studies. The poly(propylene glycol) molecular weight 2000 serves as an antifoam agent (Polysciences, Inc., Warrington, PA). Note that there is no citrate in this medium. This is primarily because this medium was designed before the effect of citrate on iron uptake was documented by von der Osten *et al.* (1989). In fact, the first version of CGM2 did not contain EDTA and a precipitate was found to form in the continuous culture feed tanks. Using such tanks, the biomass concentration in continuous cultures declined with time during the course of feeding with a given feed tank. Fresh feed tanks (free of precipitate) seemed to revive the culture, but as the feed tank was drained, precipitate formed slowly and the culture biomass declined again. Analysis of this precipitate by the MIT Central Analytical Facility showed a

Table 4.2 - CGM2 growth medium for continuous culture.

Component	Concentration†	
Portion A:		
D-Glucose	20	g/l
$MgSO_4 \cdot 7H_2O$	400	mg/l
$Na_2EDTA \cdot 2H_2O$	75	mg/l
$FeSO_4 \cdot 7H_2O$	25	mg/l
$CaCl_2 \cdot 2H_2O$	50	mg/l
NaCl	0.1	g/l
100x Mineral Salts	10	ml/l
poly(propylene glycol) MW 2000	0.1	ml/l
pH adjusted to 5.0		
Portion B:		
K_2HPO_4	3	g/l
KH_2PO_4	1	g/l
L-Threonine	100	mg/l
L-Methionine	150	mg/l
L-Leucine	400	mg/l
Biotin	1	mg/l
Thiamine·HCl	1	mg/l
$(NH_4)_2SO_4$	5	g/l
100x Salts Solution:		
$MnSO_4$	200	mg/l
H_3BO_3	6	mg/l
$(NH_4)_6Mo_7O_{24} \cdot 4H_2O$	4	mg/l
$FeCl_3 \cdot 6H_2O$	100	mg/l
$ZnSO_4 \cdot 7H_2O$	1	mg/l
$CuSO_4 \cdot 5H_2O$	30	mg/l
pH ~2 w/ HCl (to avoid precipitation)		

† Concentrations listed for Portions A and B are component concentrations per liter of final medium volume (after mixing A and B). Concentrations for 100x Salts Solution are component concentrations per liter of the 100x Salts Solution. All solutions prepared in distilled water.

high concentration of iron. It was at this point that EDTA was added to the medium (at two times the molar concentration of iron atoms) as an iron chelator. This addition greatly diminished the precipitation problem and allowed the achievement of steady states in continuous culture. Since the continuous cultures were carried out with pH control, the initial medium pH was not of critical concern. Therefore, for simplicity, the ammonium sulfate was autoclaved as part of Portion B. Autoclaving procedures were as above for MCG1 with the exception that for the preparation of 20 liter tanks of medium, which were prepared as 15 liters of portion A and 5 liters of portion B, the duration of autoclaving was 45 minutes.

Medium CGM3, listed in Table 4.3, was used for all batch and fed-batch cultivations at the 10 liter scale and is essentially a scaled-up version of CGM1 (since these fermentations were designed to achieve higher cell densities than achieved in shake flasks or continuous cultures). As with CGM2, the components are divided into two portions for sterilization. For batch fermentations and the initial reactor charges for fed-batch fermentations, portion A was sterilized in the fermentor during the fermentor sterilization cycle. Note that citric acid, rather than sodium citrate, is used in CGM3. Since the glucose concentration for batch or fed-batch initial charges was fairly high at 150 g/l, and, since the extent of glucose caramelization is reduced at low pH, the medium was sterilized at low pH (~2-3) to reduce the extent of browning. Thus, citric acid, which will lower the pH as opposed to sodium citrate's buffering behavior, was used as the iron chelator.

Since the fermentor sterilization cycle cools quite rapidly, as opposed to the several-hour natural cooling time for medium sterilized in the autoclave, the medium was held at 121°C for 40 minutes to insure proper sterilization. A temperature

Table 4.3 - CGM3 growth medium for 10 L batch and fed-batch cultures.

Component	Concentration†	
Portion A:		
D-Glucose	150-220	g/l
Citric acid	0.5	g/l
$MgSO_4 \cdot 7H_2O$	600	mg/l
$Na_2EDTA \cdot 2H_2O$	75	mg/l
$FeSO_4 \cdot 7H_2O$	50	mg/l
$CaCl_2 \cdot 2H_2O$	1	g/l
NaCl	2	g/l
100x Mineral Salts	20	ml/l
poly(propylene glycol) MW 2000	1	ml/l
Portion B:		
K_2HPO_4	4	g/l
KH_2PO_4	2	g/l
L-Threonine	733	mg/l
L-Methionine	600	mg/l
L-Leucine	1500	mg/l
Biotin	1	mg/l
Thiamine·HCl	1	mg/l
$(NH_4)_2SO_4$	40	g/l
100x Salts Solution:		
$MnSO_4$	200	mg/l
$Na_2B_4O_7 \cdot 10H_2O$	20	mg/l
$(NH_4)_6Mo_7O_{24} \cdot 4H_2O$	10	mg/l
$FeCl_3 \cdot 6H_2O$	200	mg/l
$ZnSO_4 \cdot 7H_2O$	50	mg/l
$CuCl_2 \cdot 2H_2O$	20	mg/l
pH ~2 w/ HCl (to avoid precipitation)		

† Concentrations listed for Portions A and B are component concentrations per liter based on a final medium volume of 10 liters. In other words, batch and fed-batch fermentations are carried out with the same total component amounts. Concentrations for 100x Salts Solution are component concentrations per liter of the 100x Salts Solution. All solutions prepared in distilled water.

profile during a typical fermentor sterilization cycle is shown in Figure 4.1. Using standard techniques [Wang *et al.*, 1979], one can calculate the sterility level [ln(initial spores/final spores) to be approximately 375. Thus, the sterilization cycle was certainly adequate, though probably unnecessarily long.

A few other details concerning CGM3 deserve mention. For the feed medium, portion A was brought to pH 5.0 before sterilization. Portions A and B for the feed medium were sterilized at the standard autoclave conditions described previously and aseptically mixed after cooling.

4.2.2 Fermentation Equipment

The equipment comprising the fermentation data acquisition and control system (in the case of the batch or fed-batch MBR fermentor) is shown schematically in Figure 4.2. The details of each of the fermentors used in this work, the off-gas analysis, the data acquisition hardware and software, and the on-line data manipulation are presented in this section.

4.2.2.1 Continuous Culture Fermentor

The continuous culture fermentation vessel was a 5 liter Microferm® glass bioreactor with stainless steel head plate (New Brunswick Scientific, Edison, NJ) and a 3 liter liquid working volume. This fermentor had self-contained temperature control via a thermistor-based feedback. Agitation was through a top-mounted magnetic coupling. Three six-blade Rushton-type impellers were mounted on the impeller shaft and four baffles drop down from the head plate. Control of pH was accomplished with an Ingold (Wilmington, MA) sterilizable combination pH electrode

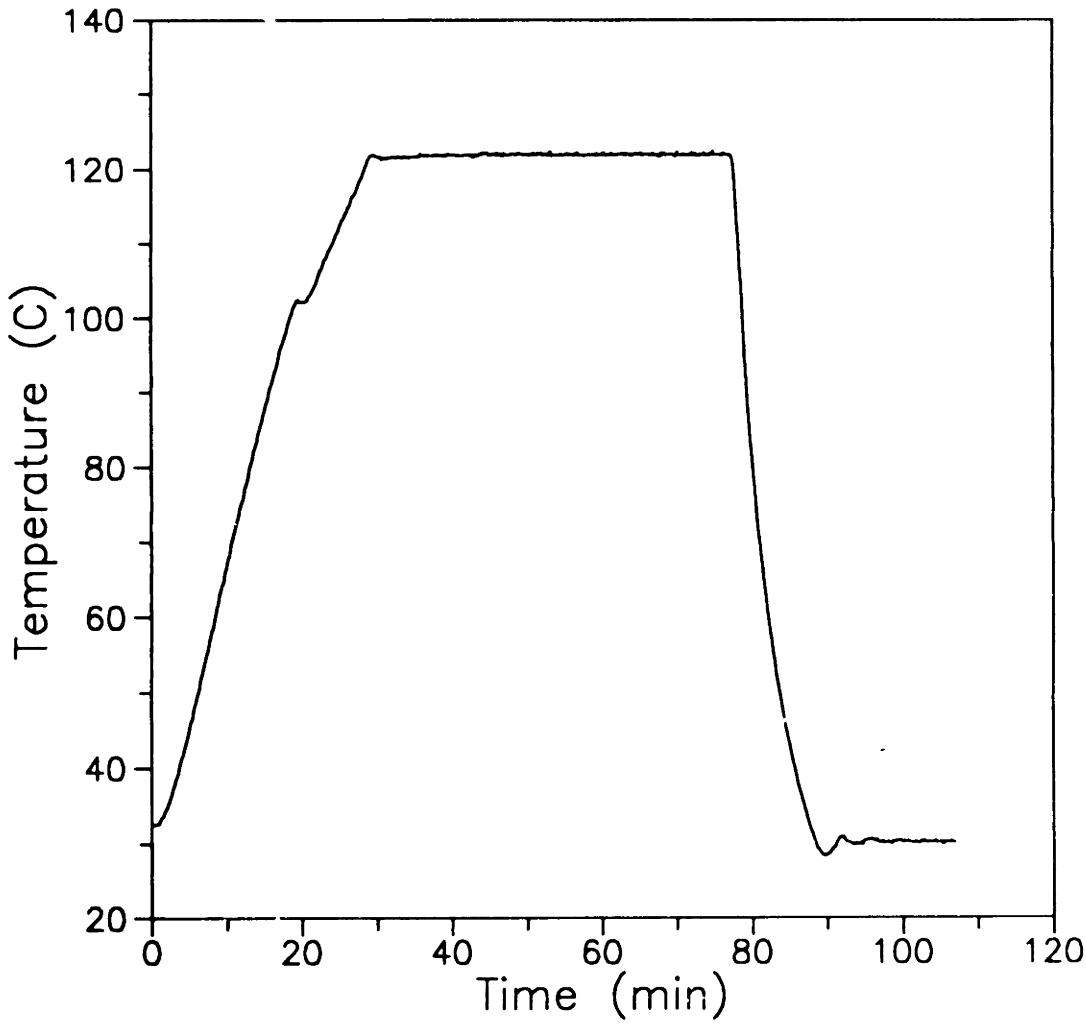

Figure 4.1. Vessel temperature profile during MBR sterilization cycle.

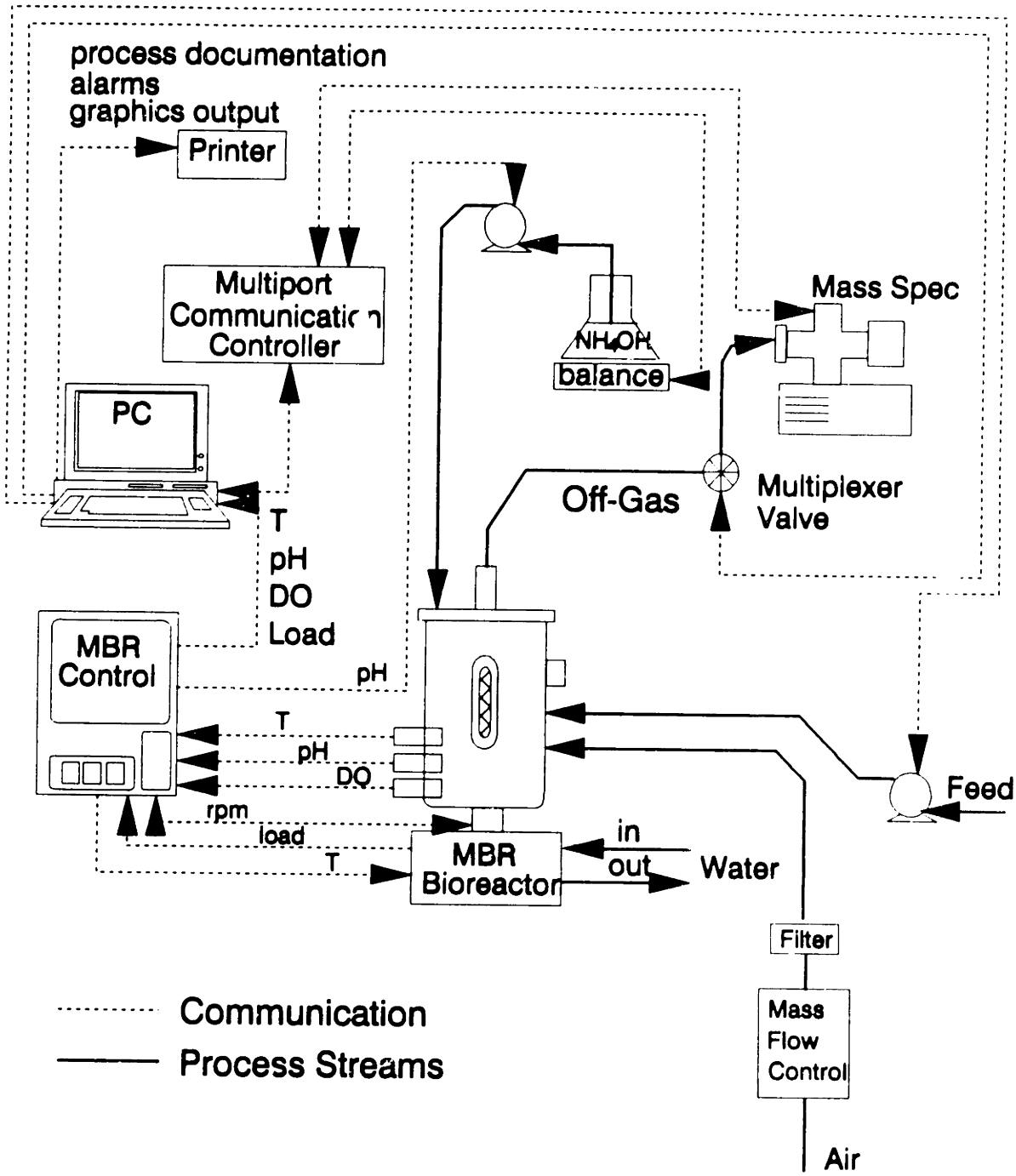

Figure 4.2. Schematic of fermentation equipment and data acquisition and control system.

(465-35-K9, A = 250 mm) and a Chemtrix (Hillsborough, OR) 45AR pH controller. Probe calibration was performed with pH 4, 7, and 10 standards. Dissolved oxygen was monitored via an ABEC (Bethlehem, PA) 9 inch galvanic dissolved oxygen probe (A316-23) and an ABEC digital display amplifier (DDA-100). Probe calibration was performed by aseptically sparging the fermentor and medium (after sterilization) with nitrogen (0% saturation) and air (100% saturation) under the typical head pressure operating condition of about 3 psig. Amplifier output was interfaced to the data acquisition and control computer for automatic data logging, as described in Section 4.2.2.3. Air flow was controlled with a Brooks (Hatfield, PA) 5850E mass flow control valve (0-10 slpm N_2 range) and a Brooks 5878 controller. Inlet air was sterilized with a Pall (Cortland, NY) Ultipor® N_{66}™ 0.2μm filter. Fermentation liquid samples were withdrawn through the built-in sampling line. The first 8 to 10 ml were discarded to flush the line, the next 10-15 ml were collected for analysis. The 3 psig head pressure, required to drive the exhaust gas to the mass spec, was sufficient to force fluid out the sampling line; suction was not required.

4.2.2.2 Batch and Fed-Batch Fermentor

All batch and fed-batch fermentations were carried out in a stainless steel MBR Laboratory Bioreactor (MBR Bio Reactor AG, division of Sulzer Bros., Inc., Wetzikon, Switzerland) at a final working volume of 10 liters (15 liter capacity). The fermentor was equipped with five 19 mm and eight 12 mm head plate ports used for purposes such as tubing, inlet air, outlet air, pressure gauge and overpressure safety valve connections; four standard 25 mm side ports occupied by temperature, pH, and dissolved oxygen probes, and a steam-sterilizable sampling valve; and one standard 25 mm bottom port occupied by a steam-sterilizable drain valve. The fermentor was

interfaced to a MBR MCS 10 control unit which was equipped with amplifiers and controllers for temperature (PID), impeller shaft rpm (PI), pH (PI), dissolved oxygen (PID), and load cell (PID). The vessel was sterilized in place and agitation was by direct drive through a steam-sterilizable double mechanical seal.

The temperature probe was supplied by MBR. The pH probe was an Ingold Type 465 combination electrode (A = 120 mm) mounted in a pressure chamber (Type 764-31) and was calibrated with pH 4 and 7 standards. When the Ingold pH probe lifetime was exhausted, it was replaced with a Broadley-James (Santa Ana, CA) F-600-B130-A06BC pH Fermprobe, a gel-filled probe not requiring pressurization or electrolyte filling/replacing. The dissolved oxygen probe was an Ingold polarographic electrode and was calibrated during vessel sterilization (0% saturation) and by aseptically sparging with air (100% saturation) following sterilization. Air flow was controlled with a Brooks (Hatfield, PA) 5850E mass flow control valve (0-20 slpm N_2 range) and a Brooks 5878 controller. Inlet air was sterilized with a Gelman Sciences (Ann Arbor, MI) 0.2 μm Mini Capsule Filter (No. 12122). Fermentation liquid samples were withdrawn through the sterilized sampling valve (valve was steam sterilized *after* each sample so that the valve was sterile and cool for the next sample). The first 20 ml were discarded to flush the line, the next 15-20 ml were collected for analysis. Steam for sterilizing the sample valve and the mechanical seal was supplied externally by an electric steam generator model PP-4 (Steamaster Co., Inc., Rutherford, NJ). Time-varying feed rates, for the feedback-controlled fed-batch experiments, were achieved by computerized control of a MBR analog variable speed peristaltic pump (0-5 volt input, 0-70 rpm range).

4.2.2.3 On-Line Exhaust Gas Analysis

The equipment setup for on-line monitoring of OUR (oxygen uptake rate) and CER (carbon dioxide evolution rate) is largely based on the description given by Coppella and Dhurjati (1987). The system is designed to allow the simultaneous monitoring of up to four fermentors. Both the continuous culture fermentor and the batch/fed-batch fermentor were interfaced to the exhaust gas analysis system.

Exhaust gas from a given fermentor flows into a 0.6 liter surge tank in which a stainless steel pressure relief valve SS-4CPA2-3 (Nupro, Willoughby, OH) maintains a 3-4 psig back pressure. This pressure provides a 1 to 2 l/min gas flow rate to a E3SC8P multiplexing valve (Valco Instruments Inc., Houston, TX). The valve is computer controlled and directs either a fermentor's exhaust gas, feed gas, or calibration gases to a 1 meter length of 50μm ID fused silica capillary tubing (part #25VS-050, Scientific Glass Engineering Inc., Austin, TX) which serves as the inlet to the Dycor quadrupole mass spectrometer (Ametek, Pittsburgh, PA). The capillary tube provides the necessary pressure drop between the sample side (atmospheric pressure) and the quadrupole (10^{-6} torr). The multiplexing valve and all stainless steel lines downstream of it toward the quadrupole, the capillary tubing, and the quadrupole itself are all maintained at 110-120°C to prevent water from condensing anywhere in the gas analysis system.

The mass spectrometer measures only ion currents at different mass to charge ratios and thus a calibration must be performed to allow calculation of gas composition. Our calibration procedure measured background noise, the contribution of CO_2 to the signal obtained at mass to charge ratio (m/q) 28 (due to CO^+), and the response factors (relative to the inert, N_2) of O_2 and CO_2. Calibration gases were from Matheson Gas Products (Gloucester, MA). Background noise was measured

by flowing pure (99.995%) helium to the mass spec. The CO_2 splitting factor was determined by flowing bone dry (99.8%) CO_2 and measuring the ratio of ion current at m/q 28 to that of m/q 44. The typical splitting factor was 0.060 ± 1%. Response factors were determined with a certified standard gas mixture containing 2% CO_2, 20% O_2, and balance N_2. Typical response factors (relative to N_2) for O_2 and CO_2 were 1.05 ± 0.4% and 0.465 ± 0.5% (the response factor for H_2O was assumed to be 1.0 in lieu of an independent measurement). The calibration factors were found to be quite reproducible from calibration to calibration, which could be weeks to months apart in time. Thus, there was no need to recalibrate the mass spectrometer during the course of a given fermentation, which might run for several days.

With these calibration parameters, the composition of a gas stream (O_2, CO_2, N_2, and H_2O mole fractions) can be determined from the following:

$$y_i = \frac{I_i \cdot RF_i}{\sum_{i=1}^{n} I_i \cdot RF_i} \qquad 4.1$$

where y_i is the mole fraction of species i, I_i is the ion current at the m/q ratio corresponding to species i, and RF_i is the response factor of species i. For this work, only ion currents corresponding to O_2, CO_2, N_2, and H_2O were monitored. Vallino (1991) discussed the fact that respiratory calculations based on measurement of only those species overestimates OUR and CER by the factor $1/(1-y_u)$, where y_u is the sum of the mole fractions of all unaccounted for species in the feed gas. For this system, y_u appears to be negligible, even if only the four species are measured.

OUR and CER (mmol/l·hr) are calculated from the inlet and exhaust gas compositions by the following equations:

$$OUR = \frac{(F_{AIR})_i}{V}\left[(y_{O_2})_i - \frac{(y_{N_2})_i}{(y_{N_2})_o}(y_{O_2})_o\right] \qquad 4.2$$

$$CER = \frac{(F_{AIR})_i}{V}\left[\frac{(y_{N_2})_i}{(y_{N_2})_o}(y_{CO_2})_o - (y_{CO_2})_i\right] \qquad 4.3$$

where $(F_{AIR})_i$ is the air inlet rate (mmol/hr), V is the fermentor liquid volume, and the y's are the gas phase mole fractions of O_2, CO_2, and N_2 in the inlet (i) and outlet (o) streams. All calculations, starting from the ion currents, were performed by the data acquisition and control computer, as discussed in the next section.

4.2.2.4 On-Line Data Acquisition and Control System

On-line data acquisition and control was accomplished through the use of a Wyse (San Jose, CA) 1400-02 pc+ computer running a modified version of a data acquisition and control program [Coppella and Dhurjati, 1987] written in Microsoft® QuickBASIC™ version 3.0. Their program was originally written to allow simultaneous utilization of a Dycor mass spectrometer by up to four fermentors, acquire analog data from a variety of devices, and display real-time graphics. We retained the main control loop structure of their original program, but made a number of significant revisions to their code. Much of the code was broken down into independent structured subroutines to facilitate debugging, all of the analog to digital (A/D), digital to analog (D/A) and digital acquisition and control functions

were rewritten to support our particular hardware, serial communications (including the mass spec data acquisition) were rewritten to increase speed (and thus, sampling frequency) and to conform to our particular hardware, the real-time graphics routines were significantly altered to meet our needs, and data filtering and feed control algorithms specific to this work were added. Our version will subsequently be referred to as FERMCON.

A Data Translation (Marlborough, MA) DT2801 analog and digital input/output (I/O) board, installed in one of the computer's expansion slots, performed the A/D inputs, the D/A outputs, and the digital I/O. The A/D inputs were operated in differential mode with a 0 - 1.25 volt range. The D/A outputs were operated with a 0 - 5 volt range.

FERMCON used the A/D inputs to acquire temperature, stirring rate (rpm), pH, dissolved oxygen, and load cell data from the MBR fermentor and dissolved oxygen data from the Microferm® fermentor. The D/A output was used to drive the variable speed pump used for on-line feed rate control. The digital I/O was used to drive the multiplexing valve which directed the appropriate gas stream to the mass spec (8 bits of output, 5 bits of input).

Control of and data acquisition from the mass spec was done by a serial communication protocol (9600 baud, 7 data bits, 2 stop bits, no parity). A digital balance model G4000-SO (Ohaus, Florham Park, NJ) was also interfaced by a serial communication protocol (300 baud, 7 data bits, 2 stop bits, no parity) to the computer to allow measurement of the base (ammonia) addition rate. An HP LaserJet series II was also interfaced by a serial protocol (9600, 8 data bits, 1 stop bit, no parity) to allow graphics screen dumps in real-time. A dot-matrix printer used

for documenting the course of a fermentation such as startup and calibration information and variable out-of-range alarm conditions occupied the computer's parallel communication port. Note that FERMCON was thus communicating with three serial devices, contrary to the two serial device limitation of the MS-DOS® operating system (ver. 3.21) the computer runs under. This limitation was circumvented by the use of a BayTech (Bay St. Louis, MS) Multiport Controller model 525H. FERMCON communicated with the Multiport Controller through one of the computer's two serial ports (9600 baud, 7 data bits, 2 stop bits, no parity). The Multiport Controller then communicated with the mass spec and balance, using the appropriate protocol, and passed the information back to FERMCON. The Multiport Controller can handle up to four serial devices (currently only interfaced to two). Additional devices, such as additional balances, may be easily interfaced for additional data acquisition and control capabilities. Further details describing FERMCON can be found in Appendix A.

4.2.2.5 On-Line Data Manipulation

The feed control algorithms employed in the restrained growth fed-batch fermentations required on-line measurements of the culture respiration, namely OUR, CER, and RQ (respiratory quotient, OUR/CER). Due to a combination of the high noise level of the Dycor mass spec and natural fermentation process noise, such as slight pH variations about the set point (due to imperfect mixing and probe lag) which can dramatically affect dissolved gas dynamics, the respiratory data were fairly noisy. In addition, noise in OUR and CER is naturally amplified in calculating RQ (CER/OUR). It was therefore desired to perform some sort of data smoothing, or filtering, prior to the control calculations.

On-line measurements of OUR and CER were smoothed using a second order Butterworth digital filter [Bozic, 1979], which is a type of recursive digital filter. This second order filter is characterized by the difference equation:

$$a(1)y(n) = b(1)x(n) + b(2)x(n-1) + b(3)x(n-2) - a(2)y(n-1) - a(3)y(n-2) \quad \textbf{4.4}$$

where **x(k)** is the sequence of raw data, **y(k)** is the sequence of filtered data, and a(i) and b(i) are the filter coefficients. Thus, the filter estimate, y(n), for the current measurement, x(n), is a linear combination of the current measurement, the previous two measurements (x(n-1) and x(n-2)), and the previous two filter estimates (y(n-1) and y(n-2)).

The filter coefficients are determined by specification of a cutoff frequency (the filter should remove the noise above the cutoff frequency). The desired cutoff frequency was obtained by Fast Fourier Transform analysis of respiratory data, obtained from the constant feed rate fed-batch fermentations, using the MATLAB™ software program (Mathworks Inc., South Natick, MA). This analysis provided a dimensionless cutoff frequency (cutoff frequency divided by one-half the sample frequency) of 0.05. This value was obtained by visual inspection of the power spectral densities shown in Figure 4.3, which correspond to 512 OUR data points (Figure 4.3A) and 512 CER data points (Figure 4.3B) obtained at a sampling rate of 0.2 min^{-1} during the 50 ml/hr constant feed rate fed-batch experiment (described further in Section 5.5.3.2). The filter coefficients corresponding to a second order low-pass Butterworth filter with a dimensionless cutoff frequency of 0.05 are shown

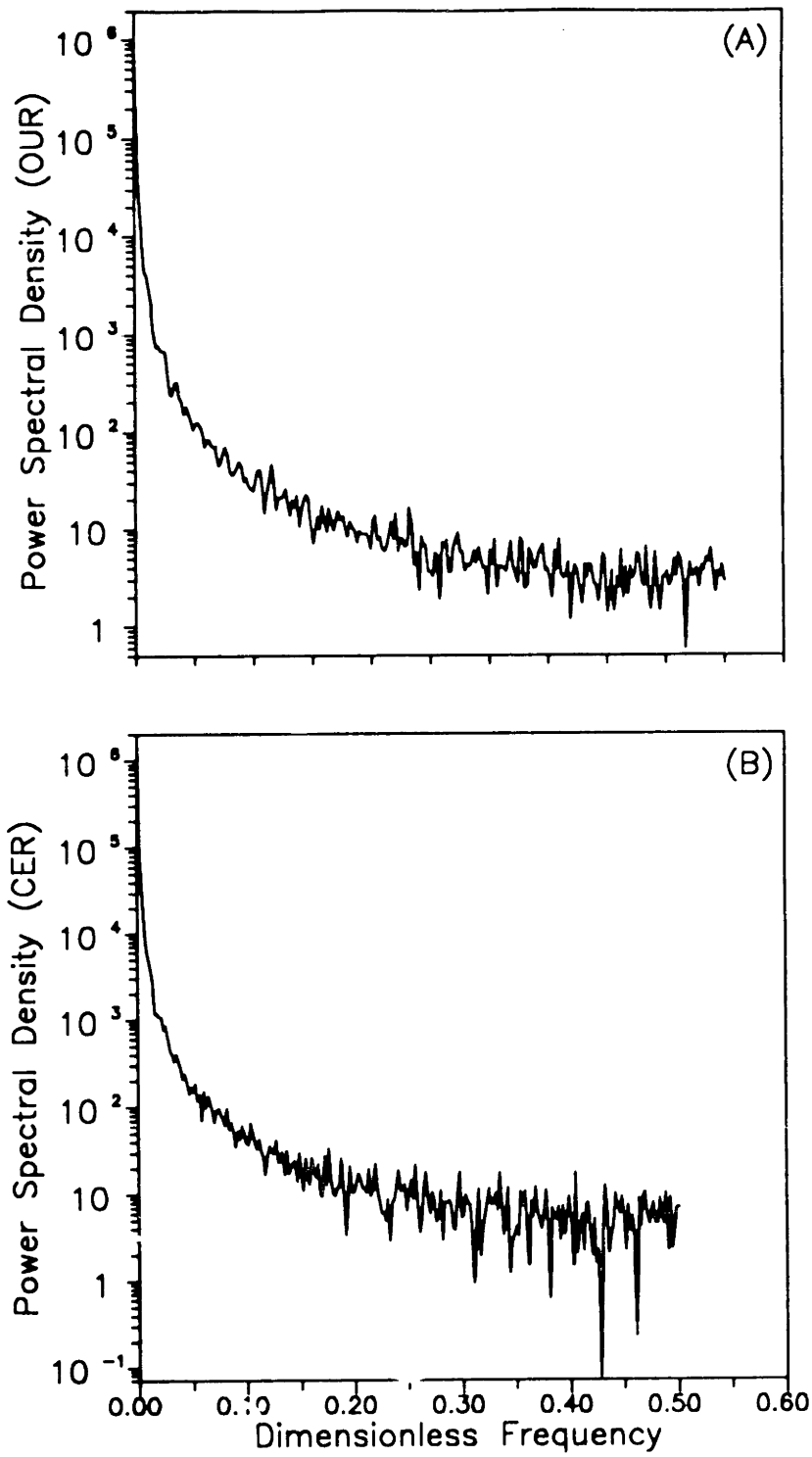

Figure 4.3. Fast fourier transformed power spectral densities for data obtained from fed-batch fermentation. (A) Spectrum for OUR data. (B) Spectrum for CER data.

below:

$$\mathbf{b} = [b(1)\ b(2)\ b(3)] = [0.0055\ 0.0111\ 0.0055] \quad (4.5)$$

$$\mathbf{a} = [a(1)\ a(2)\ a(3)] = [1.000\ -1.7786\ 0.8008] \quad (4.6)$$

Figure 4.4 shows the raw OUR and CER data the filter design was based upon along with the filtered OUR and CER calculated with the above filter coefficients. Figure 4.5 shows the raw and filtered RQ from the same data set. Since the fermentor volume changes during the course of a fed-batch fermentation, the raw OUR and CER are calculated by dividing the total respiratory rates (assuming V = 1 in Equations 4.2 and 4.3) by the load cell reading. Thus, the mass spec noise and process pH variation effects, as well as process noise in the load cell output are filtered out. The respiratory quotient, RQ, was calculated by dividing the filtered CER by the filtered OUR. The noise rejection of the filter is quite good, but the trade-off is the creation of a slight time lag, as evident in the figures.

Derivatives, or trends, in OUR, CER, and RQ were determined by applying a least squares regression analysis to a moving data window containing the most recent 30 minutes of filtered data (15 filtered measurements, including the current filtered measurement, at a sampling rate of 0.5 min^{-1}). The feed control algorithm used in the feedback controlled fed-batch experiments required only the signs (positive or negative) of the respiratory trends. To assess the reliability of the calculated trends, 95 percent confidence intervals were calculated using a t-distribution with n-(k+1) degrees of freedom, where n is the number of data points

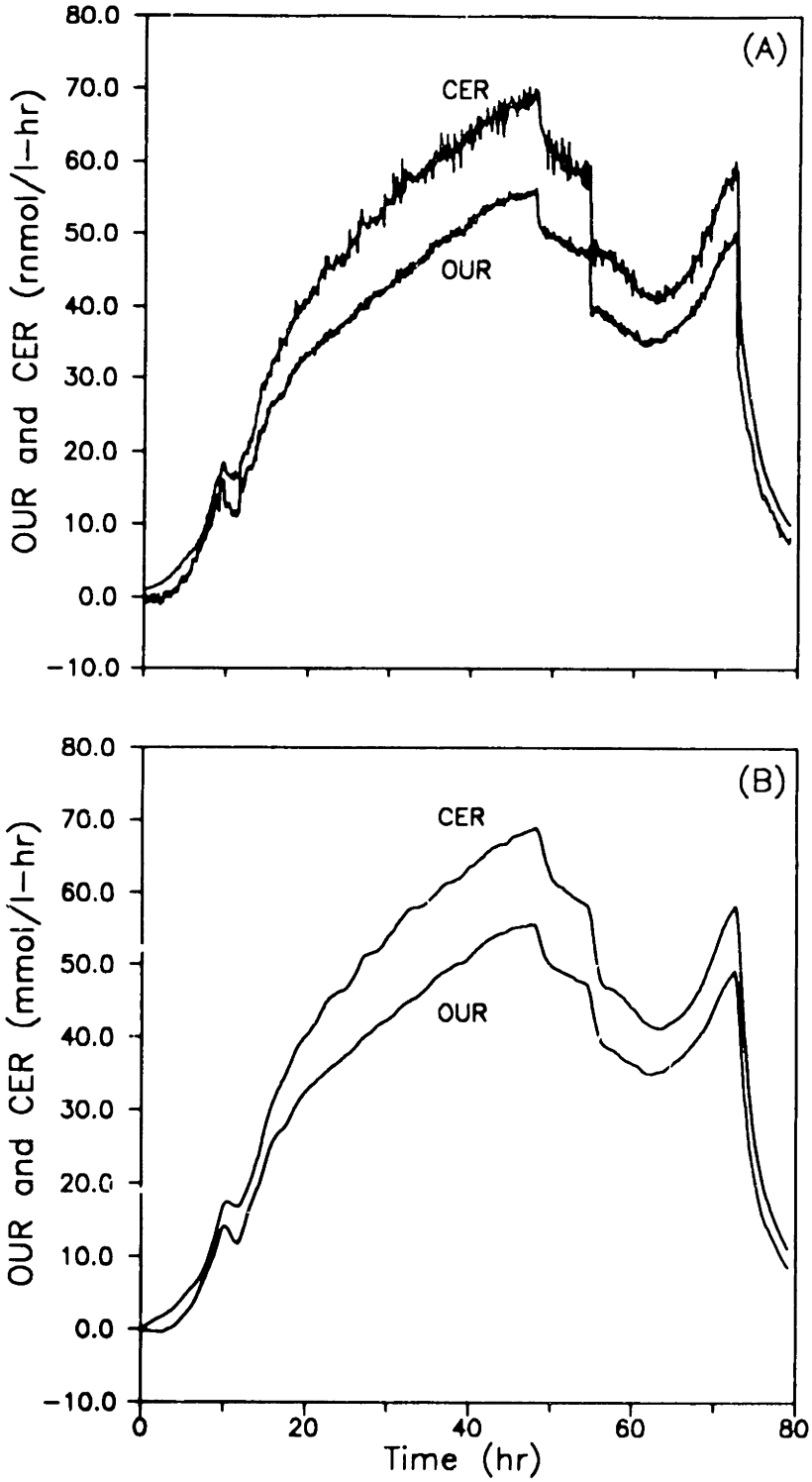

Figure 4.4. Comparison of raw and filtered respiratory rates from fed-batch fermentation, using second-order Butterworth digital filter. (A) Raw OUR and CER data. (B) Filtered OUR and CER data.

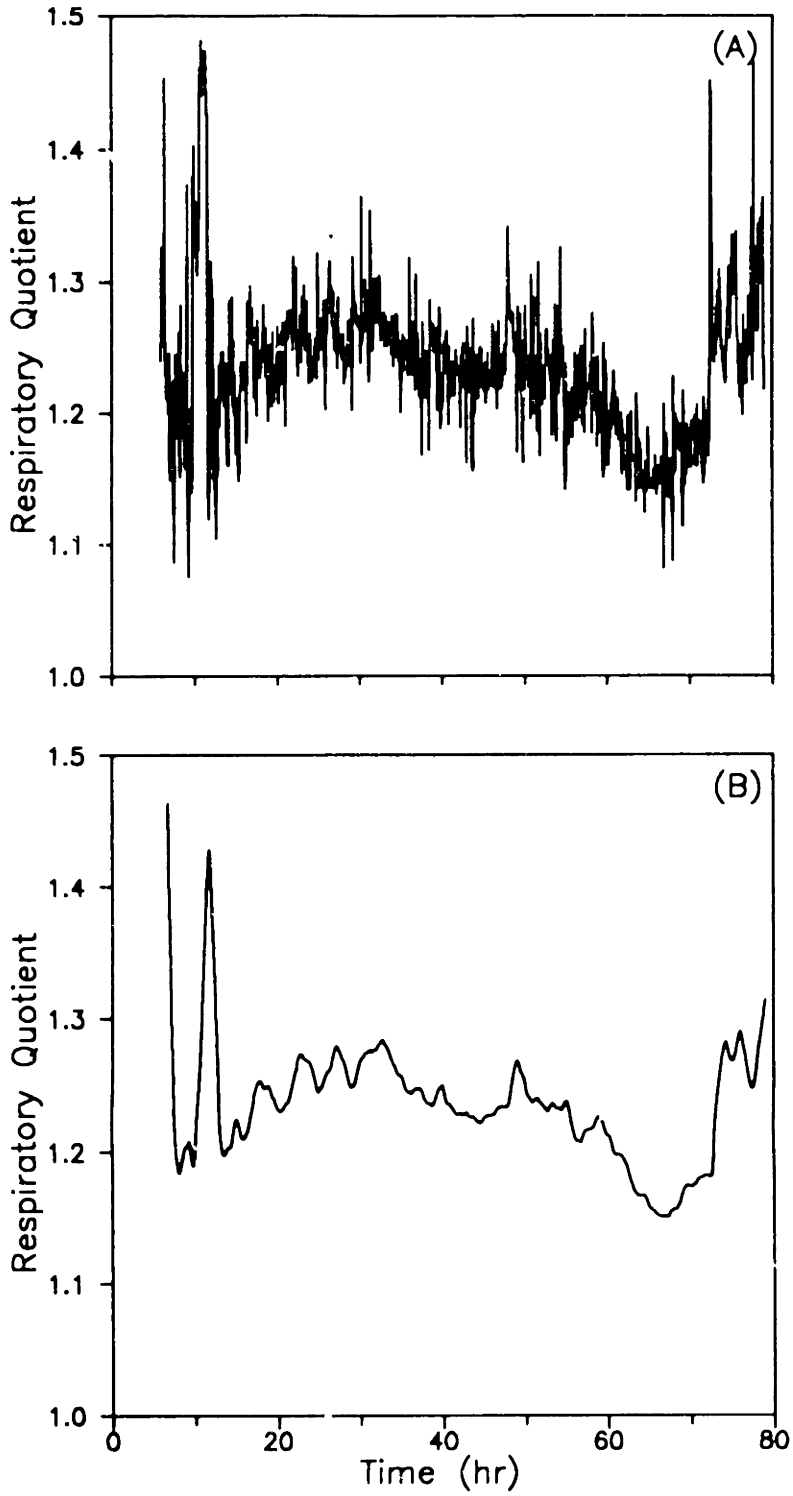

Figure 4.5. Comparison of raw and filtered respiratory quotient from fed-batch fermentation, using second-order Butterworth digital filter. (A) Raw respiratory quotient data. (B) Filtered respiratory quotient data.

regressed and k is the number of independent variables in the regression model. For 15 data points and a linear model at the 95 percent confidence level, $t_{0.025,13} = 2.160$. If a calculated trend changed sign when taking into account the confidence interval, the trend was categorized as inconclusive and the control algorithm would forgo changes in feed rate for that sampling period (2 minutes). Trends categorized as conclusive were passed on to the control algorithm for appropriate evaluation of metabolic activity and subsequent control action.

4.2.3 Cultivation Conditions

The inoculation procedure for all types of fermentations began by transferring a loopful of the organism from a LB5G plate (24 hrs. of growth) to a 250 ml shake flask containing 50 ml of LB5G broth. The shake flask was incubated for 8 - 10 hours at 30°C and 220 RPM. Further details of the procedures differ depending on the type of culture being carried out and will thus be described separately below.

4.2.3.1 Continuous Cultures

The LB5G shake flask contents were transferred to a 2 liter double-baffled shake flask containing 275 ml of the CGM2 medium and incubated under the same conditions for another 8 - 10 hours. Broth from the large shake flask was then transferred into the chemostat (resulting in a working volume of 3 liters). Temperature was maintained at 30°C and pH was maintained at 7.00±0.02 by addition of concentrated (~6 N) NH_4OH. Air was provided at a rate of 1 volume of air per volume of liquid per minute (1 VVM) and agitation rate was 600 rpm. The culture was allowed to grow in a batch mode until the cell density approached the

level which could be supported by the L-threonine limitation. Feeding was then initiated at the desired rate using a peristaltic pump (Cole Parmer, Chicago, IL). Working volume was maintained at 3 liters by rapidly pumping reactor contents through a draw-off tube positioned at the appropriate height.

4.2.3.2 Batch and Fed-Batch Cultures

The LB5G shake flask contents were transferred to a 2 liter double-baffled shake flask containing 450 ml of the defined medium and incubated under the same conditions for another 8 - 10 hours. Broth from the large shake flask was then transferred into the main fermentor. Temperature was maintained at 30°C and pH was maintained at 7.00±0.03 by addition of concentrated [~30% (w/w) NH_3] NH_4OH. Air was provided at a rate of 1 VVM. Agitation rate (rpm) was manually adjusted to maintain the dissolved oxygen concentration above 10 percent of saturation at approximately 3 psig head pressure. For the fed-batch cultures, feeding was initiated at the point of L-threonine depletion, as described further in Section 5.5.3.

4.3 Analytical Techniques

Samples were taken periodically to determine the status of a fermentation and, in the case of the continuous cultures, to follow the approach to steady state. Samples were generally analyzed for biotic measures such as optical density, cell dry weight, and viable cell count, and abiotic measures such as glucose, L-lysine, L-threonine, L-leucine, ammonium, and other side-product concentrations. In the case of the batch fermentation characterization, the biotic phase was also analyzed for intracellular protein, total DNA, and total RNA levels.

4.3.1 Biotic Phase Measurements

4.3.1.1 Dry Cell Weight

To obtain a quantity of cell mass for dry weight estimation, 10 ml fermentation broth samples were centrifuged at 10,000 rpm (12,100 x g) for 10 minutes at 4°C. The supernatant was removed and the process was repeated two more times, using cold distilled water to wash the cell mass at each stage. Dry cell weight was estimated by drying the final washed cell mass for 12 hours to constant weight at 85°C in a pre-weighed aluminum dish. Figure 4.6 shows the kinetics of drying for a typical sample, indicating that 12 hours is a sufficient drying time.

Dry cell weight could also be estimated by the use of a correlation between optical density and dry cell weight. Optical density (OD) was measured at 660 nm (4 ml volume quartz cuvette with 1 cm light path) in a Kontron (Everett, MA) Uvikon® 810 spectrophotometer (blank against distilled water). Fermentation samples were diluted sufficiently with distilled water to insure an optical density of less than 0.5 (the linear range of the spectrophotometer goes up to about 0.5). Figure 4.7 illustrates the relationship between dry cell weight and optical density with data from the batch fermentation described in Section 5.2. It should be noted that the deviation from linearity occurred when the culture reaches the late phases of batch growth. This deviation also occurred in fed-batch experiments after the feeding phase had ended and the culture entered the late phases of the post-feeding batch phase. This effect is presumably due to changes in the light absorbing properties of cell material during different phases of growth and non-growth.

A few small scale shake flask experiments used colorimetry to follow changes

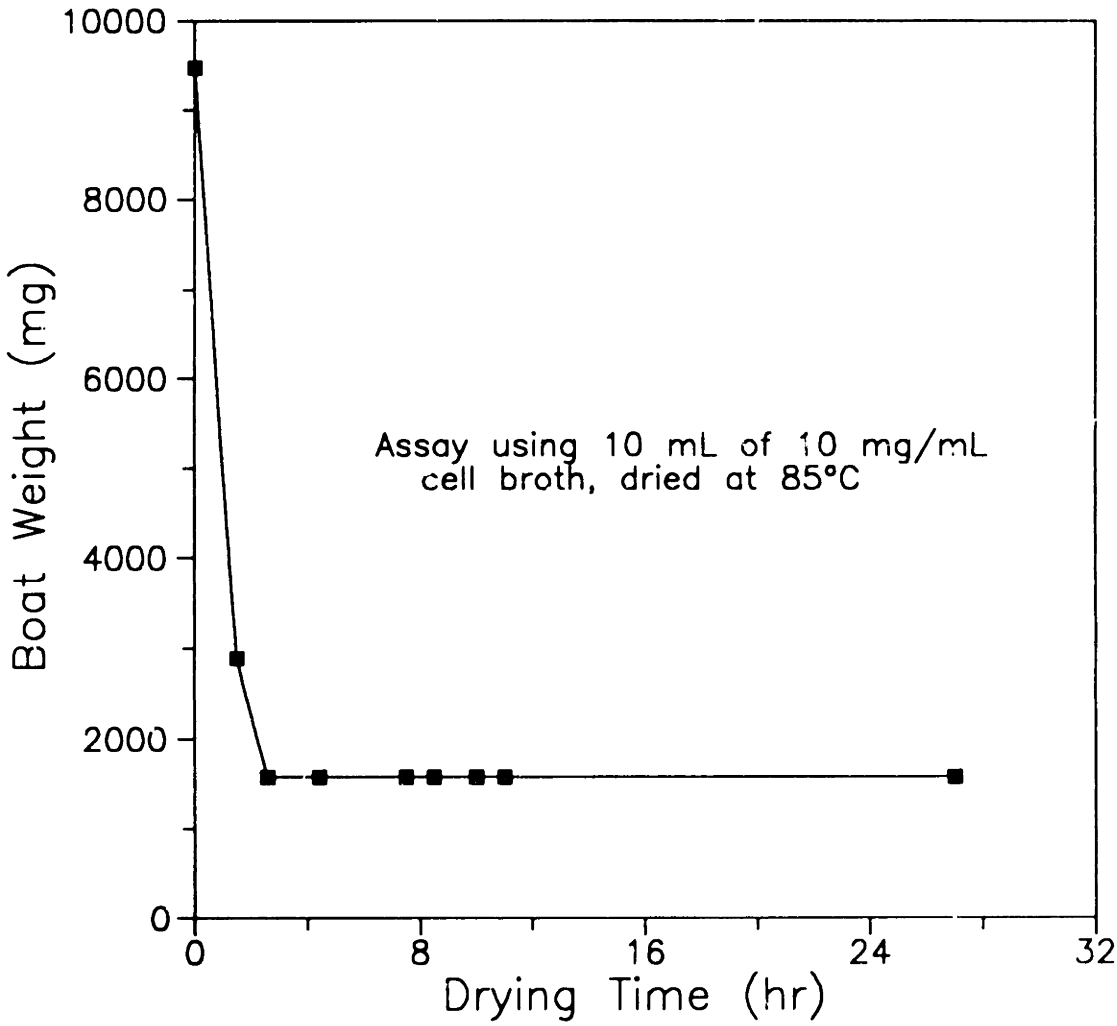

Figure 4.6. Drying kinetics for dry cell weight assay.

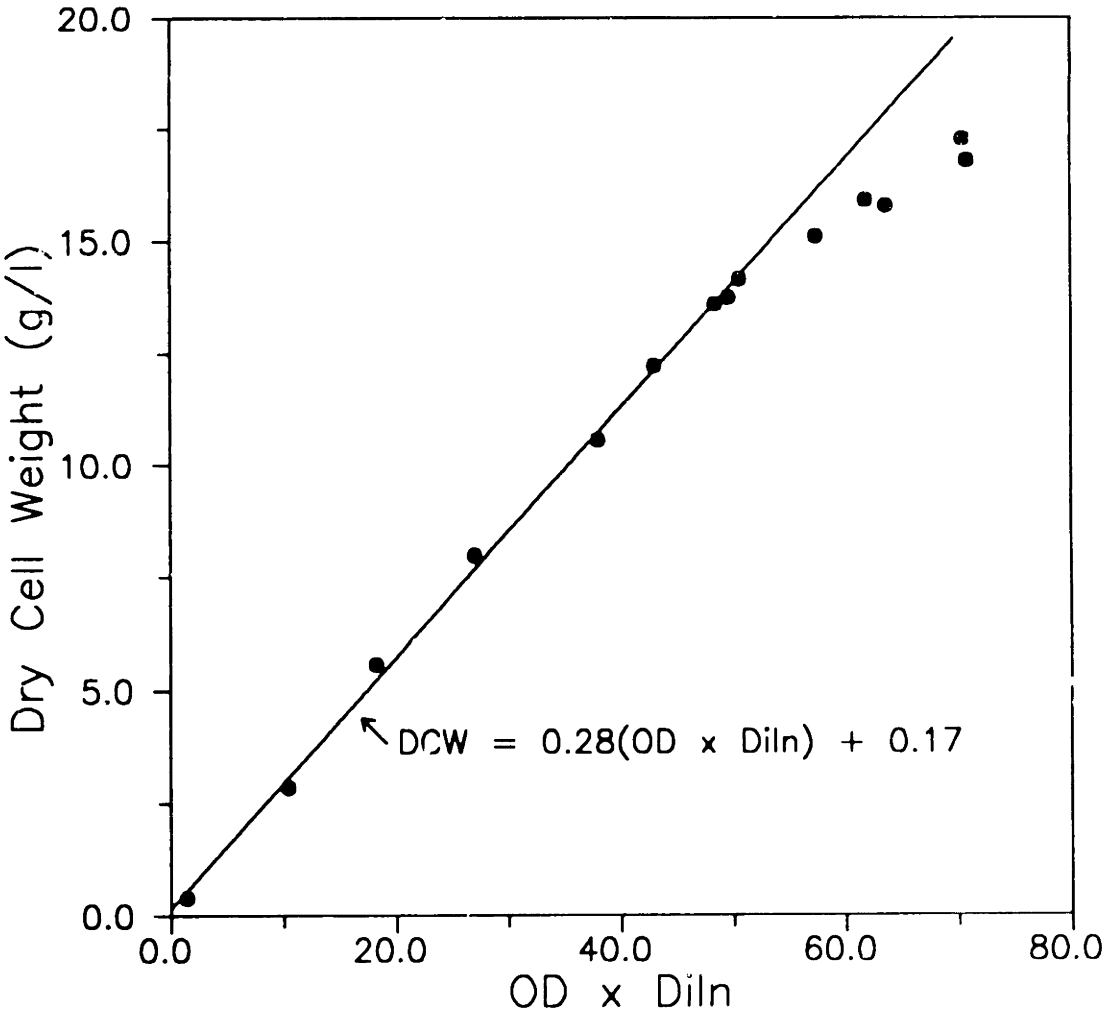

Figure 4.7. Experimental correlation between dry cell weight and optical density.

in turbidity. For those cultures, side-arm flasks were used and turbidity was measured with a Klett-Summerson (Philadelphia, PA) Model 8003 colorimeter.

4.3.1.2 Viable Cell Counts

Viable cell density, when measured, was determined by serially diluted plate counts, using sterile 1/4 strength Ringer's Solution (2.5 g NaCl, 0.105 g KCl, 0.12 g $CaCl_2 \cdot 6H_2O$, 0.05 g $NaHCO_3$ per liter of distilled water) as the diluent [Harrigan and McCance, 1966]. Platings were generally done in duplicate or triplicate, and plate dilutions with between 30 and 300 colonies were taken as the most accurate estimates of viable cell number density. Total viable cell number density was determined by serially diluted plate counts on LB5G medium.

Population distributions were determined by comparing the LB5G plate counts with plate counts on CGM1 medium lacking both L-threonine and L-methionine (for selection of homoserine revertants), lacking L-leucine (for selection of leucine revertants) and lacking all three amino acids (for selection of double revertants). When a revertant cell population was estimated to be a few percent of the total population, the distribution was also estimated by transferring colonies from the LB5G plates to the appropriate plates for revertant selection, using FMC BioProducts (Rockland, ME) RepliPlate® Colony Transfer Pads. The two independent estimates (plate count differences and replicate plate counts) agreed with one another within 5 to 10%.

4.3.1.3 Intracellular Total Soluble Protein

Cell samples from the batch characterization fermentation (Section 5.2.4) were analyzed for macromolecular (protein, DNA, RNA) content. Twenty-five ml samples were taken from the fermentor and subjected to the same centrifugation/washing

procedure as for dry cell weight analysis. The final cell pellets were frozen at -20°C until later analysis.

The assay for total intracellular protein is based on the biuret reaction as described by Herbert *et al.* (1971). This assay relies on the fact that the -CO-NH- linkages of proteins form intense reddish-violet chelation compounds when exposed to cupric ions in alkaline solution. The assay is reasonably specific as nucleic acids and most other cellular macromolecules do not interfere. In addition, most all proteins give very similar biuret absorbance values.

The assay contains a step in which a treatment in 1 N NaOH extracts protein from the given organism. In the original work, Herbert *et al.* reported that treatment in cold 1 N NaOH effected complete protein extraction from gram negative bacteria, but that a 5 minute treatment in boiling (100°C) 1 N NaOH was necessary to effect complete protein extraction from gram positive bacteria, yeasts, and molds. In this work, it was found that the time in boiling 1 N NaOH required for complete protein extraction varied between 10 and 60 minutes depending on the state of the culture at the time of cell harvest (exponentially growing cells seemed more sensitive to the treatment). Therefore, for each cell sample to be analyzed, multiple assays were run for different extraction times between 10 and 60 minutes and the maximum protein concentration obtained was taken as the true value. The assay protocol is given below:

Total Cellular Protein Assay

(1) Add to a 18 x 150 mm glass tube (with cover):

a) 2 ml cell suspension (between 2 and 10 mg/ml DCW) or standard
b) 1 ml 3 N NaOH

(2) Heat at 100°C for 10-60 minutes, cool in cold H_2O.

(3) Add 1 ml 2.5% (w/v) $CuSO_4 \cdot 5H_2O$, mix, let stand for 5 minutes.

(4) Transfer 1.4 ml into a 1.5 ml eppendorf centrifuge tube. Centrifuge 10 min. (13,300 rpm, 15,600 x g) in microcentrifuge (IEC Centra®-M Model 2399).

(5) Transfer 1 ml to microcuvette. Measure absorbance at 540 nm.

A standard curve of absorbance versus protein concentration (0, 1.0, 2.5, and 5.0 mg/ml) was prepared for sample concentration determination. Bovine serum albumin (Serva, Westbury, NY) was used for standards. A typical calibration curve appears in Figure 4.8. The sensitivity of this assay (using the above reaction volumes) is approximately 0.5 mg/ml protein (in the sample). Linearity in the standard curve extends to at least 5.0 mg/ml protein.

It should be pointed out that this whole cell biuret assay extracts cell wall and membrane associated protein in contrast to an assay which measures protein concentration in the supernatant resulting from a cellular disruption such as sonication or bead milling. As will be discussed (Section 5.2.4), it was desired to estimate total cellular protein, including that associated with the cell wall or membrane, so the whole cell biuret assay was appealing.

One further technical detail should be mentioned concerning spectrophotometric assays which measure only an end-point absorbance value, such as this assay and the DNA and RNA assays. The most convenient way to run such assays, given the large number of samples and standards, is to use individual, disposable cuvettes for each sample or standard. Although all of the cuvettes should have come from the same production line, there can be differences in absorbance

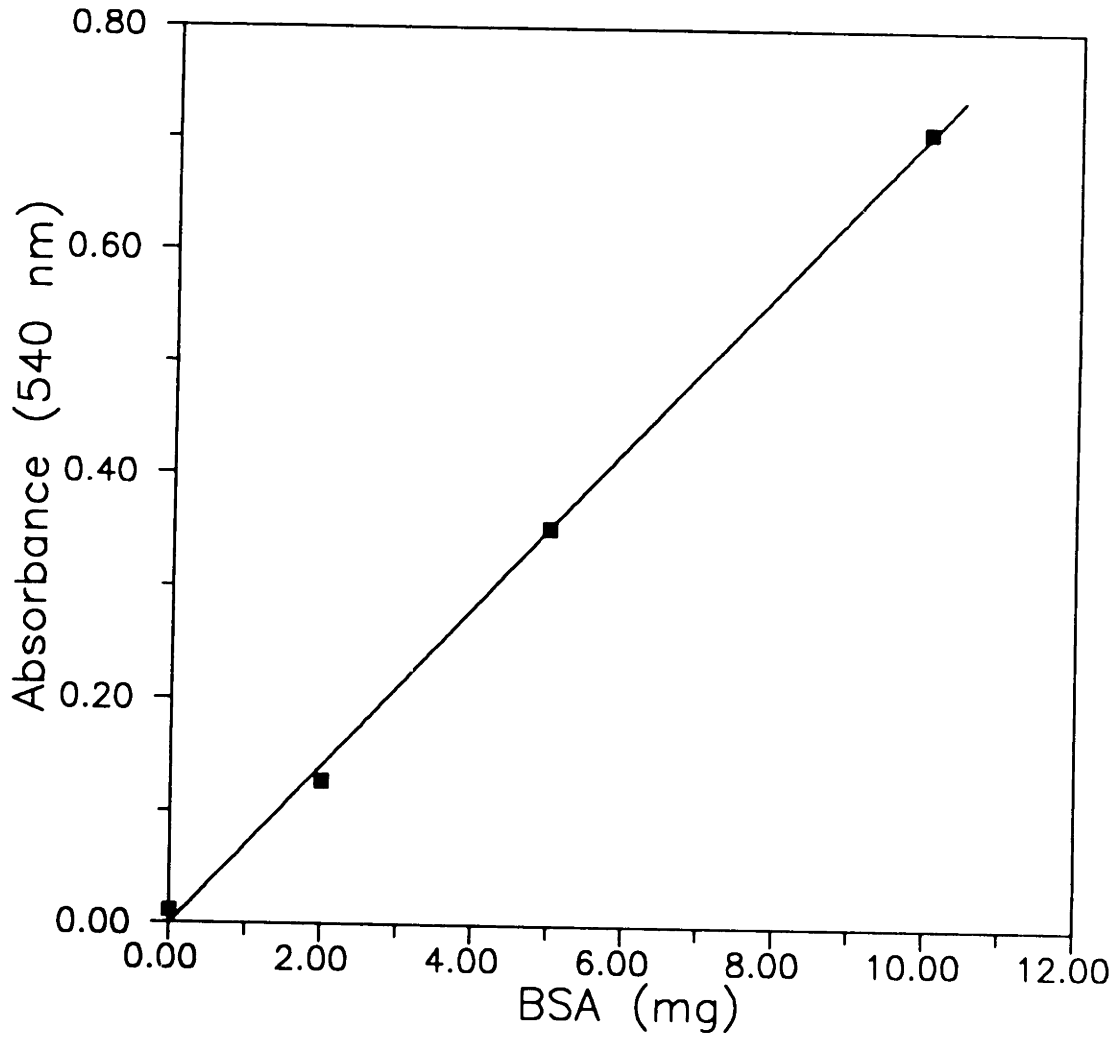

Figure 4.8. Standard curve for total protein assay.

between two cuvettes of as much as 0.040 absorbance units. If both initial (before the reaction occurs) *and* end-point absorbances could be measured, as in the L-lysine assay, using an absorbance *change* (A_0-A_F) would cancel out any differences between cuvettes. However, when using an end-point absorbance measurement only, the differences between cuvettes will not cancel and cannot be neglected. To deal with this issue, the absorbances of all cuvettes used for the assay were measured (with the cuvette empty) before addition of the reaction mixture. The spectrophotometer was then zeroed to an arbitrary cuvette. All subsequent cuvette readings could then be corrected to remove the offset.

4.3.1.4 Intracellular Total DNA

Cell samples for the DNA assay were those obtained as described above for intracellular total protein. The assay involves an extraction of nucleic acids (DNA and RNA) as described by Herbert *et al.* (1971), and the diphenylamine colorimetric reaction with DNA as described by Burton (1956) and Giles and Myers (1965).

The extraction procedure requires extracting 3 times with 0.5 N $HClO_4$ (perchloric acid) at 70°C. In an experiment designed to estimate the extraction times necessary to recover most of the cellular DNA, the DNA from each of three extracts (30, 30, and 15 minutes, in that order) and the DNA in the residue left after three extracts was estimated using the diphenylamine assay. Assuming the sum of the DNA in the four portions (three extracts and the residue) to be 100% of the cellular DNA, it was determined that about 95% of the total DNA is recovered in the three extracts, as shown in Figure 4.9A. Each of the three extracts was done in 3 ml total volume. The 1st extract used 1 ml of cell solution (cell concentration between 3 and 30 mg/ml) plus 2 ml 0.75 N $HClO_4$. For the next two extracts, 3 ml 0.5 N $HClO_4$ were

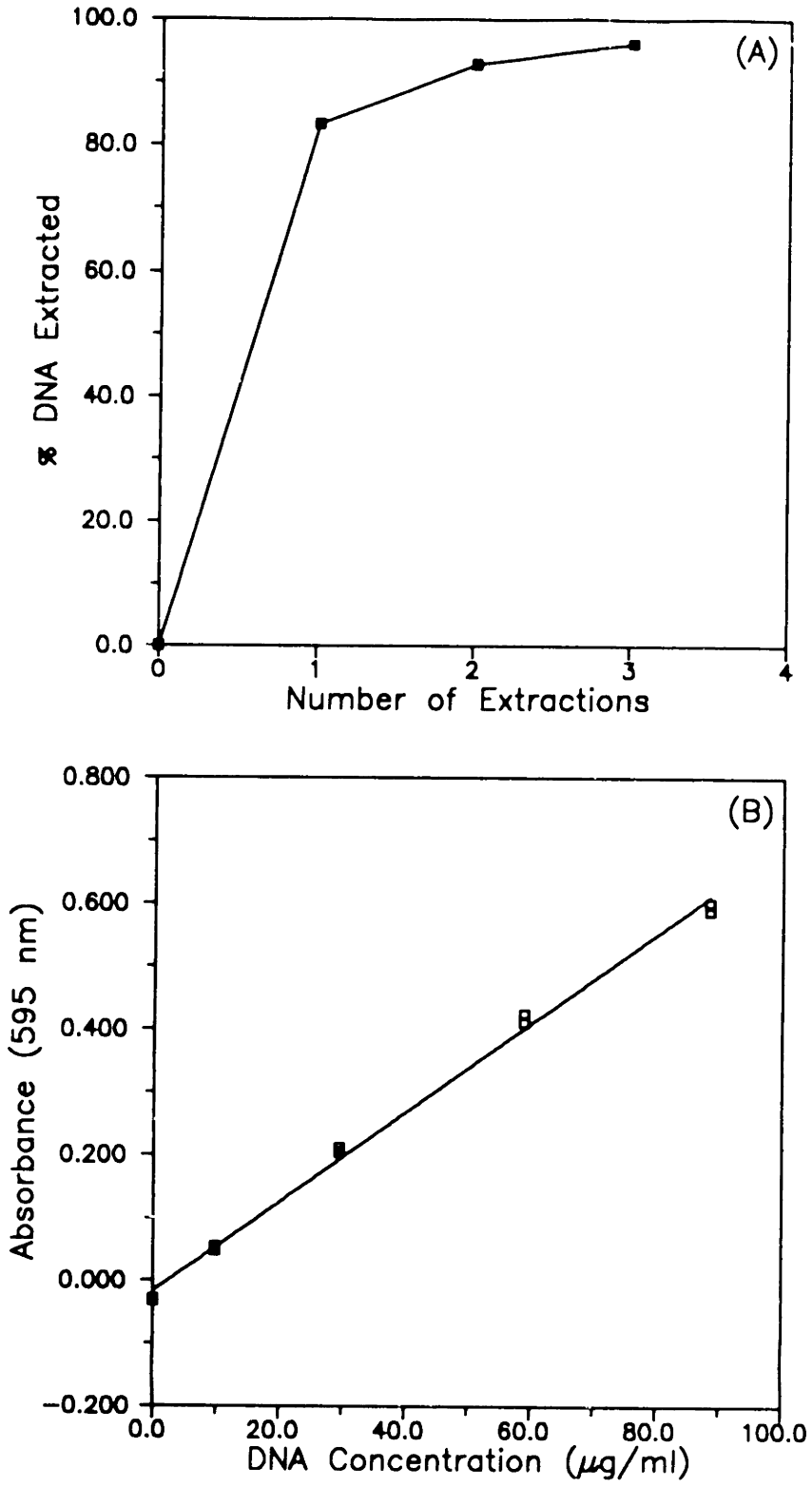

Figure 4.9. Total cellular DNA assay development. (A) Extraction protocol efficiency. (B) DNA assay standard curve.

added to the residue remaining after centrifugation for 10 minutes at 10,000 rpm (12,100 x g). The three supernatant extracts were pooled and brought to 10 ml total volume with 0.5 N $HClO_4$.

Two ml of this extract volume was then used for the diphenylamine DNA binding assay as described below:

Total Intracellular DNA Assay

(1) Add to an appropriate sized tube (with cap):

a) 2.0 ml cell extract or standard (standards must be prepared in 0.5 N $HClO_4$)
b) 2.0 ml diphenylamine solution (4 g/100 ml glacial acetic acid)
c) 100 µl 1.6 mg/ml acetaldehyde

(2) Mix contents well, incubate at 30°C overnight

(3) Transfer 1.4 ml into a 1.5 ml eppendorf centrifuge tube. Centrifuge 10 min. in microcentrifuge (13,300 rpm, 15,600 x g).

(4) Transfer 1 ml to microcuvette. Measure absorbance at 595 nm.

A standard curve of absorbance versus DNA concentration (0, 10, 30, 60, and 90 µg/ml) was prepared for sample concentration determination. Type 1 highly polymerized calf-thymus DNA (Sigma #D-1501) was used for standards. A typical calibration curve appears in Figure 4.9B. The sensitivity of this assay (using the above reaction volumes) is approximately 3.5 µg/ml DNA (in the extract). Linearity in the standard curve extends to at least 90 µg/ml DNA.

4.3.1.5 Intracellular Total RNA

Cell sample preparation is as above for the total DNA assay. Herbert *et al.* (1971) found that the $HClO_4$ procedure used for DNA extraction also extracts greater than 95% of total cellular RNA in the first extract, so an extraction efficiency

experiment was not done. The assay used to determine total RNA levels (no distinction is possible between the different types of RNA) uses the orcinol reagent. Orcinol reacts with the ribose (pentose sugar) of RNA (in the presence of a ferric catalyst and HCl) to produce a green color which can be quantitated by its absorbance at 672 nm. DNA reacts only slightly with the reagent.

The preparation of two stock solutions is convenient for this assay. The first solution consists of 0.90 g $FeCl_3 \cdot 6H_2O$ per liter of concentrated HCl (12 N). The second solution is 10 g/l orcinol. Four parts solution 1 are then mixed with 1 part solution 2 to form the "orcinol reagent". The RNA assay protocol [Herbert *et al.*, 1971] is shown below:

Total Intracellular RNA Assay

(1) Add to a 18 x 150 mm test tube (with cap):

   a) 1.0 ml cell extract or standard
   b) 3.0 ml orcinol reagent

(2) Mix contents well, heat in boiling H_2O (100°C) for 20 minutes.

(3) Cool in cold H_2O; add 11 ml n-butanol.

(4) Transfer to cuvette. Measure absorbance at 672 nm.

A standard curve of absorbance versus ribose concentration (0, 30, 60, and 90 µg/ml) was prepared for sample concentration determination. It should be noted that, since RNA standards are not used, the determination of cellular RNA is solely on a relative scale. But a relative scale of RNA concentration during a fermentation was sufficient for our purposes. A typical calibration curve appears in Figure 4.10. The sensitivity of this assay (using the above reaction volumes) is approximately 5 µg/ml ribose (in the extract). Linearity in the standard curve extends to at least 90

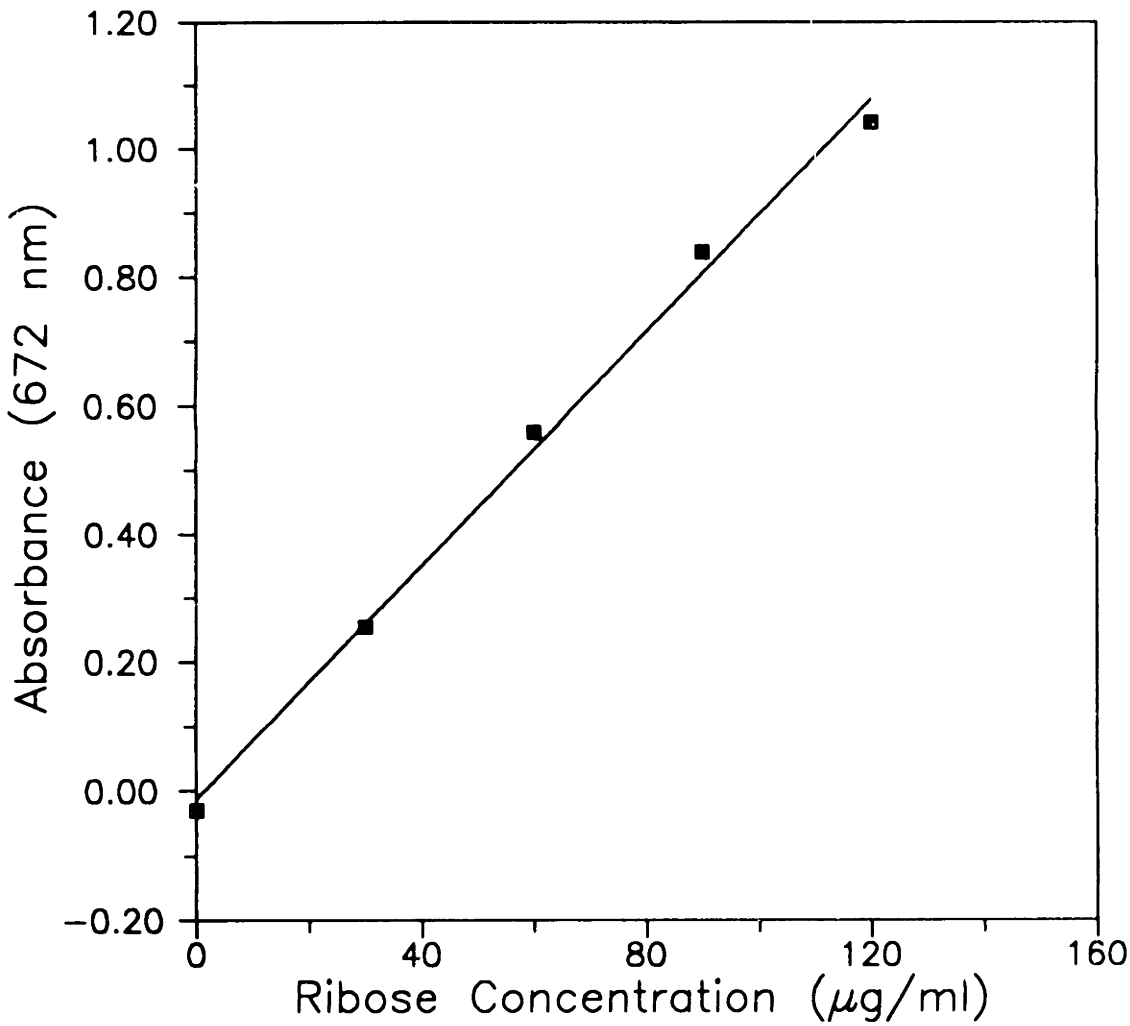

Figure 4.10. Standard curve for total RNA assay. Note that results are in "ribose-equivalents."

μg/ml ribose.

4.3.2 Abiotic Phase Measurements

The abiotic phase of the fermentation samples was analyzed for substrates and products using a variety of analytical techniques. The liquid for the analyses was obtained from the first centrifugation step of the sampling procedure. The supernatant from a centrifuge tube was filtered through a 0.22 μm Millex®-GV low protein binding filter unit (Millipore, Bedford, MA) into several individual glass storage vials. The vials were stored at -20°C until analysis.

4.3.2.1 L-Lysine Assay

L-lysine was measured by a variation of an enzymatic assay [Nakatani *et al.*, 1972] using saccharopine dehydrogenase (Product #S3633, Sigma Chemical Co., St. Louis, MO). The assay is based on the following reaction:

$$\text{L-lysine} + \alpha\text{-ketoglutarate} + \text{NADH} + \text{H}^+ \rightleftarrows \text{saccharopine} + \text{NAD}^+ + \text{H}_2\text{O} \qquad 4.7$$

The reaction is heavily in favor of saccharopine formation ($K_{eq} \approx 10^{15}$). L-lysine is quantitated by following the decrease in absorbance due to NADH at 340 nm. The assay protocol is given below:

L-lysine Assay

(1) Add (in order):

a) 2.5 ml 250 mM phosphate buffer, pH 6.8
b) 100 μl 6.4 mM NADH in 119 mM $NaHCO_3$

c) 100 µl 137 mM α-ketoglutaric acid
d) 100 µl standard or sample

(2) Mix contents well, transfer to 4.0 ml cuvette.

(3) Measure absorbance (A_0) at 340 nm (zero against phosphate buffer).

(4) Add 20 µl 25 units/ml saccharopine dehydrogenase.

(5) Incubate for 35 minutes at room temperature.

(6) Measure absorbance (A_{35}) at 340 nm.

A standard curve of ΔA (A_0-A_{35}) versus Lysine·HCl concentration (0, 0.1, 0.3, 0.5 g/l) was prepared for sample concentration determination. A typical calibration curve appears in Figure 4.11. The sensitivity of this assay (using the above reaction volumes) is approximately 0.05 g/l LysHCl (in the sample). Linearity in the standard curve extends to at least 0.5 g/l LysHCl.

Although the original work [Nakatani *et al.*, 1972] with this assay investigated the specificity of the enzyme for L-lysine, it was desired to verify the effectiveness of the assay with our fermentation samples. This was done by comparing the enzymatic assay results with the results of a L-lysine determination by high pressure liquid chromatography (HPLC). The details of the HPLC method, a pre-column derivatization with o-pthaldialdehyde (OPA), are presented in Appendix B.1. The two sets of results (from an early shake flask fermentation) agreed with each other to within 5%. Since the enzymatic assay was much simpler to perform and gave similar results to the HPLC method, it was used exclusively throughout the bulk of this work.

4.3.2.2 Ammonium Assay

Ammonium ion, NH_4^+, concentration was estimated via two methods, a

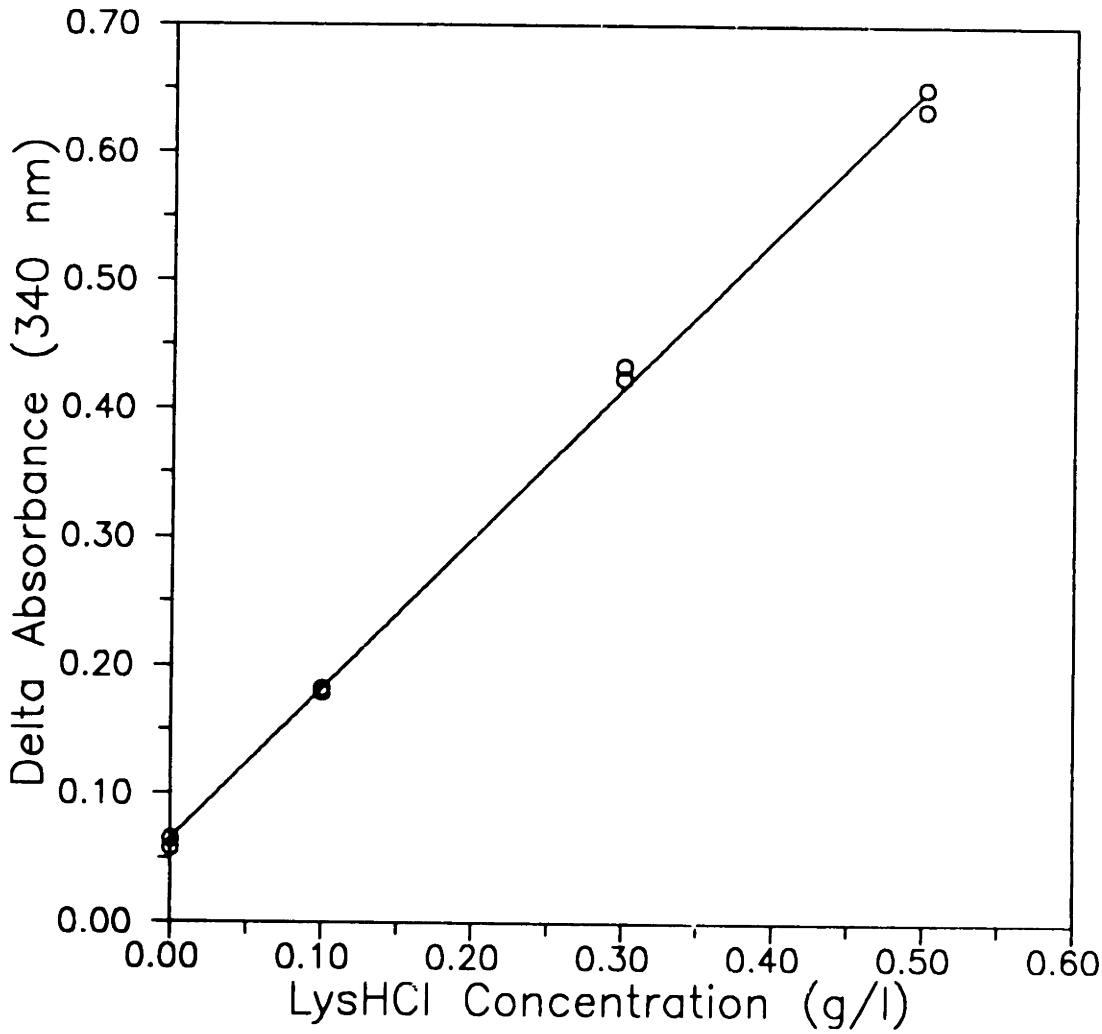

Figure 4.11. Standard curve for L-lysine enzymatic assay.

phenol/hypochlorite chemical method based on the Berthelot color reaction [Weatherburn, 1967] and an enzymatic method using glutamate dehydrogenase (Sigma). The chemical method was used in the early parts of this work (primarily for the continuous cultures). The enzymatic method became available later in the work and, due to it's greater ease of use and because it does not require the use of hazardous materials, it was implemented thereafter.

The phenol/hypochlorite ammonium assay is described below:

Phenol/Hypochlorite Ammonium Assay

(1) Add into a 18 x 150 mm glass test tube:

a) 20 µl sample or standard
b) 5 ml 50 mg/l sodium nitroprusside in 10 g/l phenol
c) 5 ml 4.2 ml/l sodium hypochlorite (5% available chlorine) in 5 g/l NaOH

(2) Mix contents well, incubate at 37°C for 20 minutes.

(3) Transfer contents to 4.0 ml cuvette.

(4) Read absorbance at 625 nm.

A standard curve of absorbance versus $(NH_4)_2SO_4$ concentration (0.1, 0.2, 0.3, 0.4, 0.5 g/l) was prepared for sample concentration determination. A typical calibration curve appears in Figure 4.12A. The sensitivity of this assay (using the above reaction volumes) is approximately 0.025 g/l $(NH_4)_2SO_4$ (in the sample). Linearity in the standard curve extends to at least 0.5 g/l $(NH_4)_2SO_4$.

The enzymatic ammonium assay is described below:

Enzymatic Ammonium Assay

(1) Add into a 4.0 ml cuvette:

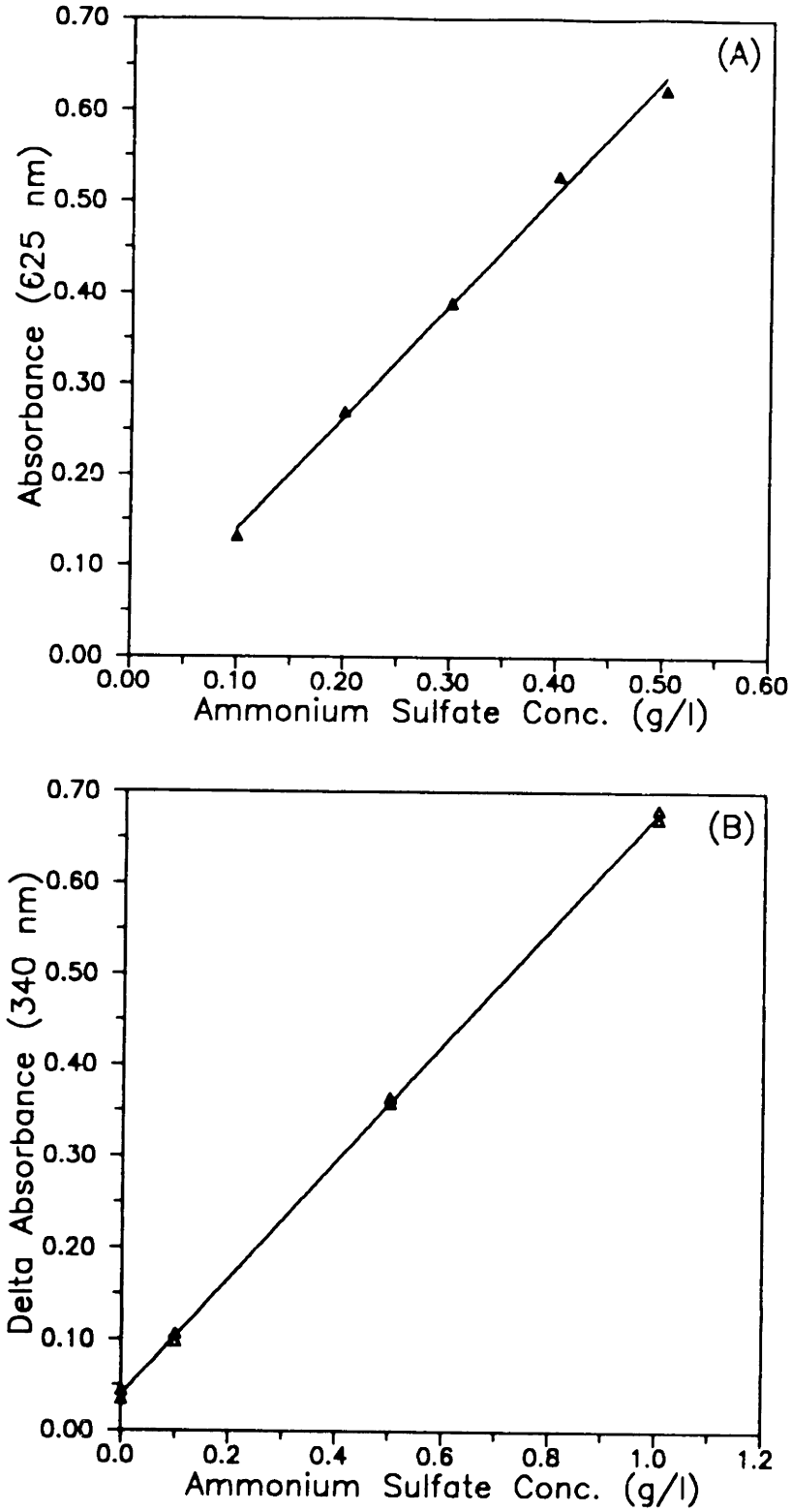

Figure 4.12. Standard curves for ammonium assays. (A) Phenol-hypochlorite assay standard curve. (B) Enzymatic assay standard curve.

a) 1.0 ml 35 mM α-ketoglutarate in 0.5 M triethanolamine·HCl buffer, pH 8.0
b) 1.68 ml distilled water
c) 100 µl 6.4 mM NADH in 119 mM $NaHCO_3$
d) 20 µl standard or sample

(2) Mix contents well by inversion.

(3) Measure absorbance (A_0) at 340 nm (blanked against 1 ml buffer + 2 ml H_2O).

(4) Add 20 µl 1200 units/ml glutamate dehydrogenase.

(5) Incubate for 15 minutes at room temperature.

(6) Measure absorbance (A_{15}) at 340 nm.

A standard curve of ΔA (A_0-A_{15}) versus $(NH_4)_2SO_4$ concentration (0, 0.1, 0.5, 1.0 g/l) was prepared for sample concentration determination. A typical calibration curve appears in Figure 4.12B. The sensitivity of this assay (using the above reaction volumes) is approximately 0.10 g/l $(NH_4)_2SO_4$ (in the sample). Linearity in the standard curve extends to at least 1.0 g/l $(NH_4)_2SO_4$.

4.3.2.3 Glucose Assay

Glucose was measured on an HPLC system consisting of a Waters (Milford, MA) 501 pump, 680 pump controller, WISP 710B automatic injector, R401 differential refractometer, a Shimadzu (Columbia, MD) C-R3A Chromatopac integrating recorder, and a BioRad (Richmond, CA) Aminex HPX-87H column. The system was run in an isocratic mode at a flow rate of 0.6 ml/min of 0.005 N H_2SO_4 (in HPLC-grade H_2O), temperature of 45°C, injection volume of 15 µl, and a refractometer attenuation of 32X. The mobile phase is prepared fresh for each run and is degassed and filtered through a 0.45 µm Millipore HVLP filter.

A sample calibration curve for glucose quantitation is shown in Figure 4.13.

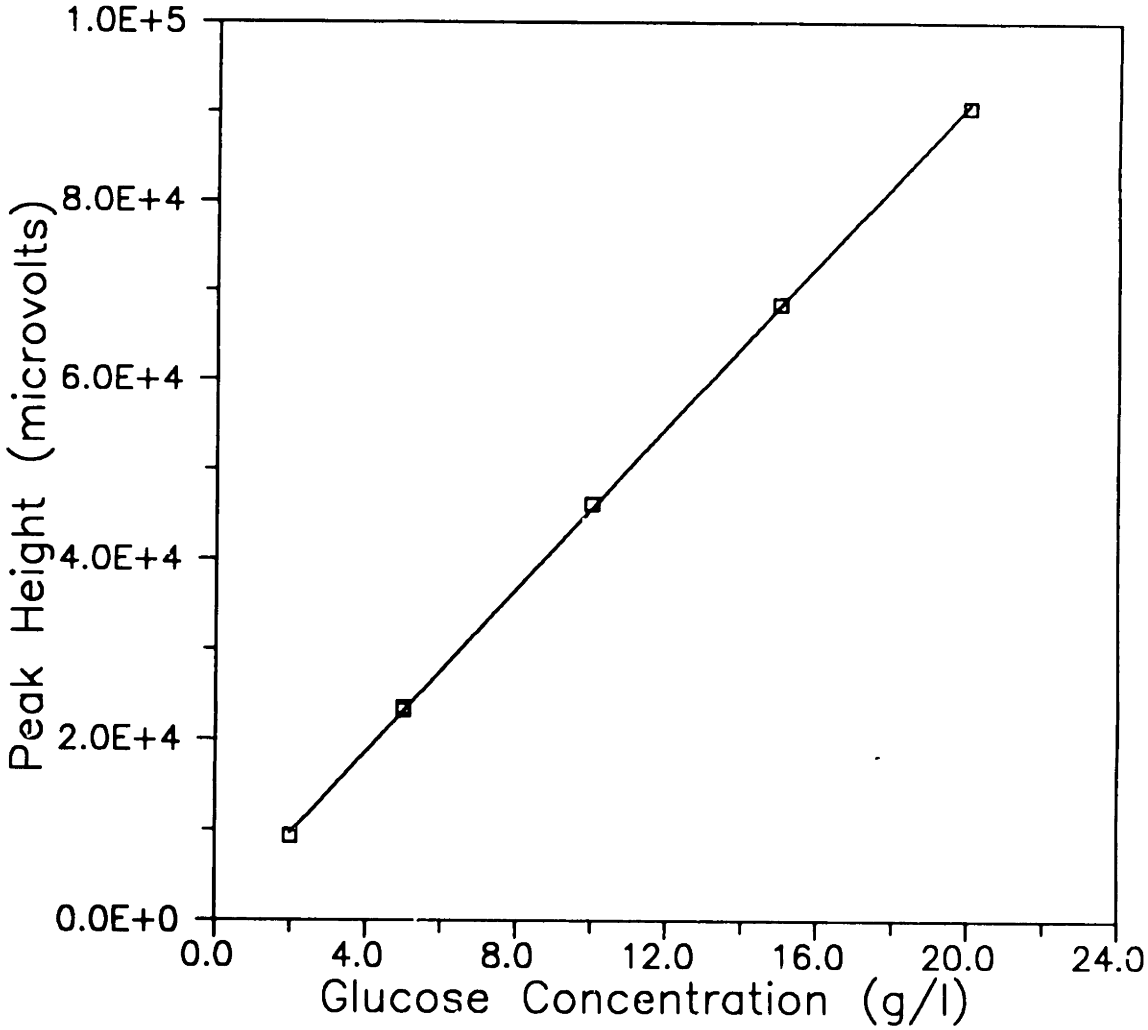

Figure 4.13. Standard curve for glucose analysis by HPLC.

The sensitivity of this assay (using the above parameters) is approximately 1.0 g/l glucose (in the injection). Linearity in the standard curve extends to at least 20 g/l glucose.

It should be mentioned that this column is also useful for quantitating other carbohydrate (trehalose) and organic acid side products (pyruvate, lactate, acetate). However, for glucose analysis, the fermentation samples typically required at least a 1:10 dilution which would dilute most side-products below their minimum detectable levels. Therefore, the fermentation samples would be run again, without dilution, to quantitate these side products.

4.3.2.4 Amino Acid Substrates and Side Products

Since this strain required L-threonine, L-methionine, and L-leucine to be provided in the medium, it was of interest to quantitate these amino acid substrates during the course of a fermentation. In addition, a number of other amino acids (L-glutamate, L-alanine, and L-valine) are known to be produced under different conditions during the L-lysine fermentation. There exist quite sensitive HPLC systems for amino acid analysis. The type of analysis our hardware was capable of performing was a pre-column derivatization method (described in Appendix B.1). Such systems are only effective if one is trying to quantitate either the highest concentration amino acid in a sample (which can be diluted down to the assay linear range) or a multitude of amino acids all at similar concentrations. This is due to the need to derivatize all amino acids before separation and detection. In a system designed to produce large quantities of L-lysine (grams per liter), it is then extremely difficult to quantitate low levels (milligrams per liter) of other amino acids, such as L-threonine [Kiss *et al.*, 1990]. It turned out that all of these amino acids, with the

exception of L-methionine and L-lysine, as well as the disaccharide side product, trehalose, could be eluted from a Biorad Aminex HPX-87C column. Although the sensitivity of an assay using RI detection is orders of magnitude less than that of a derivatization amino acid assay, it was adequate for our purposes.

The HPLC assay for these compounds used the same hardware setup as for the assay of glucose and organic acids. The Biorad HPX-87C column was run at 1.0 ml/min of 5 mM $CaSO_4$ and 85°C with an injection volume of 30 µl. The refractometer attenuation was set at 16X for additional sensitivity. Figure 4.14 shows sample calibration curves for quantitation of these compounds. Typical sensitivities under the above operating conditions were about 100 mg/l for the amino acids and about 0.5 g/l for trehalose. The linear ranges extended up to about 10 g/l for the amino acids and about 15 g/l for trehalose.

It should be mentioned that since L-threonine plays a vital role in the accumulation of L-lysine, it was of extreme interest to quantitate levels of L-threonine during all types of fermentations, especially during steady-state continuous cultures. As mentioned, a derivatization assay was unable to quantitate low levels of L-threonine in the presence of high levels of L-lysine. In addition, the HPLC assay described in this section was not sensitive enough to quantitate the expected levels of a few milligrams (or less) per liter during continuous culture. An enzymatic assay for L-threonine, with a sensitivity of approximately 5 mg/l, was developed based on the specific inhibition of homoserine dehydrogenase activity by L-threonine [Kiss *et al.*, 1990]. This assay, discussed further in Appendix B.2, was successfully employed to place an upper bound on steady-state L-threonine levels during continuous culture.

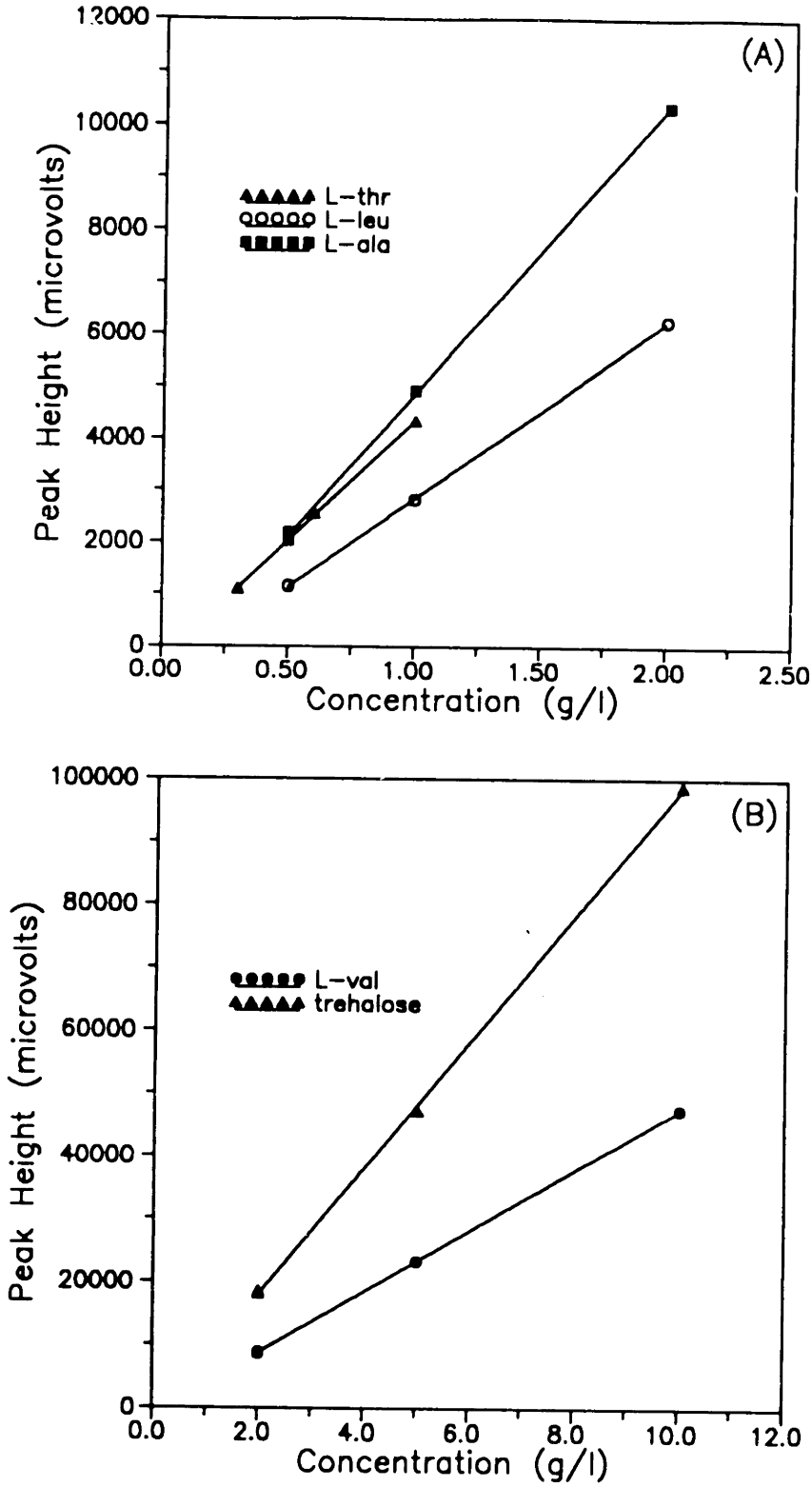

Figure 4.14. Standard curves for essential amino acid and side product analysis by HPLC. (A) L-threonine, L-leucine, and L-alanine response curves. (B) L-valine and trehalose response curves.

Chapter 5

Results and Discussion

This chapter presents the results of the work performed in meeting the stated objectives of this thesis project. The presentation of these results and the associated discussion follows the method of approach presented previously.

5.1 Strain Characterization

Several sets of experiments were carried out to determine some basic growth characteristics of the organism used in the majority of this research, *Corynebacterium glutamicum* ATCC 21253 (Thr^-, Met^-, Leu^-).

5.1.1 General Growth Characteristics

Much of the existing literature on growth of *Corynebacteria* strains reports a pH optimum of 7-8 with growth occurring in the range of 6-9, and an optimum temperature range of 25-37°C. In addition, it has been reported that most strains require biotin and some strains require thiamine (vitamin B_1) for growth [Kinoshita, 1985]. It was of interest to investigate some of these growth characteristics for this particular strain.

The effect of temperature was not investigated other than to confirm that this strain will grow in the temperature range given above. All experiments were carried out at 30°C. An optimum pH was not determined for growth of this strain, but the

time course of the pH during a shake flask fermentation conducted without pH control was obtained, as shown in Figure 5.1. Clearly, without pH control, the pH drops quite rapidly and growth ceases when pH drops below about 5. All experiments with pH control were carried out at a pH of 7.0.

This strain's need for biotin or thiamine was investigated by plating cultures grown up under standard conditions in LB5G medium onto CGM1 plates lacking either biotin, thiamine, or both biotin and thiamine (cell broth was diluted 10^6-fold with 1/4 Strength Ringers for plating, so nutrient carryover was not a concern). Not surprisingly, it was found that this strain did not actually require thiamine for growth, although growth was slightly stimulated by the presence of 1 mg/l thiamine. However, it was surprising to find that the strain apparently did not require biotin for growth (although growth was definitely stimulated by biotin at 1 mg/l). However, the possible presence of biotin as a trace contaminant in media components, such as the amino acids, was not investigated.

It was also of interest to determine the ability of this strain to grow on different carbon sources. Several carbon sources have previously been tested [Vallino, 1991], but it was desired to also investigate the possibility of this strain growing on L-lysine or trehalose as the sole carbon source. Growth tests were performed by plating cells grown in LB5G medium onto CGM1 plates with glucose replaced by 5 g/l of the carbon source under consideration. A summary of carbon source test results for this strain appears in Table 5.1. The test for growth on L-lysine was a crude method of checking whether this strain is capable of degrading L-lysine (would imply the presence of L-lysine decarboxylase). The negative result for growth on L-lysine as sole carbon source appears to indicate that this strain does

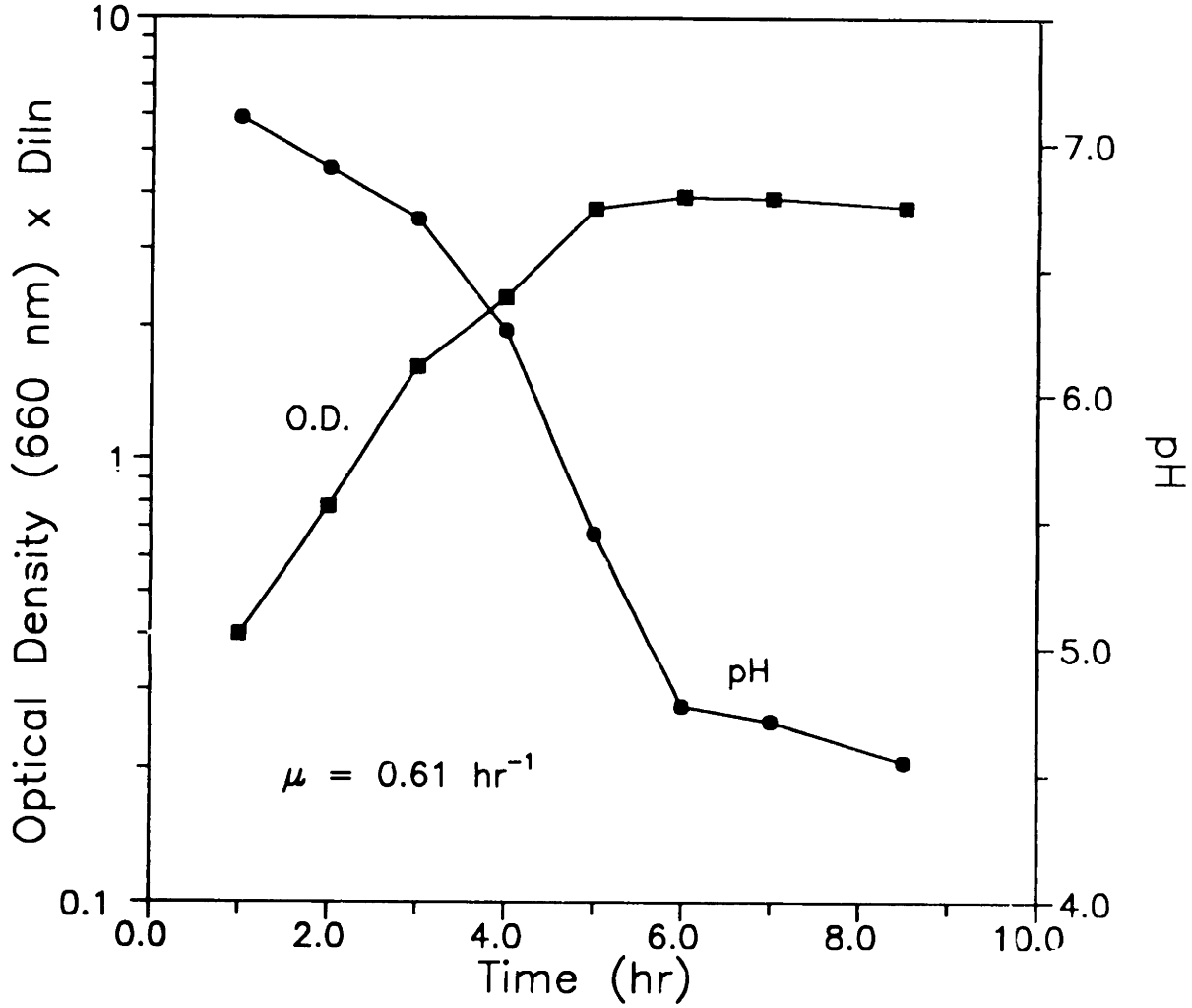

Figure 5.1. Time course of optical density and pH during typical shake flask fermentation.

not degrade L-lysine, although this result is not definitive. However, it does agree with the results of Nakayama and Kinoshita (1961a) who did not detect any L-lysine decarboxylase activity. The test for growth on trehalose was a crude method of determining whether this strain is capable of reutilizing the trehalose which it produces and secretes into the medium under certain conditions. This is of interest because trehalose is formed from glucose and any trehalose formed which is not recycled is simply lost from the glucose pool and thus will reduce the overall fermentation yield. Again, the negative result for growth on trehalose as sole carbon source appears to indicate that this strain will not reutilize the secreted trehalose, although this result is not definitive.

One further general growth characterization was performed in comparing this auxotrophic strain with the homoserine revertant strain derived from the parent auxotroph (revertants discussed in detail in Section 5.4). The main objective of the comparison was to estimate the difference in the specific growth rates of the two strains. Figure 5.2A shows the growth response of the two strains (auxotroph and revertant) in LB5G medium. Although the auxotrophs exhibited a slightly longer lag phase, the specific growth rates of the two strains were indistinguishable at approximately 0.53 hr^{-1}.

The specific growth rates of auxotrophs and revertants were also examined for growth in defined amino acid-limited media. Auxotrophs were cultured in CGM1 medium and revertants were cultured in CGM1 medium without L-threonine or L-methionine. The results of these small-scale shake flask experiments are shown in Figure 5.2B. There is relatively little difference in specific growth rate between auxotrophs limited by L-threonine and revertants limited by L-leucine. This is a

Table 5.1 - Ability of *C. glutamicum* ATCC 21253 to grow on different sole sources of carbon.

Sole Carbon Source	Growth†	Reference
Glucose	+	This work
Trehalose	-	This work
Fructose	+	Vallino (1991)
Gluconate	+	"
Acetate	+	"
Citrate	+	"
Malate	+	"
L-lysine	-	This work

† A + indicates growth; a - indicates no appreciable growth

result which is utilized further in developing the mathematical model of the continuous culture competition between auxotrophs and revertants.

5.1.2 Essential Amino Acids Requirements

Since this organism cannot synthesize the amino acids L-threonine, L-methionine, or L-leucine, they must be provided in the medium for the culture to propagate. Experiments were conducted to determine the relationships between the amount of essential amino acid provided and the cell mass synthesized. The experiments were performed in CGM1 medium plus $CaCO_3$ (dry weight measurement procedure used 1 M H_3PO_4 in washing steps to dissolve $CaCO_3$) with

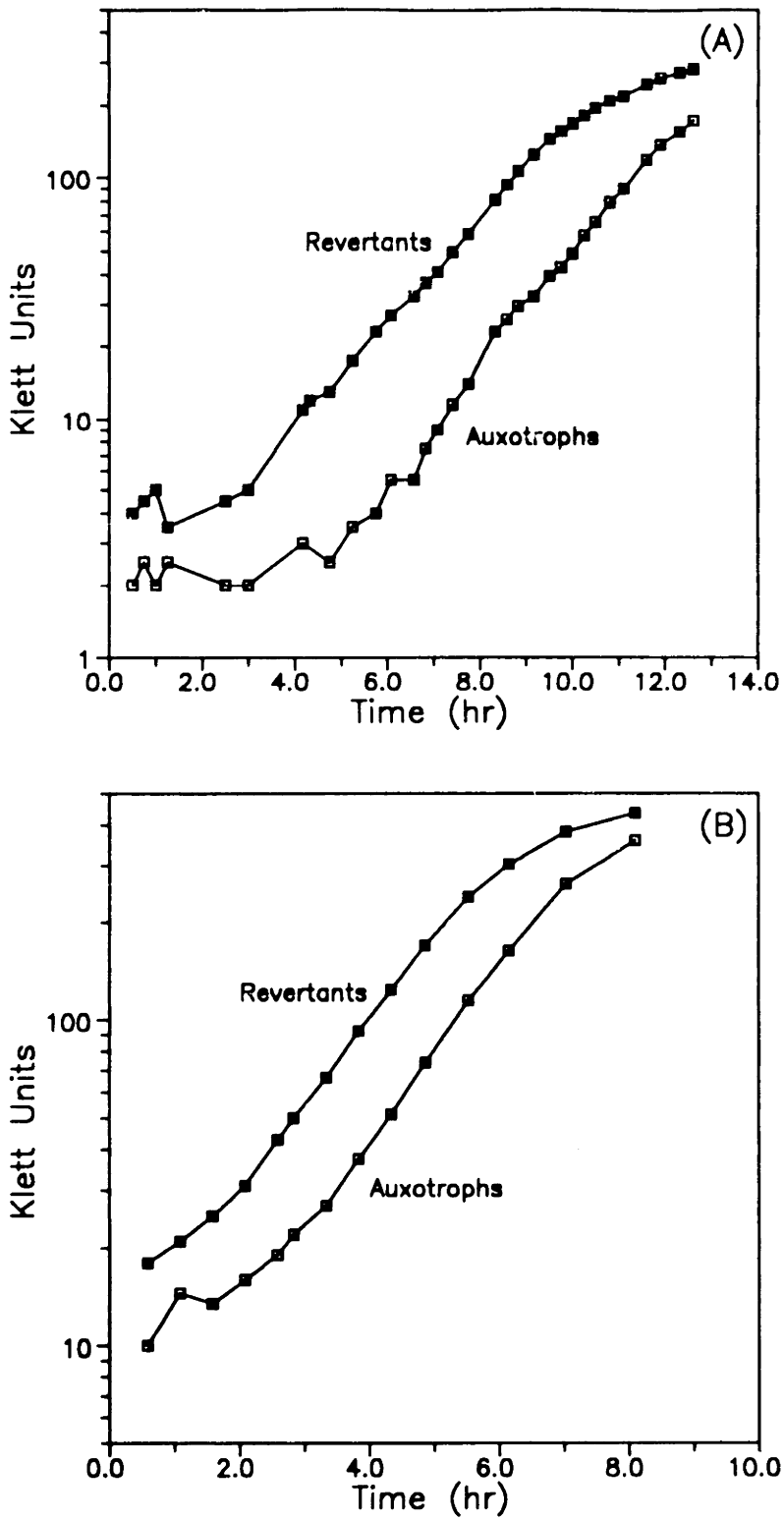

Figure 5.2. Comparison of growth profiles of auxotrophs (Thr$^-$, Met$^-$, Leu$^-$) and homoserine revertants (Leu$^-$). (A) Growth of auxotrophs and revertants on LB5G medium. (B) Growth of auxotrophs and revertants on CGM1 medium.

the amino acid under study present in growth-limiting quantities.

The results appear in Figure 5.3. The responses are linear in the ranges studied and the cell mass yield values (expressed as mg amino acid/g DCW) are obtained as the slopes of the responses. The yields are calculated to be 29.3, 7.89, and 19.5 mg amino acid/g DCW for L-threonine, L-methionine, and L-leucine, respectively. These results can be compared with the amino acid analysis of acid-hydrolyzed *C. glutamicum* biomass of Kimura (1963) which gave amino acid contents of 30.0, 10.74, and 46.4 mg amino acid/g DCW for L-threonine, L-methionine, and L-leucine, respectively. Similar content values (28.7, 21.8, 56.1 mg/g) for acid-hydrolyzed *E. coli* biomass are also given by Ingraham *et al.* (1983). Assuming that cell mass is fifty percent protein (a good assumption) and that protein consists of equal proportions of all twenty amino acids (not as good an assumption), the yields could be estimated *a priori* as 25 mg amino acid/g DCW. It is reasonable that our results show the requirement for L-threonine to be the largest of the three amino acids studied, since L-threonine is not only a direct component of protein but also a precursor for the amino acid L-isoleucine.

These experimentally determined cell mass yields are quite useful in the design of fermentation media. The yield values were used in designing all fermentation media to be L-threonine growth limiting so as to minimize concerted feedback inhibition of aspartate kinase by L-threonine plus L-lysine.

5.1.3 Growth Rate Inhibition by Glucose

It is well known [Wang *et al.*, 1979] that high concentrations of glucose can

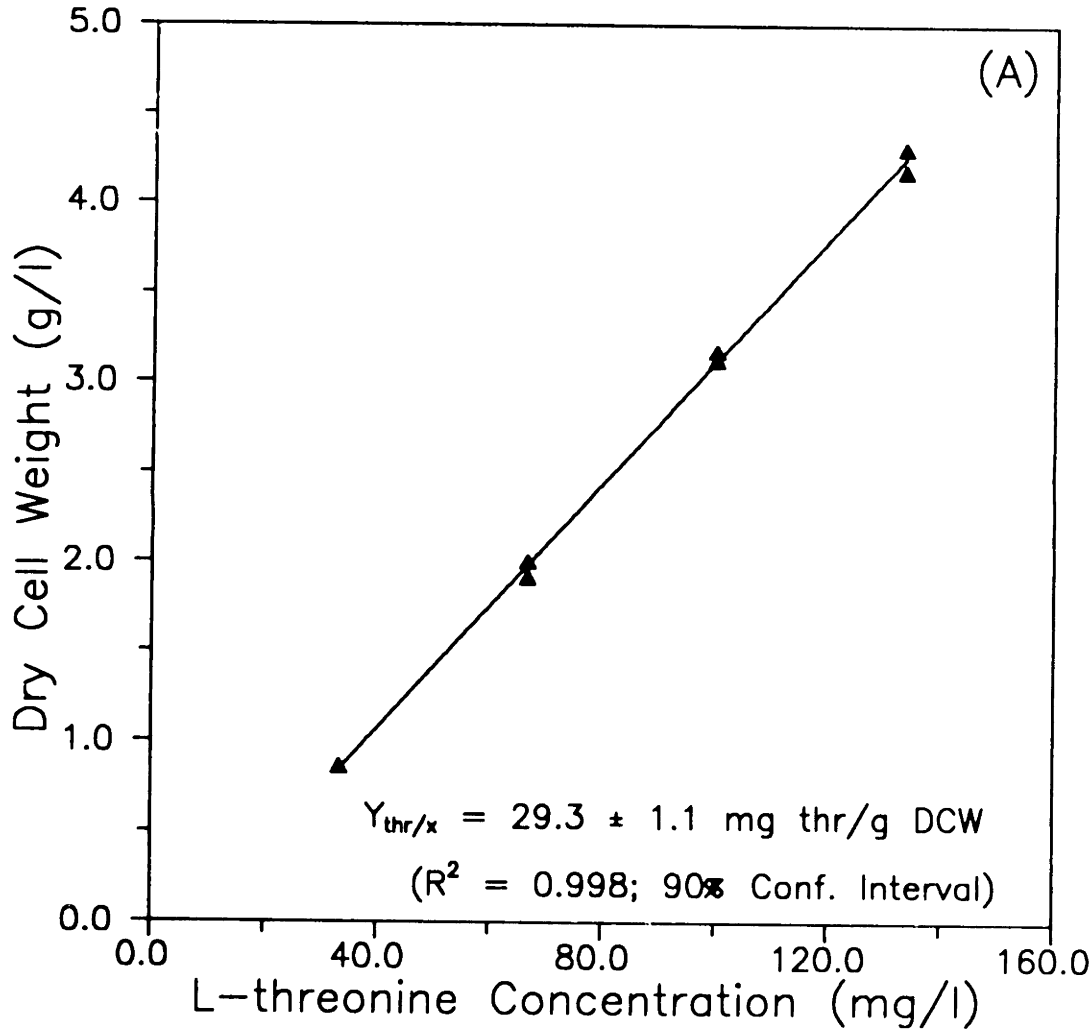

Figure 5.3. Determination of cellular requirements for essential amino acids. (A) Requirement for L-threonine.

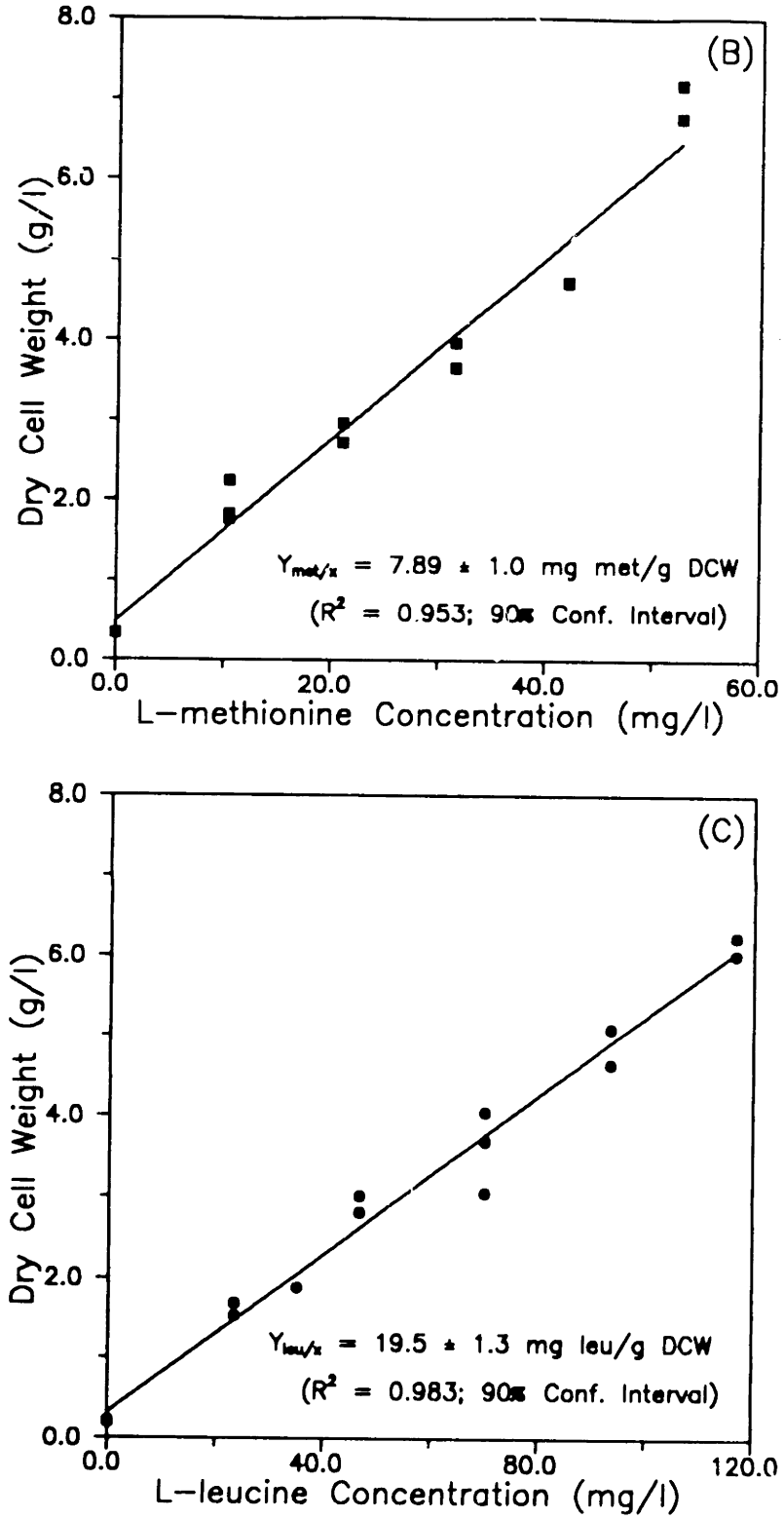

Figure 5.3. (Continued) (B) Requirement for L-methionine. (C) Requirement for L-Leucine.

retard the growth of microorganisms due to high osmotic pressure and subsequent dehydration. Since batch experiments typically utilize high initial glucose concentrations, the effect of varying levels of glucose on growth rate was investigated. Shake flask experiments were performed in CGM1 media with varying levels of glucose from 20 to 250 g/l. Figure 5.4 shows cell density (as measured by a Klett colorimeter) vs. time for various initial glucose concentrations. The initial specific growth rates are shown as a function of initial glucose concentration in Figure 5.5. Glucose concentration clearly has a strong effect on growth rate in the range studied. The maximum specific growth rate is at least 0.65 hr^{-1}, and growth is essentially shut off near 250 g/l of glucose. The data are satisfactorily modeled by substrate inhibition kinetics of the form [Han and Levenspiel, 1987]:

$$\mu = \mu_{max}\left(1 - \frac{C_s}{C_{s,crit}}\right)^n \qquad 5.1$$

which is valid when the substrate concentration is always much greater than its half-saturation constant. The lowest glucose concentration studied was 20 g/l and it is a good assumption that this is much greater than the glucose half-saturation constant, which for bacteria is typically on the order of tens of milligrams per liter.

These shake flask data may not translate directly to sparged fermentors. The continuous culture experiments performed in the sparged, 3 liter glass vessel at a glucose concentration of 20 g/l consistently gave initial growth rates between 0.3 and 0.4 hr^{-1}, and the batch and fed-batch experiments performed in the sparged, 10 liter

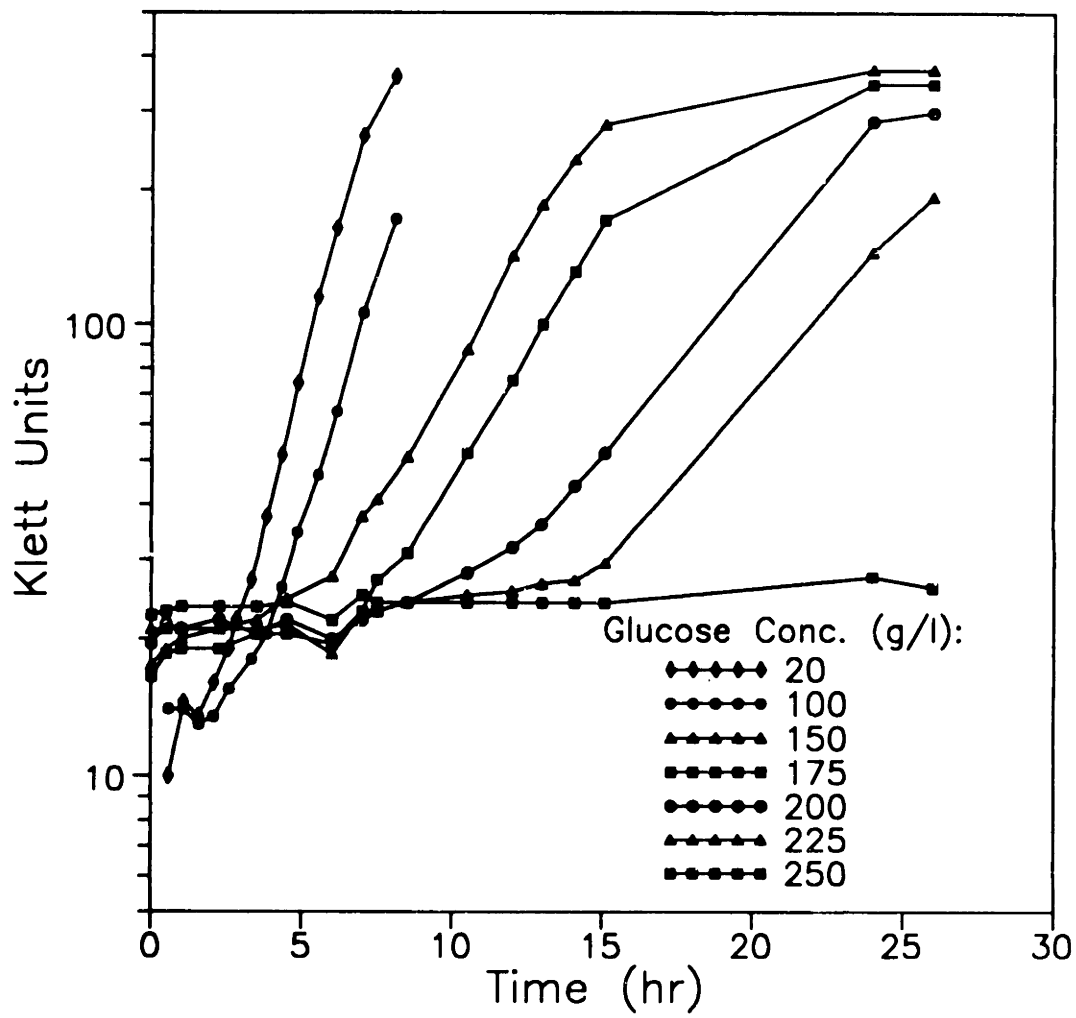

Figure 5.4. Growth profiles at varied initial glucose concentrations.

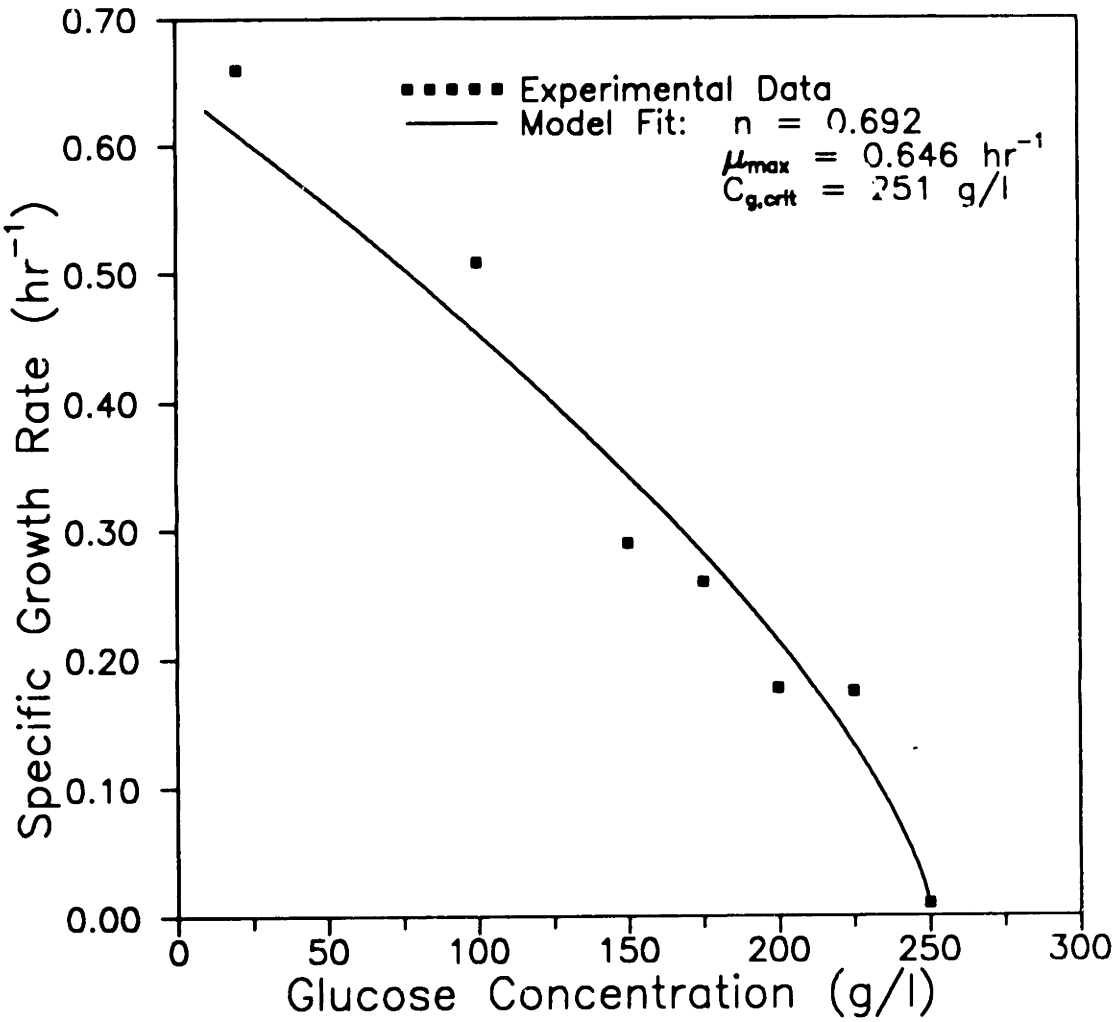

Figure 5.5. Effect of initial glucose concentration on specific growth rate.

stainless steel vessel at a glucose concentration of 150 g/l gave initial growth rates in the same 0.3 - 0.4 hr^{-1} range.

The most obvious differences between shake flask cultures and sparged vessel cultures are the dissolved oxygen and dissolved carbon dioxide concentrations. Sparged vessels typically run near 100 percent dissolved oxygen saturation (0.21 atm) in the early part of the fermentation and sparging can easily strip CO_2 from the medium. The negative effects on specific growth rate of high dissolved oxygen and low dissolved CO_2 have been documented [Pirt, 1975].

Although there are few measurements of the inhibitory levels of dissolved oxygen tension (DOT), existing data indicates that for all microorganisms there is a level of DOT above which oxygen becomes toxic and inhibits growth. The results of Wiseman *et al.* (1966) indicate that growth of *Pseudomonas*, *E. coli*, and *Staphylococci* is prevented by oxygen tension of about 1 atm.

The molecular basis for oxygen toxicity is not well understood. Hypotheses as to the role of oxygen include causing the accumulation of hydrogen peroxide by cells, indirectly inactivating essential enzymes, or oxidizing and inactivating coenzymes such as ferredoxin.

There have been relatively few studies of the effect of dissolved CO_2 on microbial growth. Dagley and Hinshelwood (1938) showed that the relation between specific growth rate and partial pressure of CO_2 was of hyperbolic form for *Klebsiella aerogenes* with a half-saturation constant of $3 \cdot 10^{-4}$ atm ($0.9 \cdot 10^{-5}$ M). Maximum specific growth rate required a CO_2 partial pressure of 10^{-3} atm.

Further investigation into the effects of O_2 or CO_2 on the growth of *C. glutamicum* was not undertaken in the course of this work.

5.2 Batch L-lysine Fermentation Characterization

Characteristic profiles for a batch L-lysine fermentation are shown in Figures 5.6A-5.6D. For two identical batch runs, the average final L-lysine titer was 23 g/l at an average volumetric productivity of 0.378 g/l-hr and an overall fermentation yield of 0.15 mol L-lysine produced/mol glucose consumed. Careful examination of the batch dynamics reveals some interesting metabolic features of this fermentation.

5.2.1 Effect of Growth-Limiting Nutrient

Figures 5.6A and 5.6B show that, at about 13 hours after inoculation, L-threonine is depleted from the medium (hereafter referred to as the depletion point), L-lysine production begins, dissolved oxygen concentration rises abruptly from a minimum, but cell mass density continues to increase, eventually reaching a maximum of approximately 1.7 times the level at the depletion point. The fact that L-lysine production begins at the point of L-threonine depletion simply confirms the feedback inhibition at sufficiently high L-threonine levels and that the level of L-threonine in the medium is critical to fermentation performance. The increasing dissolved oxygen level reflects a sharp drop in oxygen uptake rate at the depletion point. Cells reaching the depletion point appear to undergo a shift in metabolism from pure growth to both growth and lysine production. The fact that cell mass density continues to increase even after the depletion point for a required amino acid has been documented in the literature for *Streptococcus faecalis* amino acid auxotrophs [Toennies, 1963].

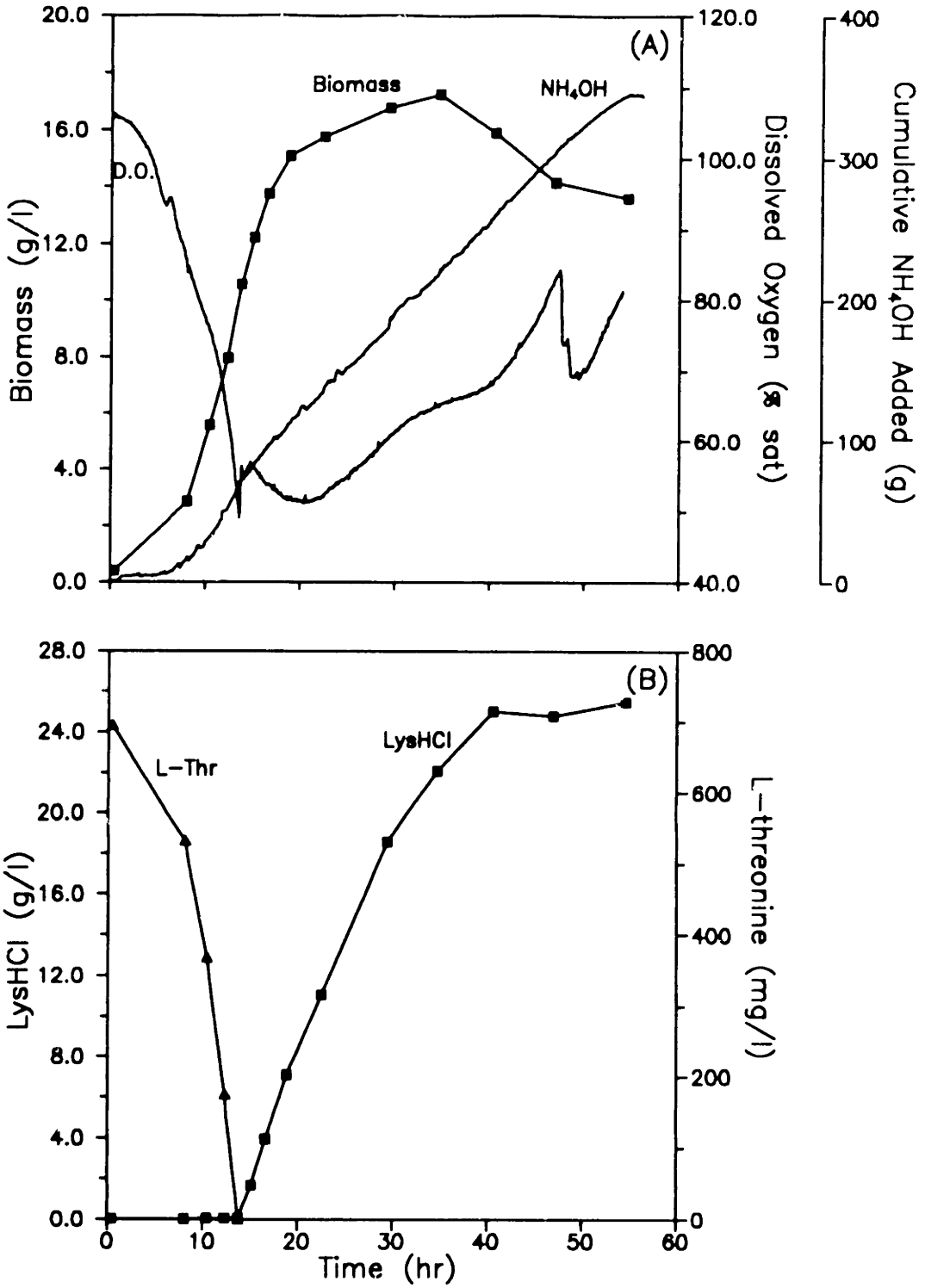

Figure 5.6. Batch L-lysine fermentation dynamic profiles. (A) Biomass and dissolved oxygen concentrations, cumulative NH_4OH added for pH control. (B) L-threonine and L-lysine·HCl concentrations.

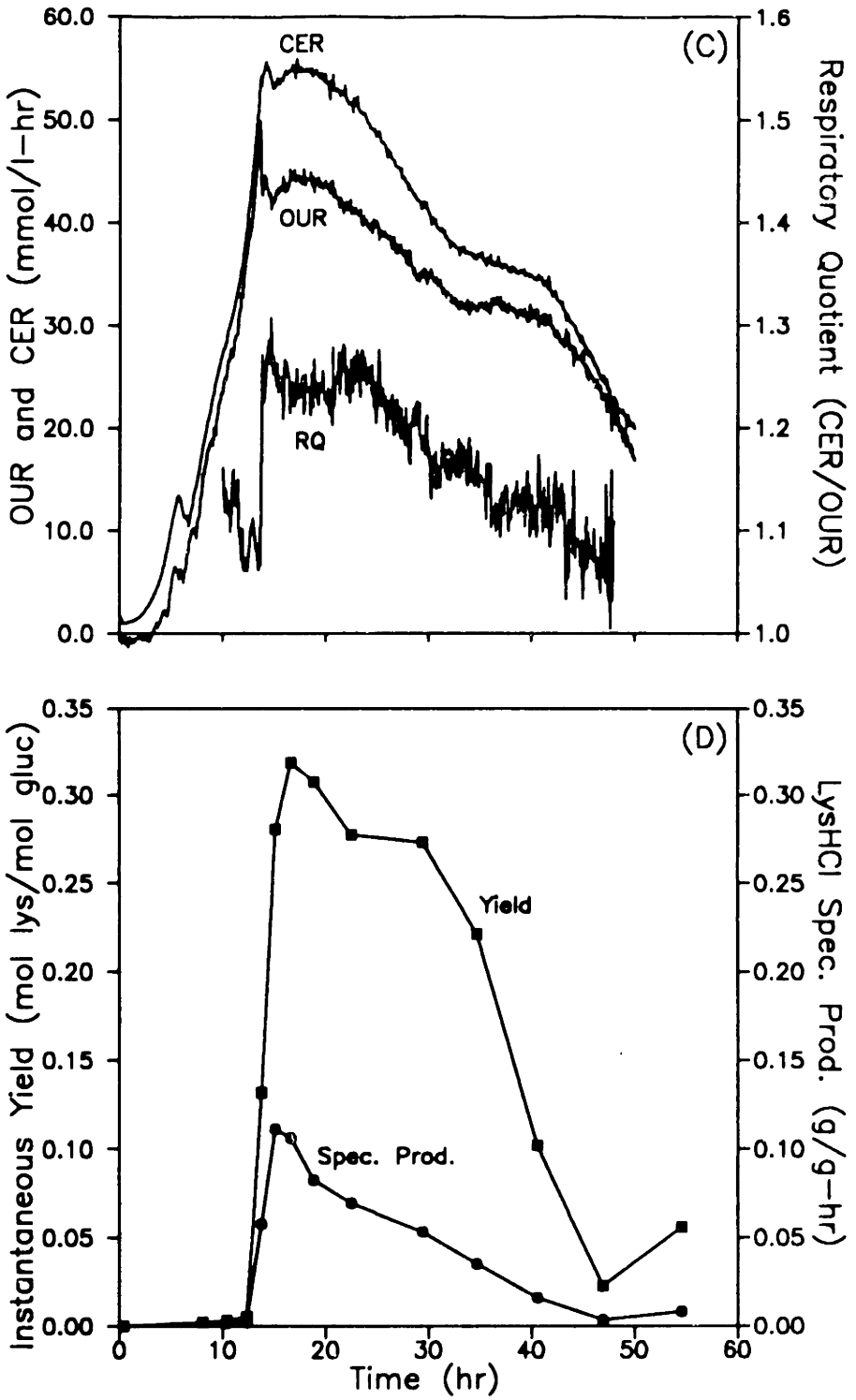

Figure 5.6. (Continued) (C) Respiration rates (OUR,CER) and respiratory quotient. (D) Instantaneous yield on glucose and specific L-lysine·HCl productivity.

5.2.2 Respiratory Dynamics

Figure 5.6C shows the batch fermentation off-gas (OUR, CER, RQ) analysis. There is a clear correlation between the dissolved oxygen and off-gas dynamics and the onset of L-lysine production. At the onset of production, there is essentially a "step-change" in respiratory behavior as OUR and, to a much lesser extent, CER decrease and RQ (CER/OUR) increases sharply from about 1.05 to nearly 1.25, where it remains for about eight hours. The increase in dissolved oxygen concentration corresponds directly to the drop in OUR. The rise in RQ is the result of a shift in metabolism from pure growth to growth and intense L-lysine accumulation (RQ = 1.25). For pure growth, RQ should be approximately 1.05 owing to the similar reductive states of the primary carbon source (glucose) and cellular biomass. As discussed previously in Section 2.4, L-lysine synthesis produces more CO_2 than it consumes O_2. Consequently, at the onset of L-lysine production, when the contribution of the L-lysine synthesis reactions to the overall culture respiration becomes more pronounced, RQ increases. The elevated value of RQ, however, persists for only a limited period of time (eight hours) due to a gradual deterioration of the culture biosynthetic activity discussed below.

5.2.3 Observed Yield and Specific Productivity Dynamics

Figure 5.6D shows the specific L-lysine productivity and the instantaneous molar L-lysine yield on glucose. There are sharp increases in both specific productivity and yield at the initial respiratory shift (coinciding with the depletion

point) with a maximum specific productivity of about 0.1 g/g-hr and a maximum instantaneous yield of about 30 percent. However, both of these performance indicators rapidly decay after reaching their maxima. The period of elevated RQ correlates directly with the period of highest specific productivity and yield, while the decays in respiratory rates (OUR and CER) correlate with the decay phase. This decay in performance may be due to an intracellular protein turnover effect. This conclusion is plausible in that L-lysine accumulation begins at the point of L-threonine depletion, and such an exhaustion of an essential amino acid should leave the cells without the means for *de novo* protein synthesis while normal protein turnover continues. Thus, the metabolic state would then be governed by the efficiency of protein turnover. It is interesting to note that the decay rates for the specific productivity and yield in batch culture are typically between about 4 and 8 percent per hour. Mandelstam (1958) directly measured a protein turnover rate of 5 percent per hour in a L-threonine and L-leucine auxotroph of *Escherichia coli* deprived of L-threonine.

5.2.4 Macromolecular Content During Batch Fermentation

To further investigate the hypothesis concerning intracellular protein turnover, cell samples were assayed for total intracellular protein, DNA, and RNA in an effort to further understand the ramifications of the L-threonine growth limitation. Figures 5.7A and 5.7B show the profiles of biomass, L-threonine, total intracellular protein, DNA and RNA during the course of the batch fermentation, with the dashed vertical line indicating the point of depletion of extracellular L-threonine.

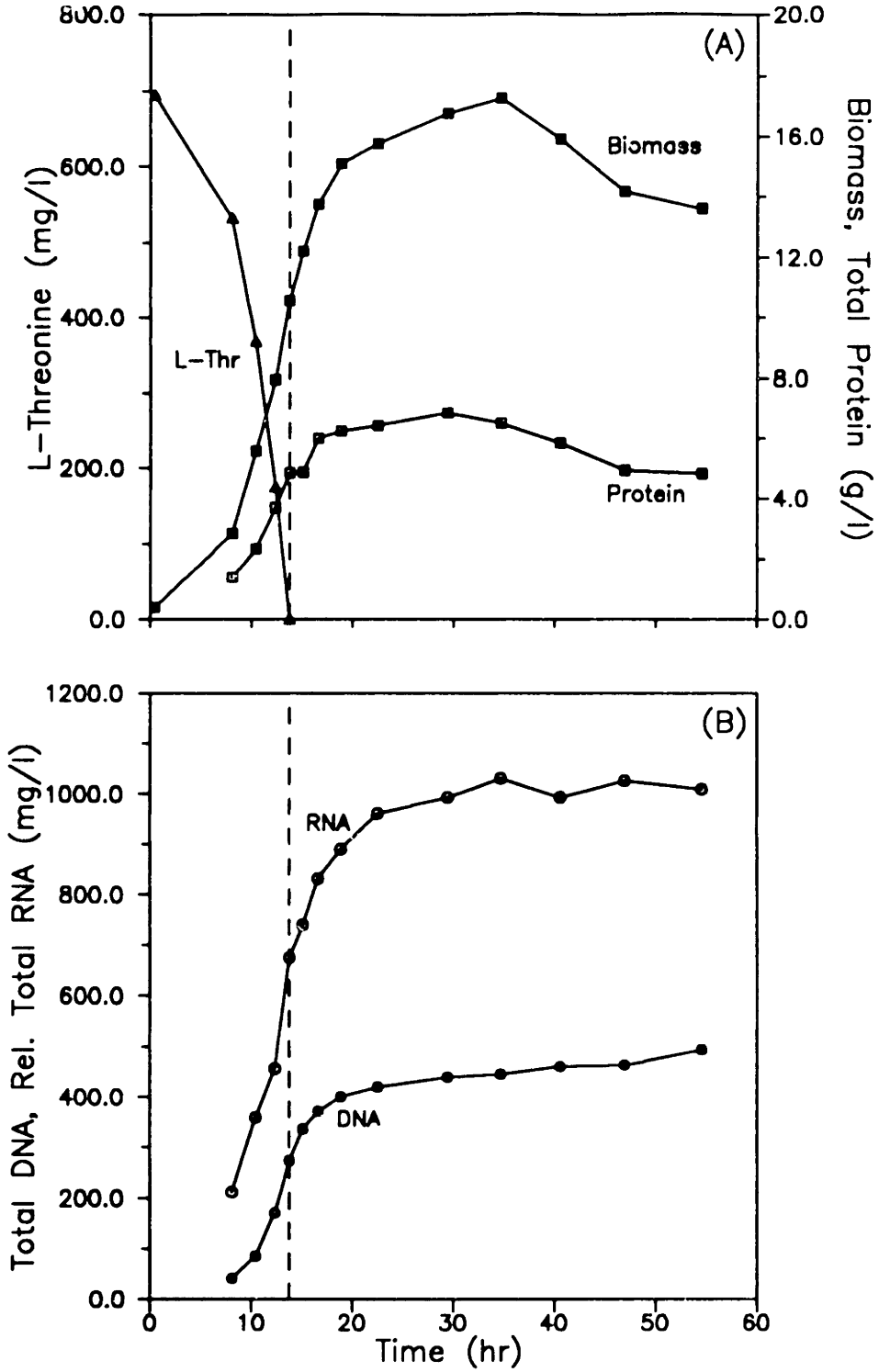

Figure 5.7. Macromolecule dynamic profiles during batch fermentation. (A) L-threonine, dry cell weight, and total intracellular protein concentrations. (B) Total culture DNA and relative RNA concentrations.

The interesting feature from this data is that between the point of depletion of extracellular L-threonine and the end of biomass accumulation, total biomass, DNA, and RNA increased approximately 70 percent while total protein increased only about 35 percent. Thus, the protein percentage of biomass continually decreased, as shown in Figure 5.8. From viable cell counts (not shown) and the DNA profile, it is also clear that the cells go through approximately one more round of replication after reaching the depletion point. The total protein data suggest that *de novo* protein synthesis does not stop precisely at the depletion point, an indication that there exist some intracellular pools of L-threonine after reaching the depletion point, though not enough to inhibit aspartate kinase. However, the fact that the increase in total protein is only half of the increase in other macromolecules indicates that a shortage of amino acid building blocks exists.

Figure 5.9 shows the enzyme specific activity data of Vallino (1991) for an identical batch fermentation. At least for the enzymes studied by Vallino, there are clear decays in specific activity with time following the depletion point. Of particular importance are the observed decays in phosphoenolpyruvate carboxylase (PPC) and pyruvate dehydrogenase (PDH), which may play key roles in governing the yield (efficiency) of L-lysine production from glucose.

The previously discussed evidence of similarity between time constants for specific productivity decay in this system and protein turnover in other bacterial systems, and the measurements [Vallino, 1991] of decay of several enzyme specific activities after the depletion point, strengthens the hypothesis that protein turnover is responsible for the rapid fermentation performance decline in batch culture. Furthermore, the evidence offers one possible biochemical explanation for the

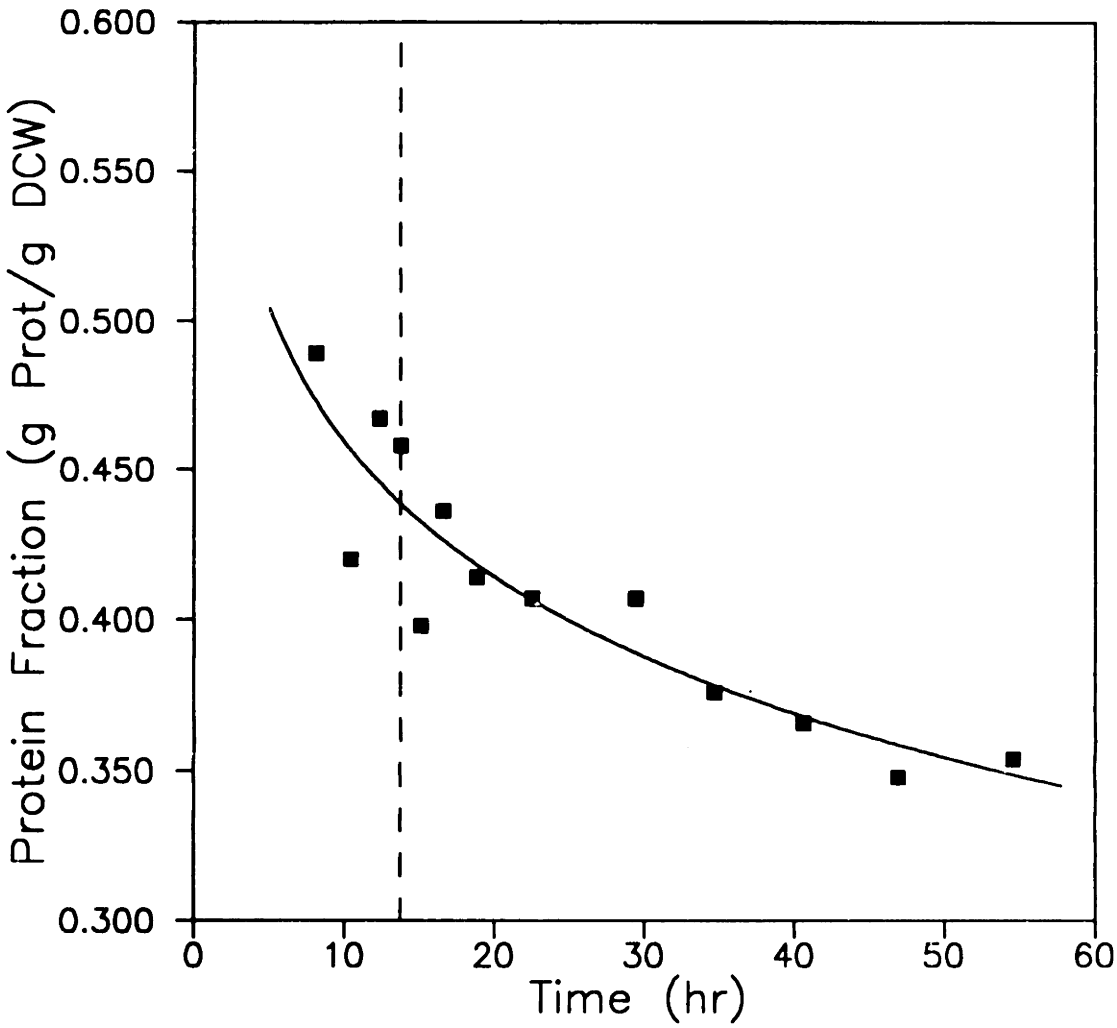

Figure 5.8. Biomass protein content during batch fermentation.

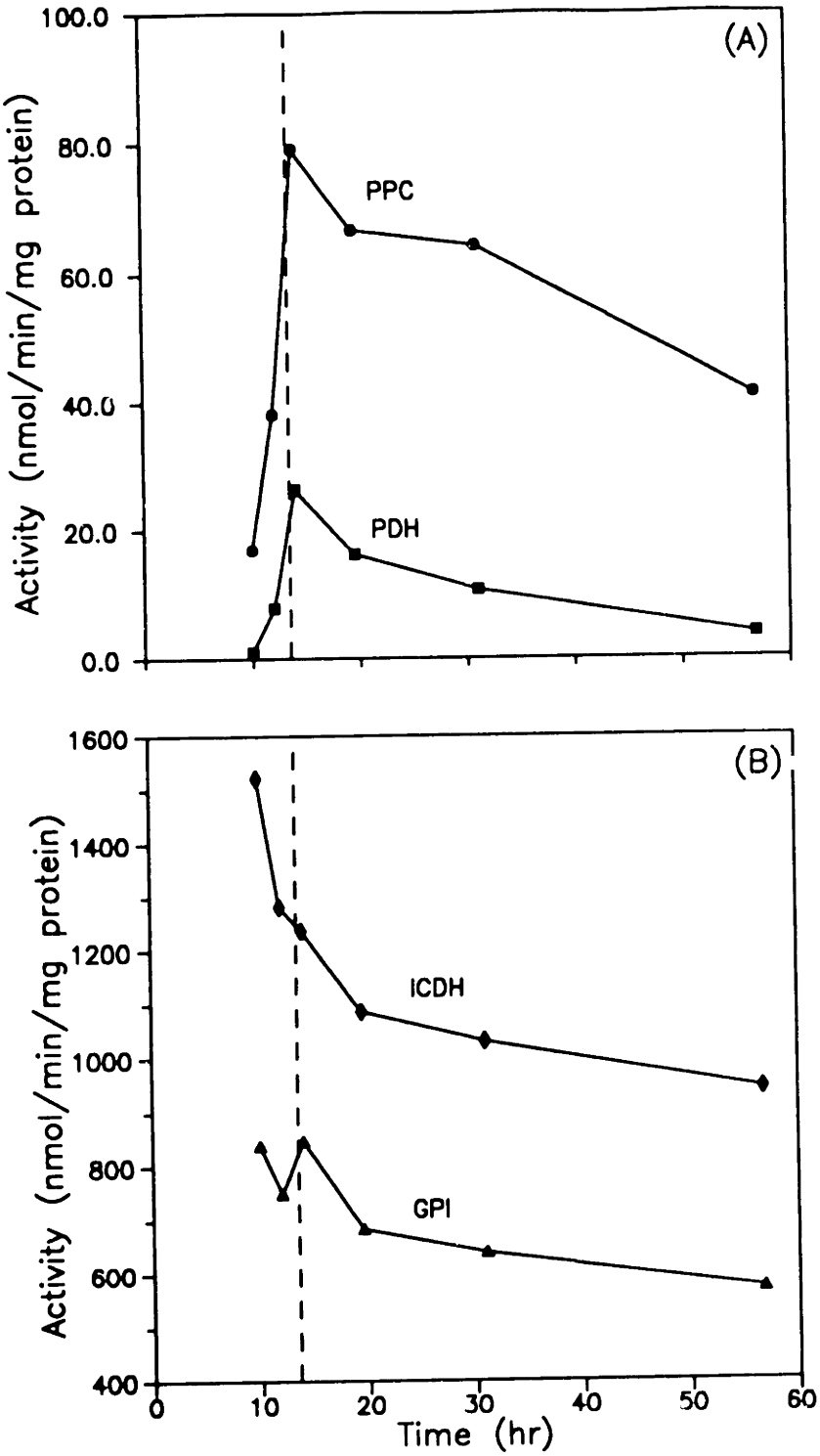

Figure 5.9. Enzyme specific activities during batch fermentation [data of Vallino (1991)]. (A) Phosphoenolpyruvate carboxylase (PPC) and pyruvate dehydrogenase (PDH) specific activities. (B) Glucose phosphoisomerase (GPI) and isocitrate dehydrogenase (ICDH) specific activities.

underlying phenomena responsible for the ability to maintain metabolic activity in fed-batch culture by the controlled addition of growth-limiting nutrients, as will be discussed in great detail subsequently.

5.2.5 Side Product Accumulation During Batch Fermentation

As discussed previously in Section 2.3.3, significant side product formation can occur during the fermentative production of L-lysine. Figure 5.10 shows the accumulation of trehalose (9.2 g/l), L-valine (5.0 g/l), L-alanine (3.7 g/l), pyruvate (1.2 g/l), and acetate (1.8 g/l) during this batch fermentation. Since it appears that this organism does not reutilize trehalose (Section 5.1.1), the excretion of trehalose is essentially a complete waste of glucose which lowers the achievable yield and cannot be recovered. The production of polysaccharides is not, however, uncommon in fermentations conducted under nitrogen limitation in the presence of excess carbohydrate substrate.

The accumulation of L-valine in such appreciable amounts is interesting for several reasons. First, it has been suggested that the production of certain amino acids (such as L-lysine) could be limited by the availability of NADPH for reductive biosynthetic reactions [Winter and Rao, 1989]. The pathway leading to L-valine was described previously in Figure 2.3. Since the synthesis of L-valine requires NADPH and since L-valine was synthesized in significant quantities along with L-lysine, it is unlikely that the availability of NADPH limits the synthesis of L-lysine.

The overproduction of L-valine under these fermentation conditions is consistent with the known regulatory mechanisms for this pathway (discussed

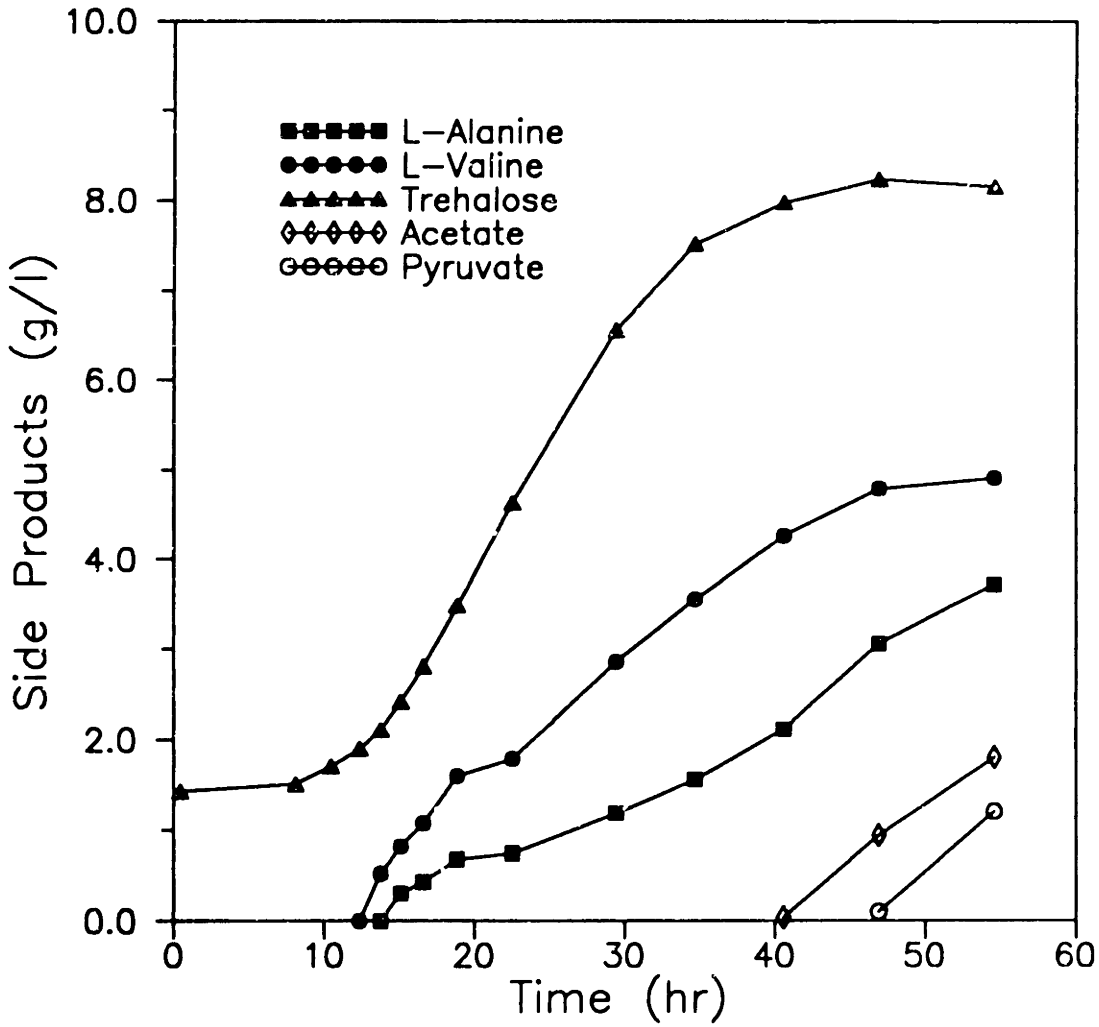

Figure 5.10. Side product accumulation during batch fermentation.

previously in Section 2.3.2). The fact that the culture is growth-limited by L-threonine requires that the culture also be starved for L-isoleucine, since L-threonine is the direct precursor to L-isoleucine. This then precludes the possibility of a concerted repressive effect of L-valine, L-isoleucine, and L-leucine upon the expression of α-acetolactate synthetase. Given that the inhibition of α-acetolactate synthetase by either L-valine, L-isoleucine, or L-leucine is only weak [Tsuchida and Momose, 1975], the possibility that pyruvate releases the enzyme from inhibition [Umbarger and Brown, 1958], and the fact that these fermentations are conducted at high glucose concentrations (thus, presumably high pyruvate levels), it is not surprising that this pathway is over-active. In addition, since this strain is auxotrophic for L-leucine, it is evident from Figure 2.4. that the flow into this pathway (from pyruvate) could easily be channeled toward L-valine, much the same as the homoserine auxotrophy causes flow to be redirected toward L-lysine. In the latter case, however, strong feedback regulation exists to minimize wasteful overproduction (this is the feedback which is bypassed by minimizing L-threonine levels).

The production of L-alanine also indicates the possibility that an excess of pyruvate stimulates side product formation. Since both L-alanine and L-valine are derived from pyruvate, their production diverts pyruvate from use in the production of L-lysine, which further decreases the observed yield of L-lysine from the carbon source. Furthermore, the slight excretion of pyruvate at the end of the fermentation suggests that even the side product pathways inactivate with time, leading to an excess of intracellular pyruvate which is subsequently excreted.

5.2.6 Summary of Batch Fermentation Results

The above features are typical of batch fermentations of *C. glutamicum* for L-lysine production. They further indicate that a batch operation is suboptimal and that an improved process could result by controlling the metabolic state of the organism through the effects that the environment can exert on the efficiency of protein turnover. This possibility is explored further in Sections 5.5 and 5.6 where a feed control law for fed-batch fermentations is developed based on the hypothesis that growth limitation by L-threonine, required to bypass the regulation of L-lysine production, results in a general decay of metabolic activity including a gradual deterioration of the L-lysine biosynthetic apparatus. This decline is evidenced by the declines in both the on-line respiratory measures and the off-line calculations of the fermentation performance variables. Clearly, both specific productivity and yield are sub-optimal during most of the time course of a typical batch fermentation. The above observations further suggest a control scheme to overcome the batch fermentation limitations based on respiration data as an on-line indicator of the biomass catalytic activity.

Furthermore, it is clear that, in the absence of any growth, biomass activity cannot be sustained and that vigorous growth will have a negative impact on overall yield. In order to optimally balance these effects, information about the dependence of the specific productivity and yield on the specific growth rate is needed. Such information, which can be quite useful in determining the appropriate growth rates for maximization of yield or productivity, is most effectively obtained through the use of continuous culture. Therefore, a fundamental study of the fermentation kinetics

was performed via an extensive set of continuous cultures, as discussed in the next section.

5.3 Steady-State Continuous Culture Characterization

Much of the literature on L-lysine overproduction has been strictly empirical and directed at analysis of strains obtained by manipulative measures such as mutation and selection. Quantitative measures have focused mainly on final L-lysine titers and yields, and average volumetric productivities obtained from batch cultures. Consequently, there is a distinct lack of kinetic data such as specific nutrient uptake and product formation rates, as well as data describing the variation, with time or specific growth rate, of important fermentation variables such as the yield or specific productivity.

In this phase of the work, the metabolic efficiency of the L-lysine producer was investigated in continuous cultures over a range of growth conditions. Continuous culture offers a sound basis for investigating relationships between fermentation variables which cannot otherwise be obtained using batch or fed-batch culture. Thus, a series of continuous culture experiments were performed to examine the effect of specific growth rate on fermentation yields, specific rates, productivities, and fluxes through the primary metabolism. This continuous culture study provides the basis for uncoupling the effects of biomass formation and L-lysine synthesis on fermentation performance, and also allows the characterization of locations within the metabolic network which are critical to the efficient overproduction of L-lysine. This is in contrast to previous studies on L-lysine production by continuous culture, which have

primarily dealt with the process aspects of the fermentation such as the operation of multi-stage systems [Beker, 1982; Michalski *et al.*, 1984] or the effects of feed sugar concentration [Hirao *et al.*, 1989], agitation rates and oxygen supply [Michalski *et al.*, 1984; Hirao *et al.*,1989] on process performance.

5.3.1 Dynamic Approach to Steady State

The chemostat was assumed to have reached a steady state when the measured variables remained constant, or near constant, for at least three to five residence times (perturbations to a process which responds exponentially in nature should be damped out by 95 - 99 percent in three to five characteristic times). Due to inherent reversion instabilities with the strain, to be discussed in Section 5.4, these steady states were never maintained indefinitely. Usually, the system progressed to a second, long-term steady state, corresponding to displacement of the L-homoserine auxotrophs by revertant cells. Only the short-term steady state behavior is discussed here as this is the most relevant and informative about L-lysine overproduction.

Examples of dynamic approaches to the short-term steady states for dilution rates of 0.0333, 0.180, and 0.301 hr^{-1} are shown in Figures 5.11 through 5.13, respectively. Minor damped oscillations are visible in the process variable data and most dramatic in the off-gas data for D = 0.18 hr^{-1} (Figure 5.12). Similar data were obtained for 10 dilution rates between 0.033 and 0.30 hr^{-1}, although off-gas, dissolved oxygen, and cell count data were not obtained in all experiments.

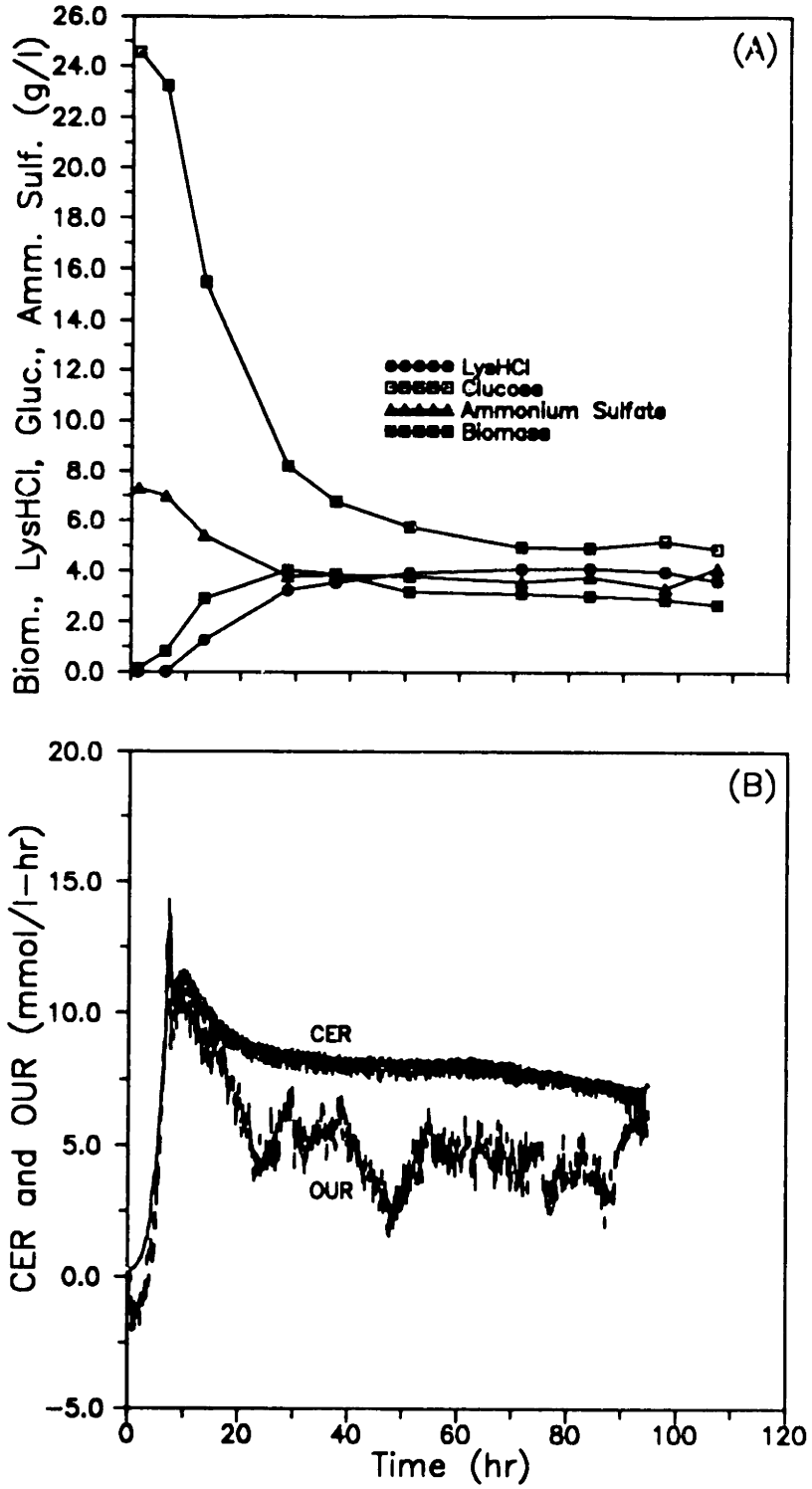

Figure 5.11. Continuous culture approach to steady state for D = 0.0333 hr^{-1}. (A) L-lysine·HCl, glucose, ammonium sulfate, and biomass concentrations. (B) Oxygen uptake and carbon dioxide evolution rates.

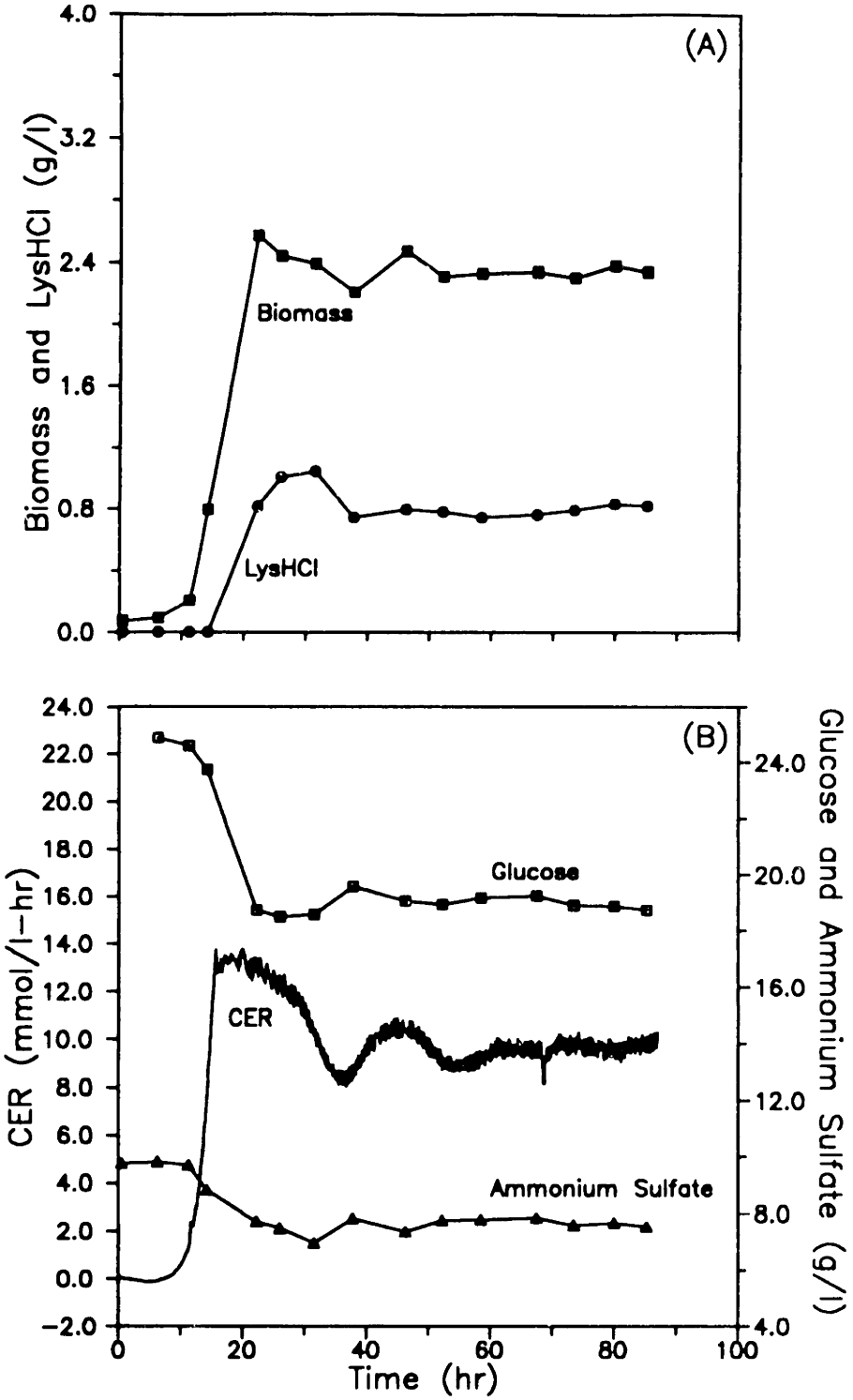

Figure 5.12. Continuous culture approach to steady state for D = 0.180 hr^{-1}. (A) L-lysine·HCl and biomass concentrations. (B) Glucose and ammonium sulfate concentrations and carbon dioxide evolution rate.

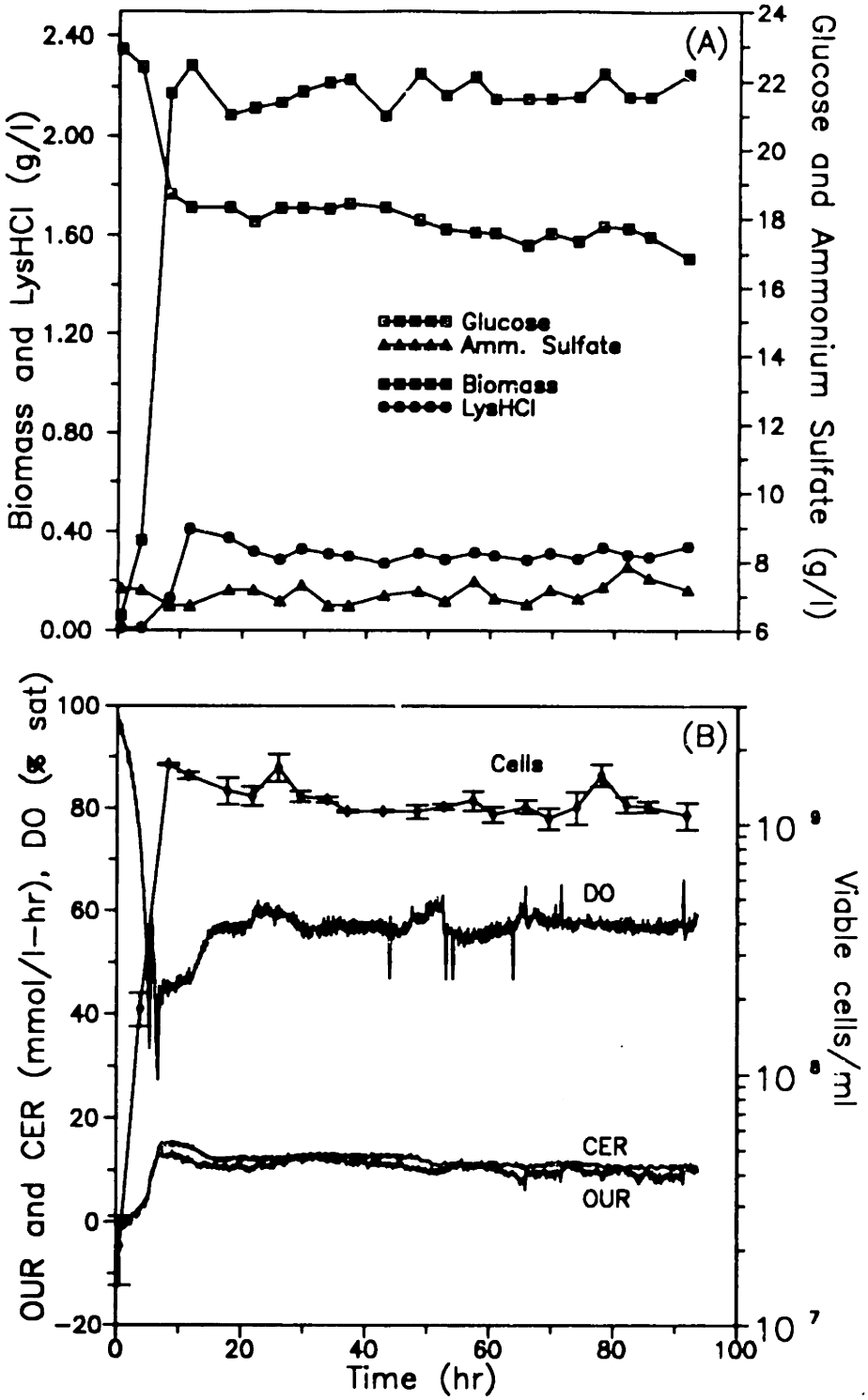

Figure 5.13. Continuous culture approach to steady state for D = 0.301 hr^{-1}. (A) Glucose, ammonium sulfate, biomass, and L-lysine·HCl concentrations. (B) Viable cell density, dissolved oxygen concentration, and oxygen uptake and carbon dioxide evolution rates.

5.3.2 Effect of Specific Growth Rate on Yields and Rates

In the continuous culture figures to follow, the error bars for directly measured quantities represent the standard deviation of multiple measurements. The error bars for derived quantities represent the statistically propagated error calculated from the standard deviations of the directly measured quantities. The steady-state data for these continuous culture experiments can be found in Table C.1 of Appendix C.

Figure 5.14 shows steady state biomass and L-lysine concentrations as a function of dilution rate, which is assumed equal to the specific growth rate. There is relatively little change in the level of biomass while there is more than an eight-fold change in L-lysine concentration over the range studied.

It is of interest to determine the yield of cell mass on the growth limiting nutrient (L-threonine). Limiting growth on an essential amino acid should, in effect, be limiting growth by limiting protein synthesis. It could be expected then to see results similar to a general nitrogen-limited (such as NH_3) continuous culture of a prototrophic microbe. The L-threonine concentration in the feed was 100 mg/l for all experiments and, at all dilution rates studied, the steady state L-threonine concentrations were found to be below the detection limit (5 mg/l). Assuming then complete consumption of L-threonine by the culture yields an error of no more than 5 percent. Based on this assumption, the specific L-threonine uptake rate and cell mass yield were determined and are shown as functions of specific growth rate in Figure 5.15. The cell mass yield on L-threonine decreases with increasing specific growth rate, a phenomenon reported by other researchers investigating nitrogen limited continuous cultures [Senior, 1975; Wang *et al.*, 1979] and attributed to the

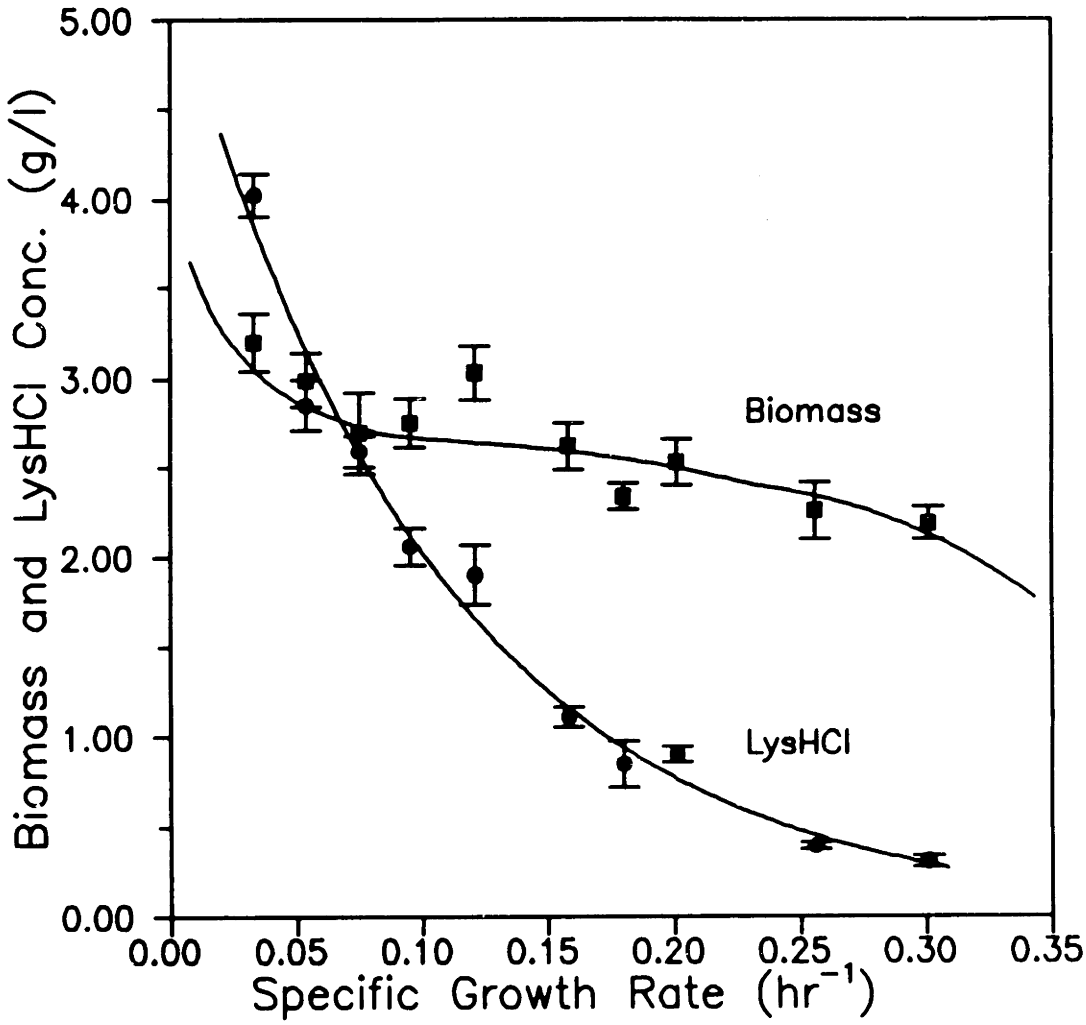

Figure 5.14. Steady-state biomass and L-lysine·HCl concentrations vs. specific growth rate.

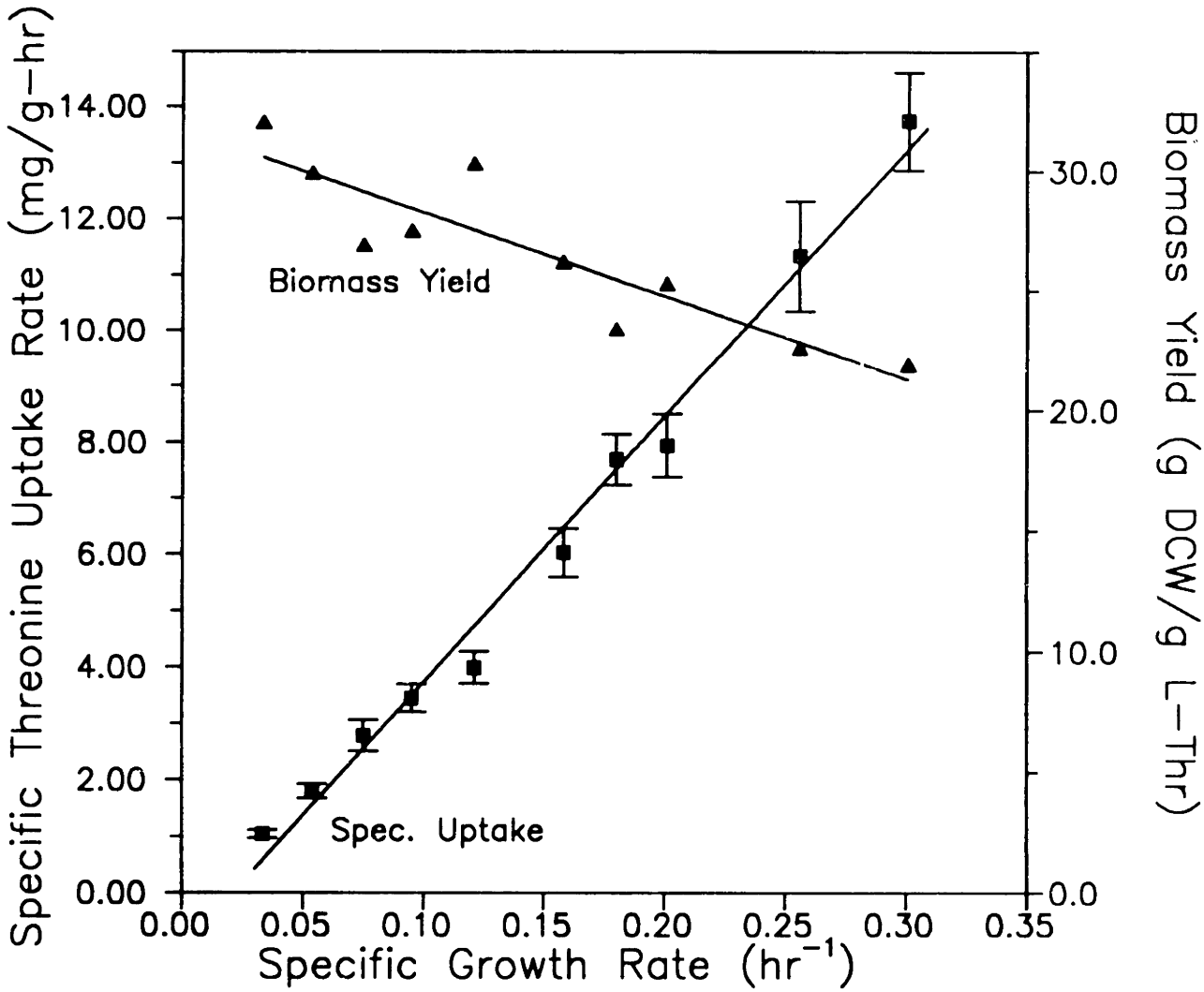

Figure 5.15. Steady-state specific L-threonine uptake rate and cell mass yield on L-threonine vs. specific growth rate.

accumulation of reserves of carbon-energy compounds such as polysaccharides. The specific L-threonine uptake rate is seen to be approximately proportional to the specific growth rate in the range of growth rate studied, a result consistent with the hypothesis that L-threonine is most likely used only for biomass production.

The specific glucose and ammonia uptake rates are shown as functions of specific growth rate in Figure 5.16A. The uptake rates of both nutrients exhibit saturation behavior with increasing growth rate. The saturation behavior is consistent with the fact that the specific productivity of L-lysine drops off at higher specific growth rates (described below) since glucose and ammonia are used not only for biomass formation but also for product formation. Figure 5.16B shows Lineweaver-Burke plots for both glucose and ammonia uptake. It is interesting to note that the "half-saturation" constants for uptake of both molecules are quite similar at about 0.12 hr^{-1}.

The L-lysine specific productivity is shown as a function of specific growth rate in Figure 5.17. The initial increase in specific productivity indicates a growth-associated type of product formation at the lower specific growth rates (less than about 0.1 hr^{-1}). The specific productivity appears to remain constant through the intermediate specific growth rate range (0.1 - 0.2 hr^{-1}), indicating a region of non-growth associated product formation. At specific growth rates greater than 0.2 hr^{-1}, the productivity appears to decrease. The reason for this decline in productivity is unknown; it may be due to sufficiently high intracellular levels of L-threonine to feedback-inhibit aspartate kinase in concert with L-lysine. The inability to measure the residual L-threonine levels in the reactor effluent makes it impossible to quantitate an effect of extracellular L-threonine on product synthesis and it was not

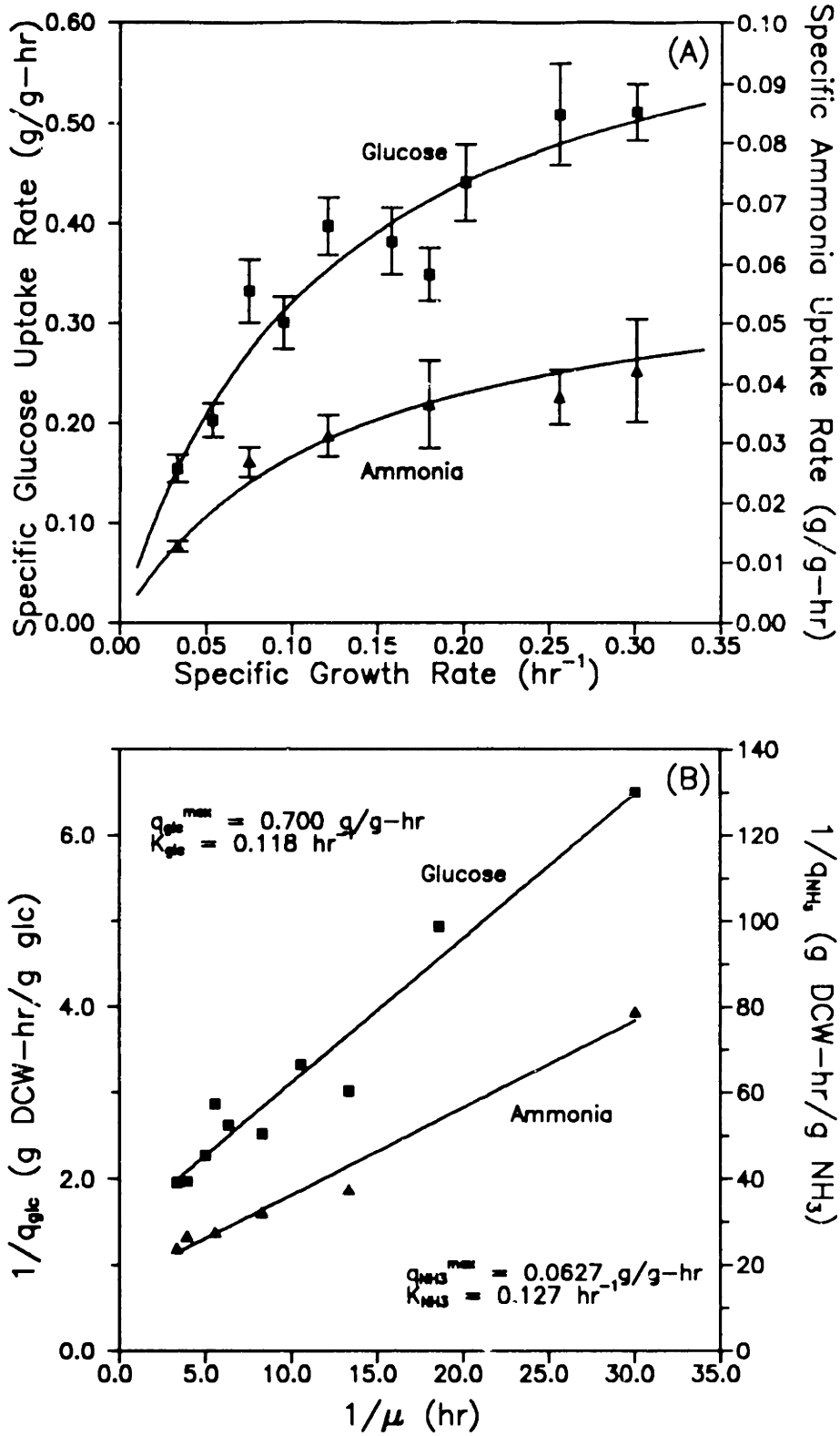

Figure 5.16. Steady-state specific glucose and ammonia uptake rate data. (A) Specific rates vs. specific growth rate. Solid lines indicate saturation model fits to the experimental data. (B) Lineweaver-Burke inverse plots for determination of saturation model parameters.

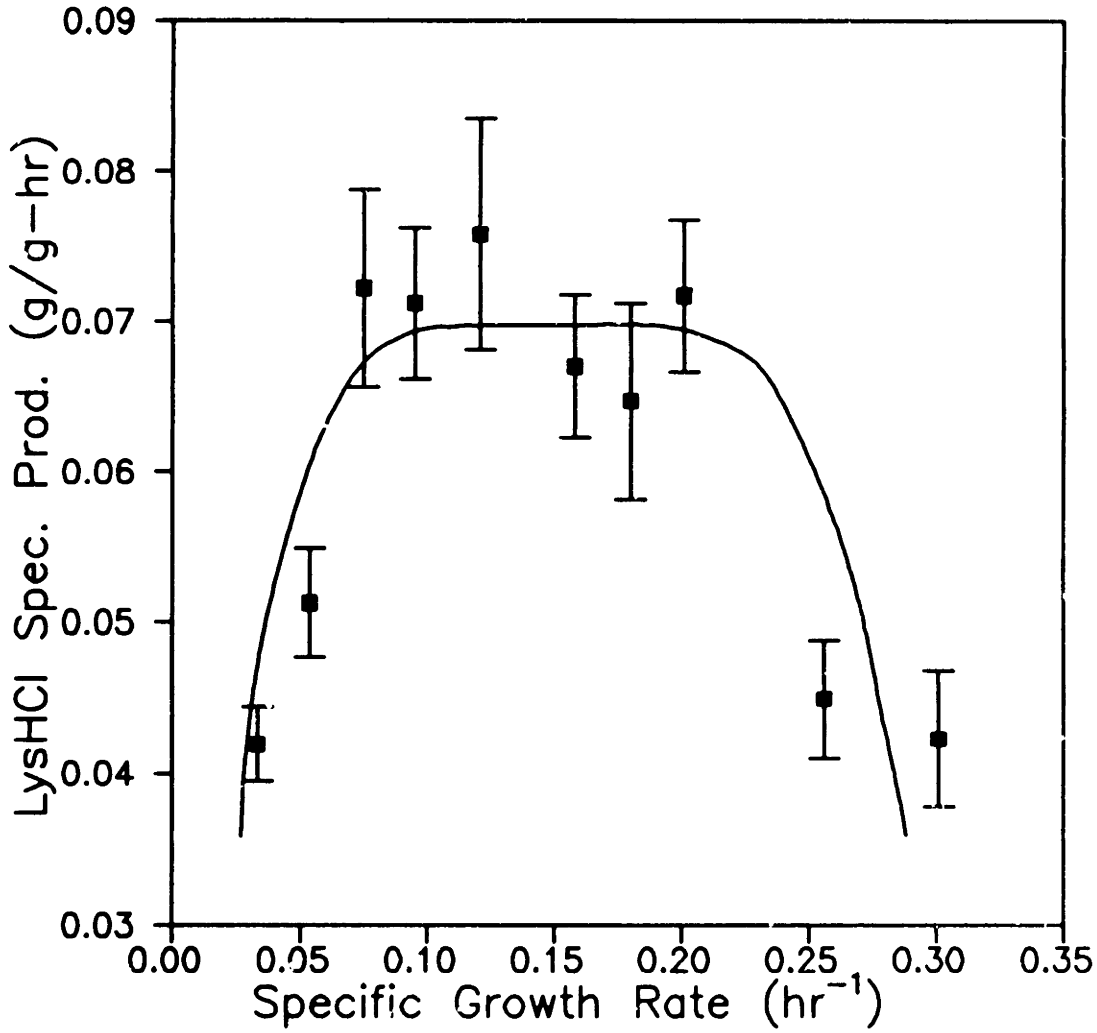

Figure 5.17. Steady-state L-lysine·HCl specific productivity vs. specific growth rate.

attempted to measure intracellular L-threonine levels.

The specific oxygen uptake and carbon dioxide production rates, and the respiratory quotient, RQ (CER/OUR), are shown as functions of specific growth rate in Figure 5.18. The striking feature here is the dramatic increase in respiratory quotient with decreasing specific growth rate. This is caused by an increasing diversion of carbon towards L-lysine synthesis, as opposed to biomass formation, as the specific growth rate decreases. Consequently, the contribution of the L-lysine synthesis reactions to the overall respiratory characteristics of the culture becomes more pronounced and RQ increases as growth rate decreases.

The observed yields of L-lysine from glucose and ammonia are shown as functions of specific growth rate in Figure 5.19. As with the case of the respiratory quotient, the observed yields increase as the specific growth rate decreases. Again, this is a reflection of the fact that the fractions of glucose and ammonia utilized for biomass synthesis decrease as the rate of growth decreases. Since L-lysine synthesis presumably continues at uninhibited rates (due to the L-threonine limitation), the fractions of glucose and ammonia diverted to L-lysine synthesis increase as growth decreases.

Figure 5.20 shows the direct relationship between observed yield and respiratory quotient. As was shown through the use of stoichiometric balances, the segment of metabolism leading to L-lysine synthesis produces more carbon dioxide than it consumes oxygen and, therefore, enhancement of L-lysine production increases the respiratory quotient above the "growth" value of unity (approximately).

The carbon and nitrogen material balances, for experiments in which sufficient measurements were available to close such a balance, typically showed near 90

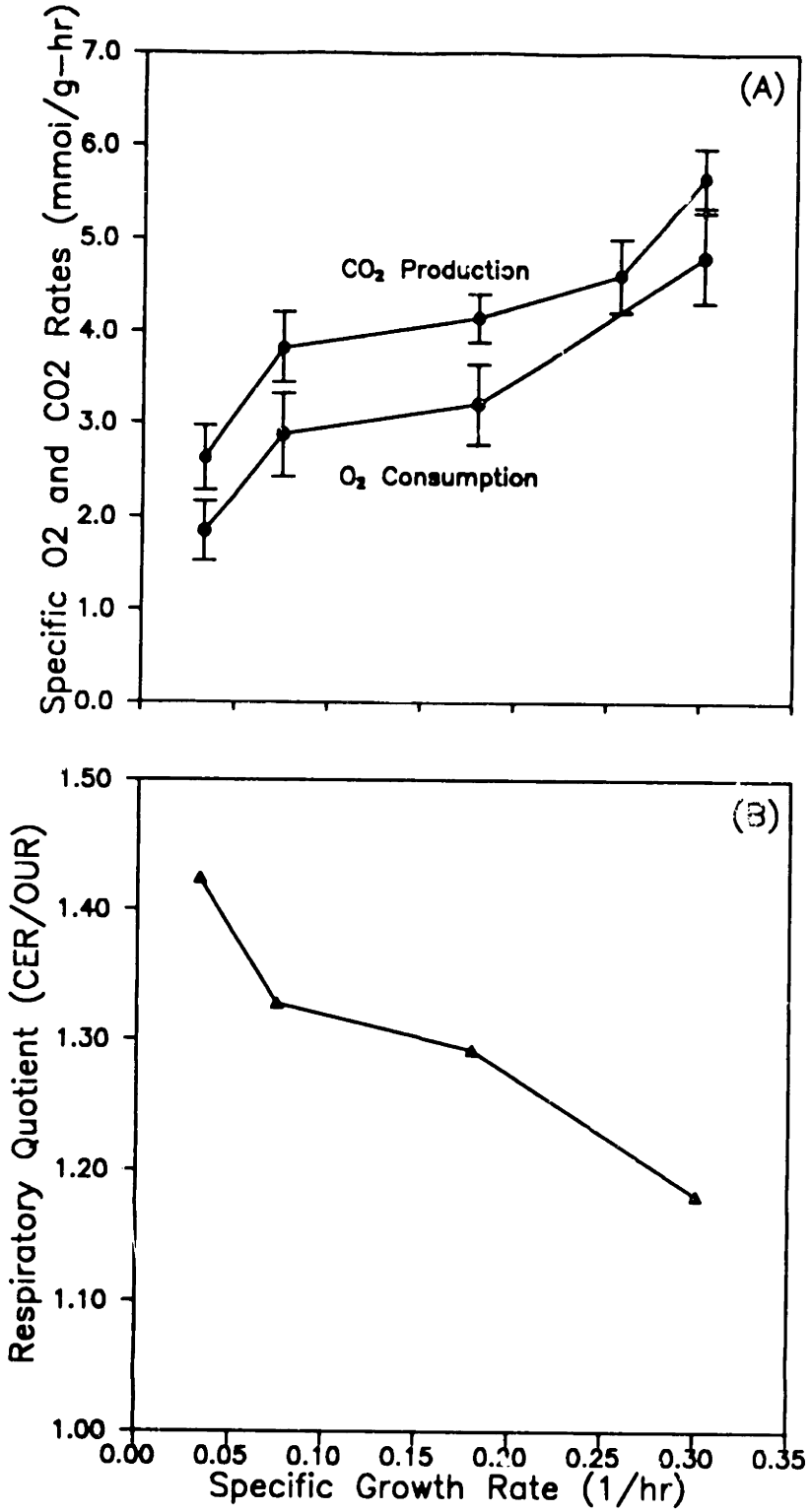

Figure 5.18. Steady-state respiratory data. (A) Specific OUR and specific CER vs. specific growth rate. (B) Respiratory quotient, RQ, vs. specific growth rate.

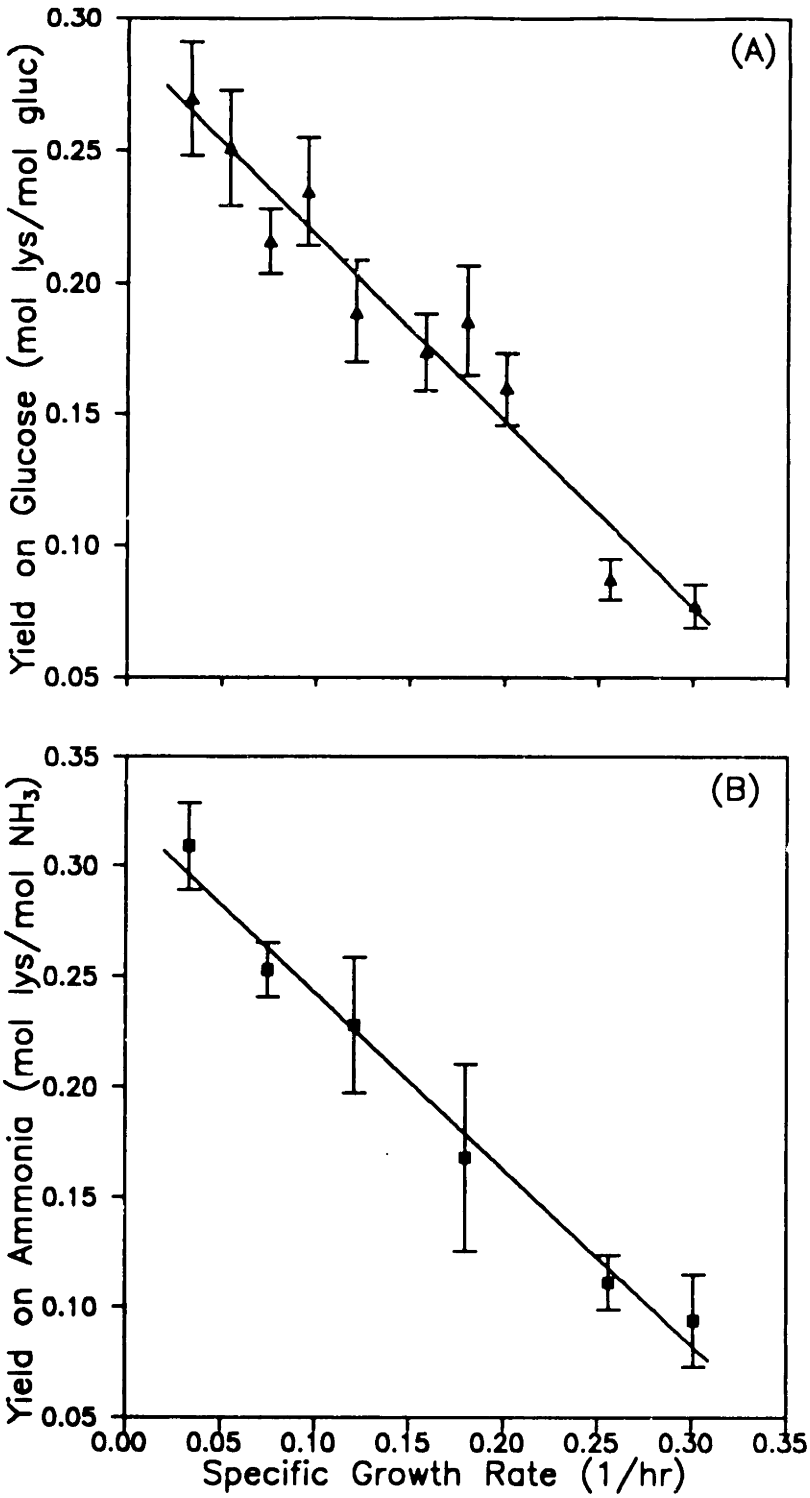

Figure 5.19. Steady-state observed L-lysine yields vs. specific growth rate. (A) L-lysine yield on glucose. (B) L-Lysine yield on ammonia.

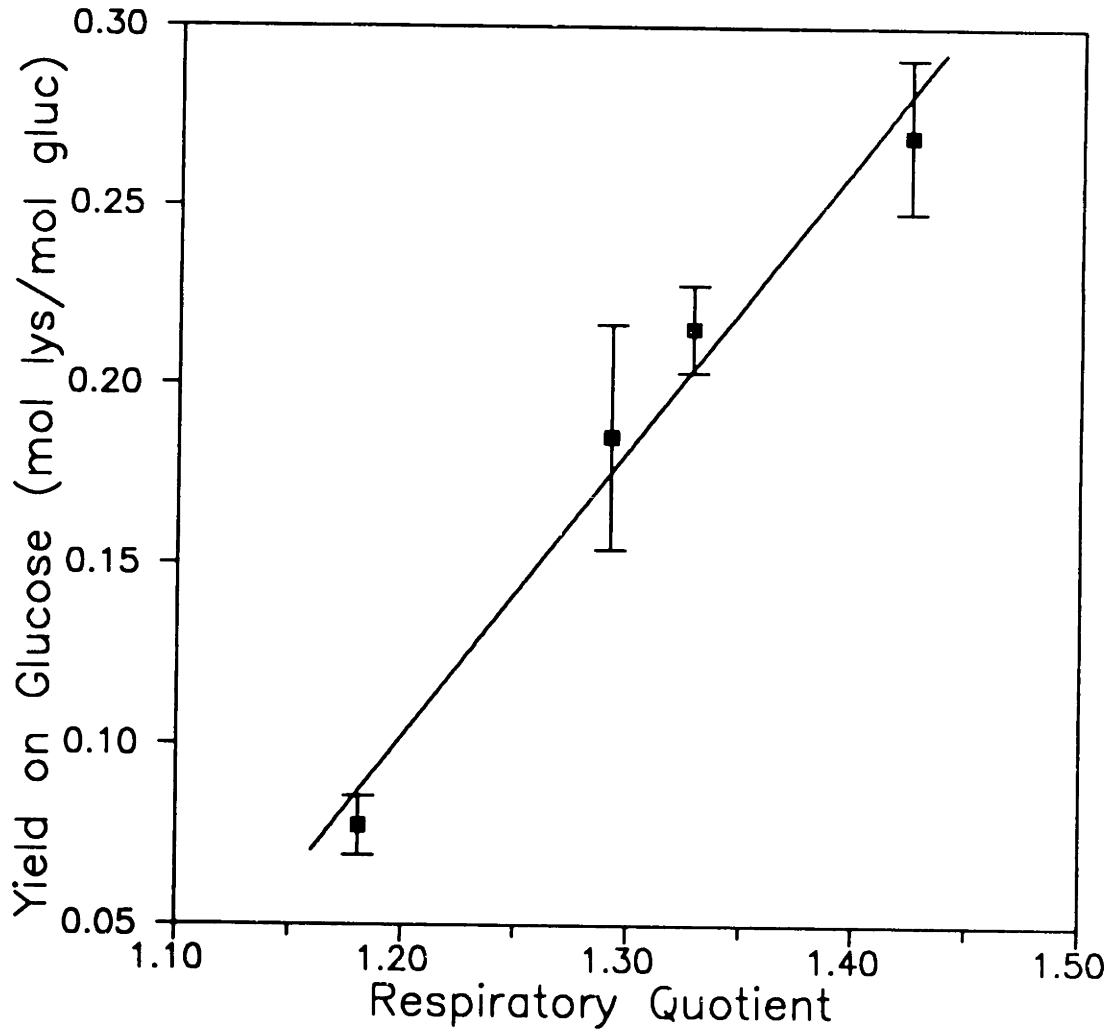

Figure 5.20. Correlation between steady-state observed L-lysine yield on glucose and steady-state respiratory quotient.

percent closure, as seen in Figure 5.21. Analyses for amino acid side products by OPA derivatization revealed the presence of only minor quantities of L-alanine (<15 mg/l), L-valine (<15 mg/l), L-glutamate (<10 mg/l), and two unknown peaks (concentrations estimated at less than 10 and 25 mg/l, assuming molecular weights of 150 g/mol).

5.3.3 Intrinsic Yield Estimation from Observed Yields

The set of continuous culture data presented in the previous section can be used to decouple the effects of biomass synthesis and product formation on overall fermentation yields. For the case of continuous L-lysine production, a steady-state glucose balance can be written as:

$$D(G_f - G) = \frac{DB}{Y_{B/G}} + \frac{DL}{Y_{L/G}} + mB \qquad 5.2$$

where D is the dilution rate, G and G_f are the residual glucose and glucose feed concentrations, B is the biomass concentration, L is the L-lysine concentration, m is the maintenance coefficient, and $Y_{B/G}$ and $Y_{L/G}$ are the conversion yields of glucose to biomass and L-lysine, respectively. Equation 5.2 assumes that the consumed glucose is converted to biomass and L-lysine and also used to satisfy any maintenance needs of the culture. Glucose oxidized to CO_2 in the generation of energy for biosynthesis is implicitly included in the term accounting for glucose converted to biomass so as to allow the obtained biomass yield coefficient to be compared with

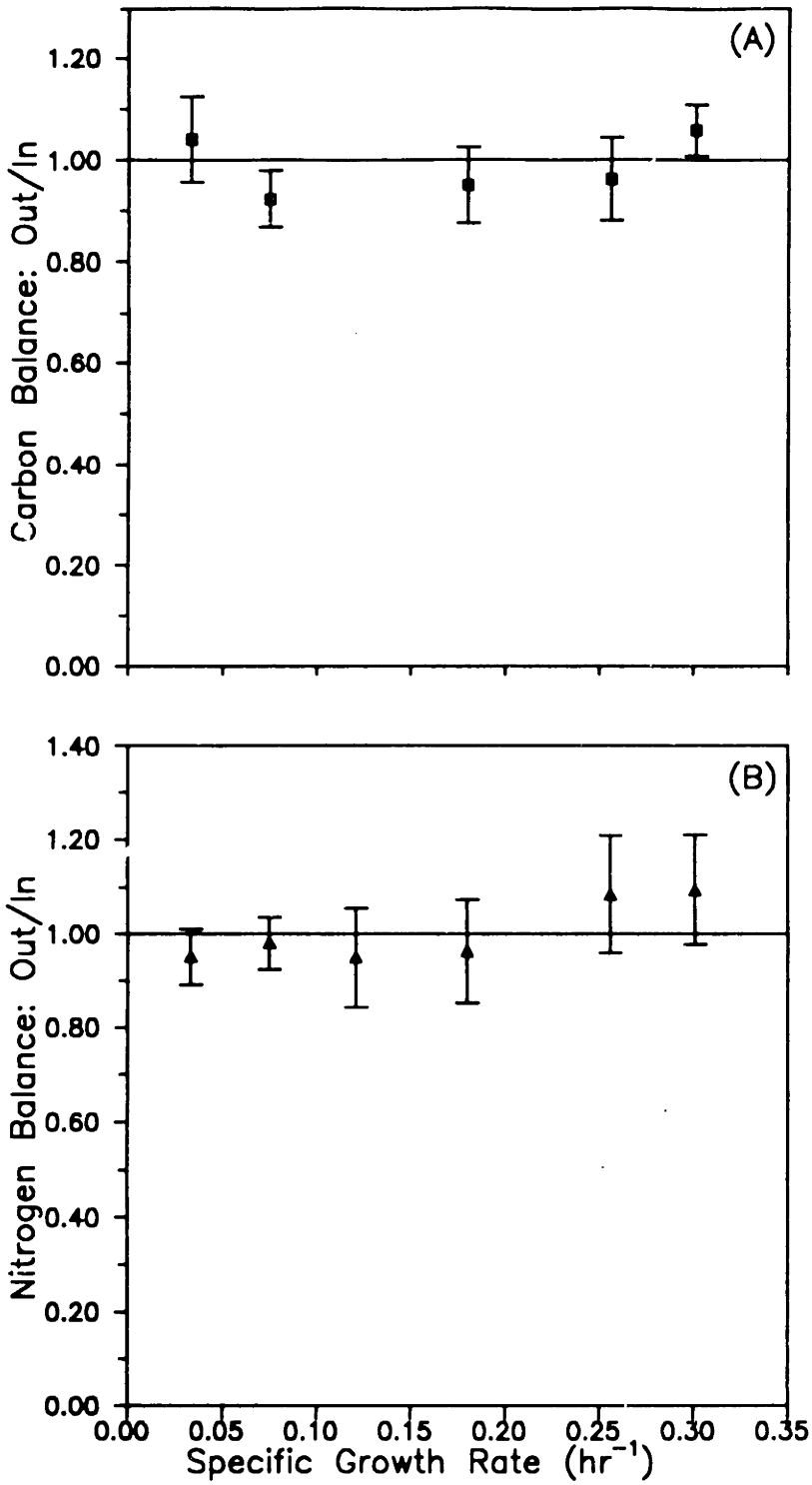

Figure 5.21. Continuous culture material balances at steady state. (A) Carbon balance. (B) Nitrogen balance.

typical biomass yields reported from aerobic growth on glucose. Since the production of L-lysine from glucose, ammonia, and oxygen provides a net ATP production, it is reasonable to conclude that the majority of CO_2 is associated with glucose dissimilation and biosynthesis purposes. Assuming that the intrinsic yields and maintenance coefficient are constant over the range of growth rate (dilution rate) studied, Equation 5.2 can be rearranged to yield the linear relationship:

$$\frac{1}{Y_o} = \frac{1}{Y_{L/G}} + \frac{1}{Y_{B/G}}\left(\frac{B}{L}\right) + m\left(\frac{B}{DL}\right) \qquad 5.3$$

where Y_o is the observed overall yield of L-lysine on glucose, $L/(G_f - G)$. Equation 5.3 suggests that plotting $1/Y_o$ versus B/L (the ratio of steady-state biomass to L-lysine concentrations), and B/DL (the ratio of steady-state biomass concentration to L-lysine volumetric productivity), in a three dimensional space should yield a plane with sufficient information to allow estimation of the yields and the maintenance term.

Due to the relatively small magnitude of the latter, such a multi-linear plot in three-dimensions was not attempted here. Figure 5.22 shows a plot of 1/Yo versus B/L (maintenance contribution assumed negligible), along with the results of the multi-linear regression of the continuous culture data to Equation 5.3. The data appear linear due to the relatively small contribution of the maintenance term to the glucose balance (assuming m to be zero in Equation 5.3 and recalculating the regression coefficients from the resulting linear relationship changes the intrinsic yield coefficients less than 2 percent). The intrinsic yield coefficient for L-lysine is 0.41±0.08 mol L-lysine/mol glucose (90% confidence interval), showing that the

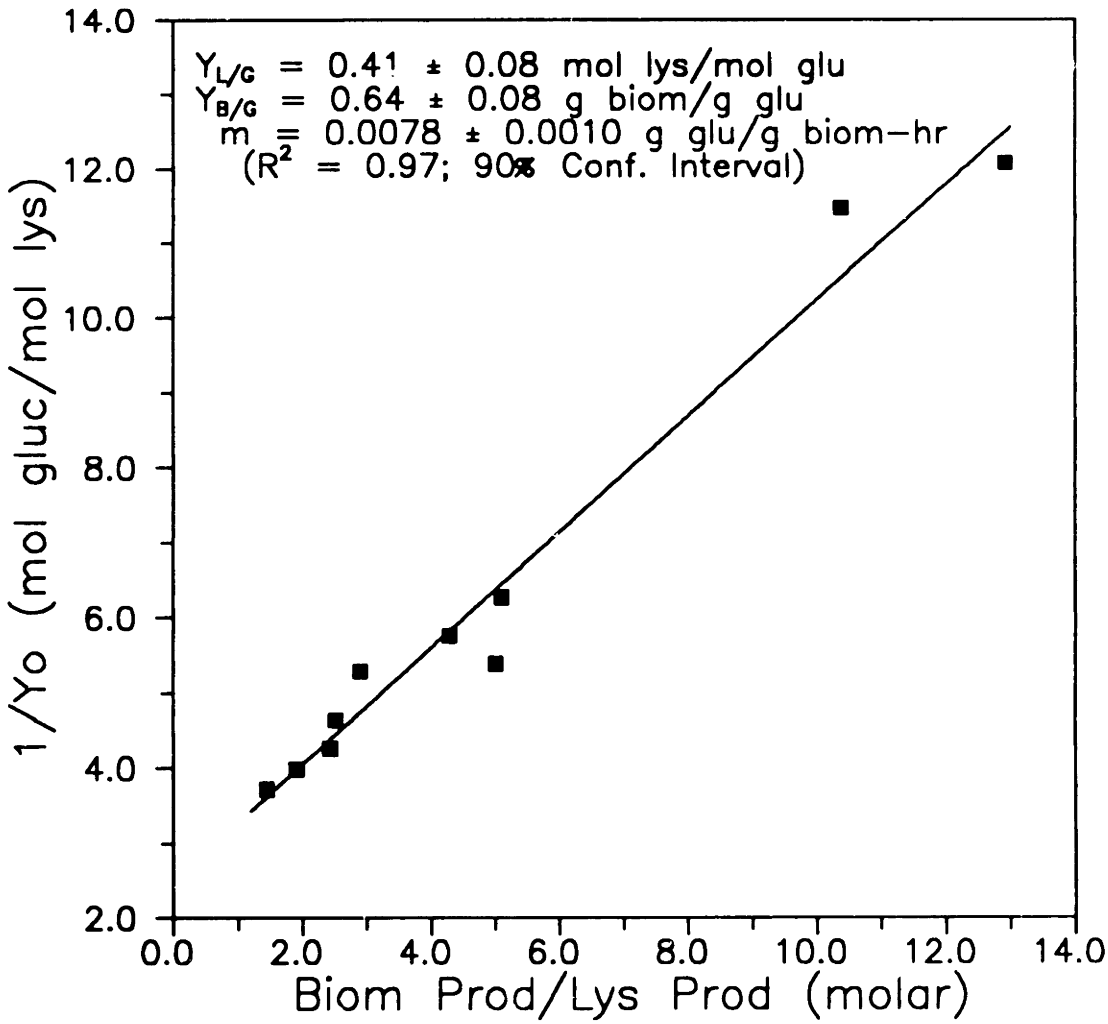

Figure 5.22. Correlation for intrinsic biomass and L-lysine yields on glucose.

observed overall yields are only about one half of the true product yield of glucose conversion to L-lysine. The fact that the intrinsic L-lysine yield coefficient is only slightly more than half of the calculated theoretical maximum yield of 0.75 may indicate losses of carbon due to futile cycles and excess activity in the TCA cycle, as will be discussed further in the next section. The intrinsic biomass yield coefficient is 0.64±0.08 g biomass/g glucose, which is at the high end of what is typically observed for aerobic biomass production (0.4 - 0.6). However, 5 to 6 percent of the biomass carbon is derived from the three essential amino acids provided in the medium and thus the yield on glucose is closer to 0.60±0.08 g/g (assuming the supplied amino acids are used exclusively for protein synthesis, which is in line with other observations). The calculated maintenance coefficient of 7.8±1.0 mg glucose/g biomass/hr is indeed small, though not unreasonable.

A similar analysis for the observed yield on the nitrogen source, NH_3, also produces useful information. Neglecting any maintenance consumption of NH_3, a steady-state balance on ammonia leads to the linear relationship:

$$\frac{1}{Y_{o,N}} = \frac{1}{Y_{L/N}} + \frac{1}{Y_{B/N}}\left(\frac{B}{L}\right) \qquad 5.4$$

where $Y_{o,N}$ is the observed yield on ammonia (mol L-lysine/mol NH_3), and $Y_{B/N}$ and $Y_{L/N}$ are the conversion yields of ammonia to biomass and L-lysine, respectively. Figure 5.23 shows a plot of $1/Y_{o,N}$ versus B/L, along with the results of the linear regression of the continuous culture data to Equation 5.4. The intrinsic L-lysine yield from ammonia, $Y_{L/N}$, is estimated to be 0.40±0.05 mol L-lysine/mol NH_3, or about 80

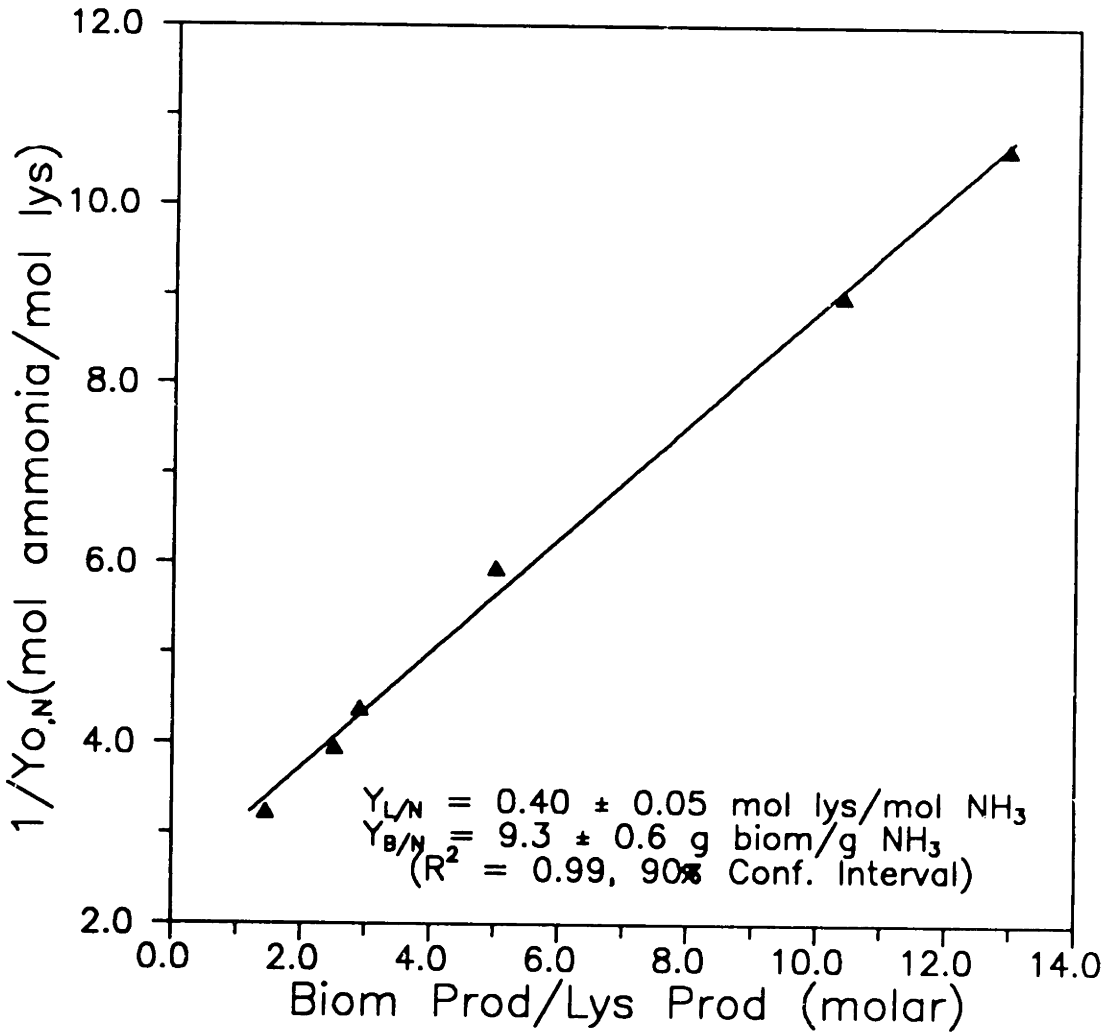

Figure 5.23. Correlation for intrinsic biomass and L-lysine yields on ammonia.

percent of the theoretical value of 0.50. The intrinsic biomass yield on NH_3, $Y_{B/N}$, is estimated to be 9.3±0.6 g biomass/g NH_3. However, between 6 and 7 percent of the biomass nitrogen is derived from the three essential amino acids provided in the medium, so this yield is closer to 8.7±0.6 g biomass/g NH_3 (assuming the supplied amino acids are used exclusively for protein synthesis).

5.3.4 Intracellular Flux Estimation

The continuous culture data provide a convenient set of extracellular flux measurements (biomass, glucose, L-lysine, ammonia, O_2, CO_2) which can be used to elucidate the biochemistry of L-lysine synthesis through intracellular flux analysis [Vallino and Stephanopoulos, 1989; Vallino, 1991]. This method combines the known metabolic pathways of the organism with a pseudo-steady-state approximation for intracellular metabolite concentrations to generate a mathematical representation of the metabolic flows. Figure 5.24 depicts a simplified network for L-lysine biosynthesis by *C. glutamicum* including the main energy and metabolite-generating bioreactions of glycolysis, the pentose phosphate cycle, and the tricarboxylic acid (TCA) cycle, as well as the aspartate family of amino acids leading to L-lysine. Biomass synthesis is treated as a lumped reaction which draws energy and metabolites from the main metabolic branches according to the stoichiometry given by Ingraham *et al.* (1983). The ATP requirement in the lumped biomass equation is the theoretical amount corresponding to an ATP yield of 28 g of biomass synthesized per mole of ATP consumed [Stouthamer, 1973] and the efficiency of oxidative phosphorylation, or P/O ratio, is taken as 2 mol ATP formed per atom of oxygen reduced [Ingraham *et al.*,

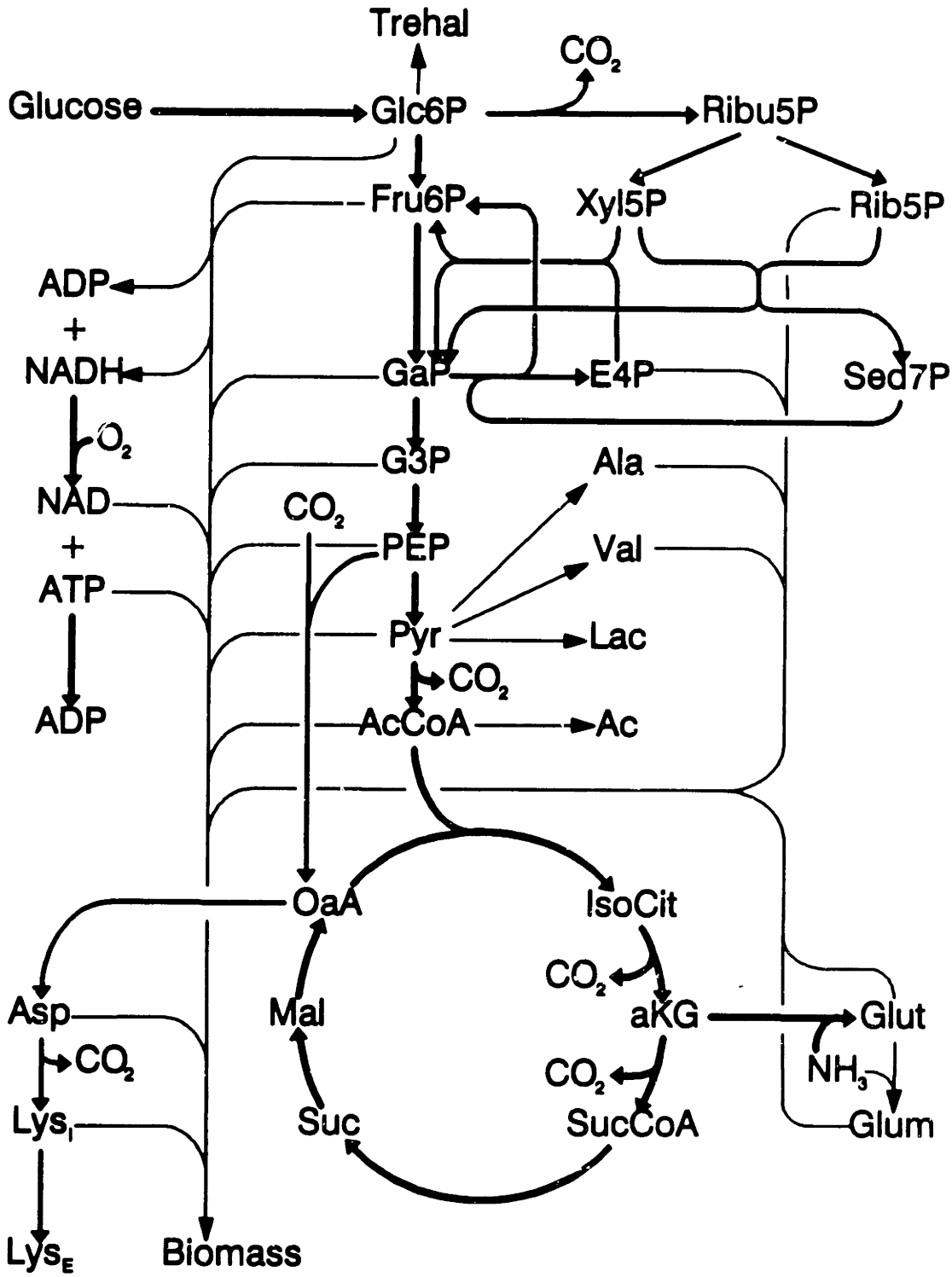

Figure 5.24. Simplified representation of *C. glutamicum* primary metabolism [adapted from Vallino (1991)].

1983].

Following a similar approach established for butyric acid bacteria [Papoutsakis, 1984], a mathematical representation of the metabolic network of Figure 5.24 is constructed by forming a material balance for each metabolite of the network as a function of the reactions producing or consuming that metabolite. The objective is to determine the fluxes of carbon through the reaction segments of Figure 5.24 from measurements of the time rates of change of extracellular metabolites, assuming that intracellular metabolite pools are at steady state. This approach yields a total of 34 unknown fluxes to be determined from 37 stoichiometric (metabolite) balances along with 6 extracellular measurements. For production of L-lysine, this system of linear equations is well-posed and can be solved by least squares inversion, provided at least three extracellular measurements are available [Vallino and Stephanopoulos, 1989; Vallino, 1991]. The analysis using this continuous culture data utilized the biochemistry set BS1 and the measurement set MS1 given by Vallino (1991) in his Appendix B.2.

A redundancy analysis [Romagnoli and Stephanopoulos, 1981; Wang and Stephanopoulos, 1983; Vallino and Stephanopoulos, 1989], which tests the consistency of the measurement set, was carried out in those instances when the number of measurements available rendered the system over-determined (hence the least squares solution rather than an exact solution of the linear equation set). This technique calculates a data set consistency index which indicates whether the extracellular metabolite flux measurement set satisfies biochemical (material balance) constraints, at a given level of statistical confidence. If a measurement set (at a given dilution rate) failed the consistency analysis at the 90 percent confidence level, the

redundant equations were used to check for the presence of gross measurement errors. In all cases in which a data set failed the consistency test, identification and deletion of a suspect measurement was always found to produce a consistent measurement set for which a least squares solution was subsequently determined.

The objective of this type of analysis is to obtain estimates of the fluxes of carbon through the primary metabolic pathways. Such estimates, in turn, provide information as to potential bottlenecks which may be limiting the rates or yields in L-lysine production.

One possibility is that the low L-lysine yields are the result of energy or ATP-limitation. The aforementioned analysis allows the calculation of the amount of ATP required for biomass and biomolecule synthesis, as well as the amount of ATP produced by the fueling reactions. Other, ill defined, ATP-consumption processes such as maintenance, futile cycles, transport costs or energy required to maintain concentration gradients have not been accounted for in the overall ATP consumption calculation. Instead, an excess of ATP, above theoretical, is determined to be produced by the cells at all continuous culture specific growth rates. This excess ATP production rate (normalized by the glucose consumption rate) is shown in Figure 5.25 as a function of the specific growth rate. Also shown in the figure is the estimated ATP consumption rate (normalized by the glucose consumption rate) for maintenance requirements, calculated by assuming that maintenance requires 10 mg glucose/g biomass/hr (8 mg/g-hr was the estimate obtained earlier) and that 26 moles of ATP can be produced per mole of glucose. Assuming that maintenance is the largest of the unaccounted ATP consumption terms, Figure 5.25 suggests that the production of L-lysine is not limited by the supply of ATP.

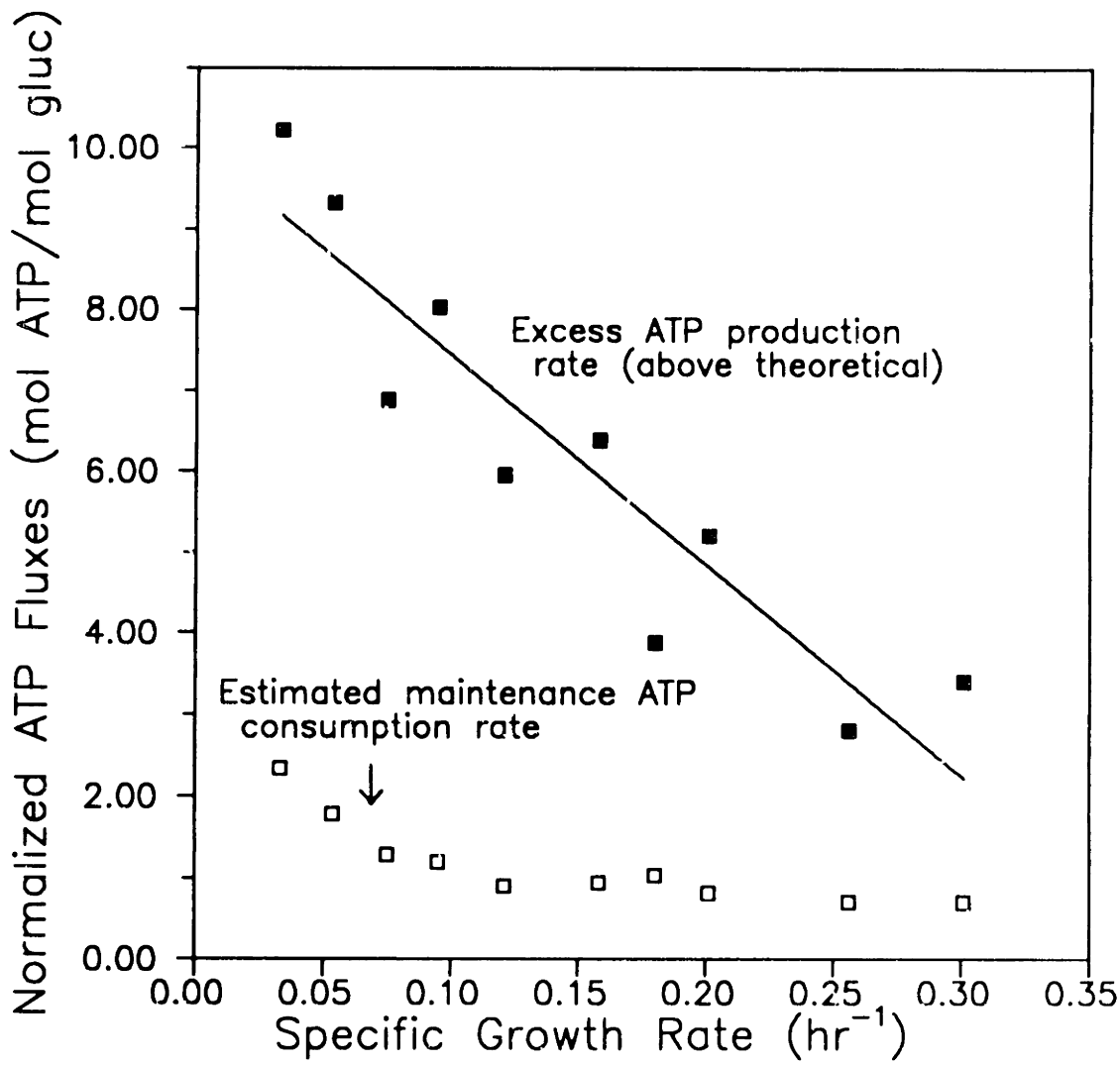

Figure 5.25. Intracellular flux calculation excess ATP production rate and calculated maintenance ATP consumption rate vs. specific growth rate.

The metabolic network for L-lysine synthesis contains about 35 nodes (branch points). However, a theoretical yield analysis [Vallino, 1991] has revealed that nodal split-ratios (the carbon flux through a branch normalized by the flux into the node) change at only a few nodes (the principal nodes), while partitioning of carbon at all other nodes remains independent of product yield. Partitioning of carbon at the principal nodes must be optimal for maximum L-lysine yield. If any of the principal nodes is rigid (*i.e.*, attempts at changing the nodal split-ratios are resisted by the imposed nodal control architecture), sub-maximal L-lysine yield will result. Therefore, investigations aimed at identifying metabolic bottlenecks need only focus at the principal nodes for L-lysine synthesis: the glucose-6-phosphate (G6P), phosphoenolpyruvate (PEP), and pyruvate (PYR) junctions. Vallino (1991) used experimental metabolic perturbations in batch culture to demonstrate that both the G6P and PYR nodes are flexible since the nodal split-ratios respond to meet metabolic requirements. Further reasoning indicated that the PEP node is strongly rigid.

Flux analysis applied to this continuous culture data yields some interesting results concerning the metabolite flow at the PEP node of the network. PEP has two metabolic fates: carboxylation (an anaplerotic reaction) to oxaloacetate (OAA) or conversion to pyruvate. Figure 5.26 shows the fraction of PEP converted to OAA by carboxylation (as opposed to being converted to pyruvate) as a function of the specific growth rate. The split at this node appears to be fairly constant over a wide range of specific growth rates, indicating that the regulation about this node may indeed be quite rigid. That is, the fraction of carbon entering the PEP node which leaves via a particular branch is strictly regulated at a relatively constant value, which

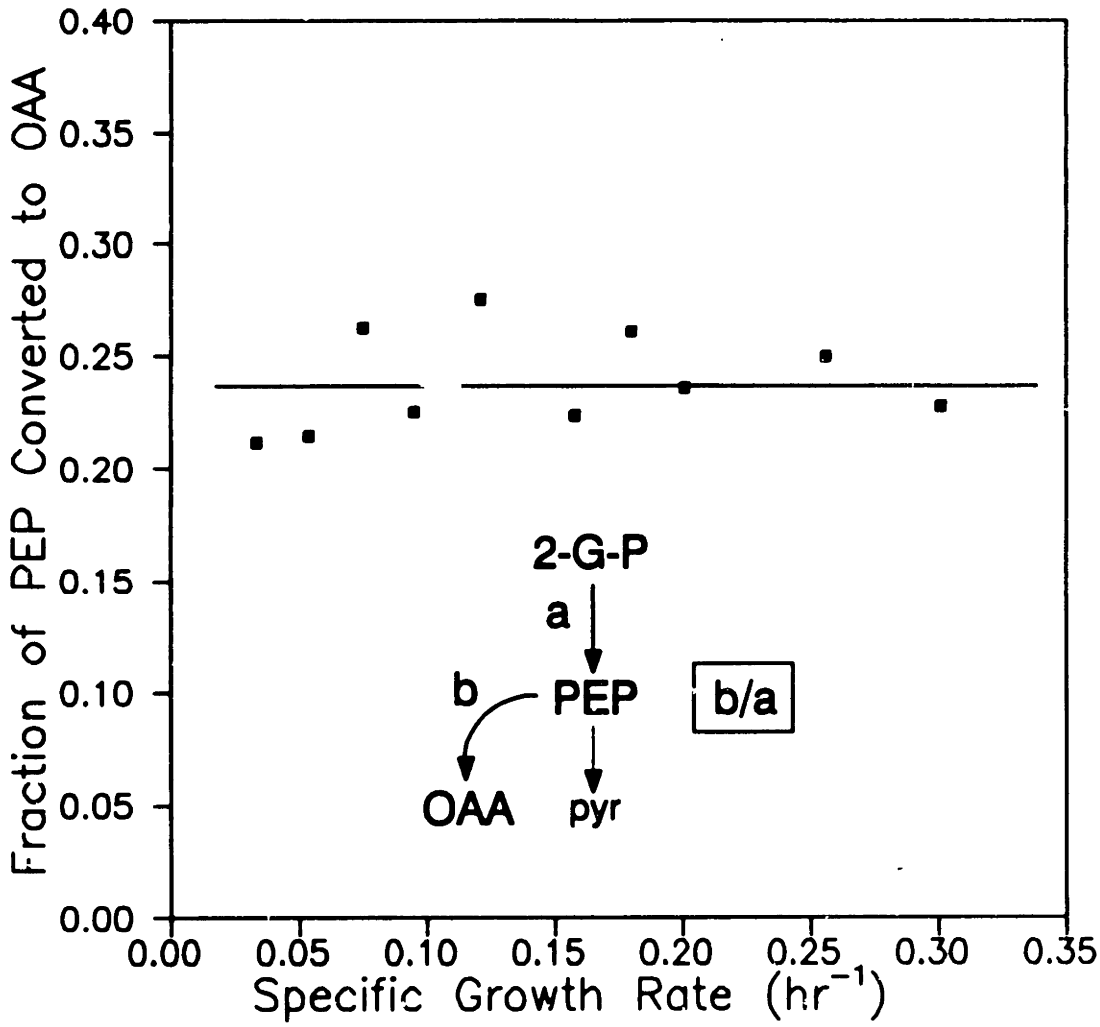

Figure 5.26. Intracellular flux calculation: fraction of PEP converted to OAA vs. specific growth rate.

makes it insensitive to metabolic perturbations. This finding is consistent with the conclusion reached by Vallino (1991) based on batch fermentation data. It is also noteworthy that three to four times as much PEP is converted to pyruvate as opposed to being converted to OAA. This may be an indication that the enzyme pyruvate kinase, PK (converts PEP to pyruvate), has a three to four-fold higher *in vivo* activity than PEP carboxylase, PPC (carboxylates PEP to OAA). Ozaki and Shiio (1979) reported that, for *B. flavum* under *in vitro* conditions, the apparent affinity of PEP for PK was about ten times higher than its affinity for PPC. It has also been documented [Mori and Shiio, 1985] that PPC is an allosteric enzyme strongly inhibited by aspartate and strongly activated by acetyl-coenzyme A. The concept of PEP nodal rigidity is consistent with these characteristics and has been verified by kinetic modeling of the enzymatic network at the PEP and PYR nodes [Vallino, 1991].

Under conditions where growth is significant, intermediates are drawn off the TCA cycle to form biomass. To replenish the TCA-cycle intermediates and keep the cycle functioning under these conditions, PEP is carboxylated to OAA. High L-lysine synthesis (even in the absence of biomass synthesis), would also require carboxylation of PEP to replace the OAA converted to aspartate en route to L-lysine.

Figure 5.27A shows, as a function of the specific growth rate, the fraction of OAA derived from PEP which ends up as aspartate. As the specific growth rate decreases, nearly all PEP converted to OAA ends up as aspartate (and is presumably converted to L-lysine). This result illustrates the increase in the carbon fraction allocated to L-lysine synthesis as the specific growth rate decreases, which is also reflected in the fact that the yield of L-lysine on glucose increases as growth rate

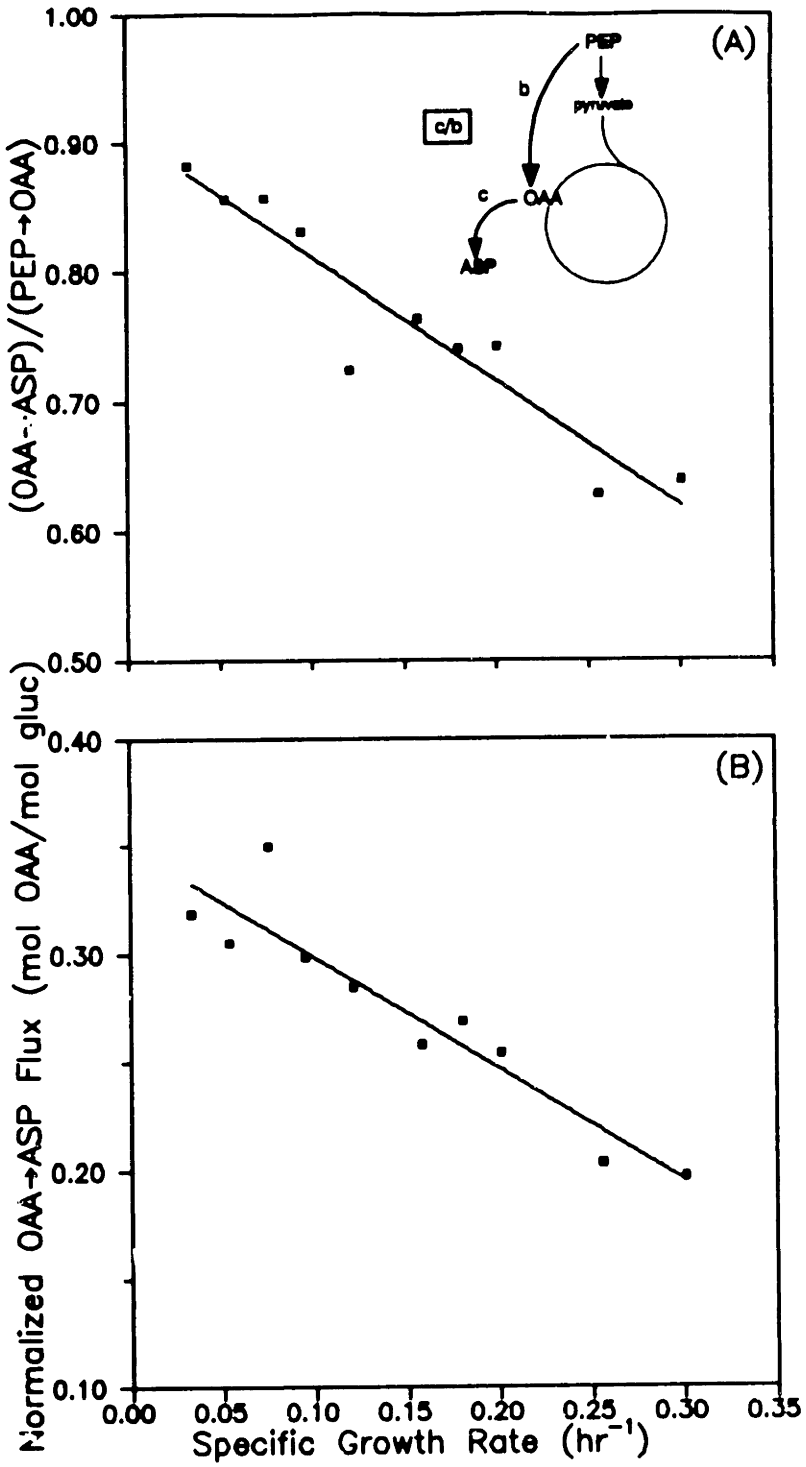

Figure 5.27. Intracellular flux calculations: fate of OAA vs. specific growth rate. (A) Fate of OAA derived from PEP. (B) OAA to ASP flux normalized by glucose flux.

decreases. As further illustration of this point, Figure 5.27B shows that the flux of OAA to aspartate, normalized by the glucose flux, increases with decreasing specific growth rate, again indicating the increased efficiency of glucose conversion to L-lysine as growth slows.

Figure 5.28 shows the fraction of OAA formed that gets converted to aspartate (OAA is formed by carboxylation of PEP and by oxidation of malate in the TCA cycle). The fraction is approximately constant at between 30 and 40 percent, indicating that there may be rigid regulation of the carbon distribution at this node as well. In light of the earlier observation of the increased conversion of PEP to aspartate with decreasing specific growth rate (Figure 5.27A), this constant split-ratio implies that the TCA cycle activity is high. Even though at low growth rates nearly all PEP carboxylated gets further converted to aspartate, significant amounts of glucose must be oxidized in the TCA cycle to maintain the constant split at the OAA node. This may be one reason the observed yields are so low, compared to theoretical, in this system. As discussed previously in Section 3.2.1, several researchers [Ozaki and Shiio, 1983; Tosaka *et al.*, 1985] have improved the L-lysine yield by using mutant strains with reduced TCA cycle enzyme activity (such as citrate synthase, pyruvate kinase, and pyruvate dehydrogenase).

5.3.5 Summary of Continuous Culture Characterization

This phase of the work investigated the effect of the specific growth rate on metabolism as it relates to overproduction of L-lysine in *C. glutamicum* fermentations. Of particular importance in such a characterization are the levels of catalytic activity

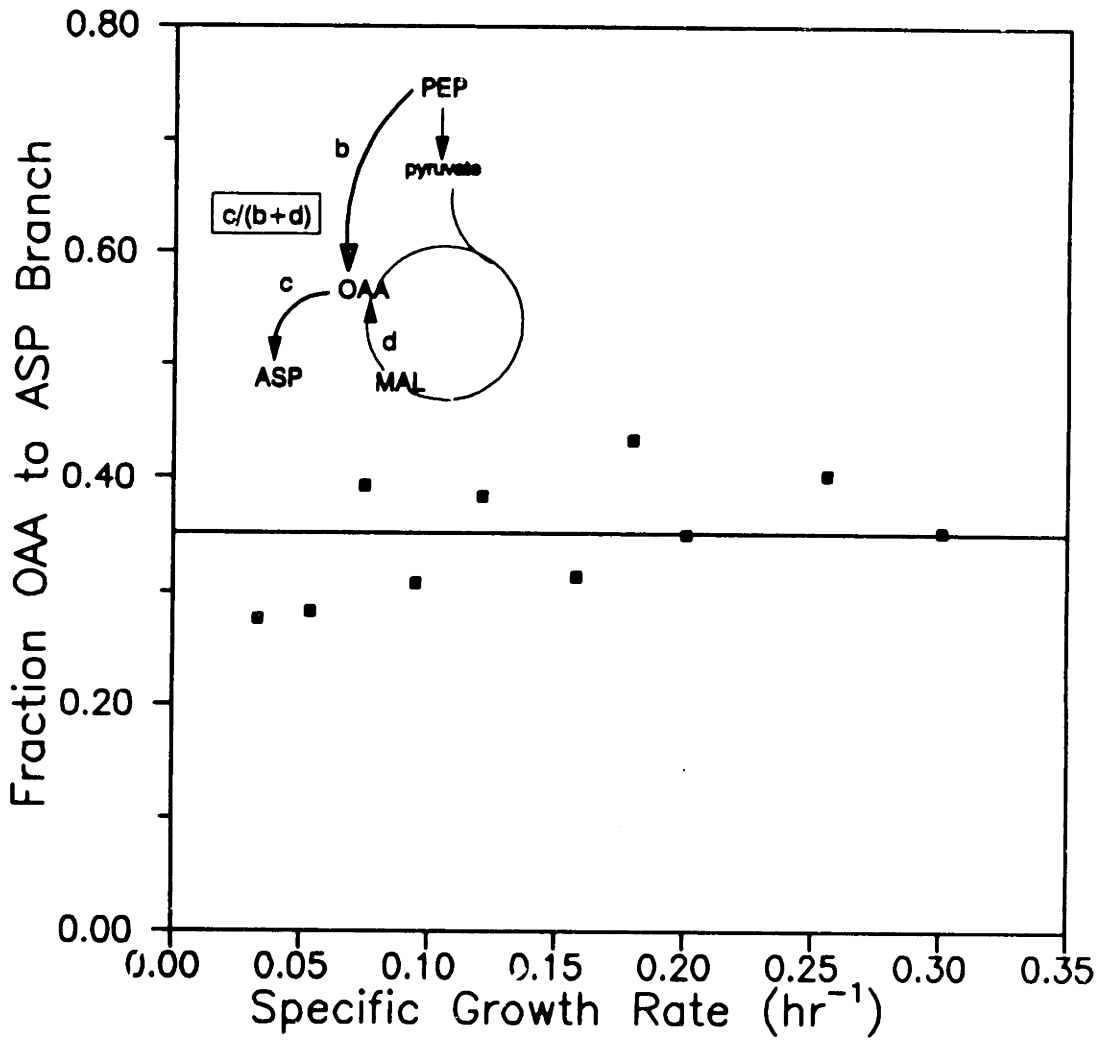

Figure 5.28. Intracellular flux calculation: fraction of OAA converted to ASP vs. specific growth rate.

achieved, namely the yield and specific productivity. Differences in the dependence of these two key parameters on the specific growth rate suggest that there may be different optimal operating strategies in continuous or fed-batch cultures for maximizing process yield or productivity. The data also show a direct correlation between the respiratory quotient and the channeling of carbon toward L-lysine synthesis, as reflected by the observed yield.

The metabolic flux modeling suggests that the production of ATP is not likely to be a limiting factor in L-lysine production and that a high TCA cycle activity coupled with rigid regulation of the metabolite flow at the PEP node is likely the cause of the large discrepancy between theoretical and actual yields. To increase product yield, it is clear that the flows of carbon at branch points must be manipulated and redirected toward L-lysine. The analysis has clearly pointed to the PEP node as a place where such modification is warranted in seeking yield improvement by strain manipulation. Recent work in this area includes the use of classical techniques to reduce the regulation of PPC [Yokata and Shiio, 1988] and recombinant DNA technology to increase the level of PPC [Sano *et al.*, 1987; Eikmanns *et al.*, 1989; Cremer *et al.*, 1991]. Current work in our laboratory by S. Park addresses the same problem (non-optimal distribution of carbon between the TCA cycle and the anaplerotic production of OAA) by the cloning and overexpression of a feedback insensitive pyruvate carboxylase to direct a greater fraction of pyruvate to OAA. The OAA node generally appears to be an important metabolic location. However, results of the intracellular flux analysis showed that under low biomass synthesis conditions, most of the PEP carboxylated eventually is converted to aspartate, and thus OAA does not really constitute a network node

under those conditions. Since most fermentations are carried out in batch mode and the majority of the L-lysine is produced after much of the biomass synthesis has occurred, OAA participates only marginally in the synthesis reactions of L-lysine. Nonetheless, reduction of carbon wasted in the TCA cycle would benefit yield, and as already mentioned, workers have looked at reduction of TCA cycle activity as a means of reducing the flow of metabolites such as pyruvate into the TCA cycle where they are simply oxidized to CO_2.

Most attempts to date at performance improvement in amino acid fermentations have involved manipulation of the biochemistry and genetics of the producing organisms. This phase of the work provides insight into how simple engineering approaches, such as manipulation of the cellular environment to maximize and maintain biomass catalytic activity, also offer promise in yield and productivity improvement.

5.4 Long-Term Continuous Culture Instability

As alluded to in the previous section, continuous cultures of this auxotrophic strain were subject to an instability which precluded the long-term maintenance of a steady state. This instability was studied over a range of dilution rates so as to develop a simple mathematical model of the system which could be used in predicting stability characteristics and consequently determining operating conditions which could minimize the instability problems.

5.4.1 Dynamics of Revertant Culture Takeover

Continuous cultures of *C. glutamicum* ATCC 21253 (Thr$^-$, Met$^-$, Leu$^-$) were periodically analyzed for revertant cells. Cells were isolated which no longer required L-threonine or L-methionine for growth, but still required L-leucine. These mutants were indistinguishable from the original strain in terms of colony morphology, size and shape under light microscopy, and gram-staining characteristics. This information strongly suggested that these mutants were *C. glutamicum* revertants which had recovered the characteristics of wild-type homoserine dehydrogenase and no longer required homoserine (or L-threonine and L-methionine) in the medium for growth (recall Figure 2.2).

Figure 5.29 shows the long term behavior of a continuous culture experiment, at a dilution rate D of 0.180 hr^{-1}, in which the homoserine dehydrogenase revertants took over the culture. A short-term quasi-steady state is achieved before the presence of the revertants is noticeable. The growth of the revertants (which are now limited in growth by the next limiting nutrient, assumed to be L-leucine) quickly outpaces the growth of the parent cells. The biomass concentration and oxygen consumption and carbon dioxide production increase exponentially as the revertant biomass concentration moves toward its steady state level.

Even though the revertant cells do not require L-threonine or L-methionine for growth, it is likely that they will consume these amino acids if they are available. They therefore directly compete with the auxotrophic parent strain for these amino acids (as well as for L-leucine and other nutrients). Their growth advantage lies in the fact that they are not growth limited by L-threonine, as are the auxotrophs, yet they will consume L-threonine and thus decrease the L-threonine available for the auxotrophs. The decreased L-threonine concentration has no effect on the revertants

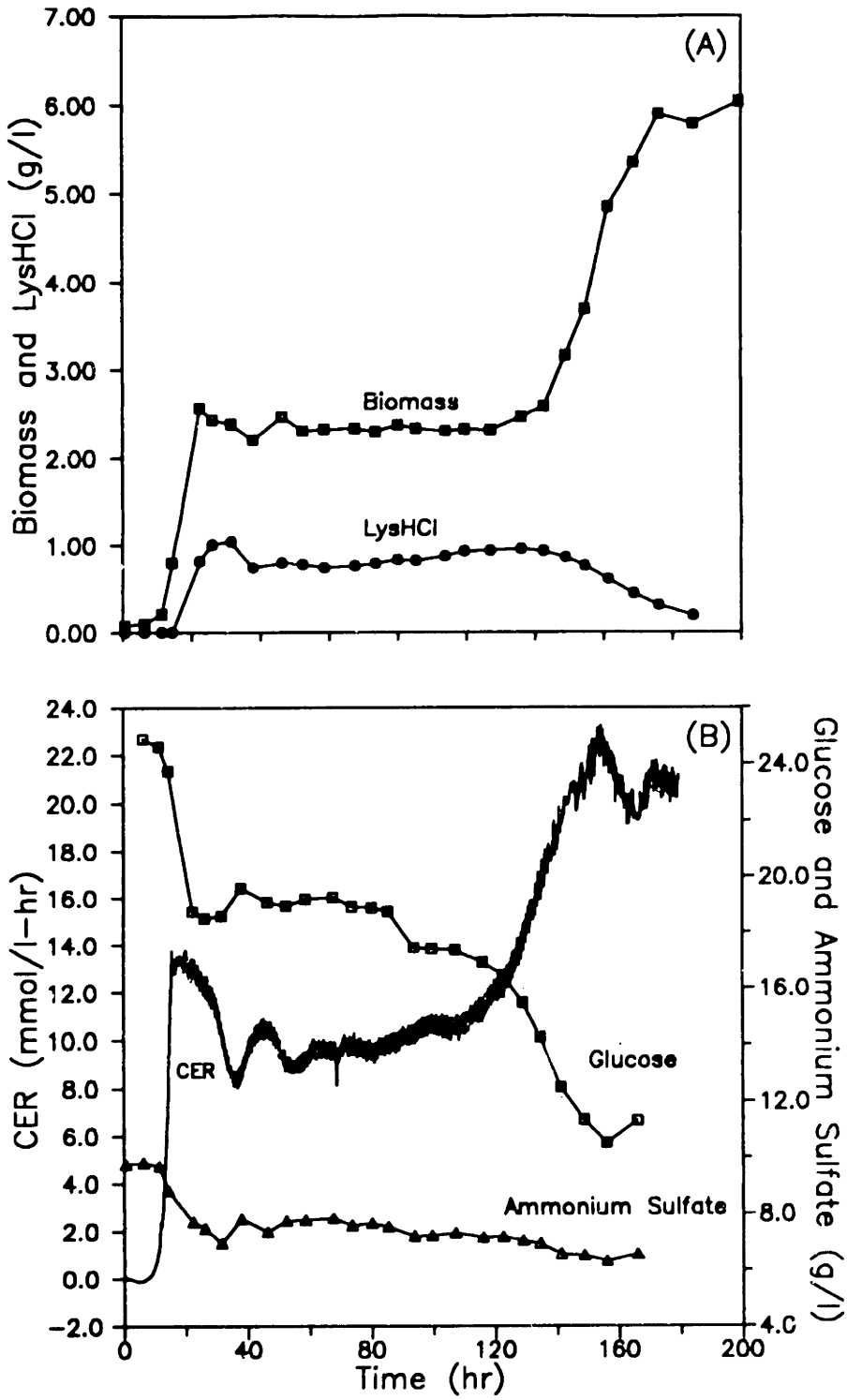

Figure 5.29. Long-term continuous culture instability for D = 0.180 hr^{-1}. (A) Dry cell weight and L-lysine·HCl concentrations vs. time. (B) Carbon dioxide evolution rate, glucose and ammonium sulfate concentrations vs. time.

since they can synthesize additional L-threonine necessary for growth, while the auxotrophs cannot. The revertant fraction of the total population thus increases with time until revertants take over the reactor. As the revertants increase, the fraction of cells producing L-lysine decreases (the reversion negates the regulatory bypass that allowed L-lysine accumulation) and the level of L-lysine in the continuous reactor falls, as seen in Figure 5.29A. Clearly, the takeover of the culture by the revertant cells ends the L-lysine fermentation.

Figure 5.30 shows the percentage of auxotrophic (Thr^-, Met^-, Leu^-) cells in the culture versus residence time (D·t) and generation time (D·t/ln(2)) for several continuous culture experiments at dilution rates ranging from 0.0333 to 0.301 hr^{-1}. The D = 0.301 hr^{-1} experiment was not carried out long enough to see a drop in the auxotroph population (on this time scale), although revertant cells were present and increasing in number when the run was terminated. In all other cases, the reactor was eventually taken over by revertant cells, which, as will be shown mathematically, is inevitable in this system.

It is interesting to note that the dynamics of the reversion process has similar qualitative features to the dynamics of continuous cultures of recombinant organisms subject to plasmid instability. Siegel and Ryu (1985) observed a decrease in plasmid loss per cell generation with increasing dilution rate with *Escherichia coli* and Watson *et al.* (1986) observed similar results with *Bacillus subtilis*. Furthermore, their data indicated that the loss of plasmid-bearing cells during continuous culture depended primarily on the growth rate differential between plasmid-bearing and plasmid-free cells. As will be discussed further in the context of the mathematical modeling for this auxotroph/revertant amino acid system, the dominant factor in governing culture

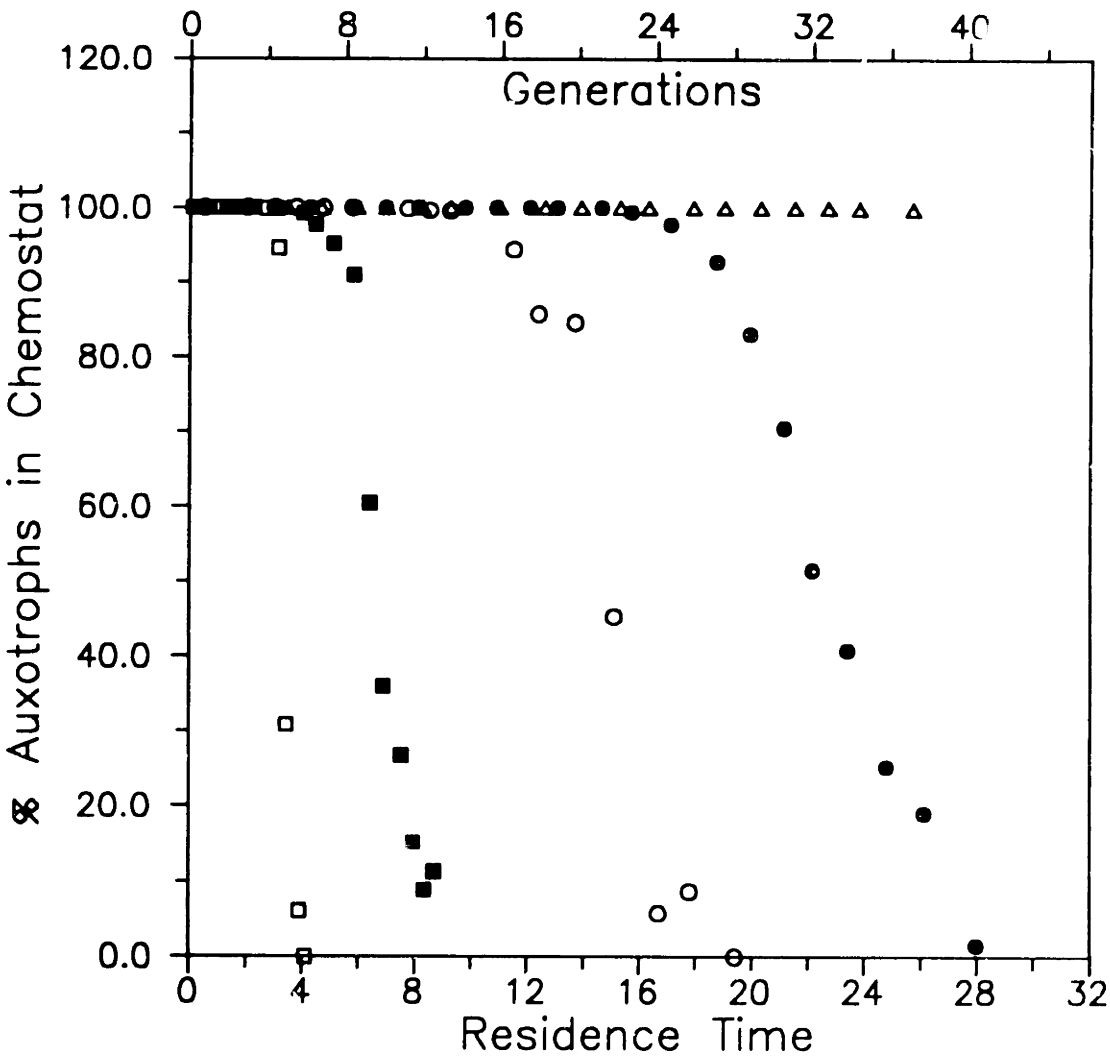

Figure 5.30. Continuous culture experimental population distributions vs. residence time and number of generations for five different dilution rates. D (hr^{-1}) = 0.0333 (□), 0.0750 (■), 0.121 (○), 0.180 (●), 0.301 (△).

stability is also the growth rate differential between competing cells.

5.4.2 Mathematical Modeling of Reversion and Competition

A mathematical model of the system was developed to aid in understanding the competition dynamics occurring in continuous cultivation of the parent double auxotrophic strain. Mass balances for two cell populations (auxotrophs requiring L-threonine, L-methionine, and L-leucine, and revertants requiring only L-leucine) and two limiting substrates (L-threonine for the auxotrophs and L-leucine for the revertants) are as follows (X_1 = auxotrophs, X_2 = revertants, S_1 = L-Thr, S_2 = L-Leu):

$$\frac{dX_1}{dt} = \mu_1 X_1 - DX_1 - p\mu_1 X_1 \qquad 5.5$$

$$\frac{dX_2}{dt} = \mu_2 X_2 - DX_2 + p\mu_1 X_1 \qquad 5.6$$

$$\frac{dS_1}{dt} = D(S_{1f} - S_1) - \sigma_{11} X_1 - \sigma_{12} X_2 \qquad 5.7$$

$$\frac{dS_2}{dt} = D(S_{2f} - S_2) - \sigma_{21} X_1 - \sigma_{22} X_2 \qquad 5.8$$

Here, μ_j is the specific growth rate of population j, p is the probability of

generating a revertant from an auxotroph upon cell division, σ_{ij} is the specific uptake rate of substrate i by population j, and subscripted f indicates feed concentration. This equation set is analogous to that given by Ryder and DiBiasio (1984) for unstable recombinant continuous cultures with the exception of the additional substrate balance (S_2) on the growth limiting nutrient for the revertant population. The specific growth rates are assumed to be solely functions of the limiting substrate for the particular population. This functionality is given by a Monod form, as has been validated experimentally for amino acid-limited growth of *E. coli* auxotrophs [Novick, 1955]:

$$\mu(S) = \frac{\mu_m S}{K_m + S} \qquad 5.9$$

Specific uptake rates are assumed to be proportional to the specific growth rate, as was experimentally determined for the specific uptake of L-threonine by the parent auxotrophs (Section 5.3.2), and are given by:

$$\sigma_{ij} = \frac{\mu_j(S_j)}{Y_{ij}} \qquad 5.10$$

where Y_{ij} is the growth yield of cells of population j on substrate i (mass of cells produced/substrate consumed).

A problem arises with the formulation of Equations 5.5-5.8 when considering the uptake of L-threonine by the revertant population. As indicated by Equations 5.9 and 5.10, neither the specific growth rate nor the specific L-threonine uptake rate of the revertants are limited by the low level of L-threonine. Consequently, the revertants can grow faster and consume L-threonine at a higher rate than that

supplied with the feed. This would drive the calculated residual L-threonine concentration to negative values. In reality, the need for additional L-threonine for growth by the revertants is met by their own synthesis of L-threonine, although they will still compete for L-threonine provided in the medium. To circumvent this problem, it is assumed that the specific uptake rate of L-threonine is equal for the auxotrophs and revertants at the level determined for the auxotrophs by the residual L-threonine concentration. This is equivalent to saying that the available L-threonine is partitioned between auxotrophs and revertants based on their respective relative proportion of the total population. With this modification and the previously mentioned forms for σ_{11}, σ_{21}, and σ_{22}, the balance equations become:

$$\frac{dX_1}{dt} = \mu_1 X_1 - DX_1 - p\mu_1 X_1 \qquad 5.11$$

$$\frac{dX_2}{dt} = \mu_2 X_2 - DX_2 + p\mu_1 X_1 \qquad 5.12$$

$$\frac{dS_1}{dt} = D(S_{1f} - S_1) - \frac{\mu_1 X_1}{Y_1} - \frac{\mu_1 X_2}{Y_1} \qquad 5.13$$

$$\frac{dS_2}{dt} = D(S_{2f} - S_2) - \frac{\mu_1 X_1}{Y_2} - \frac{\mu_2 X_2}{Y_2} \qquad 5.14$$

Note that the parent auxotrophs and revertants have been assumed to grow on

L-threonine and L-leucine with equivalent growth yields ($Y_{11} = Y_{12} = Y_1$, $Y_{21} = Y_{22} = Y_2$). This is a reasonable assumption given that the supplied amino acids are likely used exclusively for protein synthesis (Section 5.3.2) and that the two biomass types should be composed of similar proteins with similar amino acid compositions.

The model system equations (5.11-5.14) were numerically integrated using a fourth-order Runge Kutta algorithm with fixed step size. The first objective of the numerical integration was to simulate the system at conditions corresponding to the experimental runs. The second objective was to examine the effect of the second limiting substrate, L-leucine (the requirement caused by the second auxotrophic mutation), on the speed of system progression to its stable steady state (revertant takeover). Table 5.2 shows the parameter values used in the simulations. A maximum specific growth rate of 0.40 hr^{-1} was used for both auxotrophs and revertants growing on both L-threonine and L-leucine (recall that auxotrophs and revertants were found to grow at similar maximum specific growth rates in both LB5G and CGM1 media). This particular value of μ_m was based on the independent measurements for auxotrophs, discussed previously in section 5.1.3, and was assumed to be equally applicable at all dilution rates tested. The biomass yield coefficients (g biomass/mg amino acid) used were those determined independently (Section 5.1.2) for auxotrophs and were assumed to be valid for revertants. The only parameters not independently measured in some way are the reversion probability, p, which was determined by a least squared error fit to the experimental data, and the Monod saturation constants (residual steady-state L-threonine level unmeasurable [Kiss *et al.*, 1990]). The latter were taken as 1 mg/l for both auxotrophs and revertants for both L-threonine and L-leucine. The saturation constant values chosen are higher than

Table 5.2. Parameters and parameter values used in model simulations.

Parameter	Parameter Value
μ_{m1} (hr^{-1})	0.40
μ_{m2} (hr^{-1})	0.40
K_{m1} (mg L-thr/l)	1.0
K_{m2} (mg L-thr/l)	1.0
Y_1 (g biomass/mg L-thr)	0.034
Y_2 (g biomass/mg L-leu)	0.051
S_{1f} (mg L-thr/l)	100
S_{2f} (mg L-leu/l)	400
X_1 inoculum (g X_1/l)	0.1
X_2 inoculum (g X_2/l)	0.0
p (revertants/cell/generation)	3.0×10^{-13}
Integration time step (hr)	0.01 - 0.1

more realistic values of 0.1 mg/l for amino acid saturation constants. However, it was found that the model predictions are relatively insensitive to the values of the saturation constants in this range and therefore the 1 mg/l values were used in the simulations in order to increase computation speed and avoid computational instability problems resulting from very small saturation constants. It should be noted that for all simulations corresponding to experimental conditions, the large residual L-leucine levels allowed the revertant population to grow at near maximum specific growth rate, so that the value of the L-leucine saturation constant was completely unimportant.

Figure 5.31 shows simulated and experimental profiles of L-threonine, L-leucine, and percent auxotrophs for continuous culture at a dilution rate D of 0.18 hr^{-1}. The short-term steady state described earlier (and seen in the experimental data of Figure 5.29) can also be noted in the L-leucine and percent auxotrophs profiles. The model overpredicts the rate of takeover by revertants as is evidenced by the faster than experimentally measured drops in percent auxotrophs and L-leucine concentration. This could be a result of either too large of a value used for the revertant maximum specific growth rate, or an overestimation of the revertant population's effect on the L-threonine concentration. In either case, the predicted growth rate differential would be larger than that seen experimentally. The difference between the predicted and measured short-term steady-state L-leucine concentrations indicates that the model value for biomass yield on L-leucine, measured by batch cultures, may not accurately describe the yield under continuous culture conditions.

It is noted that the revertant specific growth rate can be independently estimated from the population distribution measured during the course of a continuous fermentation [Park *et al.*, 1991]. Assuming that the difference between auxotroph and revertant specific growth rates is constant and also that the reversion probability is constant, Equations 5.11 and 5.12 can be manipulated to yield a linear relationship between the continuous culture residence time and the natural logarithm of the ratio of auxotrophic to revertant cells.

These plots for the L-lysine continuous culture population data are shown in Figure 5.32. The correlation appears to be linear and, as discussed in detail by Park *et al.*, the slope and intercept at a given dilution rate provide information allowing

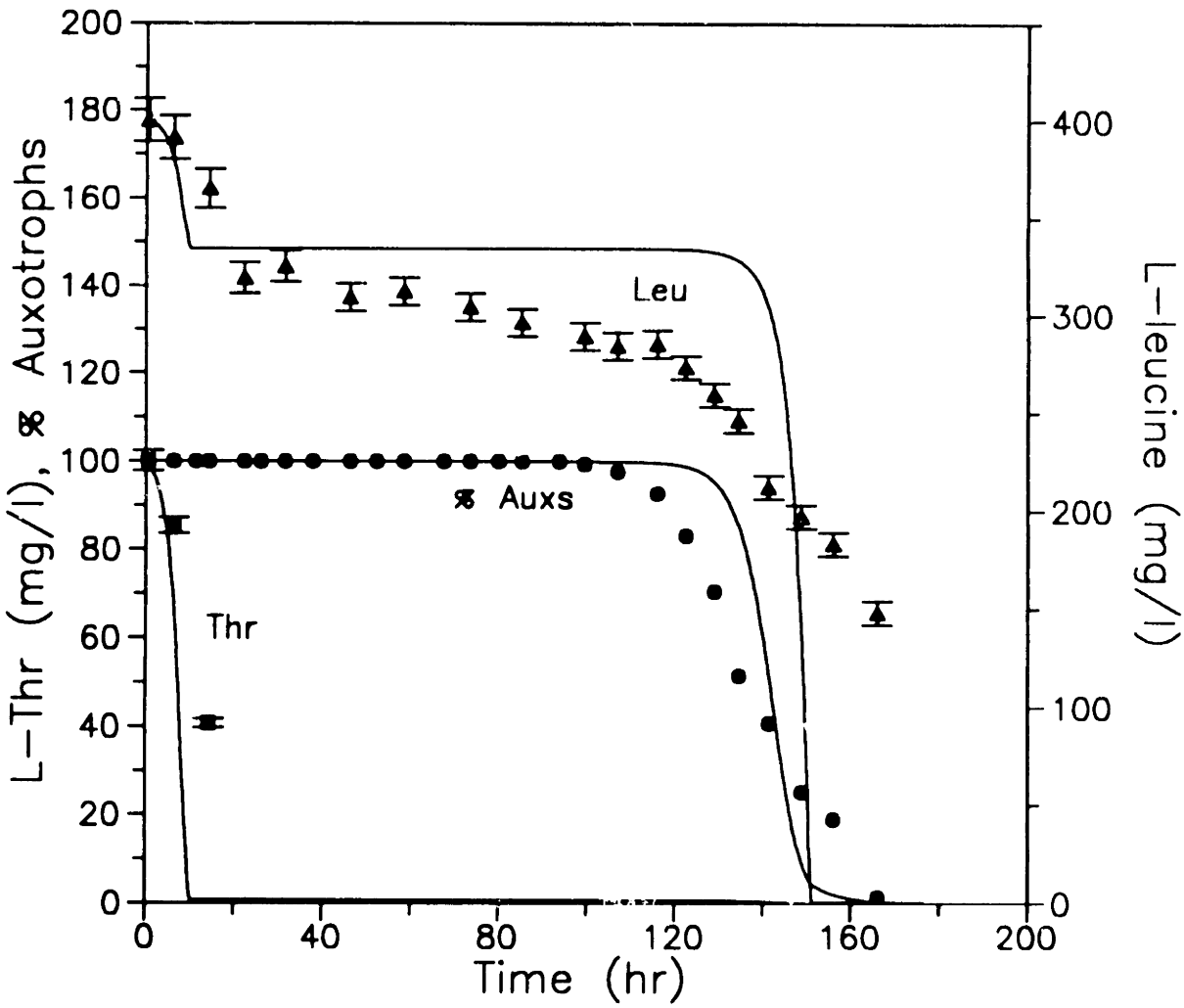

Figure 5.31. Competition model comparison to experimental L-threonine, L-leucine, and percent homoserine auxotrophs profiles for D = 0.18 hr^{-1}.

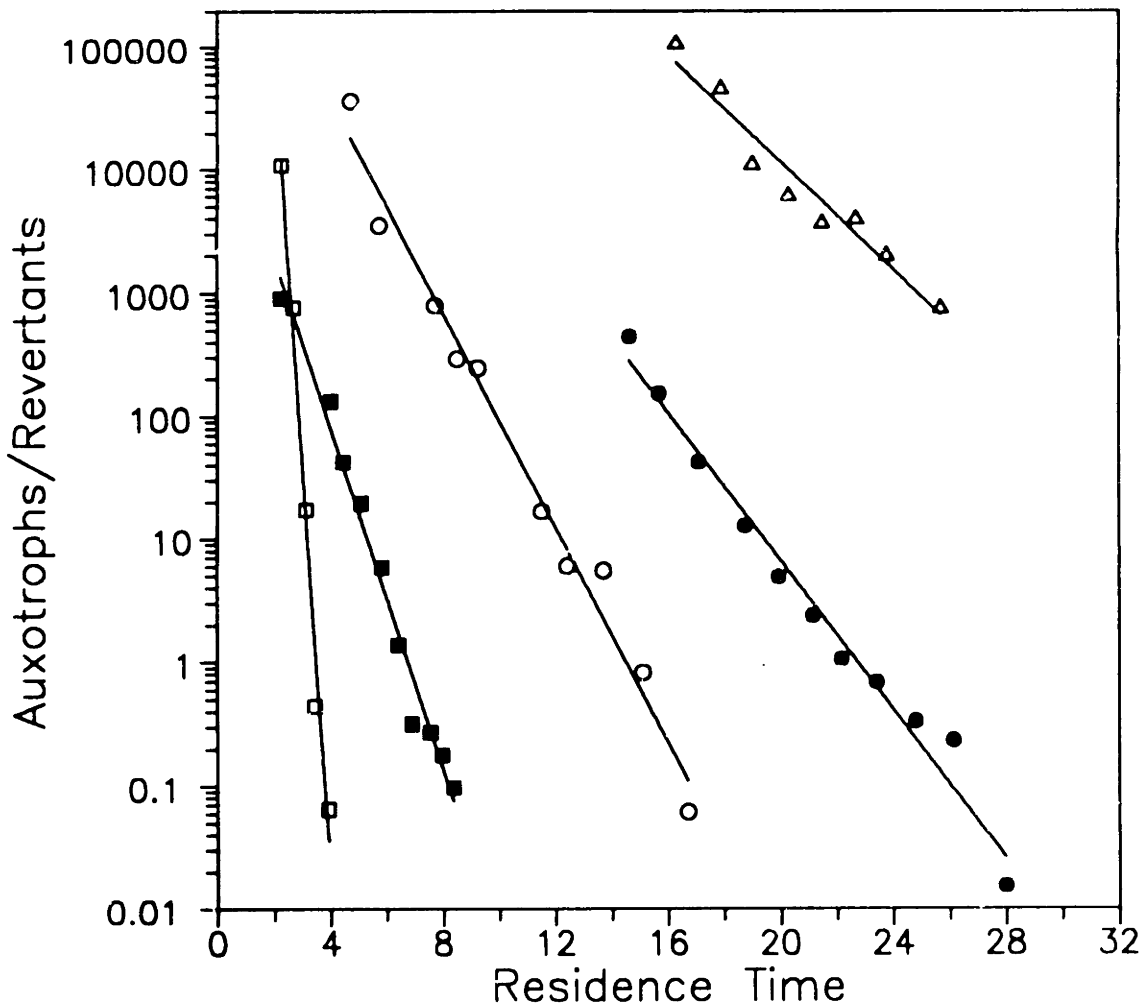

Figure 5.32. Ratio of auxotrophic to revertant cells vs. residence time for five different dilution rates. D (hr^{-1}) = 0.0333 (□), 0.0750 (■), 0.121 (○), 0.180 (●), 0.301 (△).

the estimation of the revertant population's specific growth rate. The application of the above approach to this set of data yields the values of the specific growth rates for the revertant population shown in Table 5.3 and in Figure 5.33A. The data of Table 5.3 and Figure 5.33A indicate that the revertants do not necessarily grow at maximum specific growth rate at all dilution rates, and that for dilution rates greater than 0.075 hr^{-1}, the revertant specific growth rate increases with increasing dilution rate. Also shown in Figure 5.33B is the ratio of the dilution rate to the calculated revertant specific growth rate. Similar results were obtained by Park *et al.* (1991) in their work with recombinant *E. coli.*

Using the parameters of Table 5.3, excellent agreement is obtained between the predicted and experimental auxotroph fractions in the continuous culture. This, however, requires a drastic increase in model adjustable parameters (*i.e.* the revertant specific growth rates at varying dilution rates), or the introduction of a model for the dependence of the revertant specific growth rate on dilution rate. As there is presently no mechanistic basis for the introduction of such a model, and given the objective of this work to improve the culture stability by media manipulations suggested by linearized stability analysis, it was decided that the additional complication was not warranted and a single parameter value of 0.40 hr^{-1} was used for the revertant maximum specific growth rate in all simulations. It is noted that the use of a single value for μ_m still gives a very satisfactory agreement between predicted and measured values of the auxotroph fractions as discussed below.

Figure 5.34 shows the simulated population profiles for all dilution rates for which experimental data exist, along with the data. A single, data-fitted value for the reversion probability parameter, p, was used in all simulations. Individual

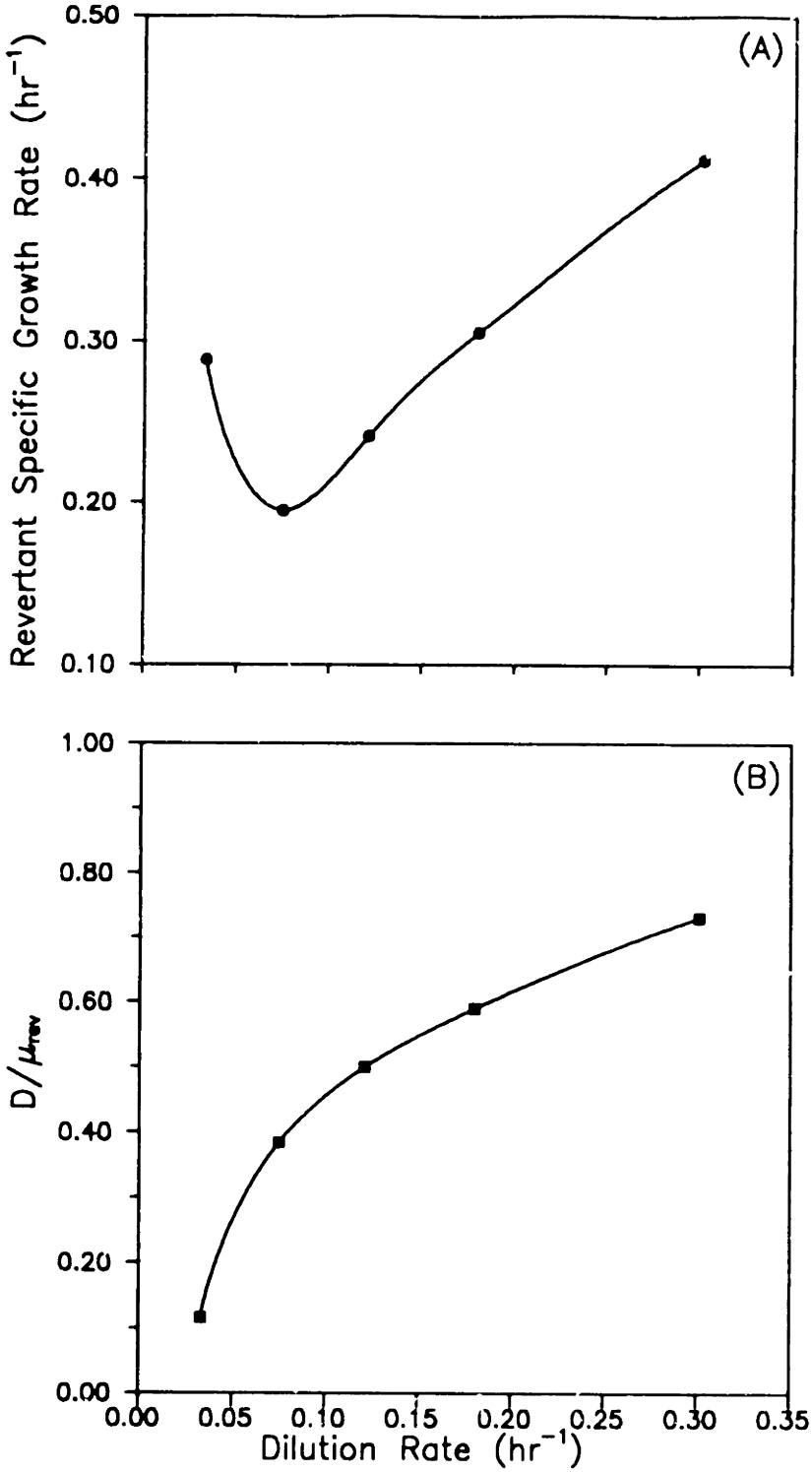

Figure 5.33. Estimated homoserine revertant growth characteristics during continuous culture. (A) Revertant specific growth rate vs. dilution rate. (B) Ratio of dilution rate to revertant specific growth rate vs. dilution rate.

Table 5.3. Estimated revertant specific growth rates during continuous culture.

Diiution Rate (hr^{-1})	Revertant Specific Growth Rate (hr^{-1})
0.0333	0.288
0.0750	0.195
0.121	0.242
0.180	0.305
0.301	0.412

determinations of p for each experimental takeover curve produced no apparent dependence of the calculated p on the auxotroph specific growth rate (dilution rate). The value of the probability p that gave the best fit is 3.0×10^{-13} reversion events per cell per generation, which corresponds to about 1 revertant appearing every generation (the reactor typically contained about 3×10^{12} cells). However, values of two revertants per generation to one revertant every four generations fit the data about equally well.

It is informative to note that the same agreement between model and experimental data can be obtained by, alternatively, assuming an identically zero reversion probability and a non-zero initial revertant cell concentration of about one cell per liter. This is a clear indication that the primary factor in driving the system toward revertant takeover is the growth advantage of the revertants over the parent auxotrophs. This can be seen by noting that, based on our experimental value of one revertant produced per generation, the number of revertants contributed to the population in N generations by back mutation upon cell division is simply N. During those same N generations, the number of revertants produced from the growth of

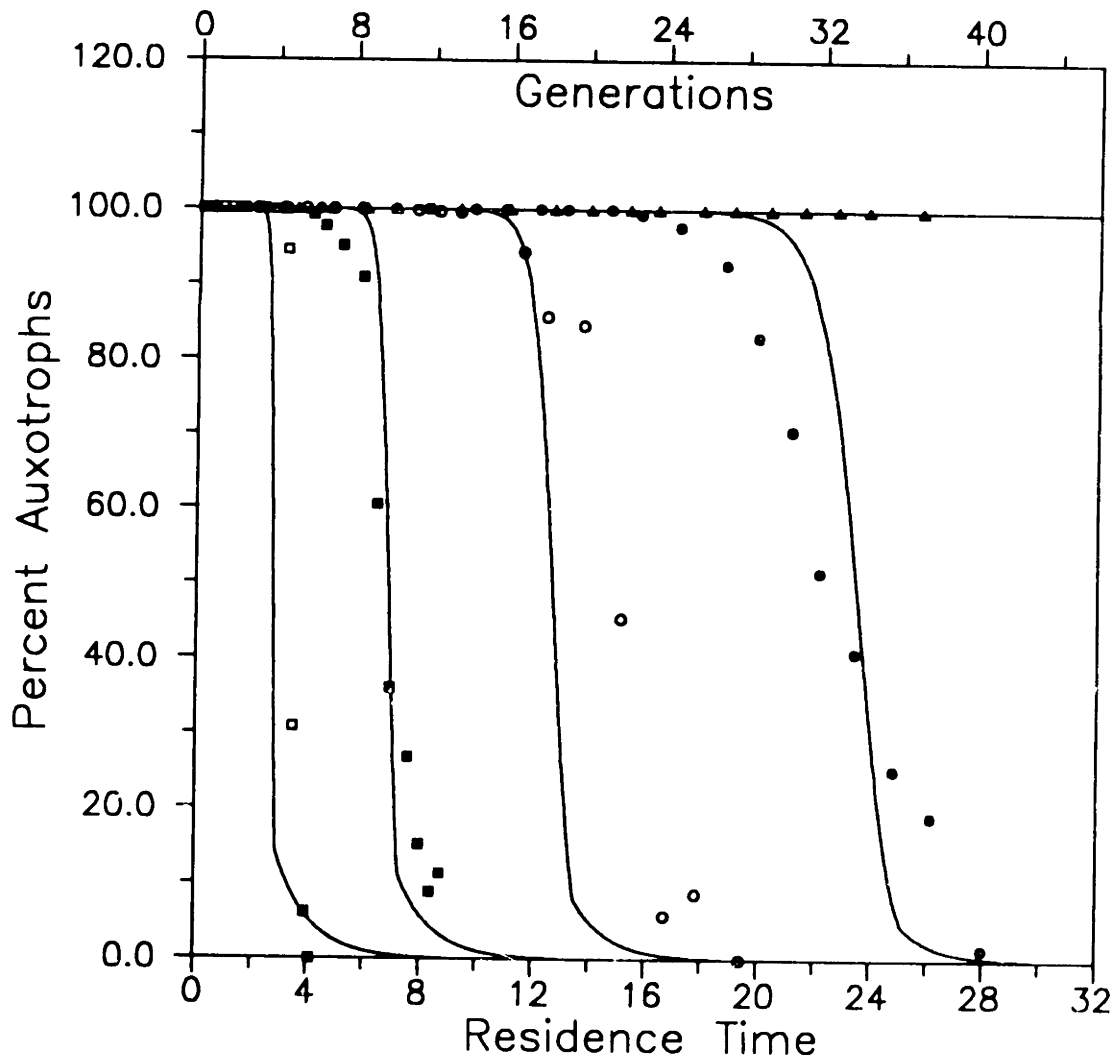

Figure 5.34. Competition model comparison to experimental population distribution profiles for five different dilution rates. D (hr^{-1}) = 0.0333 (□), 0.0750 (■), 0.121 (○), 0.180 (●), 0.301 (△).

one revertant cell is approximately given by $2^{\left(\frac{\mu_2}{\mu_1}\right)\cdot N}$. This generation of new revertants due to growth and division of existing revertants is much greater than the contribution due to reversion of auxotrophic cells for $\left(\frac{\mu_2}{\mu_1}\right)\cdot N$ greater than about 5. In this system, with the revertant population growing near its maximum specific growth rate of 0.4 hr^{-1}, and dilution rates ranging from 0.03 to 0.3 hr^{-1}, the contribution from the reversion probability term is negligible once the first revertant cell is produced. Thus, the role of the p term in the system of equations is primarily to generate the first revertant cell in the culture (assuming a zero revertant population initial condition).

In a seemingly related work, Hall (1990) has reported mutation frequencies of 10^{-10} to 10^{-11} for the reversion of a point mutation in the tryptophan (trp) operon of *E. coli* K-12, allowing a cell formerly unable to exist without supplemental tryptophan to proliferate in the absence of tryptophan. That work used the fluctuation test [Luria and Delbruck, 1943], which selects for tryptophan revertants by plating cells previously grown in excess tryptophan on plates deficient in tryptophan. Therefore, it is not directly comparable to our work conducted in continuous culture under conditions of limiting L-threonine (as opposed to a complete lack of L-threonine). Nonetheless, it suggests that our reported frequency is reasonable. Hall (1990) also reported no significant effect of specific growth rate on the mutational frequency.

5.4.3 Culture Stabililzation by Media Manipulation

In this section, the dynamic reversion/competition model is applied to investigate the importance of medium formulation in retarding revertant takeover. Linear stability analysis is used to determine the parameters which govern the rate of approach to the revertant takeover state and the stabilizing effect of proper medium formulation is determined through integration of the model system equations for various feed compositions. The theoretical predictions are then validated for the case of an extended length fed-batch fermentation.

5.4.3.1 Linear Stability Analysis

The ultimate fate of a continuous culture can be determined by examining its steady-state stability characteristics. Stability analysis is facilitated by reducing the system dimension to three following a procedure similar to Aris and Humphrey (1977). By appropriately scaling and summing Equations 5.11, 5.12, and 5.14, and then integrating the resulting differential equation, one obtains the relationship (for constant yield coefficient, Y_2):

$$\frac{X_1}{Y_2} + \frac{X_2}{Y_2} + S_2 - S_{2f} = \left(\frac{X_1}{Y_2} + \frac{X_2}{Y_2} + S_2 - S_{2f} \right)_0 e^{-Dt} \qquad 5.15$$

This equation indicates that the quantity $\frac{X_1}{Y_2} + \frac{X_2}{Y_2} + S_2 - S_{2f}$ is a culture invariant: if the initial state of the continuous culture lies on the plane defined by Equation 5.15, $S_2 = S_{2f} - \frac{X_1}{Y_2} - \frac{X_2}{Y_2}$, then it will remain there indefinitely. If the state of the culture is not on the plane initially, then the state will approach it exponentially in time with time constant 1/D. Small perturbations from this plane will

be quickly damped out and thus the time invariant characteristic can be assumed to be valid at all times. The dynamics of the continuous culture can then be described by three differential equations for X_1, X_2, and S_1, and the time invariant, or algebraic constraint relationship, for S_2:

$$\frac{dX_1}{dt} = \mu_1 X_1 - DX_1 - p\mu_1 X_1 \qquad 5.16$$

$$\frac{dX_2}{dt} = \mu_2 X_2 - DX_2 + p\mu_1 X_1 \qquad 5.17$$

$$\frac{dS_1}{dt} = D(S_{1f} - S_1) - \frac{\mu_1 X_1}{Y_1} - \frac{\mu_1 X_2}{Y_1} \qquad 5.18$$

$$S_2 = S_{2f} - \frac{X_1}{Y_2} - \frac{X_2}{Y_2} \qquad 5.19$$

The above relationship for S_2 will be used in all terms requiring S_2, such as μ_2, leaving the three differential equations for stability analysis. Ideally, one would like to find a time invariant for S_1 as well. However, the earlier assumption regarding the specific uptake of L-threonine removed a necessary symmetry from the equation set, precluding the existence of such an invariant.

There are three possible steady states for the above system of differential equations whose stability characteristics are discussed below:

Steady State I (total washout): $X_{1ss} = X_{2ss} = 0$, $S_{1ss} = S_{1f}$, $S_{2ss} = S_{2f}$

Steady State II (auxotroph washout): $X_{1ss} = 0$, $X_{2ss} > 0$,

Steady State III (coexistence): $X_{1ss} > 0$, $X_{2ss} > 0$.

A revertant washout steady state, $X_{1ss} > 0$, $X_{2ss} = 0$ is clearly not possible due to the fact that, if auxotrophs are present, they are always being converted to revertants by the term $p\mu_1 X_1$.

For the total washout steady state, the eigenvalues of the stability matrix can be solved for explicitly:

$$\lambda_1 = (1 - p)\mu_1(S_{1f}) - D \qquad 5.20$$

$$\lambda_2 = \mu_2(S_{2f}) - D \qquad 5.21$$

$$\lambda_3 = -D \qquad 5.22$$

The condition for a stable steady state is that all eigenvalues must have negative real parts. The third eigenvalue for this steady state is clearly always negative. The first eigenvalue will be negative if the dilution rate, D, is greater than the effective auxotroph specific growth rate, $(1\text{-}p)\cdot\mu_1(S_{1f})$, and the second eigenvalue will be negative if D is greater than the revertant specific growth rate, $\mu_2(S_{2f})$. If both of these conditions are met, the total washout steady state will be stable (node). If both of these conditions are not satisfied, then the total washout steady state will be unstable (an unstable node if only one condition is met and a saddle point if neither

are met).

For the auxotroph washout (revertant takeover) steady state, the eigenvalues can again be solved for explicitly:

$$\lambda_1 = (1 - p)\mu_1(S_{1ss}) - D \qquad 5.23$$

$$\lambda_2 = \mu_2(S_{2ss}) - \frac{\mu_{m2} X_{2ss} K_{m2}}{Y_2(K_{m2} + S_{2ss})^2} - D \qquad 5.24$$

$$\lambda_3 = - \frac{\mu_{m1} X_{2ss} K_{m1}}{Y_1(K_{m1} + S_{1ss})^2} - D \qquad 5.25$$

The third eigenvalue is clearly always negative. The second eigenvalue is easily seen to be always negative when one realizes that $\mu_2(S_{2ss})$ is equal to D for this steady state. For the first eigenvalue to be negative, the condition:

$$\mu_1(S_{1ss}) < \frac{D}{1 - p} \qquad 5.26$$

or

$$\mu_1(S_{1ss}) < \frac{\mu_2(S_{2ss})}{1 - p} \qquad 5.27$$

must be met. Thus, if the specific growth rate of the revertants, divided by 1-p, (which increases its magnitude), is greater than the specific growth rate of the auxotrophs, the steady state is stable. This condition can be manipulated to the form:

$$(1 - p)\frac{Y_1(S_{1f} - S_{1s})}{Y_2(S_{2f} - S_{2s})} < 1 \qquad 5.28$$

Inequality 5.28 is always satisfied for a medium designed to be L-threonine limiting. As the medium composition is shifted toward equivalent stoichiometric amounts of L-threonine and L-leucine ($Y_2S_{2f} \rightarrow Y_1S_{1f}$), λ_1 approaches zero (from the negative side). Note, however, that as this occurs, the system changes from one of L-threonine limitation toward one in which the parent auxotrophs become equally growth-limited by L-threonine and L-leucine. This is a different situation than that described by the model. In fact, all three eigenvalues approach zero (from the negative side) as the medium composition approaches the dual limitation, as can be seen in Figure 5.35. The decrease in eigenvalue magnitudes indicates that the medium composition dramatically affects the rate at which the system moves toward complete takeover. As linear stability analysis is local in nature, these results are applicable only in the neighborhood of the revertant takeover steady state. To obtain information on the global dynamics of the culture, the non-linearity of the governing differential equations must be taken into account by integrating in time from an initial condition. Some numerical results concerning the effect of medium composition on the takeover dynamics are presented in Section 5.4.3.2. Here it should be noted that, even if the specific growth rates of parent auxotrophs and revertants were equal in the culture, this steady state would still be stable since p, the reversion probability, is nonzero.

For the coexistence steady state, the eigenvalues cannot be easily solved for explicitly (a cubic equation results for λ). The Routh Hurwitz criterion [Coughanowr and Koppel, 1965] was used to determine the stability of the steady state. The details

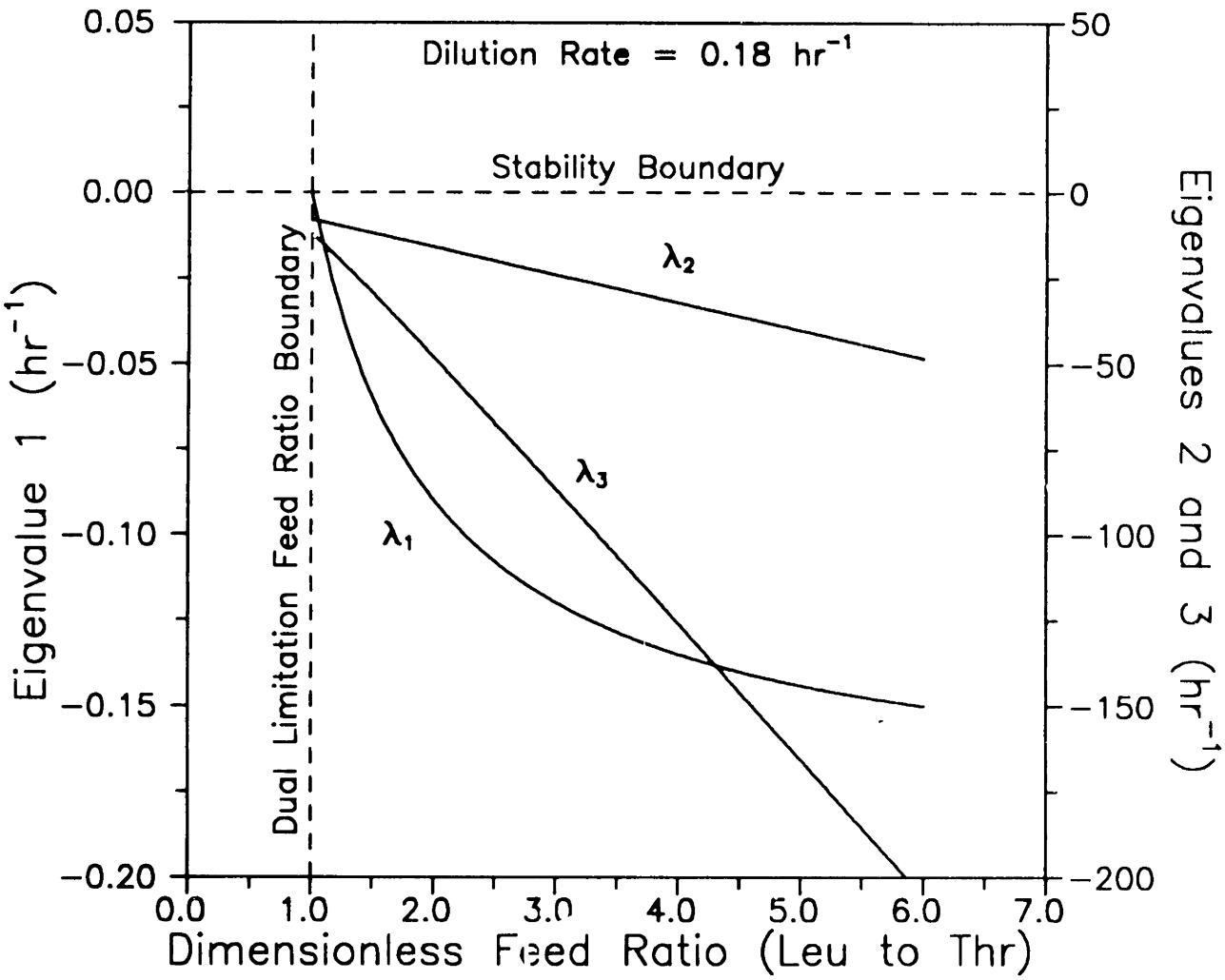

Figure 5.35. Auxotroph washout (revertant takeover) steady state eigenvalues as a function of dimensionless feed ratio, Y_2S_{2f}/Y_1S_{1f}, for D = 0.18 hr^{-1}.

are not shown here, but the analysis indicates that the coexistence steady state is always unstable when μ_2 is greater than $\mu_1 \cdot (1\text{-}p)$, the effective specific growth rate of the parent auxotrophs. Since the medium is designed to limit the parent auxotrophs on L-threonine, μ_2 will always be greater than $\mu_1 \cdot (1\text{-}p)$, and thus the coexistence steady state is always unstable.

The linearized stability analysis has showed that revertant takeover is the eventual outcome of a continuous culture of this auxotrophic strain. This is in agreement with experimental observations for a range of dilution rates and a fixed feed composition.

5.4.3.2 Effect of 2nd Limiting Nutrient on Competition Dynamics

The effect of the second limiting nutrient, L-leucine, on the outcome of the competition was further investigated by simulating the time course of continuous culture. Figure 5.36 shows the effect of varying L-leucine feed concentration on the population dynamics for two dilution rates (zero initial revertant concentration). The maximum L-leucine feed concentration, 400 mg/l, corresponds to the experimentally used feed concentration and yields a dimensionless feed ratio, $\frac{Y_2 S_{2f}}{Y_1 S_{1f}}$, of 6. The minimum value, 67 mg/l, corresponds to an amount stoichiometrically equivalent to the L-threonine feed concentration of 100 mg/l ($\frac{Y_2 S_{2f}}{Y_1 S_{1f}} = 1$). That is, feed containing 67 mg/l of L-leucine can support the same amount of cell mass as 100 mg/l of L-threonine and thus both amino acids will equally limit growth according to the model structure. This means that the specific growth rates of auxotrophs and revertants will be the same at all times, $\mu_1 = \mu_2$ (Monod growth functionalities assumed identical for growth on L-threonine and L-leucine), although the effective

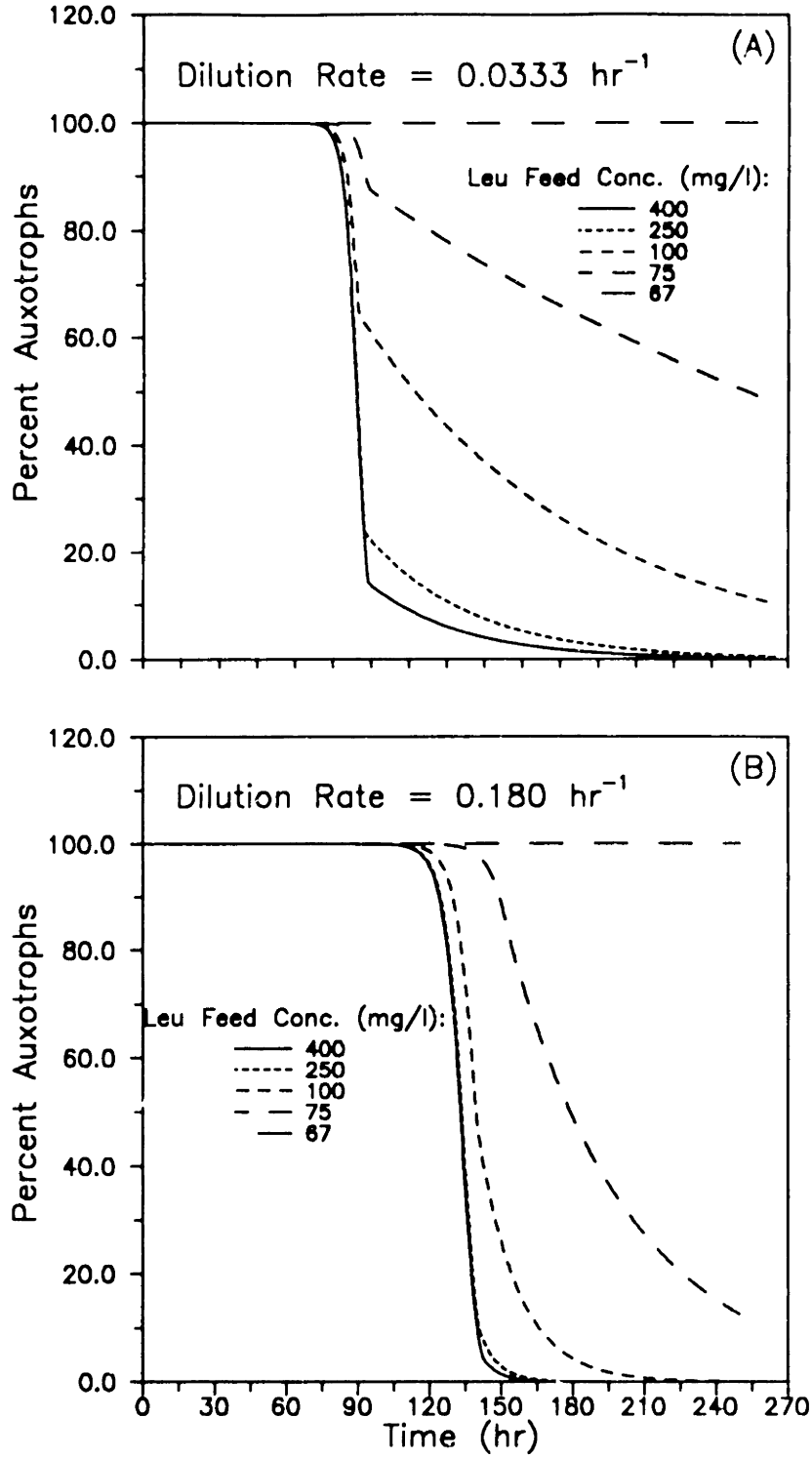

Figure 5.36. Model predictions of effect of L-leucine feed concentration on continuous culture population dynamics for D = (A) 0.0333 hr^{-1}, (B) 0.180 hr^{-1}.

specific growth rate for auxotrophs is reduced by the factor [1-p]. For the stoichiometric feed cases, the simulations were not carried out to long enough times to show that the revertants will eventually take over the reactor due to the very slow approach to this steady state. Nevertheless, the presence of the [1-p] term in the stability requirement for the auxotroph washout steady state, Equation 5.27, insures that this steady state is indeed a stable one. The simulations show clearly that decreasing the second limiting nutrient concentration has a beneficial effect on the stability of the system with respect to revertant takeover.

This stabilizing factor is further illustrated in Figure 5.37 where the time required for the culture to reach 50 percent revertants is plotted versus the dimensionless feed ratio of L-leucine to L-threonine for a dilution rate of 0.18 hr^{-1}. The stabilizing effect is clearly most dramatic for dimensionless feed ratios less than 2. This effect is a manifestation of the fact that growth of revertant cells is held in check by the lower residual levels of L-leucine, the second auxotrophic growth factor requirement.

It should be mentioned that the homoserine revertant cells themselves are capable of reverting further to L-leucine independence as well. Such a double reversion would require the occurrence of two low probability mutations in sequence. The model does not allow for that possibility. Similarly, since the medium is designed to be L-threonine limited, the possibility of parent auxotrophs reverting to L-leucine independence has not been accounted for in the model.

5.4.3.3 Extension of Model Predictions to Stabilization of Fed-Batch Cultures

The theoretical predictions of the previous section indicate the importance of

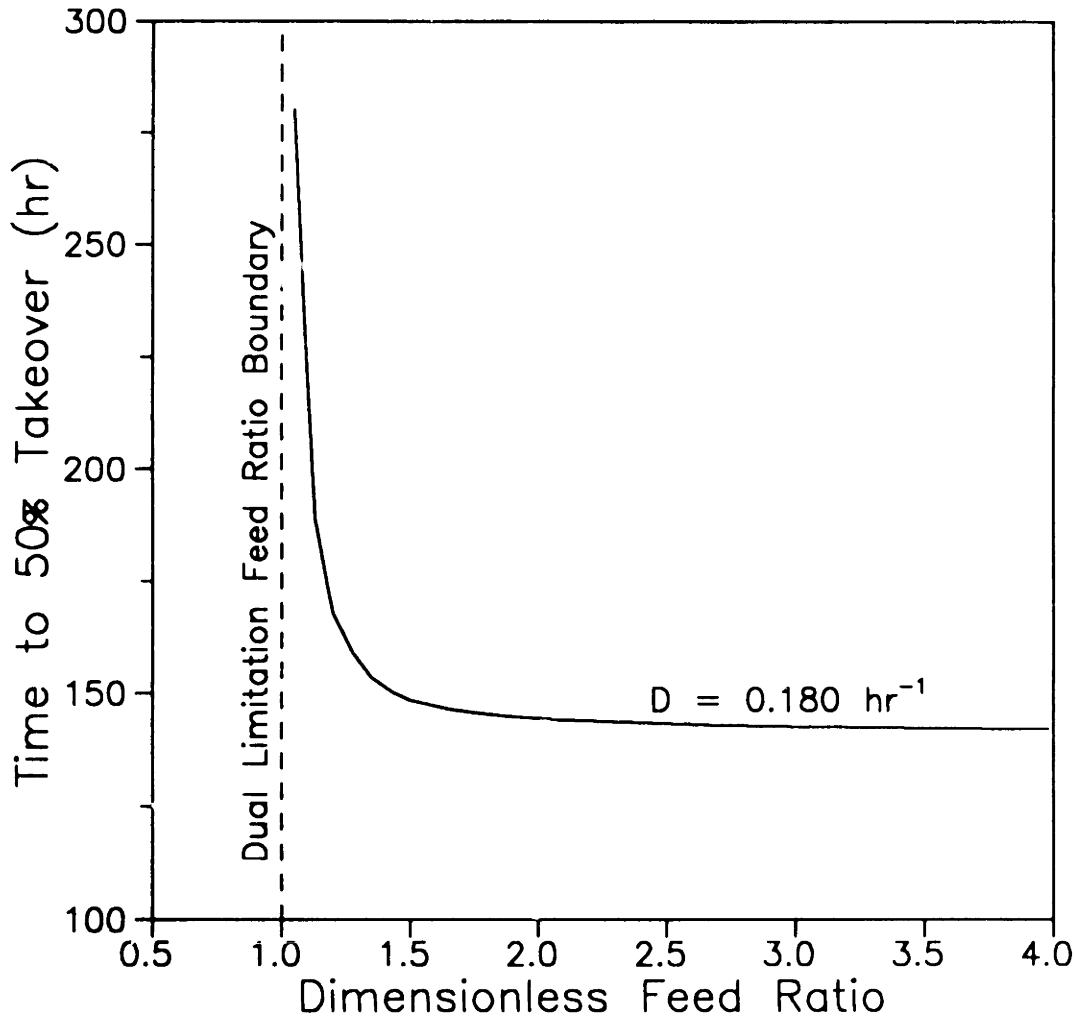

Figure 5.37. Model predictions of effect of dimensionless feed ratio, Y_2S_{2f}/Y_1S_{1f}, on the time required to reach 50 percent takeover for D = 0.18 hr^{-1}.

proper medium design in maintaining the integrity of the culture for extended lengths of time. One might expect the reversion problem to be important in lengthy fed-batch experiments considering that any revertant cell formed will remain in the reactor with no possibility of being washed out as in continuous culture. In fact, fed-batch experiments (for example, experiment FB4 discussed in Section 5.5.3.2) carried out with this auxotrophic strain at dimensionless feed ratios of 4.0 have ended in revertant takeover in less than 80 hours (7 to 8 generations). Although fed-batch experiments will be discussed in detail in Section 5.5 and 5.6, it is appropriate here to discuss the application of the theoretical medium design criterion to the stabilization of fed-batch cultures.

The model predictions suggest that a continuous culture could be stabilized by using a dimensionless feed ratio much closer to unity. Although the calculations were performed for the case of continuous culture, the results are expected to be valid for the stabilization of long-term fed-batch cultures as well since the critical concern is the minimization of the growth rate advantage possessed by revertant cells, which should be independent of reactor operating mode. As a test of that prediction, a fed-batch experiment was carried out using conditions identical to a previous fed-batch experiment (FB4 of Section 5.5.3.2) which had been taken over in 80 hours, except that a much lower L-leucine feed concentration was used such that the dimensionless feed ratio was reduced from 4.0 to 1.4.

The population profiles for the control experiment (feed ratio = 4.0) and the reduced dimensionless feed ratio experiment are shown in Figure 5.38. Figure 5.38A shows the stability of the population in terms of the percentage of the population still possessing the homoserine requirement (and therefore, still capable of overproducing

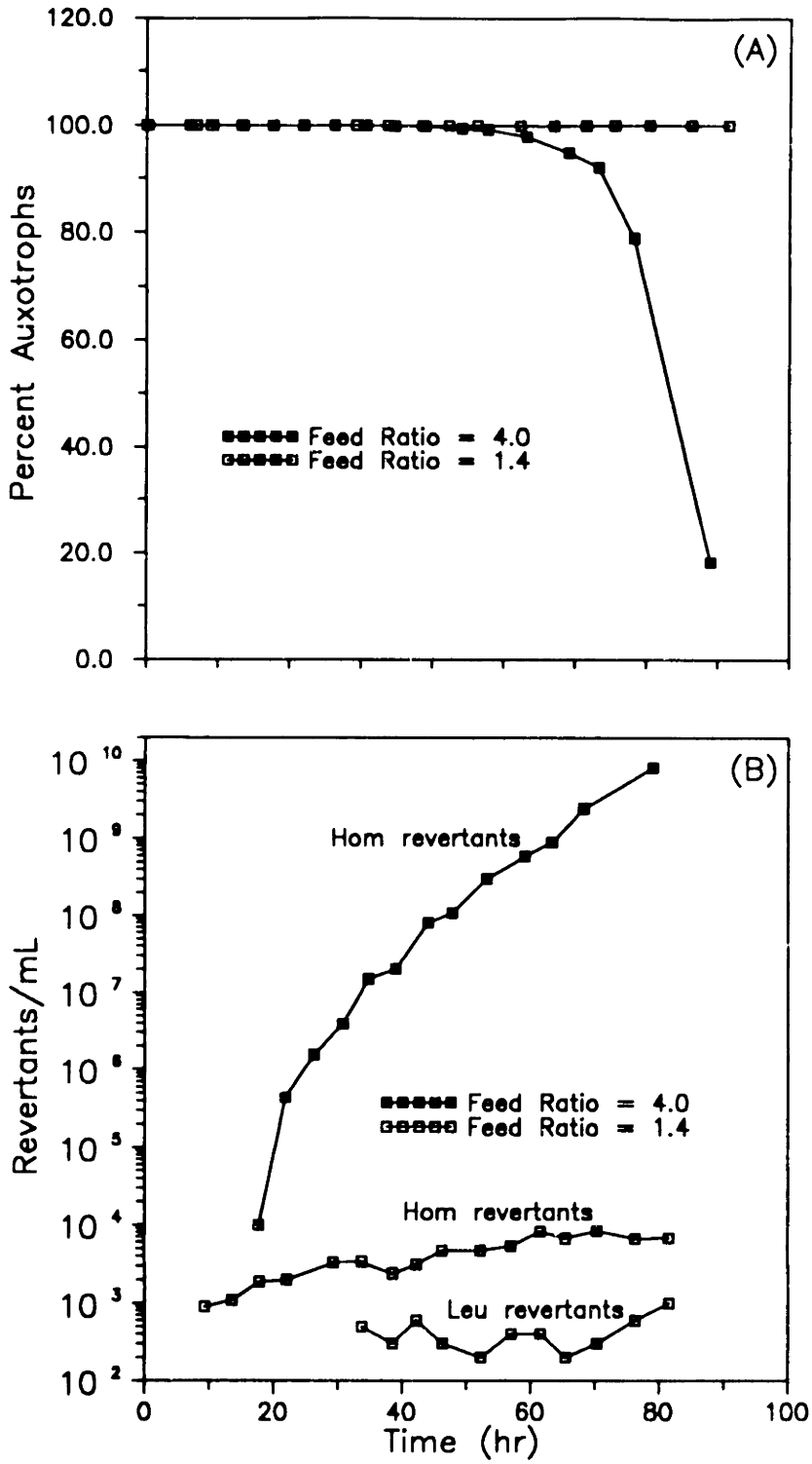

Figure 5.38. Stabilization of fed-batch culture against revertant takeover by medium manipulation. (A) Percentage of cells capable of overproducing L-lysine vs. time. (B) Revertant cell counts vs. time.

L-lysine). Figure 5.38B shows the revertant cell densities during the two experiments, illustrating the ability of the reduced feed ratio medium to retard the proliferation of homoserine revertant cells (Also shown are the counts of L-leucine revertant cells for the low feed ratio experiment. Such counts for the control experiment were only capable of determining that the L-leucine revertant population density was less than 10^4 cells/ml). Clearly, reducing the feed ratio has been successful in stabilizing the culture for upwards of 80 hours. In the reduced ratio experiment, the revertants comprised less than 10^{-5} percent of the total cell population when the fermentation was ended. The benefits in preventing excessive growth of revertant cells are evident in the fact that the reduced feed ratio increased both average volumetric productivity and final L-lysine concentration by 20 percent (48 vs. 40 g/l for equivalent fermentation time) over the control experiment.

It should be mentioned that another test of the medium design criterion was performed in a fed-batch mode at a dimensionless feed ratio of 1.0. This feed composition was also effective in maintaining the integrity of the auxotrophic population for upwards of 80 hours. However, L-lysine accumulation was markedly reduced, reaching a final concentration of only 8.4 g/l. This is an indication that a feed ratio of 1.0 (as calculated based on the experimentally determined batch culture biomass-amino acid yield coefficients) actually results in a L-leucine growth limitation with enough excess residual L-threonine to cause inhibition of aspartokinase. The L-threonine concentration was always less than the minimum detectable level (HPX-87C analysis) of about 100 mg/l after the first 9 hours of culture. This, then, is further evidence of the critical importance of proper control of the L-threonine concentration in this fermentation.

5.4.4 Summary of Culture Instability Work

The implications of strain instability on the use of continuous culture for L-lysine production are serious. The productivity of the bioreactor drops off rapidly as revertant cells become a significant proportion of the population and the fermentation yield decreases as revertant cells consume glucose for growth without producing L-lysine.

This phase of the work has shown, both experimentally and through a mathematical model, that revertant takeover in continuous cultures of auxotrophic mutants is inevitable, given a non-zero probability of reversion, with the primary driving force being the growth rate differential between auxotrophs and revertants. However, the analysis has demonstrated that additional auxotrophic marker mutations can be employed to extend the productive length of a culture, given that the fermentation medium is properly formulated to exploit the auxotrophic growth factor requirements. Such a simple medium manipulation was successfully employed in this work to stabilize the performance of a fed-batch L-lysine fermentation. This observed effect of medium design on culture stability provides a plausible explanation for the results of Woodruff and Jackson (1970), who observed a stabilization of L-lysine producing cultures by the addition of a second auxotrophic mutation in addition to the homoserine auxotrophic requirement, but were unable to provide a mechanism for the stabilizing effect.

As discussed by Ollis (1982) in regards to unstable recombinant cultures, the question may not be whether to run a continuous production system at all, but rather how long to run such a system. For the continuous culture conditions studied, stable

operation was maintained only for a few days due to the large growth advantage of revertant cells. As was demonstrated with fed-batch cultures, proper formulation of the medium with respect to the second growth-limiting nutrient would likely lengthen the productive life of continuous cultures as well as extended fed-batch cultures. The benefit of such a stabilizing effect is especially important for fed-batch culturing since much of industrial fermentation is performed in repeated fed-batch type operations. As the need for improved productivity and improved yield processes increases, the importance of maintaining active, productive biomass, free from culture instability problems, becomes even more pronounced.

5.5 Rationale for Restrained Growth Fed-Batch Fermentations

In summarizing the information gained about the microbial production of L-lysine through batch and continuous cultures, several key observations stand out and point to a rational strategy for improving fermentation yield, productivity, and product titer.

5.5.1 Key Observations of Batch and Continuous Cultures

The batch culture characterization results show that the instantaneous process yield and specific productivity are both sub-optimal during most of the fermentation. This results in a poor overall process yield, low volumetric productivity, and low L-lysine titer. The batch cultures also indicate that a direct relationship exists between the culture respiratory characteristics and the level of biomass catalytic

activity (yield and specific productivity), suggesting the use of on-line respiratory data as a real-time monitor of fermentation performance.

Continuous culture results showed that the instantaneous process yield increases as the growth rate decreases, while the specific productivity was shown to be maximum over a broad, intermediate range of growth rates. The continuous culture studies also showed a clear correlation between the respiratory quotient and the channeling of carbon toward L-lysine synthesis.

These yield and specific productivity relationships suggest that, at least in continuous culture, there exist different optimal operating conditions for maximizing fermentation yield or productivity. The data imply that the yield would be maximized at a zero growth rate. It is not possible to maintain a zero growth rate indefinitely (nor is it desirable from the standpoint of biomass activity decline), but very low growth rates could conceivably be maintained using a respiratory-based methodology. To maximize productivity, the goal would be to grow the maximum amount of active biomass as quickly as possible, implying that the fermentation should be operated at the largest specific growth rate which still allows maximum specific productivity. Thus, in both cases, some degree of control over the specific growth rate is required; in the case of yield maximization a strategy would need to minimize growth rate while keeping the specific growth rate from falling too low. In the case of productivity maximization, a strategy would need to maximize growth rate just short of the point where specific L-lysine productivity is negatively affected.

5.5.2 Restrained Growth/Performance Improvement Hypothesis

The combined results of the batch and continuous culture characterizations suggest that improved fermentation performance (yield, productivity, and titer) can be expected by cultivating the organism under conditions of controlled, or restrained growth. This controlled growth can be conveniently achieved in a fed-batch operation using on-line respiratory measurements as a metabolic activity indicator for feed rate control.

Before attempting to formulate control algorithms based on this restrained growth/performance improvement hypothesis, constant feed rate fed-batch fermentations were conducted to verify the hypothesis as to the effect of growth restraint on fermentation performance and examine the suitability of the respiratory data as an on-line basis for control strategies. Two experiments were performed: one experiment was a four cycle repeated fed-batch culture at relatively high feed rate (250 ml/hr) and the other a single cycle fed-batch run at reduced feed rate (50 ml/hr). Both experiments showed a maintenance of high specific productivity, instantaneous yield, and respiratory quotient over their entire duration following initiation of L-lysine production, in marked contrast to the sub-optimal dynamic behavior of the typical batch fermentation. The details of these two open-loop fed-batch experiments and their subsequent validation of the restrained growth hypothesis will now be discussed.

5.5.3 Hypothesis Verification by Open-Loop Fed-Batch Fermentations

The base case for comparison of all fed-batch fermentation results is the batch fermentation discussed previously in Section 5.2. To insure a meaningful comparison,

the media for the fed-batch experiments was identical to the batch experiment on a total volume basis. That is, the batch experiment was carried out in 10 liters of liquid volume while the fed-batch experiments were designed to end with final volumes of 10 liters with the same total amounts of nutrients provided as in the batch case. The key parameters of interest to be compared are the L-lysine titer, total L-lysine produced, specific productivity, average volumetric productivity, and the instantaneous and overall yields of L-lysine from glucose.

5.5.3.1 Repeated Fed-Batch Fermentation

Experiment FB1 was a repeated fed-batch experiment in which the initial reactor volume was 6 liters. Feed was supplied at a constant rate of 250 ml/hr for four consecutive fed-batch phases. When the reactor liquid volume reached 10 liters, the reactor was drained to approximately 6 liters and feeding was restarted. At the end of the fourth fed-batch phase, the fermentation was allowed to run in batch mode for approximately another 12 hours (glucose was exhausted during this final batch stage).

For the first three fed-batch phases, the feed medium was identical to the initial reactor medium (L-threonine limited, all media components present), while the fourth feed tank consisted only of L-threonine and glucose, to prove that L-threonine was indeed the limiting nutrient. Dissolved oxygen concentration was maintained by manual agitation (rpm) control to be not less than 10% of saturation. The feed to the first fed-batch phase was begun at the "step-change" condition in RQ and dissolved oxygen, which is characteristic of the depletion of L-threonine from the medium, as discussed previously.

Figures 5.39A through 5.39F show the time courses of the fermentor liquid

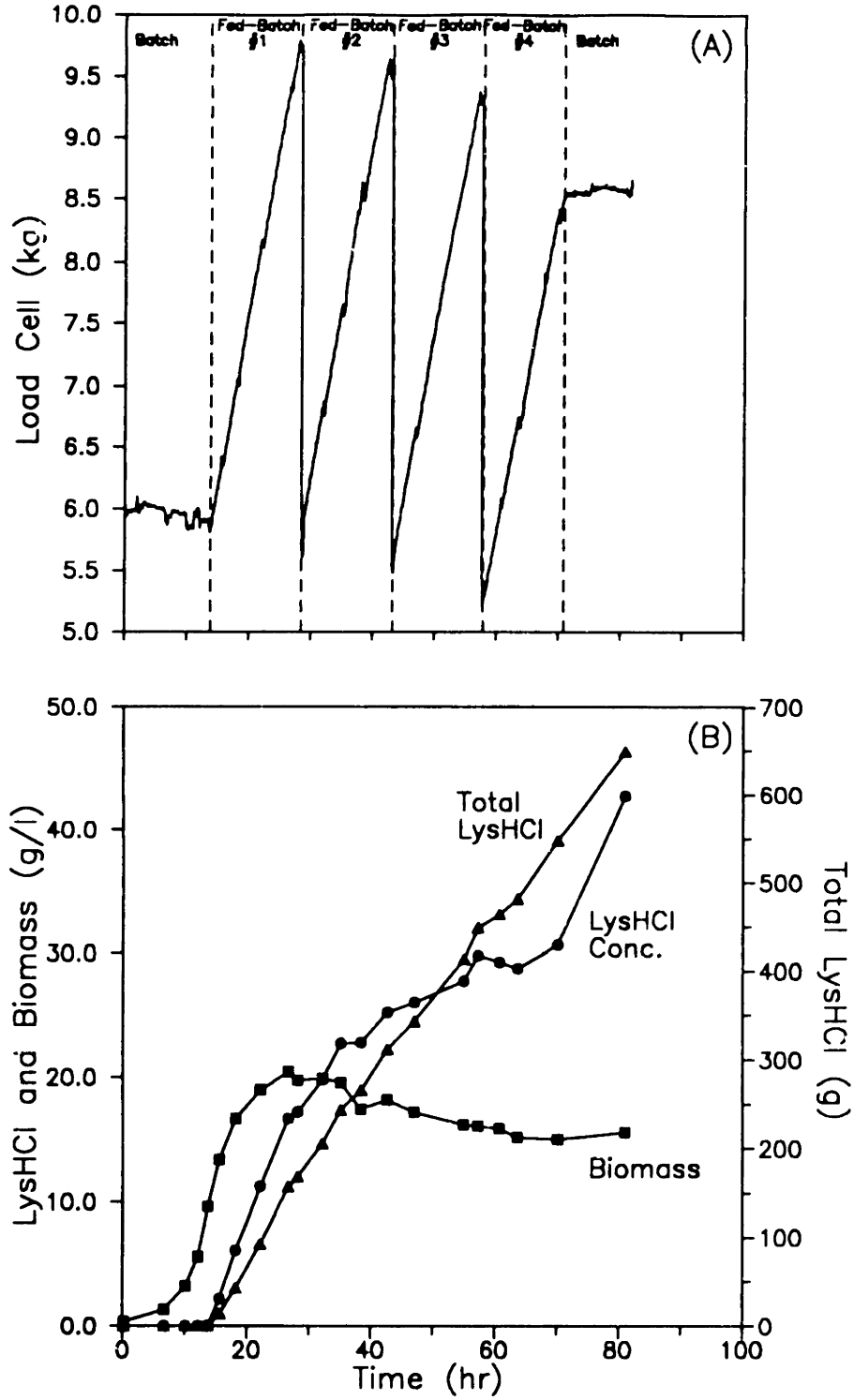

Figure 5.39. Open-loop, repeated fed-batch fermentation dynamic profiles. (A) Load cell reading. (B) Biomass and L-lysine·HCl concentrations and total L-lysine·HCl.

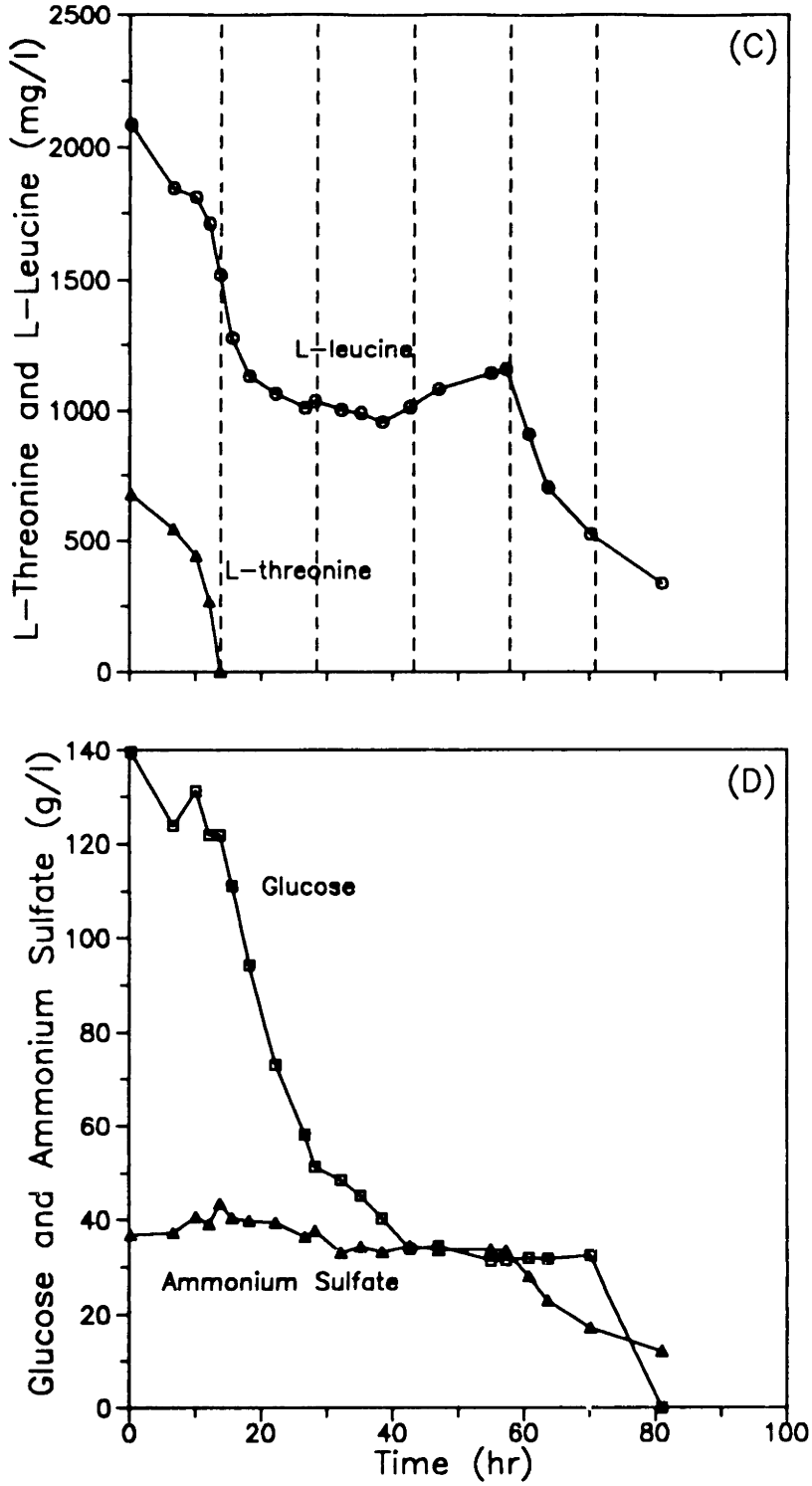

Figure 5.39. (Continued) (C) L-threonine and L-leucine concentrations. (D) Glucose and ammonium sulfate concentrations.

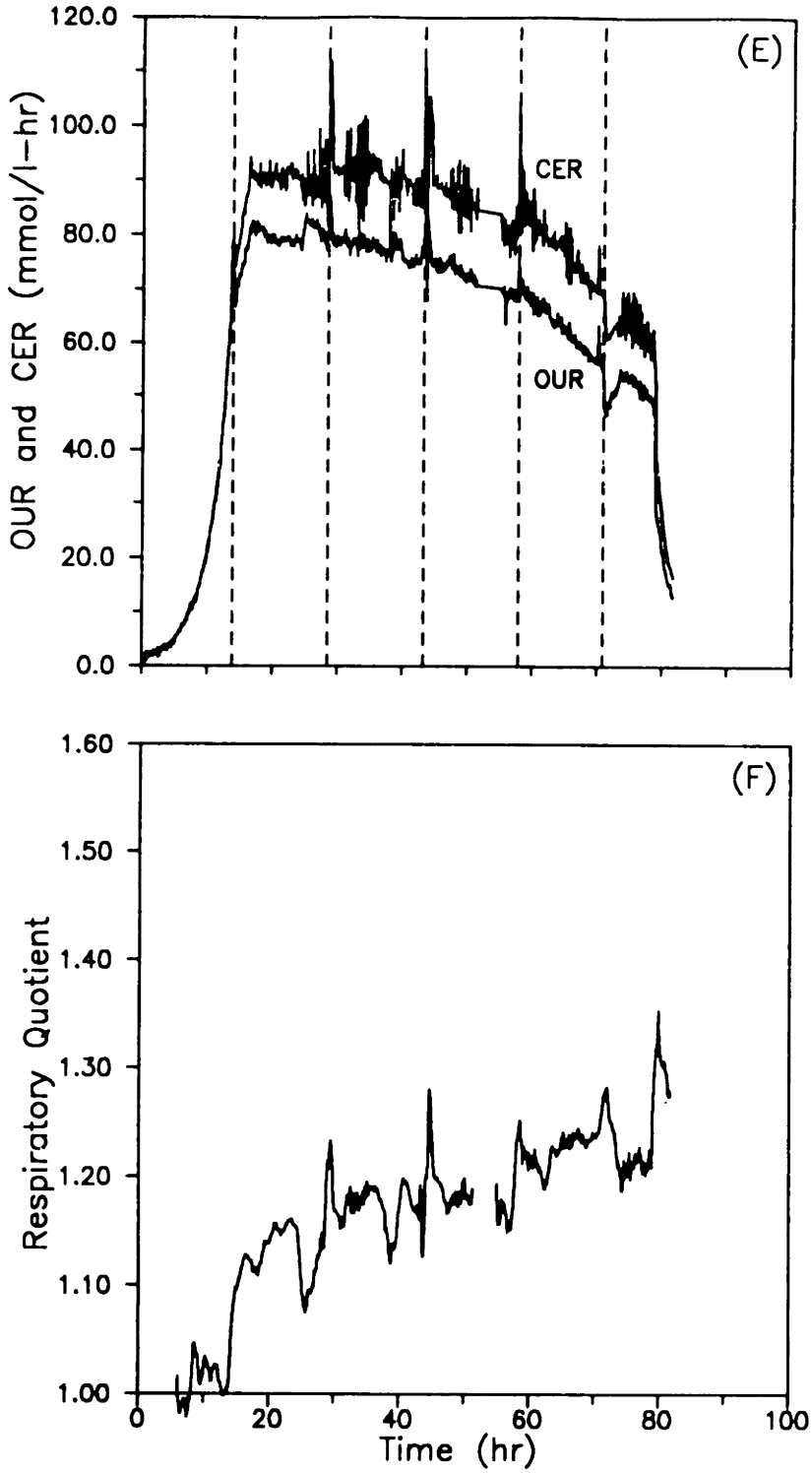

Figure 5.39. (Continued) (E) Oxygen uptake and carbon dioxide evolution rates. (F) Smoothed respiratory quotient (7 point moving average smoothing).

volume, various substrate concentrations, biomass concentration, L-lysine concentration, total L-lysine produced, OUR, CER, and RQ during this experiment. The L-threonine profile (Figure 5.39C) shows a rapid drop in concentration down to levels below assay sensitivity in about 14 hours. This corresponds to the point of respiratory "step-change" and the start of feeding for the fed-batch phases. Although L-threonine was being fed for the duration of this experiment, its concentration remained below measurable levels once feeding was begun. The most striking feature of the L-lysine profile (Figure 5.39B) is the fact that the final product titer was about 42 g/l, as compared to the batch case of about 23 g/l, an increase of over 80 percent in final titer (the total L-lysine produced was nearly three times that produced in the base case). The biomass (Figure 5.39B) reached a maximum of nearly 21 g/l before leveling off at about 16 g/l, compared to a maximum of about 17 g/l in the batch case. Glucose (Figure 5.39D) is seen to be exhausted when the run was stopped and it is therefore possible that the L-lysine titer could have reached higher levels had there been more glucose.

The off-gas data shows OUR and CER (Figure 5.39E) maintained at levels much higher than in the batch fermentation for nearly 80 hours, with RQ (Figure 5.39F) maintained at elevated levels above 1.1 for the entire experiment after the initiation of feed flow. The off-gas data itself is a clear indication that the level of biomass catalytic activity is being maintained at much higher levels than in the batch case and for long periods of operation.

To see the ramifications of this maintenance of the biomass catalytic activity, one needs to look at the time course of the L-lysine specific productivity and instantaneous and cumulative yields. Figure 5.40 shows the specific productivity and

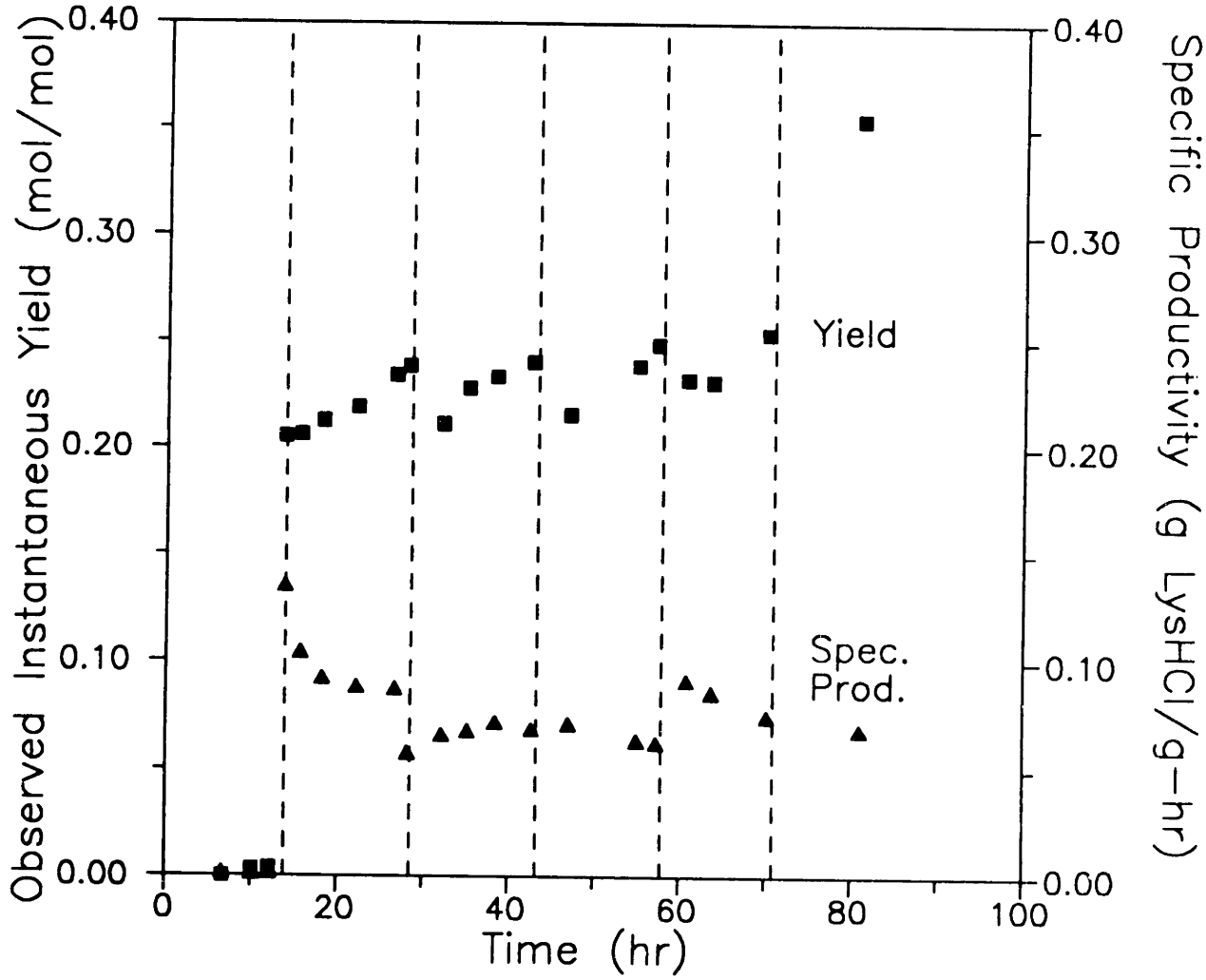

Figure 5.40. Specific L-lysine·HCl productivity and observed yield vs. time during repeated fed-batch fermentation.

instantaneous observed yield as functions of time during this experiment. The specific productivity is seen to stabilize at a level of between 0.06 and 0.08 g/g-hr for nearly 80 hours of culture, in marked contrast to the base case where there was a rapid decline in specific productivity to negligible levels after 40 hours. The comparison of the specific productivities for the two experiments is given in Figure 5.41. The elevated specific productivity resulted in a more than two-fold increase in average volumetric productivity over the batch base case (0.854 vs. 0.378 g/l-hr).

An interesting feature concerning the time course of the instantaneous yield is the increase in yield during the course of each fed-batch phase from about 0.20 to 0.25 mol/mol. A plausible explanation for this lies in the fact that the fed-batch dilution rate decreases linearly during the course of each fed-batch phase as the reactor volume increases. It has already been shown (for continuous culture) that the yield increases with decreasing growth rate. Depending on the rate at which the culture responds to dynamic changes in its environment, the growth rate of the culture should follow, to some extent, the changes in dilution rate. The fact that the concentrations of substrates and biomass were seen to reach quasi steady state values for much of the experiment implies that the growth rate was indeed closely following the dilution rate. The maintenance of the instantaneous yield at elevated levels for the duration of the experiment resulted in a 33 percent increase in overall yield over the batch base case (0.20 vs. 0.15 mol/mol).

Analysis of the fermentation broth for side products revealed the accumulation of L-valine (14 g/l) and L-alanine (1 g/l), and of the disaccharide trehalose (5 g/l), as shown in Figure 5.42. All three of these side products were produced during the base case experiment - L-valine at lower levels, but L-alanine and trehalose at slightly

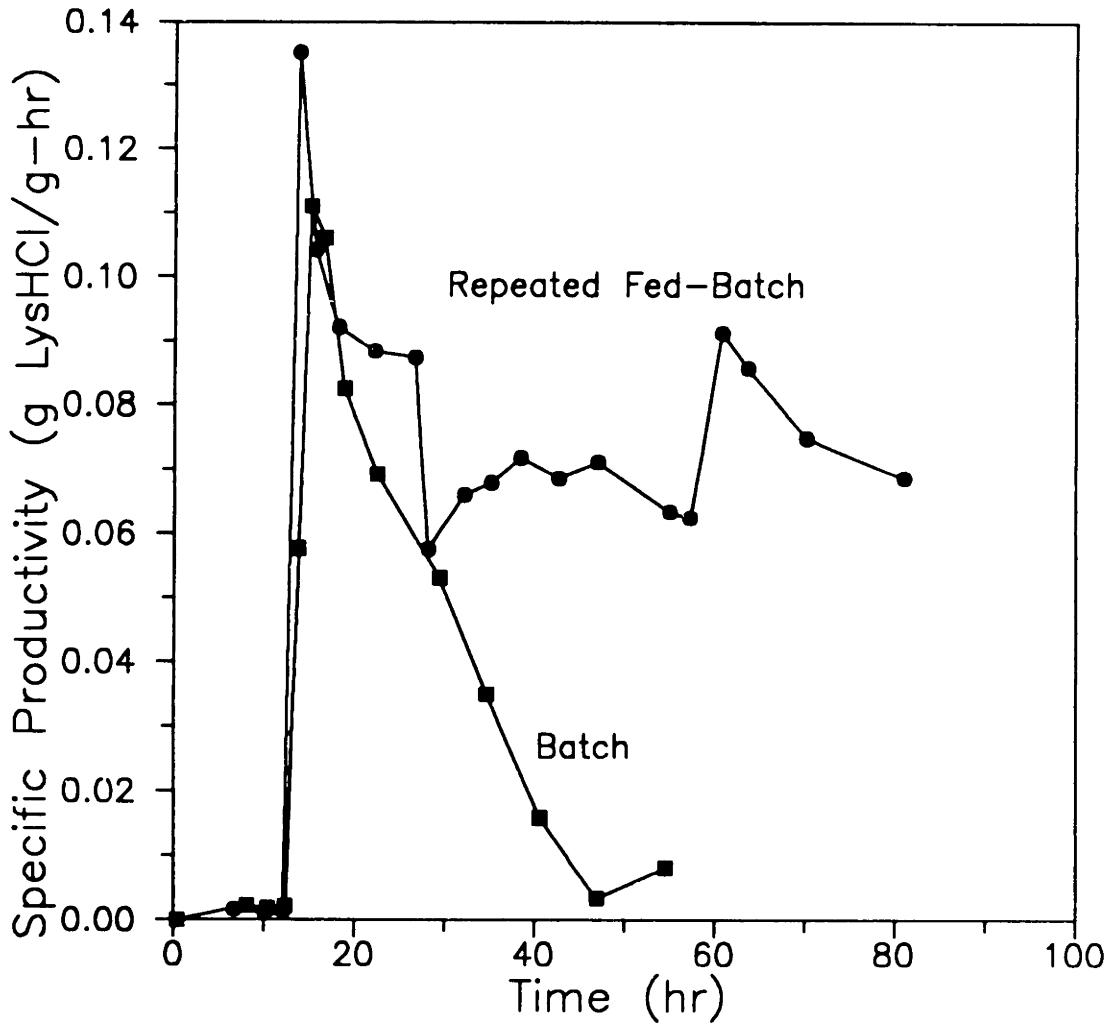

Figure 5.41. Comparison of specific L-lysine·HCl productivities for base case batch fermentation and repeated fed-batch fermentation.

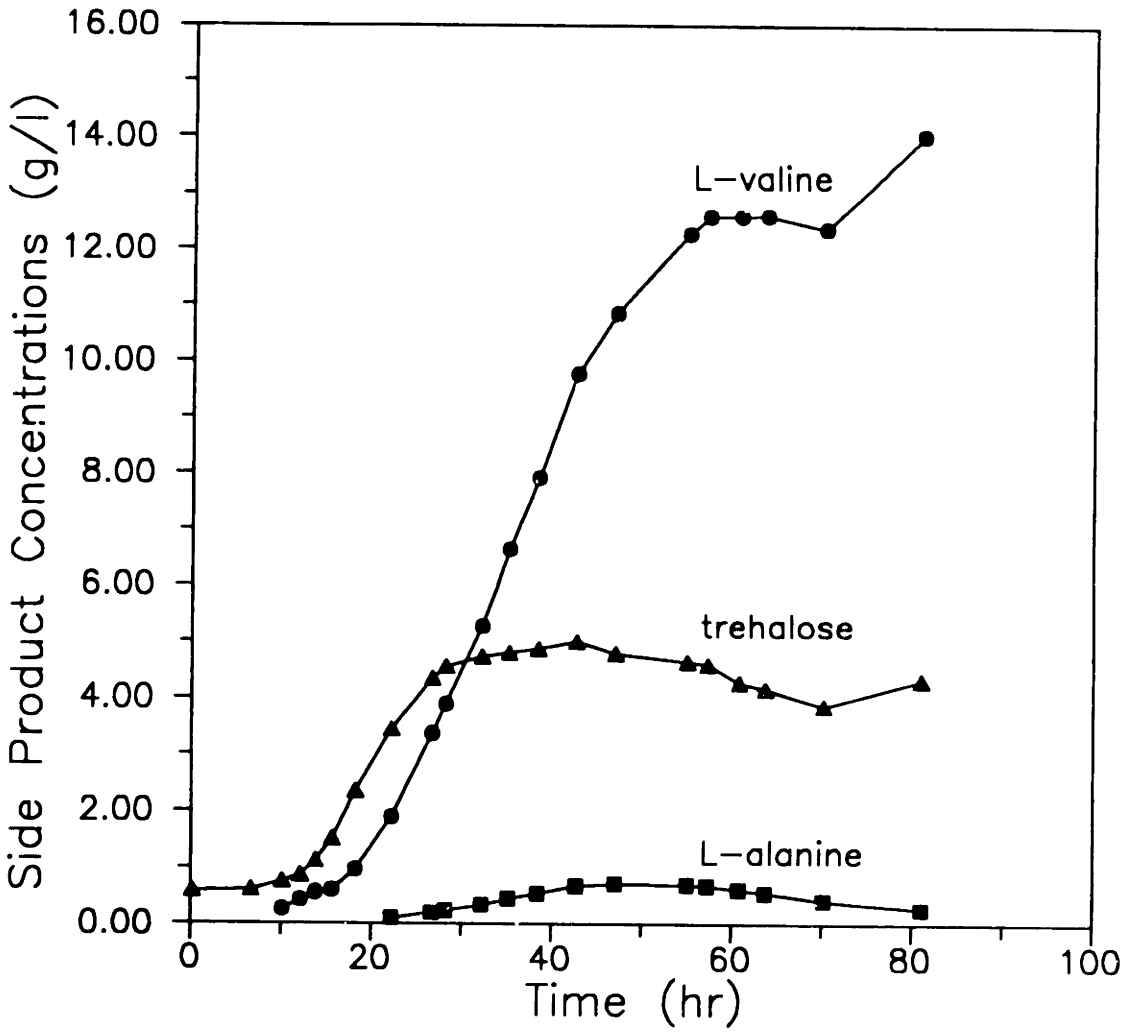

Figure 5.42. Side product accumulation during repeated fed-batch fermentation.

higher levels. The overall yield of amino acids (L-lysine and L-valine) from glucose is about 0.33 mol amino acid/mol glucose for this fed-batch experiment and the carbon material balance closes to 90 to 95 percent. The fact that high levels of L-lysine were accumulated in the presence of more than 1 g/l of L-leucine casts doubt on any negative effect of L-leucine on L-lysine biosynthesis, as discussed in Section 2.3.1.

5.5.3.2 Reduced Dilution Rate Fed-Batch Fermentation

The previous fed-batch experiment operated at feed rates which were somewhat high in that the reactor would be filled with liquid after about 16 hours of feeding. The initial reactor liquid volume cannot be less than about 6 liters due to probe constraints and thus 4 liters is about the maximum amount of feed which can be delivered to the process. Since the feed time was so short, the total fermentation time for one fed-batch phase would have been less than 30 hours. So, to make the fermentation more directly comparable to the base case (as well as to investigate the recyclability, or durability of the catalyst), the fed-batch operation was repeated several times so that reactor productivities could be compared over approximately equal time frames.

The next open-loop fed-batch experiment, denoted FB4, was designed to run for about the same time as the base case batch fermentation using only a single fed-batch phase plus additional batch fermentation once the reactor was filled. The feed rate for FB4 was 50 ml/hr (2 liters total feed) and the initial reactor volume was approximately 8 liters. The dissolved oxygen concentration was maintained at or above 20 percent of saturation at all times by manual adjustment of the agitation rate. As far as keeping the biomass active, the important variable is not necessarily

the volumetric feed rate, but the rate of addition of the growth limiting nutrient, L-threonine. It was thought that 50 ml/hr of feed at the same L-threonine feed concentration as FB1 might not be sufficient to maintain catalytically active biomass, so the L-threonine was partitioned more toward the feed rather than the initial reactor fill. Thus, the initial L-threonine concentration for batch growth before feeding began was lower than that in FB1 or the base case, and the L-threonine feed concentration was higher than that in FB1 (feed concentration was 2.93 g/l L-threonine as opposed to the standard CGM3 concentration of 0.733 g/l). The total L-threonine provided to the culture was, however, exactly the same as in FB1 and the base case. The L-threonine addition rate (mg/hr) for FB4 was about 80 percent of that for FB1.

Since the initial L-threonine concentration was reduced in this experiment, one would expect to reach the depletion point earlier in the experiment and at a lower biomass concentration than in either FB1 or the base case. This was indeed the case, and feeding was begun at about 9 hours and 2.5 g/l of biomass as compared to 14 hours and 9.7 g/l of biomass in FB1.

Figures 5.43A through 5.43E show the time course of various substrate concentrations, biomass and L-lysine concentrations, total L-lysine produced, OUR, CER, and RQ for this experiment. It should be noted that additional glucose (500 g) was added at about 54 hours, resulting in about a 1 liter dilution effect. In Figure 5.43B, the L-threonine concentration is seen to drop rapidly to unmeasurable values (at which point feeding was initiated) and remains undetectable for the remainder of the experiment. The L-leucine concentration never achieves a quasi steady state level as in FB1. The same can be said for the biomass profile (Figure 5.43A) and the

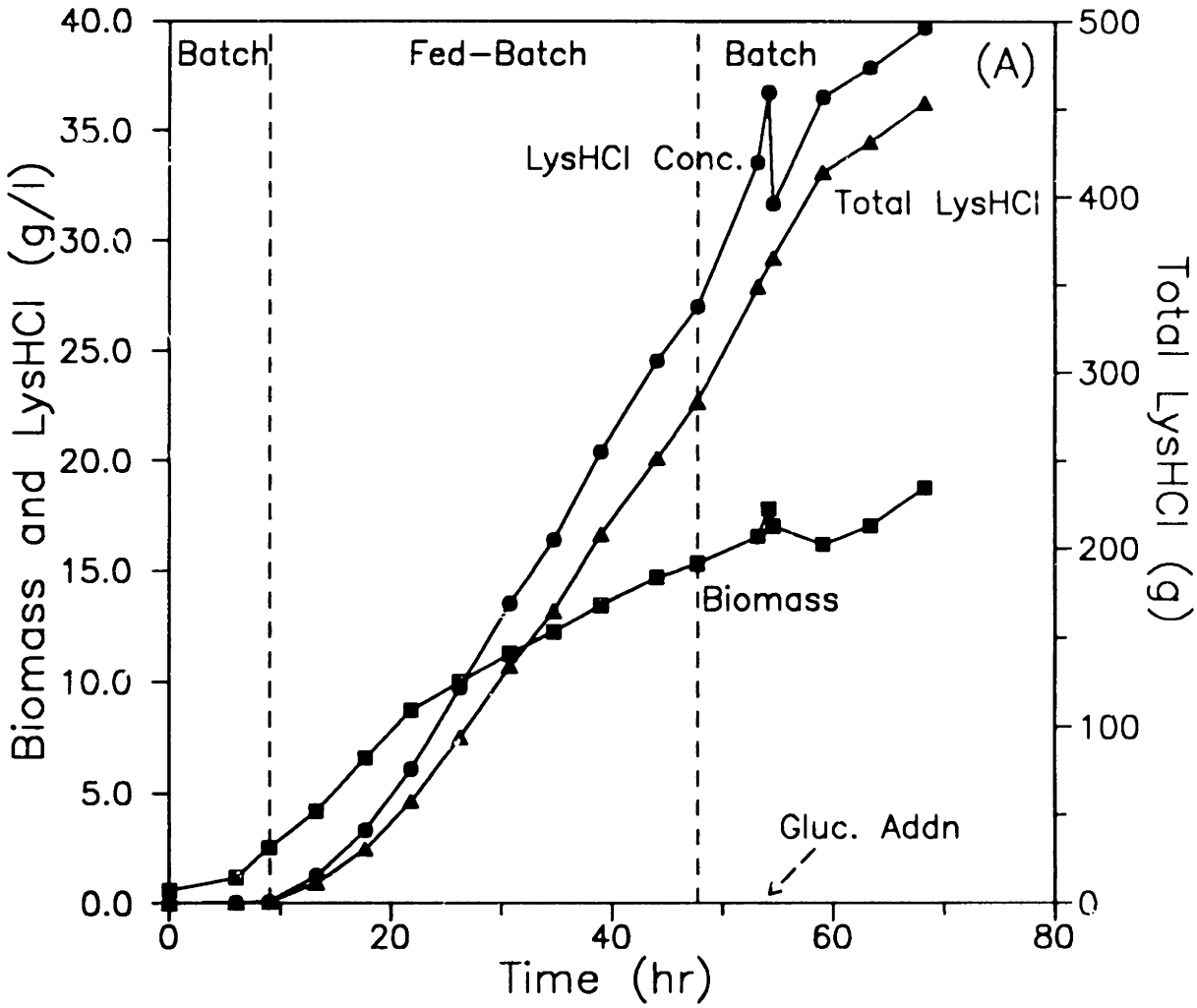

Figure 5.43. Open-loop, reduced dilution rate fed-batch fermentation dynamic profiles. (A) Biomass and L-lysine·HCl concentrations and total L-lysine·HCl.

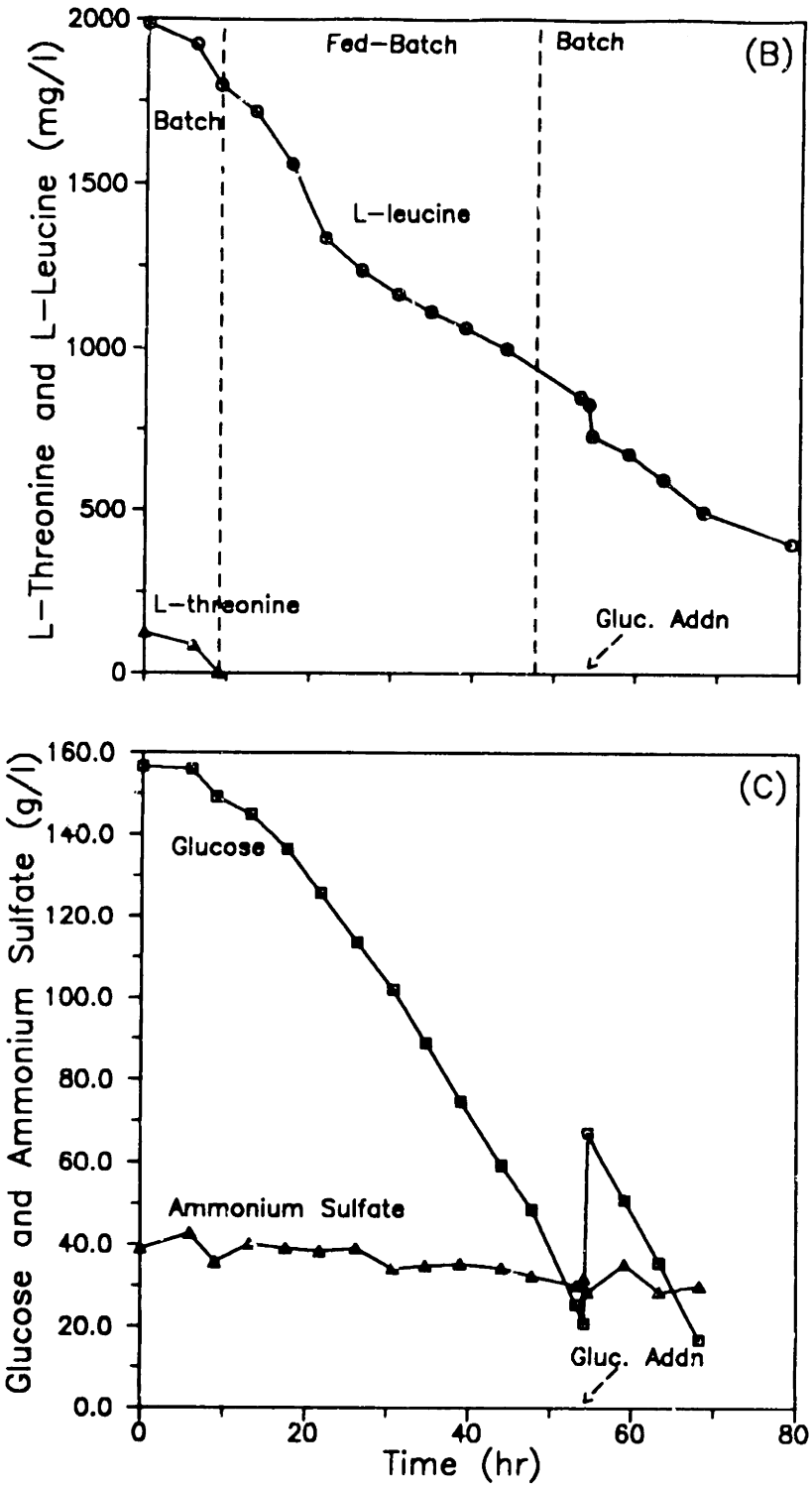

Figure 5.43. (Continued) (B) L-threonine and L-leucine concentrations. (C) Glucose and ammonium sulfate concentrations.

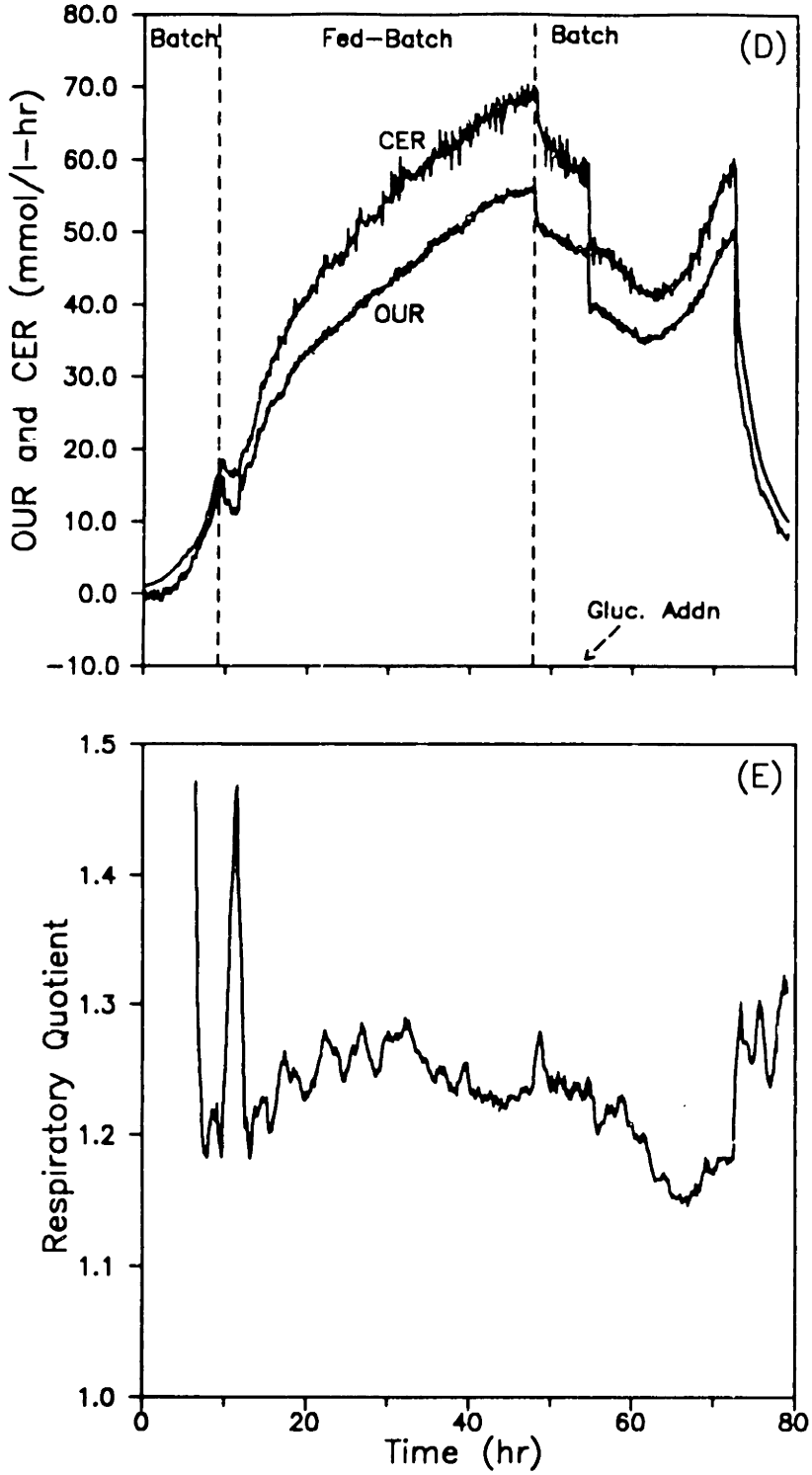

Figure 5.43. (Continued) (D) Oxygen uptake and carbon dioxide evolution rates. (E) Smoothed respiratory quotient (7 point moving average smoothing).

glucose profile (Figure 5.43C). Figure 5.43A shows L-lysine accumulation beginning right at the point of feeding initiation (corresponding to the depletion point) and continuing until the level reaches about 40 g/l. As in FB1, this product titer was nearly twice that of the base case (total L-lysine produced was twice that of the base case), and as we will see, maintenance of the specific productivity over the course of the fermentation was the reason for this increased titer.

Off-gas data for this experiment are shown in Figures 5.43D and 5.43E. OUR and CER (Figure 5.43D) are seen to increase steadily during the entire course of feeding due to the fact that the culture never reaches a quasi steady state. The respiratory quotient profile (Figure 5.43E) shows this indicator to be near about 1.2 for the duration of the experiment after the initiation of feed flow. The spike at approximately 12 hours followed a temporary accidental shutoff of the feed flow.

Figure 5.44 shows the specific productivity and instantaneous observed yield as functions of time for this experiment. As in FB1, the specific productivity remains in the range of 0.06 to 0.08 g/g-hr and the instantaneous yield is between 0.20 and 0.25 for most of the experiment. Again, the maintenance of the specific productivity, in direct contrast with the base case, results in the increased product titer and volumetric productivity seen in this run. The maintenance of the instantaneous yield at elevated levels results in an increase of about 40 percent in the overall yield over the base case (0.21 versus 0.15 mol/mol). The drops in yield and productivity at the end of the final batch phase are due not only to normal batch culture decay, but also to the appearance of a significant proportion of homoserine revertant cells toward the end of the experiment (note the increasing respiratory rates prior to glucose exhaustion). Recall that this cultural instability problem was successfully addressed

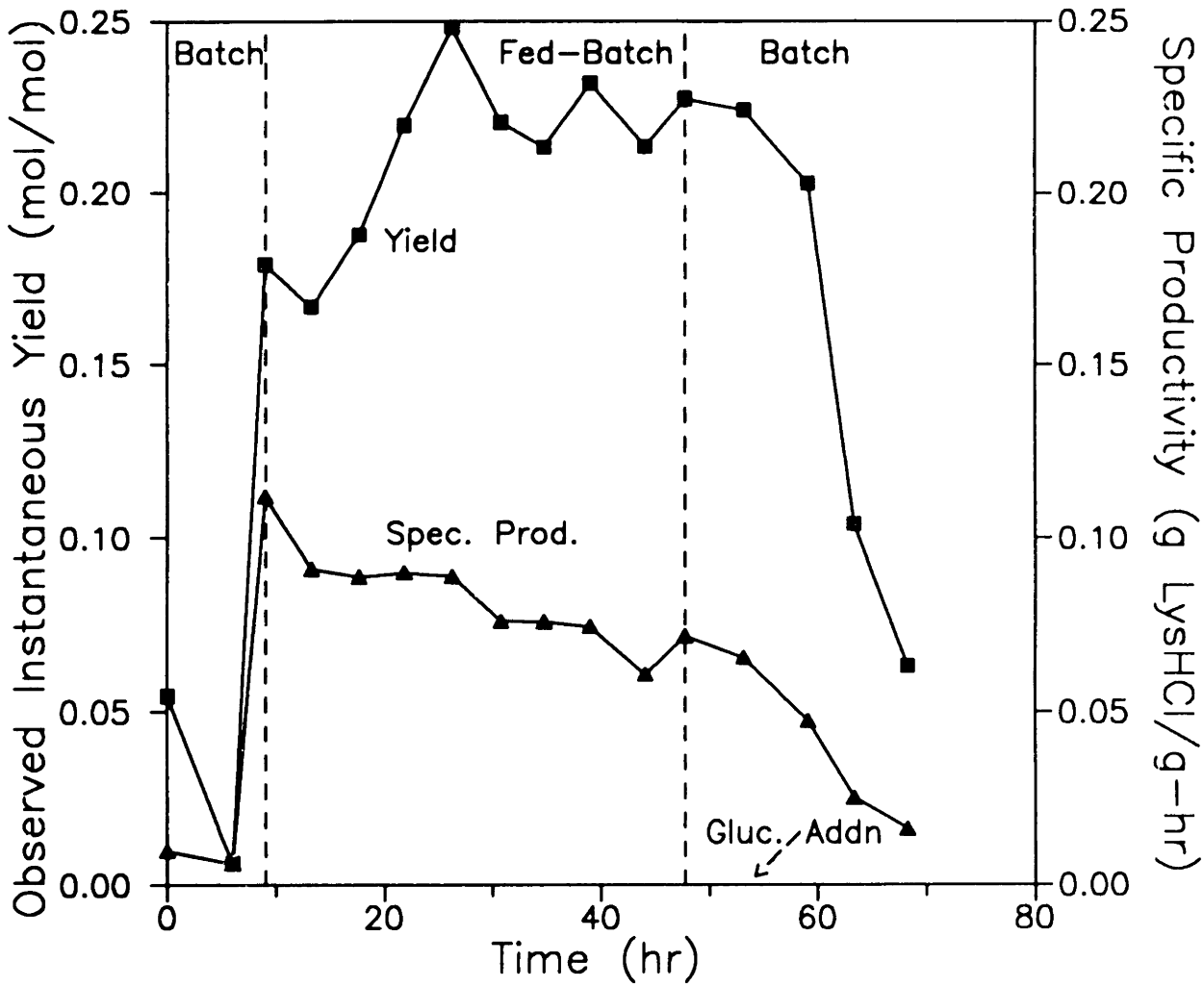

Figure 5.44. Specific L-lysine·HCl productivity and observed yield vs. time during reduced dilution rate fed-batch fermentation.

via media manipulations.

As in experiment FB1, there was significant side product accumulation in experiment FB4. Figure 5.45 shows the time profiles of L-valine (20 g/l), trehalose (6 g/l), L-alanine (1 g/l), and pyruvate. The small amount of pyruvate excreted was later consumed by the culture when glucose was exhausted. The overall yield of L-lysine and L-valine from glucose reached about 0.35 mol/mol.

5.5.3.3 Summary of Open-Loop Fed-Batch Experimental Results

Both of the open-loop fed-batch experiments have clearly demonstrated the advantages of restraining growth in this amino acid fermentation. Culturing the cells at a slow, controlled rate of growth for a large portion of the fermentation time results in high levels of specific productivity and instantaneous yield being maintained throughout the fermentation. The ramifications of the maintenance of the biomass catalytic activity were seen in the near doubling of the final product concentration (1.7 to 2.2-fold increases in average volumetric productivity) and overall fermentation yields of 20 to 21 molar percent. The fed-batch cultures have also shown the respiratory quotient to remain elevated throughout the process once the L-threonine limitation has been reached and feeding is initiated. Table 4 gives a performance comparison between the base case batch fermentation and the two open-loop fed-batch fermentations.

The shift of the fermentation final state from low L-lysine, low L-valine (base case) to high L-lysine and high L-valine with increased yield by a simple fed-batch strategy clearly demonstrates the promise of environmental manipulation as a means of influencing the metabolic outcome of a microbial fermentation. These results provided further support for the performance improvement hypothesis and the utility

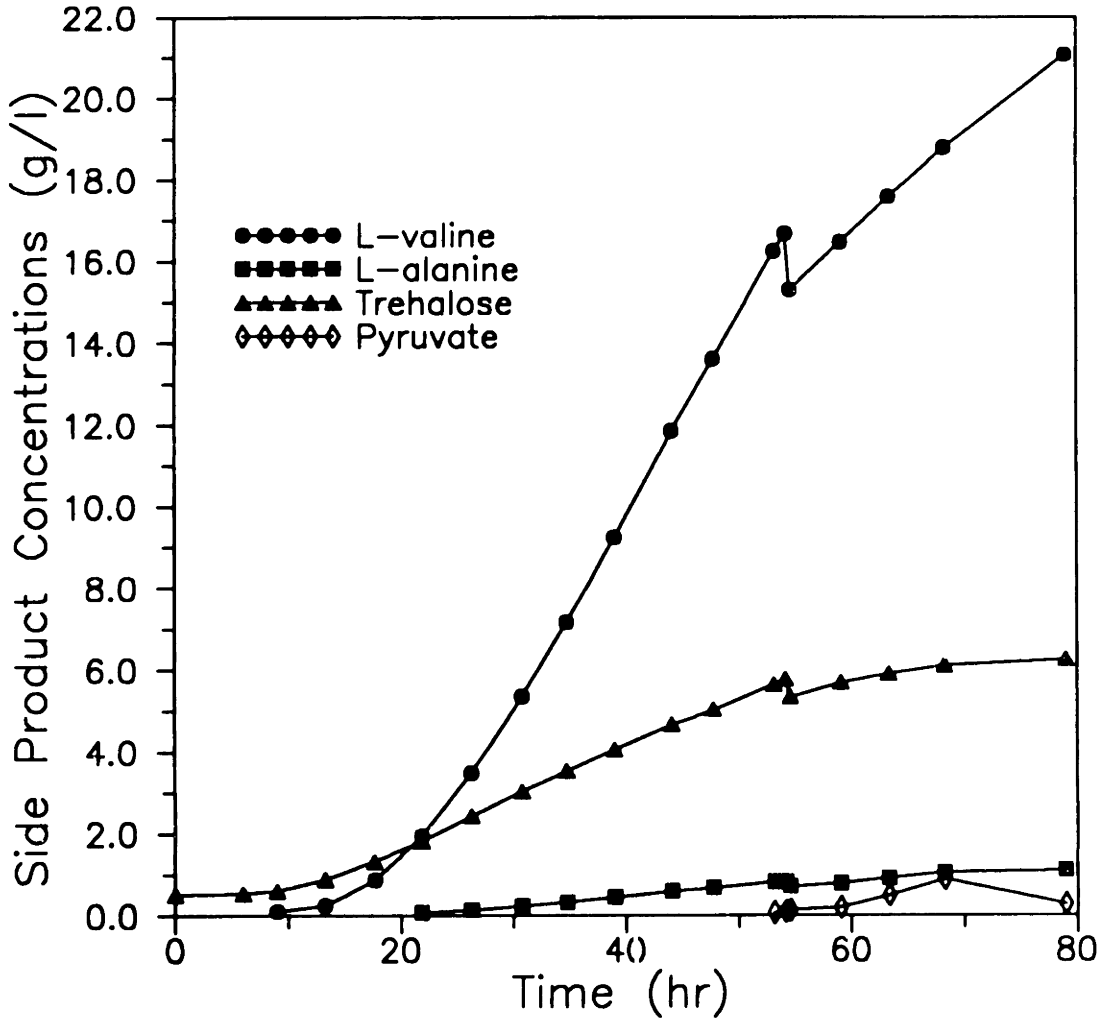

Figure 5.45. Side product accumulation during reduced dilution rate fed-batch fermentation.

Table 5.4 - Performance comparison between base case batch fermentation and constant feed rate fed-batch fermentations.

Experiment Type	Batch	Fed-Batch	
Experiment ID	Batch Base Case	FB1	FB4
Final L-Lys·HCl Titer (g/l)	23	42	40
Ratio to Base Case	-	1.83	1.74
Total L-Lys·HCl Produced (g)	230	649	456
Ratio to Base Case	-	2.82	1.98
Avg. Vol. Prod. (g/l-hr)	0.378	0.854	0.639
Ratio to Base Case	-	2.26	1.69
Avg. Mass Productivity (g/hr)	3.82	8.54	6.71
Ratio to Base Case	-	2.24	1.76
Observed Yield (mol/mol)	0.15	0.20	0.21
Ratio to Base Case	-	1.33	1.40

of the respiratory data as an on-line metabolic activity indicator for closed-loop feedback controls. The development of such controls, and experimental demonstration of their effectiveness are discussed next.

5.6 Development and Demonstration of Restrained Growth Feedback Control Strategies

This section describes the development of the control algorithms used for feed rate control in restrained growth fed-batch fermentations. After development of the necessary software and hardware, the strategies were tested in two fermentations, one with a goal of overall productivity maximization and the other with a goal of overall

yield maximization.

5.6.1 General Strategy Description

As previously mentioned, maximization of either the overall productivity or the overall yield will require different control strategies. These strategies are derived from the batch and continuous culture characterization data and rely on the on-line determination of trends (increasing or decreasing behavior) in the respiratory parameters. These trends (i.e. derivatives) in OUR, CER, and RQ are indicative of the culture's metabolic activity towards L-lysine overproduction. Appropriate control action (feed rate manipulation) is taken based on a heuristic, or decision tree, analysis of the fermentation respiratory trends. The details of the on-line data analysis and manipulation have been previously discussed in Section 4.2.2.4.

5.6.2 Productivity Maximization Strategy

5.6.2.1 Algorithm

The control strategy for maximizing productivity is based on the premise that the volumetric productivity will be maximized when the highest possible growth rate, within the range of maximum specific productivity, is maintained throughout the course of the fermentation. A control algorithm attempting to continually increase the specific growth rate through feed rate increases is shown in Figure 5.46. Respiratory trends were used as feedback indicators of under- or over-feeding.

Following along the right branch of the decision tree of Figure 5.46, an increasing RQ implies that production of L-lysine is increasing; consequently, an even higher specific growth rate should be sought by further increasing the feed rate.

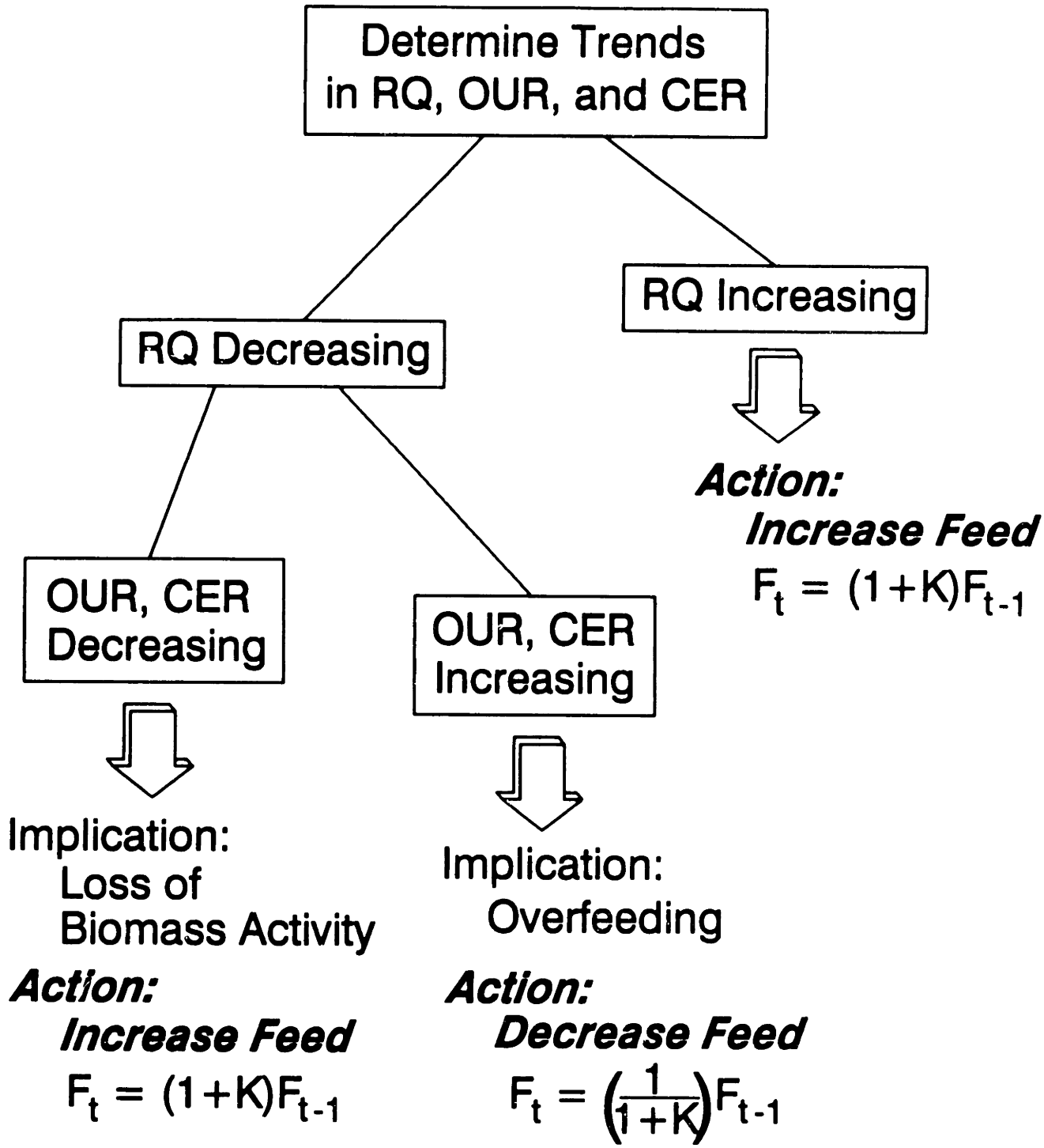

Figure 5.46. Control policy structure for productivity maximization goal.

Looking at the left branch of the decision tree, a decreasing RQ, in itself, does not uniquely determine the course of action to be taken since this can be indicative of either a loss of biomass catalytic activity due to under-feeding or of feedback inhibition by L-threonine due to over-feeding. Discrimination between these two possibilities is possible through examination of the individual trends in OUR and CER. If respiratory rates are decreasing while RQ is decreasing, this implies that the supply of the growth-limiting nutrient (L-threonine) is insufficient and the biomass activity is deteriorating, indicating the need for an increased feed rate. If the respiratory rates are increasing while RQ is decreasing, this implies that biosynthesis is being favored over L-lysine formation, indicating the need for a reduced feed rate.

As indicated in Figure 5.46, in all feed rate actions taken, the feed rate was adjusted to be proportionately higher or lower, as appropriate, than the feed rate at the previous sampling epoch. The proportionality constant K (equal to 0.005) was selected solely on the basis of system constraints such as total reactor volume and pumping capacity, and the desire to pump in all available feed in a physically reasonable amount of time. In the event that the control algorithm repeatedly takes the same action (such as repeated increases or decreases of the feed rate) the feed profile will be governed by a power-law expression and will thus be exponential in character. If the calculated respiratory trends do not follow one of the decision tree branches (i.e. OUR increases while CER decreases), no changes in feed rate are made for that sampling period.

Although correct in assigning the cause-effect relationships and identifying the proper control and manipulated variables, the control law of Figure 5.46 can be further improved by applying modern control theory in the determination of the

control parameter K. One possibility is to couple the control law with a model for the process dynamics and tune the parameter K on the basis of the characteristic time constants of the system and the anticipated rates of L-threonine consumption. Yet another possibility might be, especially in light of the time-varying nature of a fermentation system, to provide for variable values of the parameter K determined from adaptive control theory. None of the above possibilities were considered in this work which focused primarily on the establishment of the cause-effect relationships and the elucidation of the role of L-threonine in balancing cell viability and L-lysine overproduction.

5.6.2.2 Experimental Results

The results of the experiment carried out utilizing this productivity maximization feed control strategy appear in Figures 5.47A to 5.47F. The experimental details were similar to experiment FB1 with 6 liters of initial reactor volume and 4 liters of CGM3 feed. The feed rate, calculated on-line by the control algorithm, is seen to increase rapidly, and nearly continually, between the initiation of feeding at the depletion point and the exhaustion of the feed supply (Figure 5.47A). Inspection of the respiratory data in Figure 5.47B and the respiratory trend data of Figures 5.47C and 5.47D reveals how such a feed profile was generated. First, however, it should be pointed out that the filtering algorithm satisfactorily extracted the fermentation respiratory trends from the on-line respiratory data. Note that OUR and CER trends were only determined when the RQ was found to be decreasing; otherwise they were not required and thus do not appear in the figure.

For approximately the first half of the feeding phase, RQ continued to increase and the controller responded by trying to increase growth further by

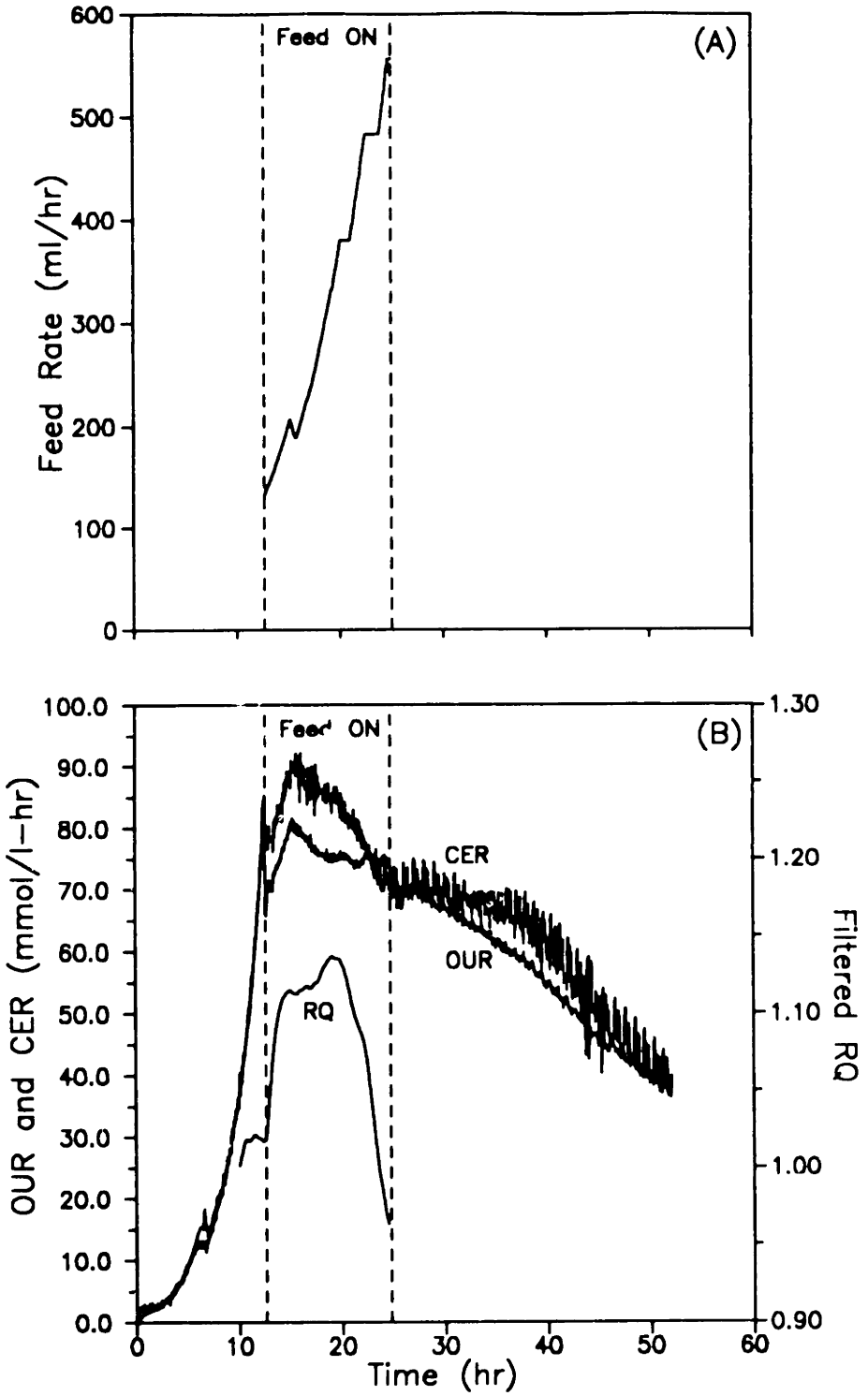

Figure 5.47. Experimental results for feedback controlled fed-batch fermentation utilizing productivity maximization algorithm. (A) Feed rate vs. time. (B) Respiration rates (raw) and filtered respiratory quotient vs. time.

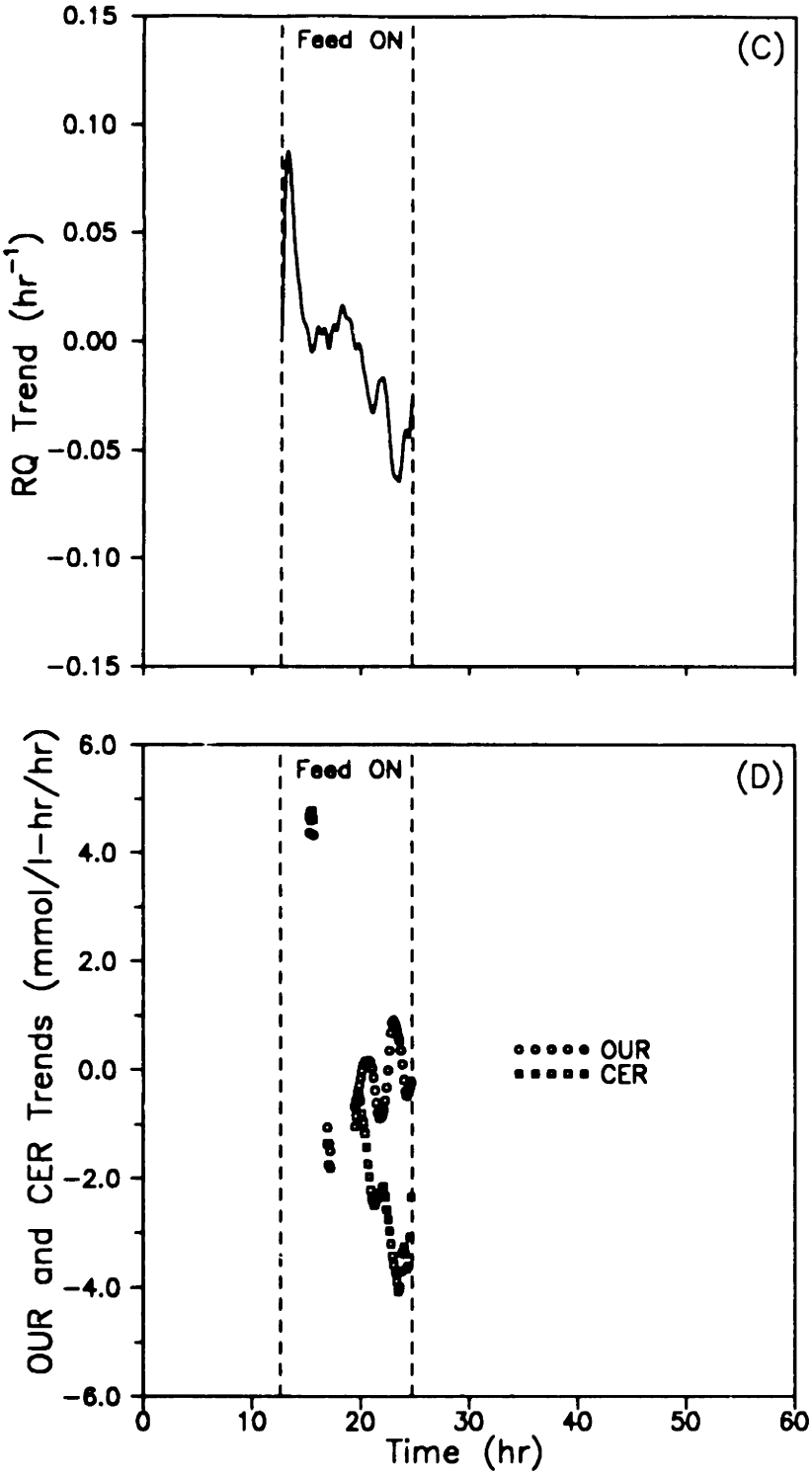

Figure 5.47. (Continued) (C) On-line respiratory quotient trends vs. time. (D) On-line OUR and CER trends vs. time.

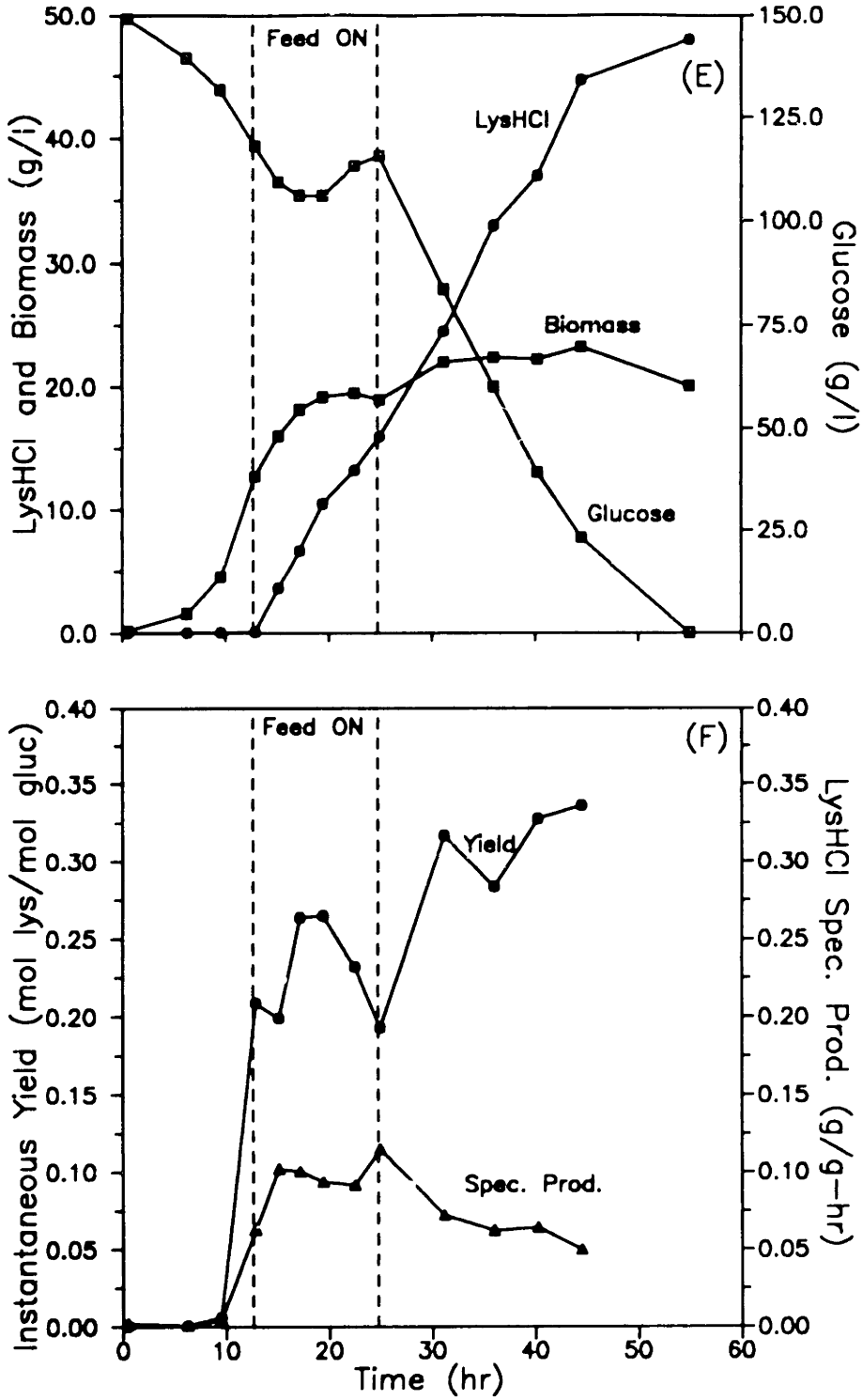

Figure 5.47. (Continued) (E) Biomass, L-lysine·HCl, and glucose concentrations vs. time. (F) Instantaneous yield on glucose and specific L-lysine·HCl productivity vs. time.

increasing the feed rate. About half way through the feeding phase, RQ began to decrease with OUR and CER also decreasing. This was correctly interpreted as a decline in metabolic activity due to underfeeding (as opposed to feedback inhibition) and the feed rate was increased further. However, the feed rate increases were insufficient to arrest the decline in RQ and respiratory rates which continued unabated to the end of the feeding phase. Apparently the value of K chosen was inadequate during the later phase of feeding, to supply L-threonine in amounts needed to support the large amount of biomass that had accumulated. Considering the need for a small value of K during the initial phase of the fermentation to avoid feedback inhibition by L-threonine, a variable K value would likely be optimal for this fermentation. As discussed earlier, adaptive control theory could be applied in addressing this problem.

As alluded to in the discussion of dynamic optimization in Section 3.3.3, this experimentally obtained feed rate profile agrees with the optimal profile determined by the dynamic optimization of Modak *et al.* (1986). This is an appealing result since the experimental profile was determined on-line based solely upon the heuristic interpretation of the culture respiration. No mathematical model for the fermentation dynamics was required; the interpretation relied only upon the phenomenological relationships between metabolic activity and respiration developed through the batch and continuous culture characterizations.

Figure 5.47E shows that this feed strategy resulted in a final L-lysine titer of 48 g/l and Figure 5.47F shows the maintenance of both specific productivity and yield at elevated levels for the duration of the fermentation. This strategy resulted in an overall average volumetric productivity 2.5 times that of the batch fermentation with

final L-lysine titer increased by a factor of 2.1. It should also be mentioned that this fermentation ended due to glucose exhaustion at a time when the biomass was still productive and thus higher titer could likely have been obtained. Side product accumulation was similar to experiment FB1 (Section 5.5.3.1) with 1.5 g/l of L-alanine, 11 g/l of L-valine, and 12 g/l of trehalose.

A further experiment was performed with productivity maximization as the goal, but at approximately twice the batch culture cell density. To achieve the increased cell density, the CGM3 medium was scaled up by doubling the L-threonine concentration and increasing all other components, except glucose, by 1.5-fold. Total glucose was increased to 3300 g (6 liters initial reactor volume at 150 g/l plus 4 liters of feed at 600 g/l). A linearized approximation to the experimentally determined continually increasing feed rate was applied in an open-loop mode.

The results of this "high-density" experiment are shown in Figures 5.48A to 5.48D. The fermentation profiles are quite similar to those of the productivity maximization run just described, indicating a more general applicability of this strategy. L-lysine titer reached 77 g/l (3.3 times the batch titer) at an average volumetric productivity of about 1.2 g/l-hr (3.2 times the batch case) and an overall yield of about 0.22 mol/mol. The maximum instantaneous productivity (specific productivity·biomass concentration) was about 1.8-2.2 g/l-hr. The higher biomass density led to higher final side product concentrations: 2.5 g/l of L-alanine, 22 g/l of L-valine, 19 g/l trehalose and about 0.2 g/l pyruvate. Note that this fermentation resulted in more than 100 g/l of total amino acid production.

The increased final L-lysine concentration dispels any notion that the 40 g/l range of L-lysine is inhibitory toward aspartate kinase. Under the fermentation

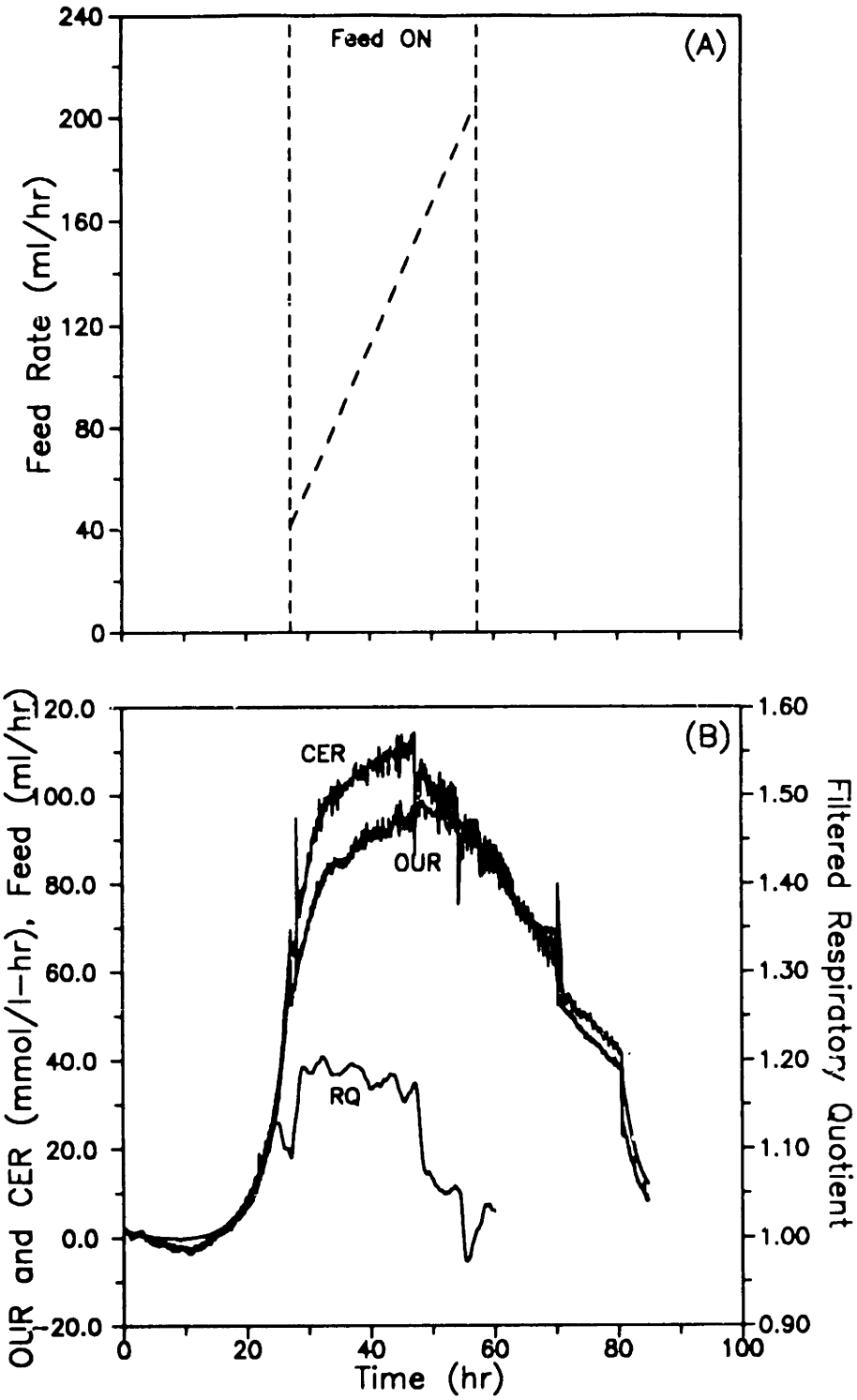

Figure 5.48. Experimental results for high cell density fed-batch culture using open-loop approximation to productivity maximization feed profile. (A) Feed rate vs. time. (B) Respiration rates (raw) and filtered respiratory quotient vs. time.

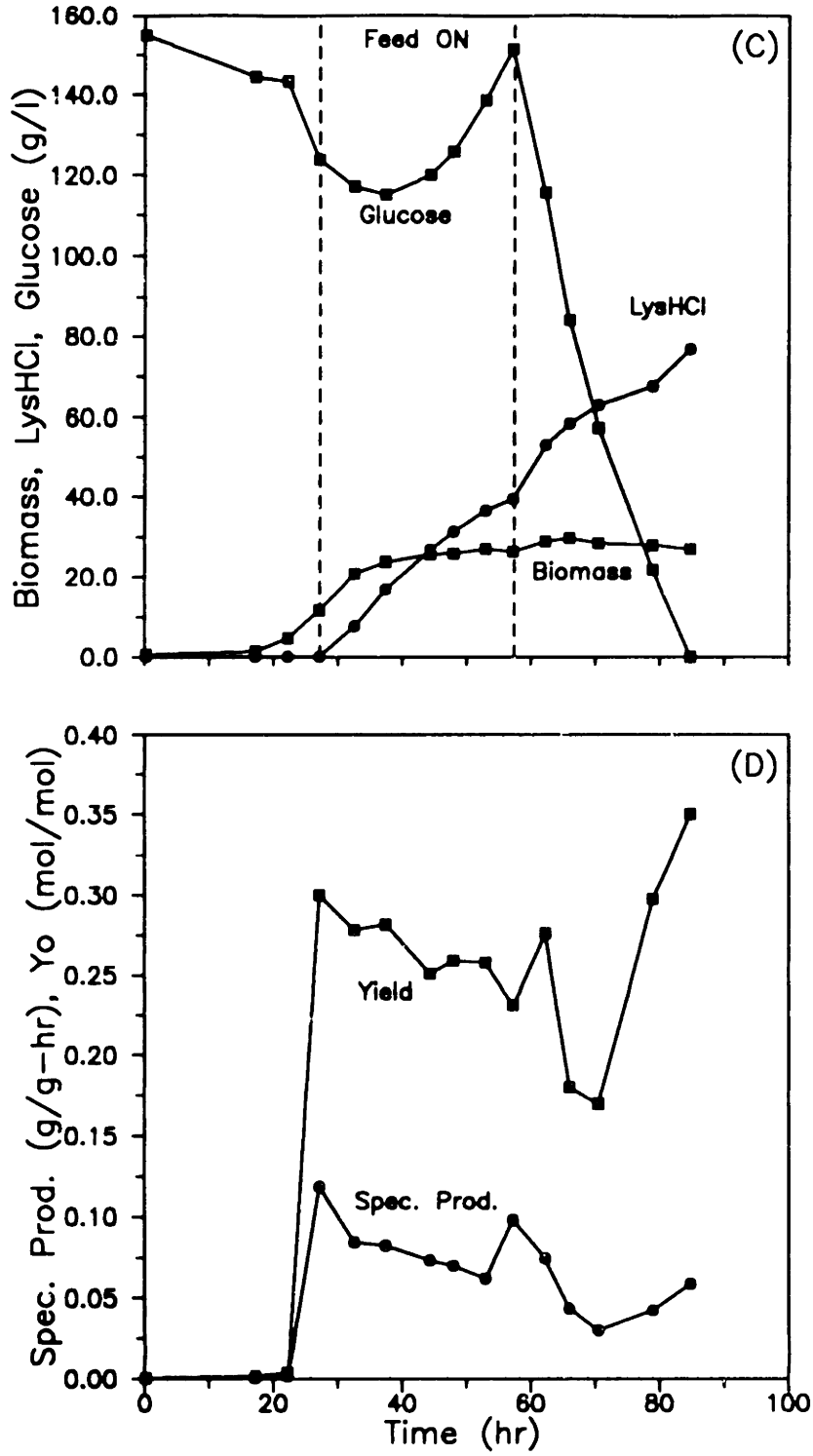

Figure 5.48. (Continued) (C) Biomass, L-lysine·HCl, and glucose concentrations vs. time. (D) Instantaneous yield on glucose and specific L-lysine·HCl productivity vs. time.

conditions of these experiments, it is likely that the L-threonine is low enough that there is effectively no inhibition of aspartate kinase. Thus, this "simple" auxotrophic strain is entirely capable of producing quite high concentrations of L-lysine (comparable to the more highly touted AEC resistant strains). Also, these results indicate a lack of any negative regulatory effect of L-leucine on L-lysine formation since levels of L-leucine were consistently above 1 g/l.

It should be mentioned that due to the increased cell density in this experiment, higher rates of oxygen transfer were required compared to all other runs. This was achieved by manually adjusting both agitation rate and vessel head pressure to maintain the DO level at 10 percent of saturation or greater. The maximum vessel head pressure used was approximately 7 psig.

5.6.3 Yield Maximization Strategy

5.6.3.1 Algorithm

Maximization of the overall fermentation yield can be achieved through maximization and maintenance of the instantaneous yield throughout the fermentation. The instantaneous yield in turn will be maximized when the growth rate is minimized to a level just sufficient to maintain the L-lysine biosynthetic apparatus (Figure 5.19A). The strategy then is to force the culture to produce L-lysine at the lowest possible growth rate by minimizing feed rate.

The control algorithm for yield maximization is shown in Figure 5.49. The on-line respiratory measurements indicate whether the culture can produce at even lower feed rates or if maintaining sufficient metabolic activity requires higher rates of feed.

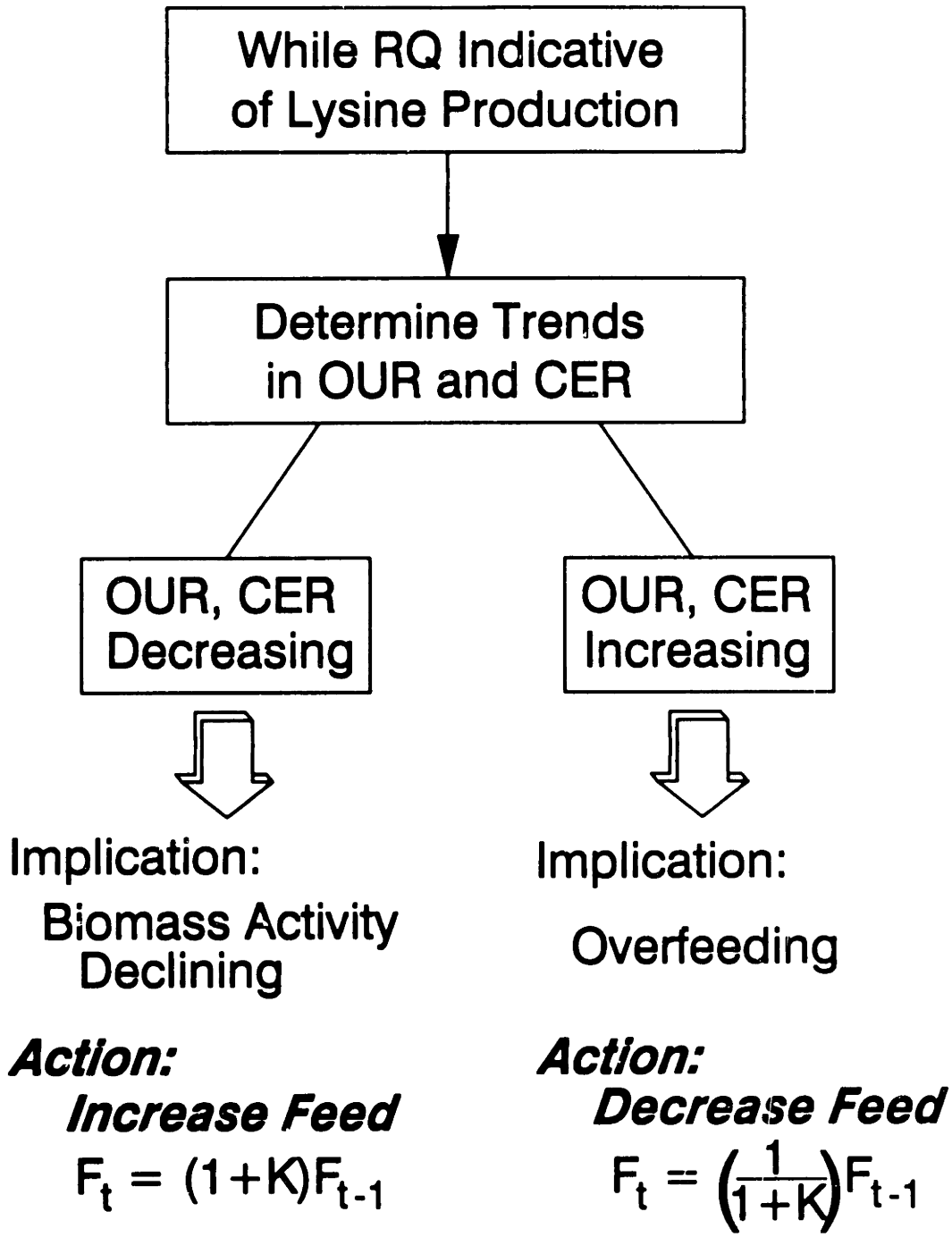

Figure 5.49. Control policy structure for yield maximization goal.

Since the emphasis is on minimizing growth rate, the only two metabolic conditions which should arise in the application of this strategy are the case of declining metabolic activity due to insufficient nutrients and the case of excessive nutrient addition leading to more growth than required to maintain maximum conversion efficiency. In this control algorithm, then, as opposed to the productivity algorithm, effective monitoring of the biomass catalytic activity requires only the trends in OUR and CER, given that the respiratory quotient is elevated above the pure growth value and is thus indicative of L-lysine production. Thus, the simplified decision tree of Figure 5.49 is sufficient for proper culture control.

5.6.3.2 Experimental Results

The results of the experiment carried out utilizing this yield maximization strategy appear in Figures 5.50A to 5.50D. The experimental details were similar to experiment FB4: 8 liters initial reactor volume and 2 liters of CGM3 feed modified to contain 2.93 g/l L-threonine. In Figure 5.50A, the feed rate is seen to decrease continually from the point of feed initiation. The control algorithm correctly interpreted increasing respiration rates as an indication of excessive biomass production (at the expense of the yield). Figure 5.50B illustrates the respiratory trends in OUR and CER utilized by the control algorithm.

At 20 hours, an approximately constant feed rate was reached, and subsequently maintained by control action for the duration of the fermentation. This constant feed rate corresponded to a specific L-threonine feed rate of about 0.5 mg L-threonine/g DCW·hr, and was sufficient to maintain constant levels of respiration at a RQ of between 1.25 and 1.35. Thus, this experiment determined the minimum specific L-threonine addition rate required to restrain the growth of the organism at

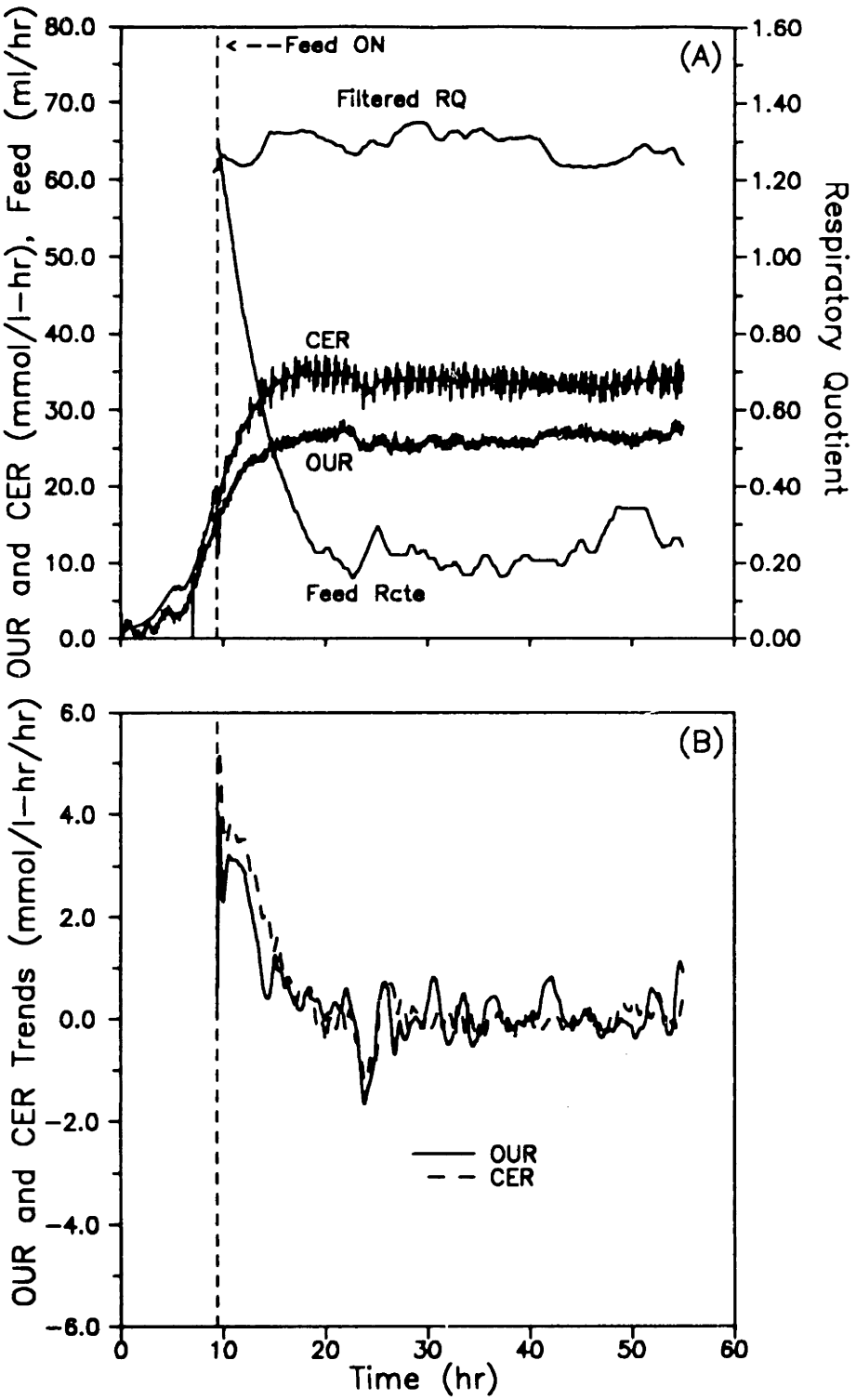

Figure 5.50. Experimental results for feedback controlled fed-batch fermentation utilizing yield maximization algorithm. (A) Feed rate, respiration rates (raw) and filtered respiratory quotient vs. time. (B) On-line OUR and CER trends vs. time.

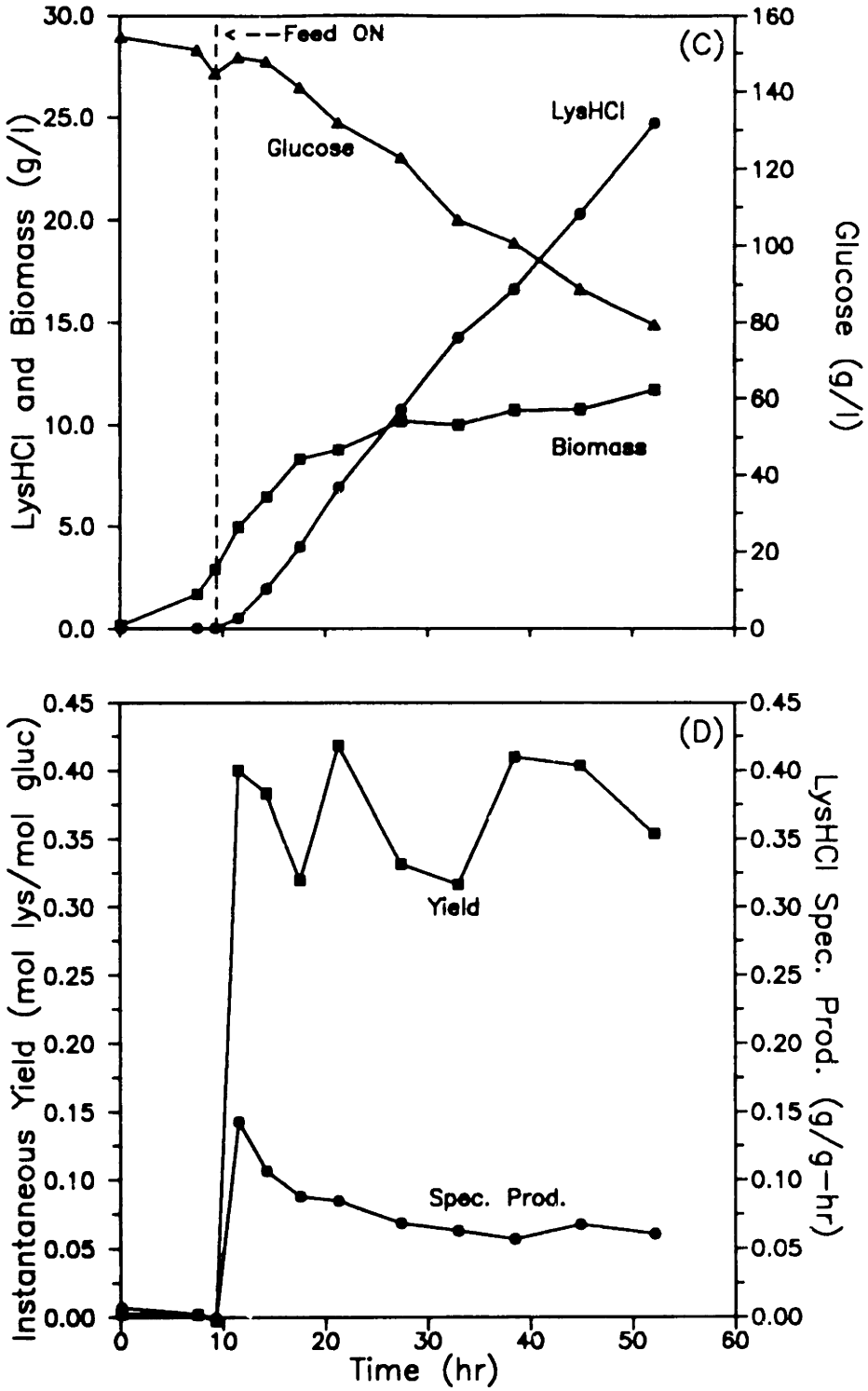

Figure 5.50. (Continued) (C) Biomass, L-lysine·HCl, and glucose concentrations vs. time. (D) Instantaneous yield on glucose and specific L-lysine·HCl productivity vs. time.

minimum levels while maintaining the metabolic activity of the biomass at sufficient levels for efficient overproduction of L-lysine. Based on the specific L-threonine uptake rate - specific growth rate data of the continuous culture work, this minimum specific feed rate corresponds to a minimum specific growth rate of approximately 0.01 hr^{-1}. The highly elevated RQ is a strong indication of enhanced yields and, as Figure 5.50D shows, this strategy led to sustained instantaneous yields of 30 to 40 mol percent for upwards of 50 hours resulting in an overall fermentation yield of 0.24 mol/mol as compared to the batch fermentation's overall yield of 0.15 mol/mol (60% increase). Side product accumulation was measured to be 1.4 g/l of L-alanine, 13 g/l of L-valine, and 7 g/l of trehalose.

5.6.4 Summary of Restrained Growth Strategies

A summary of the results from the base case batch fermentation and the two feedback-controlled fed-batch fermentations is given in Table 5.5. Both control strategies achieved superior levels of metabolic activity when compared to batch culture, as evidenced by the fact that *both* productivity and yield were increased under either strategy.

These strategies have demonstrated the benefits of controlling biological activity through control of the microbial environment and its effects on microbial metabolism. Simply stated, rather than allowing the production organism to grow at maximum rates in batch culture, which leads to a rather unproductive stationary phase, fed-batch culturing at lower rates of growth for extended periods of time has been shown to allow significant improvement in fermentation performance. On-line

Table 5.5 - Effect of restrained growth control strategies on fermentation performance. Parenthetical quantities indicate the ratio relative to the base case.

Experiment	Batch Base Case	Yield Max. Strategy	Prod. Max. Strategy
Final L-lysine·HCl Concentration (g/L)	23	25 (1.09)	48 (2.09)
Average Volumetric Productivity (g/L·hr)	0.378	0.479 (1.27)	0.925 (2.45)
Overall Fermentation Yield (mol/mol)	0.15	0.24 (1.60)	0.22 (1.47)

respiratory data have provided the required on-line indicator of metabolic activity for use in the feedback control algorithm which maintained environments conducive to meeting fermentation performance goals.

These controls of metabolic activity are appealing in several respects. First, the basis of the control algorithm requires only qualitative relationships between fermentation parameters and readily available on-line respiratory measurements. No detailed mathematical models or state estimation algorithms are required and thus modeling errors and sensitivity problems typically associated with such schemes are avoided.

Second, when attempting to control a bioprocess in which there are two products (biomass and L-lysine), closure of a material balance for use with an on-line bioreactor estimation algorithm would require three on-line measurements. In addition to OUR and CER, a liquid phase concentration would have to be measured, which is difficult in practice (base addition rate is of limited use when products are acidic or basic, as in the case of amino acids).

Third, in some cases it is desired to control a fermentation subject to substrate

inhibition of product formation by adjusting the feed rate based on a measurement of the inhibitory substrate concentration. In the restrained growth strategies employed in this work, the respiratory data are, in some sense, being used as an indirect sensor for L-threonine, thus eliminating the need for a liquid phase L-threonine measurement. Such a measurement is presently unavailable for industrial application.

5.6.5 Applicability to Other Fermentation Systems

This approach to fermentation control may offer promise in other systems as well, particularly for products of primary or intermediary metabolism in which there is likely to be some growth-associated behavior of product formation [Shimizu *et al.*, 1991]. In addition, for such metabolites, the yield - specific growth rate correlation is likely to be similar to the relationship found in this work. Thus, a goal of yield maximization might be achieved through a similar strategy of restraining growth at the lowest rate which still maintains catalyst activity. Furthermore, if the reductive state of the product is such that significant deviations from a "pure growth respiratory quotient" will occur upon initiation of product accumulation, on-line respiratory measurements can serve as accurate indicators of metabolic activity. For example, Figure 5.51 shows the predicted relationships between observed respiratory quotient and observed yield for several amino acid fermentations (based on the lumped stoichiometric approach developed in Section 2.4.1). A productivity maximization strategy similar to the one employed in this work may be quite useful for those fermentations as well. However, it is clear that a strategy based solely on RQ would

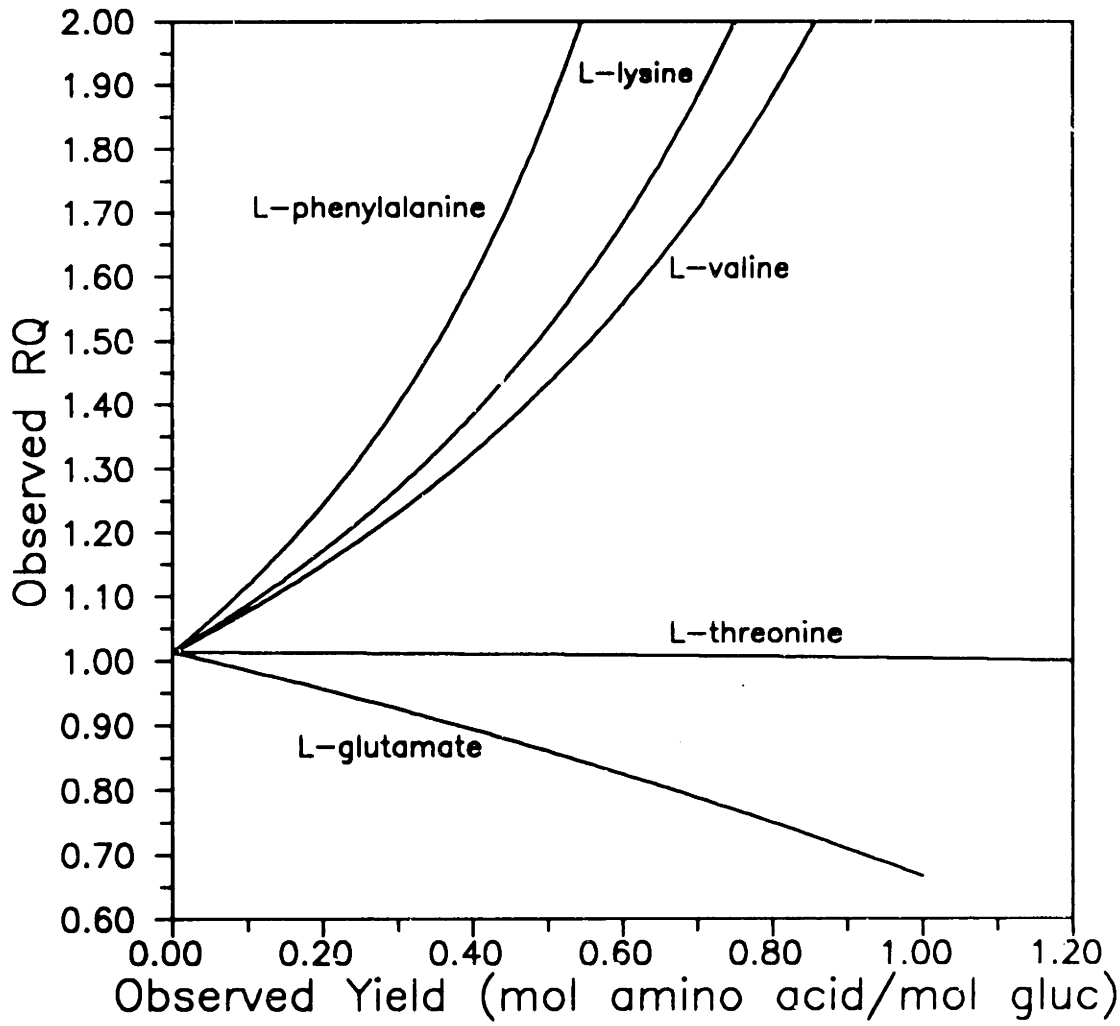

Figure 5.51. Simulated relationship between observed RQ and observed yield on glucose for several amino acid fermentations, accounting for both biomass and amino acid production.

be of little use in the fermentative production of L-threonine, because the respiratory quotients for pure biomass synthesis and pure L-threonine synthesis are nearly identical.

The key requirement for translating the restrained growth fed-batch strategy to other systems is only the need for qualitative relationships between fermentation performance variables, such as yield or specific productivity, and some form of on-line indicator of culture metabolic activity toward product formation. Such information should generally be available for a well-characterized fermentation system.

Chapter 6

Conclusions and Recommendations

6.1 Summary

This work began by investigating various properties of the *C. glutamicum* L-lysine producing strain such as basic growth requirements, specific essential amino acid requirements, and the effect of glucose concentration on the specific growth rate. An extensive characterization of the batch L-lysine fermentation was then performed, determining the dynamic behavior of the culture when grown in the L-threonine-limited medium necessary to achieve L-lysine overproduction. The fermentation performance indicators, specific L-lysine productivity and instantaneous L-lysine yield from glucose, were shown to be suboptimal for most of the time course of the batch fermentation. The decay in time of the specific productivity and yield were shown to be correlated to decays in on-line respiratory measures. Investigation of intracellular macromolecular content (protein, RNA, DNA) indicated that the growth limitation by L-threonine results in a general decay of metabolic activity including a gradual deterioration in the L-lysine biosynthetic apparatus. These batch characterization results suggested that an improved fermentation could result by controlling the metabolic state of the culture through the effects that the environment can exert on the efficiency of protein turnover and further suggested that such a control might be based on respiratory data as an on-line indicator of biocatalyst activity.

Although the batch culture work yielded tremendous insight into the factors affecting the dynamics of the L-lysine fermentation, continuous culture studies were necessary to elucidate the effect of culture specific growth rate on metabolic efficiency in producing L-lysine. Steady-state L-lysine yield from glucose was found to increase with decreasing specific growth rate and the steady-state specific L-lysine productivity was found to be maximized only over an intermediate range of specific growth rates, suggesting that there exist different optimal operating conditions for maximization of yield or productivity. In addition to establishing the specific growth rate dependence of specific consumption and production rates and conversion yields, the continuous culture data also provided sufficient information to decouple the effects of biomass and L-lysine production on substrate utilization. A material-balance based analysis then provided estimates of the intrinsic, or true, efficiencies of carbon and nitrogen incorporation into L-lysine. Furthermore, continuous culture provided a convenient set of flux data for the estimation of intracellular carbon fluxes and carbon partitioning at key locations within the metabolic network, providing both an understanding of the underlying causes of the low observed yields and rational directives for future strain manipulations.

The continuous culture work also provided an opportunity to study a culture instability which could result in the takeover of both continuous and extended-length fed-batch fermentations by revertant (unproductive) cells. A deterministic mathematical model which incorporated two growth-limiting substrate balances satisfactorily described the dynamics of the reversion and competition phenomena. Linear stability analysis showed that eventual takeover of any continuous culture by revertant cells is inevitable. However, the model predicted a stabilizing role for the

second growth-limiting nutrient (L-leucine) in slowing the growth of revertant cells. Such a stabilizing role was verified by conducting a fed-batch experiment at conditions corresponding to an extended-length fed-batch culture which was taken over by revertants with the exception of an adjustment to the L-leucine feed concentration to satisfy the theoretical medium design criterion. The medium manipulation successfully stabilized the performance of the extended fed-batch fermentation and increased L-lysine titer, productivity, and yield when compared to the culture taken over by revertant cells.

The results from the batch and continuous culture characterizations provided sufficient information to identify the proper reactor operating mode and control strategy for manipulating the culture metabolic activity and improving fermentation performance. The working hypothesis was known as the restrained growth/metabolic activity/fermentation performance hypothesis. This hypothesis held that improved fermentation performance could be expected by cultivating the organism under conditions of controlled, or restrained, growth. Furthermore, this restrained growth could be successfully achieved in a fed-batch operation using on-line respiratory measurements as a metabolic activity indicator for feed rate control. Before developing such restrained growth fed-batch control strategies, constant feed rate fed-batch fermentations were conducted and subsequently verified the hypothesis as to the positive effect of restrained growth on fermentation performance and the suitability of the on-line respiratory measurements as an indicator of metabolic activity towards L-lysine overproduction.

Following the successful verification of the working hypothesis, two different control strategies were developed, both heuristic in nature, for maximization of the

fermentation yield and maximization of the fermentation productivity, respectively. These strategies rely on the determination of trends (increasing or decreasing behavior) in the on-line respiratory measurements; that is, the algorithms require knowledge of the change with time (*i.e.*, derivatives) of the oxygen utilization and carbon dioxide evolution rates (OUR and CER) and the respiratory quotient (RQ). Appropriate control actions are taken based on a heuristic evaluation of the trends in OUR, CER, and RQ.

Both fed-batch control strategies were successful in maintaining the yield and specific productivity at high levels for extended times, resulting in significant improvements in the overall fermentation yield, volumetric productivity, and titer. These feedback-controlled fed-batch experiments thus demonstrated that proper environmental control can be an effective means of manipulating microbial metabolism to favor metabolite overproduction. Coupled with the results from the culture stabilization work, these efforts combine to present a complete picture of a novel method of biocatalyst activity control including a design criterion for insuring the culture integrity for extended fed-batch fermentations.

6.2 Conclusions

The following major conclusions can be drawn from this thesis work:

(1) *C. glutamicum* ATCC 21253 incorporates its essential amino acids (L-threonine, L-methionine, and L-leucine) into biomass at respective yields of 29.3, 7.89, and 19.5 mg amino acid/g DCW.

(2) High levels of glucose have a detrimental effect on the specific growth rate of this strain. Growth is completely inhibited by about 250 g/l of glucose.

(3) Batch cultivation of this strain results in sub-optimal performance. The

growth limitation by L-threonine, required to bypass the regulation of L-lysine biosynthesis, results in a general decay of metabolic activity and a subsequent deterioration of the L-lysine production capacity. The decay in fermentation performance (as quantified by the specific L-lysine productivity and yield of L-lysine from glucose) is observable on-line through measurements of the culture respiration.

(4) The production of L-lysine is growth associated for specific growth rates up to about 0.1 hr^{-1} and non-growth associated for specific growth rates in the range of 0.1-0.2 hr^{-1}.

(5) This strain incorporates ammonia into L-lysine at an intrinsic efficiency of about 0.40 mol/mol (80% of the theoretical maximum) and incorporates glucose into L-lysine at an intrinsic efficiency of about 0.41 mol/mol (55% of the theoretical maximum).

(6) Intracellular flux calculations, based on steady-state continuous culture data, indicate that the overproduction of L-lysine is not likely limited by the production of ATP or NADPH. Furthermore, the calculations suggest that a tightly controlled split of metabolite flow at the PEP node coupled with a high TCA cycle activity is likely a cause of the large discrepancy between theoretical and actual yield from glucose in L-lysine fermentations.

(7) An inherent culture instability, due primarily to a growth rate advantage of non-productive cells over productive cells, makes long-term continuous cultivation with this type of auxotrophic organism impractical and can also cause difficulties with extended-length fed-batch cultures. The dynamics of this instability can be satisfactorily predicted using a deterministic model incorporating two growth-limiting substrate balances.

(8) The use of multiple auxotrophic markers in conjunction with a rational medium design tailored to the auxotrophic requirements is effective in controlling the rate of culture takeover by non-productive cells in extended fed-batch fermentations.

(9) Restraining the growth of this organism by fed-batch cultivation employing on-line respiratory trends as a metabolic activity indicator for feed rate control significantly improves fermentation performance (L-lysine titer, productivity, and yield). These restrained growth fed-batch strategies can be utilized for maximizing either overall volumetric productivity or overall yield and require only qualitative relationships between fermentation performance parameters and readily available on-line respiratory measurements.

6.3 Recommendations for Future Work

Their are several areas in which interesting future work with the L-lysine fermentation may lie. These issues deal with both further investigation into the biological nature of L-lysine overproduction and further development of controls of metabolic activity.

The batch culture characterization suggested a gradual deterioration of metabolic activity with time upon reaching the L-threonine depletion point. It also showed an apparent excess of intracellular pyruvate which led to excretion of L-alanine and L-valine. Are all enzymes subject to the same degree of inactivation during this period or are some enzymes selectively degraded or more labile under conditions of L-threonine starvation? This may be an ideal situation for the application of 2-D electrophoresis to examine the time course of intracellular proteins and shed more light on this organism's response to the stress of amino acid deprivation.

As mentioned in the text, the value of the proportionality constant, K, used in the feed control algorithms was selected on the basis of engineering judgement. The experimental data suggested that a variable K may be more appropriate for this system. Future work may be directed at improving the control law by applying modern control theory, such as adaptive control, to continuously optimize the value of K.

One area which was not addressed in the course of the fed-batch experimentation was that of optimal switching time. If a model for the process dynamics in fed-batch culture, particularly the relationship between L-threonine

uptake and biomass density, could be developed, the effect of varying the switching time between batch and fed-batch phases could be examined. This may provide the ability to further improve the performance of the L-lysine fermentation.

Finally, this type of approach should be applied to other fermentation systems, particularly amino acid systems. Enough similarity likely exists between the L-lysine fermentation and other amino acid fermentations that only minor modifications to the restrained growth fed-batch strategies need be made.

Chapter 7

Nomenclature

CER carbon dioxide evolution rate, mmol/l·hr

D dilution rate, hr^{-1}

K_{mi} saturation constant for substrate i, mg/l

m maintenance coefficient, g glucose/g DCW·hr

N number of generations

OUR oxygen uptake rate, mmol/l·hr

p reversion probability, revertants/cell/generation

q_{glc} specific glucose uptake rate,

q_p specific productivity, g/g DCW·hr

Q_p volumetric productivity, g/l·hr

RQ respiratory quotient (CER/OUR), mmol CO_2/mmol O_2

S_i reactor substrate concentration, mg/l

S_{if} feed substrate concentration, mg/l

x(k) sequence of raw on-line measurements

X_i cell concentration of population i, g/l or cells/l

y_i gas phase mole fractions

y(k) sequence of filtered on-line measurements

Y_{ij} cell yield of population j on substrate i, cells/mg

$Y_{B/G}$ intrinsic yield of biomass from glucose, g biomass/g glucose

$Y_{L/G}$ intrinsic yield of L-lysine from glucose, mol L-lysine/mol glucose

Y^{MAX} maximum theoretical yield of L-lysine from glucose, mol L-lysine/mol glucose

Y_o observed yield of a metabolite from glucose, mol metabolite/mol glucose

λ_i i^{th} eigenvalue of the steady state under consideration, hr^{-1}

σ_{ij} specific uptake rate of substrate i by population j, mg/cell-hr or mg/g-hr

μ_i specific growth rate based on substrate i, hr^{-1}

μ_{mi} maximum specific growth rate based on substrate i, hr^{-1}

Chapter 8

Literature References

Abe, S., Takayama, K.-i., Kinoshita, S. (1967). Taxonomical studies on glutamic acid-producing bacteria. *J. Gen. Appl. Microbiol.* **13**: 279-301.

Akashi, K., Shibai, H., Hirose, Y. (1979). Effect of oxygen supply on L-lysine, L-threonine, and L-isoleucine fermentations. *Agric. Biol. Chem.* **43(10)**: 2087-2092.

Archer, J.A.C., Follettie, M.T., Sinskey, A.J. (1989). Biology of *Corynebacterium glutamicum*: a molecular approach. p. 27-33 In: *Genetics and Molecular Biology of Industrial Microorganisms*, C.L. Hershberger, S.W. Queener, G. Hegeman (eds.), American Society for Microbiology, Washington, D.C.

Aris, R., Humphrey. A. (1977). Dynamics of a chemostat in which two organisms compete for a common substrate. *Biotechnol. Bioeng.* **19**: 1375-1386.

Azuma, T., Nakanishi, T., Hagino, H. (1987). Properties of revertants appearing in L-leucine fermentation culture broth. *Agric. Biol. Chem.* **51(12)**: 3245-3249.

Azuma, T., Nakanishi, T., Hagino, H. (1988a). Mechanism for the stabilization by L-valine of L-leucine fermentation using an unstable mutant of *Corynebacterium glutamicum*. *Agric. Biol. Chem.* **52(5)**: 1129-1133.

Azuma, T., Nakanishi, T. (1988a). Stabilization of an unstable L-leucine producing strain of *Corynebacterium glutamicum* by enhancement of L-valine biosynthesis. *Agric. Biol. Chem.* **52(6)**: 1521-1524.

Azuma, T., Nakanishi, T. (1988b). Enzymatic background for the reversion or stabilization of an L-leucine producing strain of *Corynebacterium glutamicum*. *Agric. Biol. Chem.* **52(6)**: 1525-1528.

Azuma, T., Nakanishi, T., Sugimoto, M. (1988b). Isolation and characterization of a stable L-arginine producer from continuous culture broth of *Corynebacterium acetoacidophilum*. *J. Ferment. Technol.* **66**: 279-284.

Bailey, J. (1991). Toward a science of metabolic engineering. *Science* **252**: 1668-1675.

Beker, M. (1982). Product biosynthesis in continuous fermentation. *Folia Microbiol.* **27**: 315-318.

Beppu, T. (1986). Breeding of amino acid-producing strains. p. 24-35 In: *Biotechnology of Amino Acid Production.* K. Aida, J. Chibata, K. Nakayama, K. Takinami, H. Yamada (eds.), Elsevier Publishing, New York.

Bozic, S.M. (1979). *Digital and Kalman Filtering: An Introduction to Discrete-Time Filtering and Optimum Linear Estimation.* Edward Arnold Publishing, London.

Burton, K. (1956). A study of the conditions and mechanism of the diphenylamine reaction for the colorimetric estimation of deoxyribonucleic acid. *Biochem. J.* **62**: 315-323.

Chemical Marketing Reporter. June 24, 1985; July 1, 1991.

Cooney, C.L., Acevedo, F. (1977). Theoretical conversion yields for penicillin biosynthesis. *Biotechnol. Bioeng.* **19**: 1449-1462.

Coppella, S., Dhurjati, P. (1987). Low cost computer-coupled fermentor off-gas analysis via quadrupole mass spectrometer. *Biotechnol. Bioeng.* **29**: 679-689.

Coughanowr, D., Koppel, L. (1965). *Process Systems Analysis and Control.* McGraw-Hill Publishing, New York.

Cremer, J., Treptow, C., Eggeling, L., Sahm, H. (1988). Regulation of enzymes of lysine biosynthesis in *Corynebacterium glutamicum. J. Gen. Microbiol.* **134**: 3221-3229.

Cremer, J., Eggeling, L., Sahm, H. (1991). Control of the lysine biosynthesis sequence in *Corynebacterium glutamicum* as analyzed by overexpression of the individual corresponding genes. *Appl. Env. Microbiol.* **57(6)**: 1746-1752.

Crueger, W., Crueger, A. (1984). *Biotechnology: A Textbook of Industrial Microbiology.* Sinauer Associates, Inc., Sunderland, MA.

Dagley, S., Hinshelwood, C.N. (1938). Physiochemical aspects of bacterial growth Part II. Quantitative dependence of the growth rate of *Bact. lactis aerogenes* on the carbon dioxide content of the gas atmosphere. *J. Chem. Soc.* (London) 1936-1942.

Dairaku, K., Izumoto, E., Morikawa, H., Shioya, S., Takamatsu, T. (1983). An advanced micro-computer coupled control system in a baker's yeast fed-batch culture using a tubing method. *J. Ferment. Technol.* **61(2)**: 189-196.

D'Amore, T., Crumplen, R., Stewart, G. (1991). The involvement of trehalose in yeast stress tolerance. *J. Ind. Microbiol.* **7**: 191-196.

Daoust, D., Stoudt, T. (1966). The biosynthesis of L-lysine in a strain of *Micrococcus*

glutamicus. *Dev. Ind. Microbiol.* **7**: 22-34.

Dattas, P., Dungan, S., Feldberg, R. (1973). Regulation of the amino acid biosynthesis of the aspartate pathway in different microorganisms. In: *Genetics of Industrial Microorganisms*, Vol. **I**. Z. Vanek, Z. Hostalek, J. Cudlin (eds.), Elsevier Publishing, Amsterdam.

Demain, A., Birnbaum, J. (1968). Alteration of permeability for the release of metabolites from the microbial cell. p. 1-25 In: *Current Topics in Microbiology and Immunology*, Vol. **46**. Springer-Verlag, New York.

Demain, A. (1972). Cellular and environmental factors affecting the synthesis and excretion of metabolites. *J. Appl. Chem. Biotechnol.* **22**: 345-362.

Eikmanns, B., Follettie, M.T., Griot, M., Sinskey, A.J. (1989). The phosphoenolpyruvate carboxylase gene of *C. glutamicum*: molecular cloning, nucleotide sequence, and expression. *Mol. Gen. Genet.* **218**: 330-339.

Erickson, L.E., Minkevich, I.G., Eroshin, V.K. (1979). Utilization of mass-energy balance regularities in the analysis of continuous-culture data. *Biotechnol. Bioeng.* **21**: 575-591.

Follettie, M.T., Peoples, O.P., Archer, J.A.C., Sinskey, A.J. (1990). Metabolic engineering of *Corynebacteria*. In: *Genetics of Industrial Microorganisms*, Proceedings of the 6th International Symposium on Genetics of Industrial Microorganisms, Vol. **I**.

Follettie, M., Shin, H., Sinskey, A. (1988). Organization and regulation of the *Corynebacterium glutamicum* hom-thrB and thrC loci. Molec. Microbiol. **2(1)**: 53-62.

Giles, K.W., Myers, A. (1965). An improved diphenylamine method for the estimation of deoxyribonucleic acid. *Nature* **206**: 93.

Gottschalk, G. (1986). *Bacterial Metabolism*, 2nd Ed. Springer-Verlag, New York.

Greer, J. (1991). Personal communication.

Greer, J., Bakker, J., Kitai, A. (1983). CEH Marketing Research Report: Amino Acids. p. 503.5000B-503.5004G In: *Chemical Economics Handbook*. SRI International, Menlo Park, CA.

Grosz, R., Stephanopoulos, G., San, K.-Y. (1984). Studies on on-line bioreactor identification. III. Sensitivity problems with respiratory and heat evolution measurements. *Biotechnol. Bioeng.* **26**: 1198-1208.

Hadj, S.A., Queric, M.P., Deschamps, A.M., Lebeault, J.M. (1988). Optimisation of

L-lysine production by *Corynebacterium* sp. in fed-batch cultures. *Biotechnol. Lett.* **10(8)**: 583-586.

Hall, B.G. (1990). Spontaneous point mutations that occur more often when advantageous than when neutral. *Genetics* **126**: 5-16.

Harrigan, McCance (1966). *Laboratory Methods in Microbiology.* Academic Press, New York.

Herbert, D., Phipps, P.J., Strange, R.E. (1971). Chemical analysis of microbial cells. p. 210-344 In: *Methods in Microbiology*, Vol. **5B**. J.R. Norris, D.W. Ribbons (eds.), Academic Press, New York.

Hilliger, M., Hanel, F. (1981). Process analysis of L-lysine fermentation under different oxygen supply. *Biotechnol. Lett.* **3(5)**: 219-224.

Hilliger, M., Mockel, H.-O., Forberg, W. (1984). The optimization of L-lysine fermentation and a mass transfer model. *Acta Biotechnol.* **4**: 355-360.

Hirao, T., Nakano, T., Azuma, T., Sugimoto, M., Nakanishi, T. (1989). L-Lysine production in continuous culture of an L-lysine hyperproducing mutant of *Corynebacterium glutamicum*. *Appl. Microbiol. Biotechnol.* **32**: 269-273.

Hirose, Y., Okada, H. (1979). Microbial production of amino acids. p. 211-240 In: *Microbial Technology*, Vol. **1**, 2nd Ed. H. Peppler, D. Perlman (eds.), Academic Press, New York.

Hunter, D., Morris, G. (1990). ADM has world-scale biochemical ambitions. *Chem. Wk.* July 25, 1990.

Ikeda, K. (1908). *J. Tokyo Chem. Soc.* **30**: 820.

Inbar, L., Kahana, Z., Lapidot, A. (1985). Natural-abundance ^{13}C nuclear magnetic resonance studies of regulation and overproduction of L-lysine by *Brevibacterium flavum*. *Eur. J. Biochem.* **149**: 601-607.

Ingraham, J., Maaloe, O., Neidhardt, F. (1983). *Growth of the Bacterial Cell.* Sinauer Associates, Inc., Sunderland, MA.

Ishino, S., Yamaguchi,K., Shirahata, K., Araki, K. (1984). Involvement of meso-α-ϵ diaminopimelate D-dehydrogenase in Lysine Biosynthesis in *Corynebacterium glutamicum*. *Agr. Biol. Chem.* **48(10)**: 2557-2560.

Kimura, K. (1963). The effect of biotin on the amino acid biosynthesis by *Micrococcus glutamicus*. *J. Gen. Appl. Microbiol.* **9(2)**: 205-212.

Kinoshita, S., Udaka, S., Shimono, M. (1957). Studies on the amino acid

fermentation. Part I. Production of L-glutamic acid by various microorganisms. *J. Gen. Appl. Microbiol.* **3**: 193-205.

Kinoshita, S., Nakayama, K., Kitada, S. (1958). L-Lysine production using microbial auxotroph. *J. Gen. Appl. Microbiol.* **4(2)**: 128-129.

Kinoshita, S. (1985). Glutamic acid bacteria. p. 115-142 In: *Biology of Industrial Microorganisms.* Demain, A.L., Solomon, N.A. (eds.), Benjamin/Cummings Publishing Co., Inc., London.

Kiss, R., Follettie, M., Stephanopoulos, G. (1990). Quantitative assay for low levels of L-threonine in amino acid fermentation broths. *Biotechnol. Bioeng.* **35**: 1169-1173.

Klausner, A. (1985). Building for success in phenylalanine. *Bio/Technol.* **3(4)**: 301-307.

Liao, J., Perkins, W. (1990). Analysis of yield and productivity using metabolic constraints. Presented at American Chemical Society National Meeting, Washington, D.C., August, 1990.

Luntz, M.G., Zhdanova, N.I., Bourd, G.I. (1986). Transport and excretion of L-lysine in *Corynebacterium glutamicum. J. Gen. Microbiol.* **132**: 2137-2146.

Luria, S.E., Delbruck, M. (1943). Mutations of bacteria from virus sensitivity to virus resistance. *Genetics* **28**: 491-511.

Mandelstam, J. (1958). Turnover of protein in growing and non-growing populations of *E. coli. Biochem. J.* **69**: 110-119.

Mandelstam, J., McQuillen, K., Dawes, I. *Biochemistry of Bacterial Growth*, 3rd Ed. Blackwell Scientific Publications, New York.

Mavrovouniotis, M. (1990). Group contributions for estimating standard Gibbs energies of formation of biochemical compounds in aqueous solution. *Biotechnol. Bioeng.* **36**: 1070-1082.

Menkel, E., Thierbach, G., Eggeling, L., Sahm, H. (1989). Influence of increased aspartate availability on lysine formation by a recombinant strain of *Corynebacterium glutamicum* and utilization of fumarate. *Appl. Environ. Microbiol.* **55(3)**: 684-688.

Michalski, H., Krzystek, L., Blaszczyk, R., Jamroz, T., Wieczorek, A. (1984). The effect of mean residence time and aeration intensity on the L-lysine production in a continuous system. *Proceedings of The Third European Congress on Biotechnology* **2**: 527-532.

Misono, H., Togawa, H., Yamamoto, T., Soda, K. (1979). Meso-α,ϵ-diaminopimelate D-dehydrogenase: Distribution and the reaction product. *J. Bacteriol.* **137**: 22-27.

Miyajima, R., Otsuka, S., Shiio, I. (1968). Regulation of aspartate family amino acid biosynthesis in *Brevibacterium flavum*. I. Inhibition by amino acids of the enzymes in threonine biosynthesis. *J. Biochem.* **63(2)**: 139-148.

Miyajima, R., Shiio, I. (1970). Regulation of aspartate family amino acid biosynthesis in *Brevibacterium flavum*. III. Properties of homoserine dehydrogenase. *J. Biochem.* **68**: 311-319.

Modak, J.M., Lim, H.C., Tayeb, Y.J. (1986). General characteristics of optimal feed rate profiles for various fed-batch fermentation processes. *Biotechnol. Bioeng.* **28**: 1396-1407.

Mori, M., Shiio, I. (1985). Purification and some properties of phosphoenolpyruvate carboxylase from *Brevibacterium flavum* and its aspartate-overproducing mutant. *J. Biochem.* **97**: 1119-1128.

Mori, M., Shiio, I. (1987). Phosphoenolpyruvate:sugar phosphotransferase systems and sugar metabolism in *Brevibacterium flavum*. *Agric. Biol. Chem.* **51(10)**: 2671-2678.

Nakatani, Y., Fujioka, M., Higashino, K. (1972). Enzymic determination of L-lysine in biological materials. *Anal. Biochem.* **49**: 225-231.

Nakayama, K., Kinoshita, S. (1961a). Studies on lysine fermentation. II. α,ϵ-diaminopimelic acid and its decarboxylase in lysine production strain and parent strain. *J. Gen. Appl. Microbiol.* **7**: 155-160.

Nakayama, K., Kinoshita, S. (1961b). Studies on lysine fermentation. III. α,ϵ-diaminopimelic acid accumulation and diaminopimelic acid decarboxylase. *J. Gen. Appl. Microbiol.* **7**: 161-172.

Nakayama, K., Sato, Z., Kinoshita, S. (1964a). Growth of a glutamic acid producing bacterium and related bacteria I. Effect of iron salts, ferrichrome, amino acids and some other compounds. *J. Gen. Appl. Microbiol.* **10(2)**: 143-155.

Nakayama, K., Sato, Z., Tanaka, H., Kinoshita, S. (1964b). Growth of a glutamic acid producing bacterium and related bacteria II. Effect of chelating agent and it relation to inorganic salt. *J. Gen. Appl. Microbiol.* **10(3)**: 181-199.

Nakayama, K., Kinoshita, S. (1966). Some considerations on the mechanism in biosynthesis of lysine. *Dev. Ind. Microbiol.* **7**: 16-21.

Nakayama, K., Tanaka, H., Hagino, H., Kinoshita, S. (1966). Studies on lysine fermentation. Part V. Concerted feedback inhibition of aspartokinase and the absence of lysine inhibition on aspartic semialdehyde-pyruvate condensation in *Micrococcus glutamicus*. *Agr. Biol. Chem.* **30(6)**: 611-616.

Nakayama, K. (1972). Lysine and diaminopimelic acid. p. 369-397 In: *The Microbial Production of Amino Acids*. K. Yamada, S. Kinoshita, T. Tsunoda, K. Aida (eds.), John Wiley and Sons, New York.

Nakayama, K. (1985). Lysine.. p. 607-620 In: *Comprehensive Biotechnology*, Vol. **3**. H.W. Blanch, S. Drew, D.I.C. Wang (eds.), Pergammon Press, New York.

Novick, A. (1955). Growth of bacteria. *Ann. Rev. Microbiol.* **9**: 97-110.

Ohno, H., Nakanishi, E. (1976). Optimal control of a semibatch fermentation. *Biotechnol. Bioeng.* **18**: 847-864.

Ollis, D. (1982). Industrial fermentations with (unstable) recombinant cultures. *Phil. Trans. R. Soc. London*, Series B **297**: 617-629.

Ozaki, H., Shiio, I. (1979). Regulation of the TCA and glyoxylate cycles in *Brevibacterium flavum*. II. Regulation of phosphoenolpyruvate carboxylase and pyruvate kinase. *J. Biochem.* **66**: 297-311.

Ozaki, H., Shiio, I. (1983). Production of lysine by pyruvate kinase mutants of *Brevibacterium flavum*. *Agric. Biol. Chem.* **47(7)**: 1569-1576.

Ozaki, A., Katsumata, R., Oka, T., Furuya, A. (1985). Cloning of the genes concerned in phenylalanine biosynthesis in *Corynebacterium glutamicum* and its application to breeding of a phenylalanine producing strain. *Agric. Biol. Chem.* **49(10)**: 2925-2930.

Papoutsakis, E.T. (1984). Equations and calculations for fermentations of butyric acid bacteria. *Biotechnol. Bioeng.* **26**: 174-187.

Park, S.H., Ryu, D.D.Y., Lee, S.B. (1991). Determination of kinetic parameters related to the plasmid instability: for the recombinant fermentation under repressed condition. *Biotechnol. Bioeng.* **37**: 404-414.

Pirt, S.J. (1967). Steady-state processes for cell growth and product formation. p. 162-172 In: *Microbial Physiology and Continuous Culture*. E.O. Powell (ed.), Her Majesty's Stationary Office, London.

Pirt, S.J. (1975). *Principles of Microbe and Cell Cultivation*. John Wiley and Sons, New York.

Plachy, J. (1975). The effect of medium composition on the production of valine by

Corynebacterium 9366-EMS/184. *Folia Microbiol.* **20**: 346-350.

Radji, M.K., Hatch, R.T., Cadman, T.W. (1984). Optimization of amino acid production by automatic self-tuning digital control of redox potential. p. 657-679 In: *Biotechnol. Bioeng. Symposium* No. **14**, Wiley and Sons, New York.

Romagnoli, J., Stephanopoulos, G. (1981). Rectification of process measurement data in the presence of gross errors. *Chem. Eng. Sci.* **36**: 1849-1863.

Rutkov, A.B. (1984). Microbiological production of L-lysine by employing feed batch cultivation. *Bulg. Akad. Nauk.* **37(12)**: 1677-1680.

Ryder, D., DiBiasio, D. (1984). An operational strategy for unstable recombinant DNA culture. *Biotechnol. Bioeng.* **26**: 942-947.

Sano, K., Shiio, I. (1970). Microbial production of L-lysine. III. Production by mutants resistant to S-(2-aminoethyl)-L-cysteine. *J. Gen. Appl. Microbiol.* **16**: 373-391.

Sano, K., Ito, K., Miwa, K., Nakamori, S. (1987). Amplification of the phosphoenolpyruvate carboxylase gene of *Brevibacterium lactofermentum* to improve amino acid production. *Agric. Biol. Chem.* **51(2)**: 597-599.

Senior, P.J. (1975). Regulation of nitrogen metabolism in *Escherichia coli* and *Klebsiella aerogenes*: Studies with the continuous-culture technique. *J. Bacteriol.* **123(20)**: 407-418.

Shiio, I. (1961). Glutamic acid formation from glucose by bacteria. *J. Biochem.* **50(1)**: 34-40.

Shiio, I., Miyajima, R. (1969). Concerted inhibition and its reversal by end products of aspartate kinase in *Brevibacterium flavum*. *J. Biochem.* **65(6)**: 849-859.

Shiio, I., Miyajima, R., Sano, K. (1970). Genetically desensitized aspartate kinase to the concerted feedback inhibition in *Brevibacterium flavum*. *J. Biochem.* **68(5)**: 701-710.

Shiio, I. (1973). Lysine and threonine production by *Brevibacterium flavum* mutants and their regulatory mechanisms. p. 249-265 In: *Genetics of Industrial Microorganisms*. Z. Vanek, Z. Hostalek, J. Cudlin (eds.), Elsevier Publishing, New York.

Shiio, I., Toride, Y., Sugimoto, S.-i. (1984). Production of lysine by pyruvate dehydrogenase mutants of *Brevibacterium flavum*. *Agric. Biol. Chem.* **48**: 3091-3098.

Shiio, I., Sugimoto, S.-i., Kawamura, K. (1990). Effects of carbon source sugars on

the yield of amino acid production and sucrose metabolism in *Brevibacterium flavum*. *Agric. Biol. Chem.* **54(6)**: 1513-1519.

Shimizu, H., Araki, K., Shioya, S., Suga, K. (1991). Optimal production of glutathione by controlling the specific growth rate of yeast in fed-batch culture. *Biotechnol. Bioeng.* **38**: 196-205.

Shvinka, J., Viesturs, U., Ruklisha, M. (1980). Yield regulation of lysine biosynthesis in *Brevibacterium flavum*. *Biotechnol. Bioeng.* **22**: 897-912.

Siegel, R., Ryu, D. (1985). Kinetic study of instability of recombinant plasmid pPLc23 trpA1 in *E. coli* using two-stage continuous culture system. *Biotechnol. Bioeng.* **27**: 28-33.

Simon, J., Engasser, J., Germain, P. (1984). Substrate flux mapping in *Corynebacteria* for amino acids production. *Proceedings of The Third European Congress on Biotechnology* **2**: 49-54.

Slezak, J., Sikyta, B., Plachy, J. Brecka, A. (1969). Problems in continuous lysine biosynthesis. p. 505-510 In: *Continuous cultivation of microorganisms*. I. Malek, K. Beran, Z. Fencl, V. Munk, J. Ricica, H. Smrckova (eds.), Academia, Prague.

Sprugytenberg, R., Dunn, I.J., Bourne, J.R. (1979). Computer control of a glucose feed to a continuous aerobic culture of *Saccharomyces cerevisiae* using the respiratory quotient. p. 359-368 In: *Biotechnol. Bioeng. Symposium* No. **9**, John Wiley and Sons, New York.

Stephanopoulos, G., Vallino, J.J. (1991). Network rigidity and metabolic engineering in metabolite overproduction. *Science* **252**: 1675-1681.

Stouthamer, A. (1973). A theoretical study on the amount of ATP required for synthesis of microbial cell material. *Antonie van Leeuwenhoek* **39**: 545-565.

Svedas, V.-J.K., Galaev, I.J., Borisov, I.L., Berezin, I.V. (1980). The interaction of amino acids with o-pthaldialdehyde: A kinetic study and spectrophotometric assay of the reaction product. *Anal. Biochem.* **101**: 188-195.

Toennies, G. (1963). Differential responses to amino acids in bacterial growth. p. 118-127 In: Proceedings of the 142nd meeting of the American Chemical Society, No. 44.

Tosaka, O., Takinami, K., Hirose, Y. (1978a). L-Lysine production by S-(2-aminoethyl) L-cysteine and α-amino-β-hydroxyvaleric acid resistant mutants of *Brevibacterium lactofermentum*. *Agric. Biol. Chem.* **42(4)**: 745-752.

Tosaka, O., Takinami, K., Hirose, Y. (1978b). Production of L-lysine by leucine auxotrophs derived from AEC resistant mutants of *Brevibacterium lactofermentum*. *Agric. Biol. Chem.* **42(6)**: 1181-1186.

Tosaka, O., Hirakawa, H., Takinami, K., Hirose, Y. (1978c). Regulation of L-lysine biosynthesis by leucine in *Brevibacterium lactofermentum*. *Agric. Biol. Chem.* **42(8)**: 1501-1506.

Tosaka, O., Hirakawa, H., Yoshihara, Y., Takinami, K., Hirose, Y. (1978d). Production of L-lysine by alanine auxotrophs derived from AEC resistant mutant of *Brevibacterium lactofermentum*. *Agric. Biol. Chem.* **42(9)**: 1773-1778.

Tosaka, O., Morioka, H., Takinami, K. (1979). The role of biotin dependent pyruvate carboxylase in L-lysine production. *Agric. Biol. Chem.* **43(7)**: 1513-1519.

Tosaka, O., Yoshihara, Y., Ikeda, S., Takinami, K. (1985). Production of L-lysine by fluoropyruvate-sensitive mutants of *Brevibacterium lactofermentum*. *Agric. Biol. Chem.* **49(5)**: 1305-1312.

Tsuchida, T., Momose, H. (1975). Genetic changes of regulatory mechanisms occurred in leucine and valine producing mutants derived from *Brevibacterium lactofermentum* 2256. *Agric. Biol. Chem.* **39(11)**: 2193-2198.

Tsuchida, T., Yoshinaga, F., Kubota, K., Momose, H., Okumura, S. (1975). Cultural conditions for L-leucine production by strain no. 218, a mutant of *Brevibacterium lactofermentum* 2256. *Agric. Biol. Chem.* **39(5)**: 1149-1153.

Ueda, K. (1972). Continuous fermentation. p. 181-201 In: *The Microbial Production of Amino Acids*. K. Yamada, S. Kinoshita, T. Tsunoda, K. Aida (eds.), John Wiley & Sons, New York.

Umbarger, H.E. (1969). Regulation of the biosynthesis of the branched-chain amino acids. p. 57-76 In: *Current Topics in Cellular Regulation*, Vol I. E. Bern, L. Horecher, E. Stadtman (eds.). Academic Press, New York.

Vallino, J.J. (1991). *Identification of branch-point restrictions in microbial metabolism through metabolic flux analysis and local network perturbations*, Ph.D. thesis, Massachusetts Institute of Technology, Cambridge, MA.

Vallino, J.J., Stephanopoulos, G. (1989). Flux determination in cellular bioreaction networks: Applications to lysine fermentations. p. 205-219 In: *Frontiers in Bioprocessing*. S. Sikdar, M. Bier, P. Todd (eds.), CRC Press, Boca Raton, FL.

von der Osten, C., Gioannetti, C., Sinskey, A. (1989). Design of a defined medium

for growth of *Corynebacterium glutamicum* in which citrate facilitates iron uptake. *Biotech. Lett.* **11(1)**: 11-16.

Wang, H., Cooney, C.L., Wang, D.I.C. (1977). Computer-aided baker's yeast fermentations. *Biotechnol. Bioeng.* **19**: 69-86.

Wang, D.I.C., Cooney, C.L., Demain, A.L., Dunnill, P., Humphrey, A.E., Lilly, M.D. (1979). *Fermentation and enzyme technology*, John Wiley and Sons, New York.

Wang, N.S., Stephanopoulos, G. (1983). Application of macroscopic balances to the identification of gross measurement errors. *Biotechnol. Bioeng.* **25**: 2177-2208.

Watson, T. Pinches, A., Louw, M. (1986). Effect of growth rate on the maintenance of a recombinant plasmid in *Bacillus subtilis*. *Biotech. Lett.* **8(10)**: 687-690.

Weatherburn, M. (1967). Phenol-hypochlorite reaction for determination of ammonia. *Anal. Chem.* **39(8)**: 971-974.

Wilkinson, J., Munro, A. (1967). The influence of growth limiting conditions on the synthesis of possible carbon and energy storage polymers in *Bacillus megaterium*. p. 173-185 In: *Microbial physiology and continuous culture*, E.O. Powell (ed.), Her Majesty's Stationary Office, London.

Winter, E., Rao, G. (1989). Metabolic engineering of the amino acid fermentation via reduction state control. Presented at American Chemical Society National Meeting, Miami Beach, Sept 1989.

Wiseman, G., Violago, F., Roberts, E., Penn, I. (1966). The effect of hyperbaric oxygen upon aerobic bacteria: I. *In vitro* studies. *Canad. J. Microbiol.* **12**: 521.

Woodruff, H., Jackson, M. (1970) US Patent 3,524,797 (1970).

Yokata, A., Shiio, I. (1988). Effects of reduced citrate synthase activity and feedback-resistant phosphoenolpyruvate carboxylase on lysine productivities of *Brevibacterium flavum*. *Agric. Biol. Chem.* **52(2)**: 455-463.

Yoshihama, M., Higashiro, K., Rao, E., Akedo, M., Shanabruch, W., Follettie, M., Walker, G., Sinskey, A. (1985). Cloning vector system for *Corynebacterium glutamicum*. *J. Bacteriol.* **162**: 591-597.

Appendices

A. FERMCON Description

The software which acquires analog data, controls the mass spectrometer, acquires digital balance data, controls an analog-driven feed pump and performs various other functions during the course of a fermentation is named FERMCON. As discussed briefly in Section 4.2.2.4, the program is written in Microsoft® QuickBASIC™ version 3.0.

A flowsheet detailing the functions that FERMCON performs is given in Figure A.1 and a sample video monitor output is shown in Figure A.2. The program was designed to allow the simultaneous use of a mass spectrometer by up to four different fermentors [Coppella and Dhurjati, 1987]. The program simulates a multi-tasking capability by continually running through a main control loop which determines when automatically activated events (such as off-gas sampling) need to occur. At the same time, as long as a device is not being sampled or a user activated event is not occurring, the user may interrupt the program flow away from the main control loop to request user activated events. Whenever input is requested from the user (such as the value of a desired parameter update), the flow returns to the main control loop to continue its automatic tasks while waiting for the user to input the desired information. When input is triggered by the user, the flow returns to handle the user request further, and so on.

The program size is quite large. In fact, the program requires more memory than is allowed under QB version 3.0 for a single program (64K). Consequently, two

FERMCON Flow Sheet

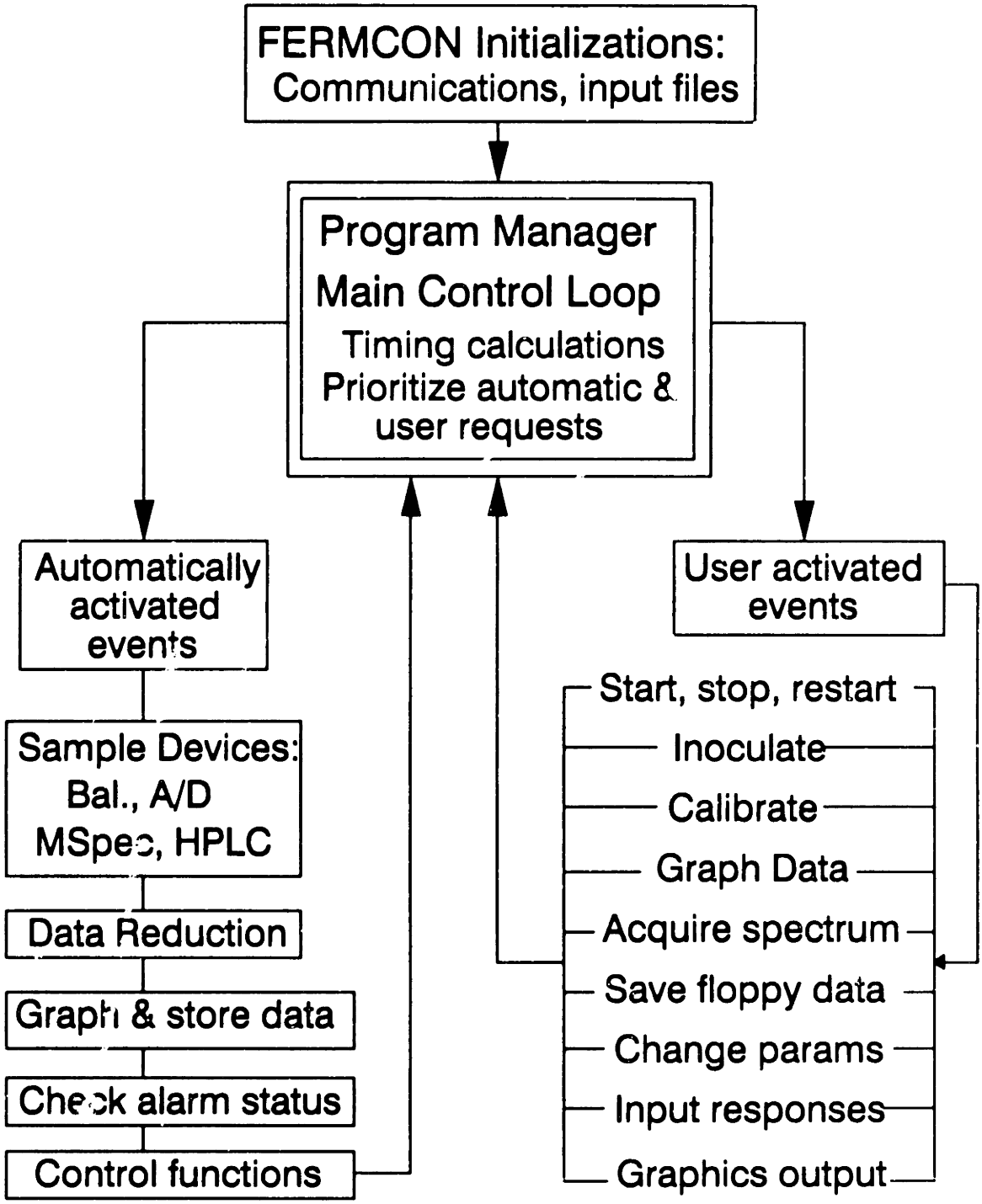

Figure A.1. Flowsheet detailing the fermentation data acquisition and control program, FERMCON.

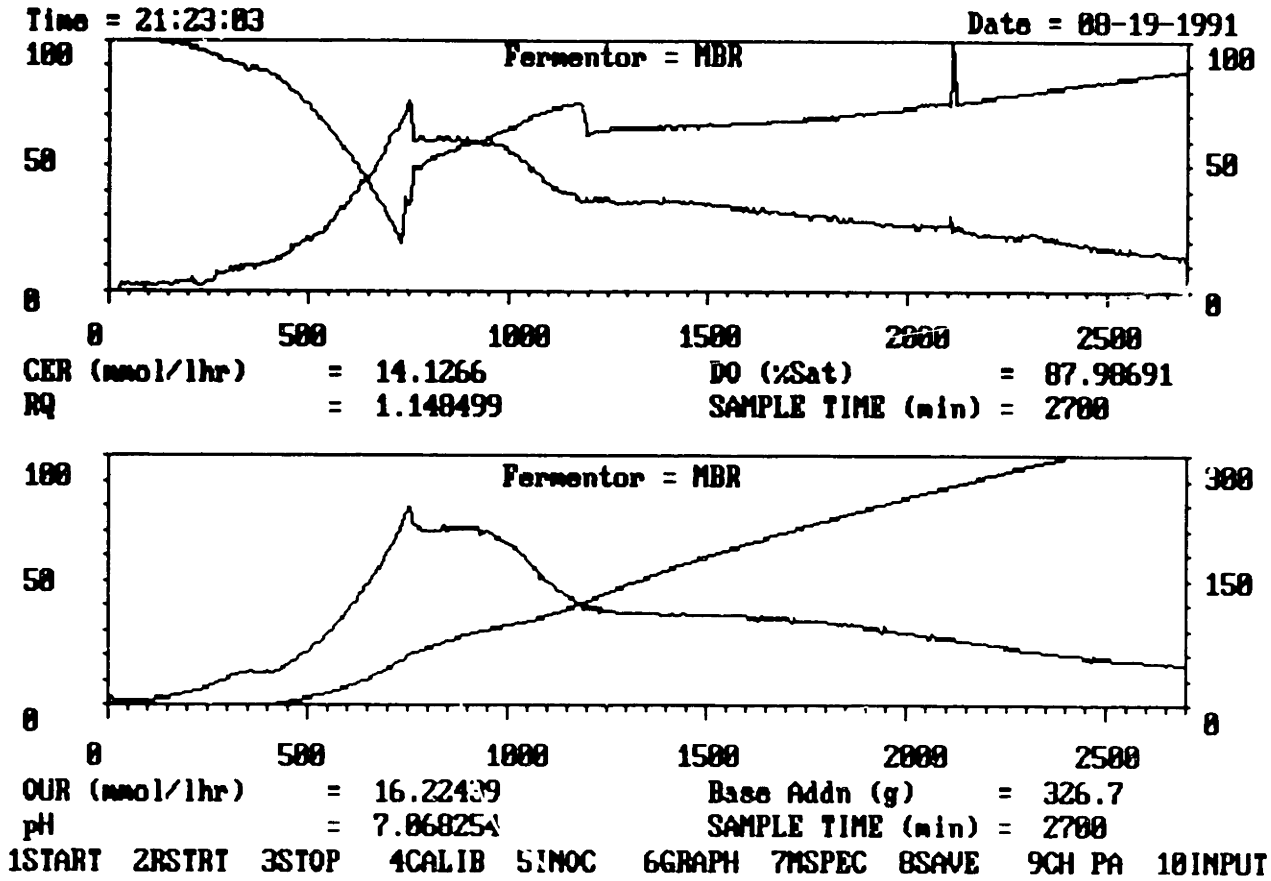

Figure A.2. Sample video monitor output during a run monitored by FERMCON.

programs (FERMCON.BAS and FERMCON3.BAS) are "chained" together and a library of compiled subroutines (FCONLIB.EXE) contains much of the programming code. FERMCON is started by running FERMCON.EXE. This program mainly performs equipment initializations and reads input files and then transfers control to FERMCON3.EXE.

FERMCON and FERMCON3 are compiled from source code and linked using the following commands:

```
QB87 c:\masspec\work3\fermcon /L FCONLIB.EXE/w/d/x/c:4096; >FCERR.LST
LINK c:\masspec\work3\fermcon,,,BRUN3087
QB87c:\masspec\work3\fermcon3/LFCONLIB.EXE/w/d/x/c:4096; >FC3ERR.LST
LINK c:\masspec\work3\fermcon3,,,BRUN3087
```

Here, w,d,x, and c are compile options that must be specified (consult the QB manual for details).

The subroutine library is created by the command:

```
Buildlib @FCONLIB.LST, FCONLIB.EXE/SEG:384;
```

Here, FCONLIB.LST is a text file containing the names of the approximately 75 object files that are placed into the library. Of course, each of those object files is compiled separately prior to building the library.

Before running FERMCON, a number of steps must be taken. First, the mass spec should be calibrated. The program to do this is in directory

C:\MASSPEC\CAL and is named MSCAL.BAS. Run the executable version, MSCAL.EXE, to perform the calibration. At the end of the calibration routine, make sure to save the calibration results to MSPARAM.DOC by choosing item 5) on the main menu. If this is not done, FERMCON will read in the calibration data from the last time MSCAL saved to MSPARAM.DOC, which will not be appropriate. Historical records of the mass spec calibration can be found in the files with a .HIS extension. The response factor part of the calibration uses a gas mixture to measure the responses of O_2 and CO_2 relative to N_2. The composition of the gas mixture is found in CALGAS.INP and is read by MSCAL. Consequently, when a new gas standard is purchased, CALGAS.INP must be updated.

The next item to be taken care of before running FERMCON is to set up the appropriate input files. FERMCON reads the following input files:

FIN?.DOC, VARF?.DOC, VARIABLE.DOC, MSPARAM.DOC

where the question mark is either 1, 2, 3, or 4 depending on which fermentor the file pertains to (1 = MBR fermentor, 2 = Microferm fermentor, 3 and 4 not specified at this time). The FIN?.DOC file will usually need to be updated for each fermentation since it contains information particular to the run such as sampling increments, initial operating parameters, and the name of the file to be used for output. The other files contain information which is not changed too frequently. All the input files are commented sufficiently.

The output data file will be stored in the directory c:\MASSPEC\DATA with a filename corresponding to the name given in FIN?.DOC with a .DAT extension

added. The output file contains some initial descriptive information followed by the fermentation data in the format: sample #, t (min), var 1, var2, ... , var31 (*i.e.*, 31 variables are stored to the output file). These output files can get quite large. To create smaller output files, from the original output file, with only the desired data (such as for creating plots), the utility RDFOUT.BAS was written. It is located in c:\MASSPEC\DATA and the executable form is RDFOUT.EXE. This utility will create a file containing only fermentation time and the value of the variable of choice.

As with virtually every piece of software of this size, "there's always one more bug!"

B. Additional Analytical Methods Details

B.1 OPA HPLC Analysis

The following information describes the procedure for quantitative analysis of primary amino acids by high pressure liquid chromatography. The system employed consisted of a Waters WISP 710B, Waters Automated Gradient Controller, two Waters 501 HPLC pumps, Waters Resolve C_{18} 5 micron Reversed Phase Column, Waters 441 Absorbance Detector, Waters 420E Fluorescence Detector, and a Shimadzu C-R3A Chromatopac Integrator.

General System Information:

1. A two buffer gradient program (#7) is utilized for the separation.
2. Pre-column derivatization of free amino acids by o-Phthaldialdehyde (OPA) is carried out automatically by the WISP.
3. The C_{18} column is used at room temperature (usual max. back pressure is about 3000 - 3500 psig).
4. A guard column packed with C_{18} precedes the column.
5. A micro-reactor packed with 500 micron beads precedes the guard column.
6. UV (340nm) or Fluorescence (334 nm excitation, 425 nm emission) detection can be used.
7. The Shimadzu Chromatopac uses the file 7 parameters.

System Specifics:

Gradient Programming:

Gradient program 7 contains the following lines of code:

Time	Flow	%A	%B	Curve
Initial	0.0	100	0	*
3.0	0.0	100	0	06
5.0	0.1	100	0	01
5.5	1.5	100	0	06
17.0	1.5	50	50	07
26.0	1.5	0	100	07
31.0	1.5	100	0	11
38.0	0.0	100	0	11
45.0	0 05	0	100	06

The last line of code is reached only at the end of the run, at which time solvent B (methanol/water) flows at 0.05 ml/min through the system.

Solvent Preparation:

Solvent A:
7.1 g anhydrous Na_2HPO_4 (0.05M Phosphate)
6.8 g $NaOAc*3H_2O$ (0.05M Acetate)
20 ml HPLC grade Methanol
20 ml HPLC grade Tetrahydrofuran (THF)
960 ml HPLC grade Water
Adjust pH to 7.5 with glacial acetic acid.

Solvent B:
650 ml HPLC grade Methanol
350 ml HPLC grade Water

WISP Programming:

To carry out the derivatization, it is necessary to use the WISP in auto mode. The OPA should go in position 1 with a run time of 1 minute. Samples go in positions 2 onward with run times of 38 minutes. The following system messages are required (unless you only have one sample):

System Message 7201 - programs for one sample per standard (OPA).
System Message 8201 - sets standard protocol at 1.

OPA Derivatizing Solution:

Prepare under hood

Dissolve 50 mg OPA in 1 ml absolute HPLC grade Methanol.
Add 40 microliters of 2-mercaptoethanol.
Dilute to 10 ml with Borate buffer (see below).
Add 10 microliters of 30% aqueous brij 35 surfactant.
(Prepare this fresh every run)

Borate Buffer:

Dissolve 12.36 g boric acid in 900 ml HPLC grade water.
Add 10.5 g KOH until dissolved.
Adjust pH to 10.4 with KOH.
Bring to 1 liter with HPLC grade water, filter.

Most people agree that the OPA solution is unstable when not flushed and stored under nitrogen in the dark. The solution described above is about 5 g/l (0.0373M) in OPA. Since OPA itself will both absorb UV and fluoresce, the smaller the volume used for derivatization, the less noise will corrupt the chromatogram. Use the results of the minimum required OPA study (detailed below) and an estimate of the amino acid content of the sample to set the minimum necessary OPA volume. For example, for a 100 microliter sample of 100 micromolar amino acid, 10 - 20 microliters of OPA should do.

Comments on Column Performance:

1. Retention times are fairly consistent. For the amino acids looked at, the following retention times were observed:

   L-Lysine: 29.7 - 30.1 min
   L-Methionine: 26.5 -26.7 min
   L-Threonine: 19.5 - 19.7 min
   L-Leucine: 28.7 - 28.8 min
   L-Glutamate: 9.5 - 9.7 min
   L-Glutamine: 17.8 - 17.9 min
   L-Alanine: 23.4 - 23.6 min
   L-Valine: 28.1 - 28.2 min

   If the samples contain ammonia (i.e. fermentation broth), the ammonia derivative will elute just before L-methionine and cause problems with methionine quantitation.

2. When starting a run, the column requires 1 or 2 runs to equilibrate fully (water will do as the sample).

3. The guard column and bead reactor should be washed and repacked frequently (Waters recommends weekly). The guard resin tended to develop a blue color after about 50 injections. This is likely a result of the high

ammonia content of our samples. Periodic backflushing with pure methanol (at 0.1 ml/min overnight) will help clean the column and reduce the backpressure.

Comments on Detection:

Both UV and Fluorescence detection methods have been investigated. The fluorescence method is one to two orders of magnitude more sensitive than the UV method. For samples full of "junk", this means that higher sample dilutions along with the use of the fluorescence method may offer cleaner chromatograms with better quantitation.

Linearity and sensitivity considerations:

UV: The linear range of this detector is up to at least 10,000 picomoles for all the amino acids studied. However, note that the UV detector puts out a 0 - 2 volt signal, whereas the maximum input voltage to the Shimadzu is 1 volt. A voltage divider which cuts the detector output in half has been constructed and installed. This allows the linear range to be extended to at least 20,000 picomoles. The minimum sensitivity is approximately 100 picomoles.

Fluorescence: The linear range of this detector also goes beyond the input range of the Shimadzu. The gain setting will set the sensitivity of the instrument. Thus, the gain allows you to "set" the maximum amount of amino acid which will cause the Shimadzu to see an input voltage of 1 volt. At a gain of 8, this value is about 1000 picomoles (about 2500 for threonine). The sensitivity of this detector is down to about 10 picomoles. Figure B.1 shows a typical set of calibrations for the fluorescence detector.

Figure B.2 shows the fluorescence detector response as a function of the molar ratio of OPA to L-lysine. As can be seen, a ratio of about 10 is the minimum necessary to insure "true" results. This result is expected to hold for other amino acids as well (possibly with the exception of glycine and histidine) since the bimolecular rate constants for reaction with OPA and the unimolecular decomposition rate constants of the derivatives for the different amino acids are similar (Vytas *et al.*, 1980).

B.2 L-threonine Assay Development

As was discussed in the text, an assay was needed for the detection of low concentrations of L-threonine in the presence of much higher levels of L-lysine. An

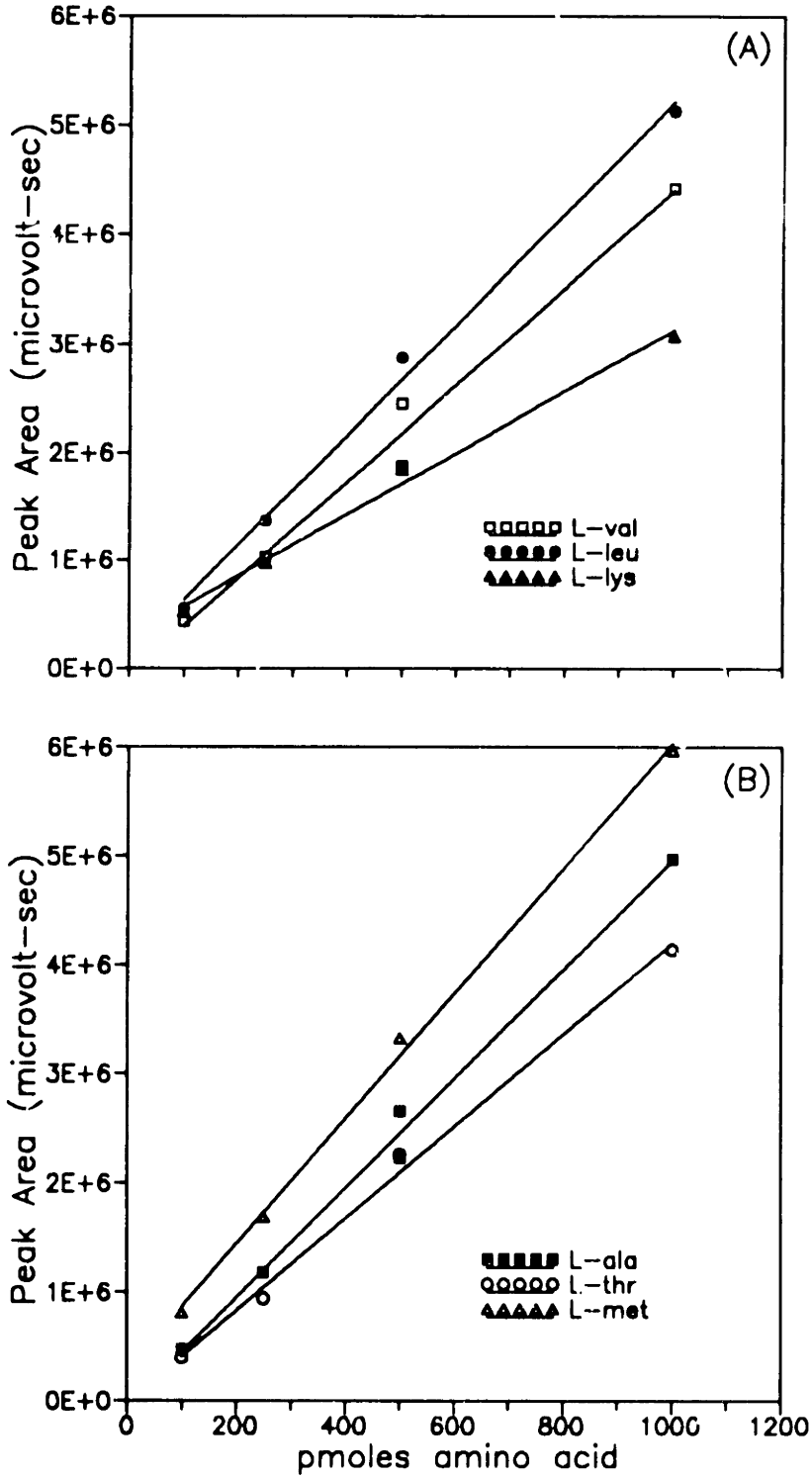

Figure B.1. Standard curves for OPA amino acid analysis calibration. Conditions as described in the text. (A) L-valine, L-leucine, L-lysine. (B) L-alanine, L-threonine, L-methionine.

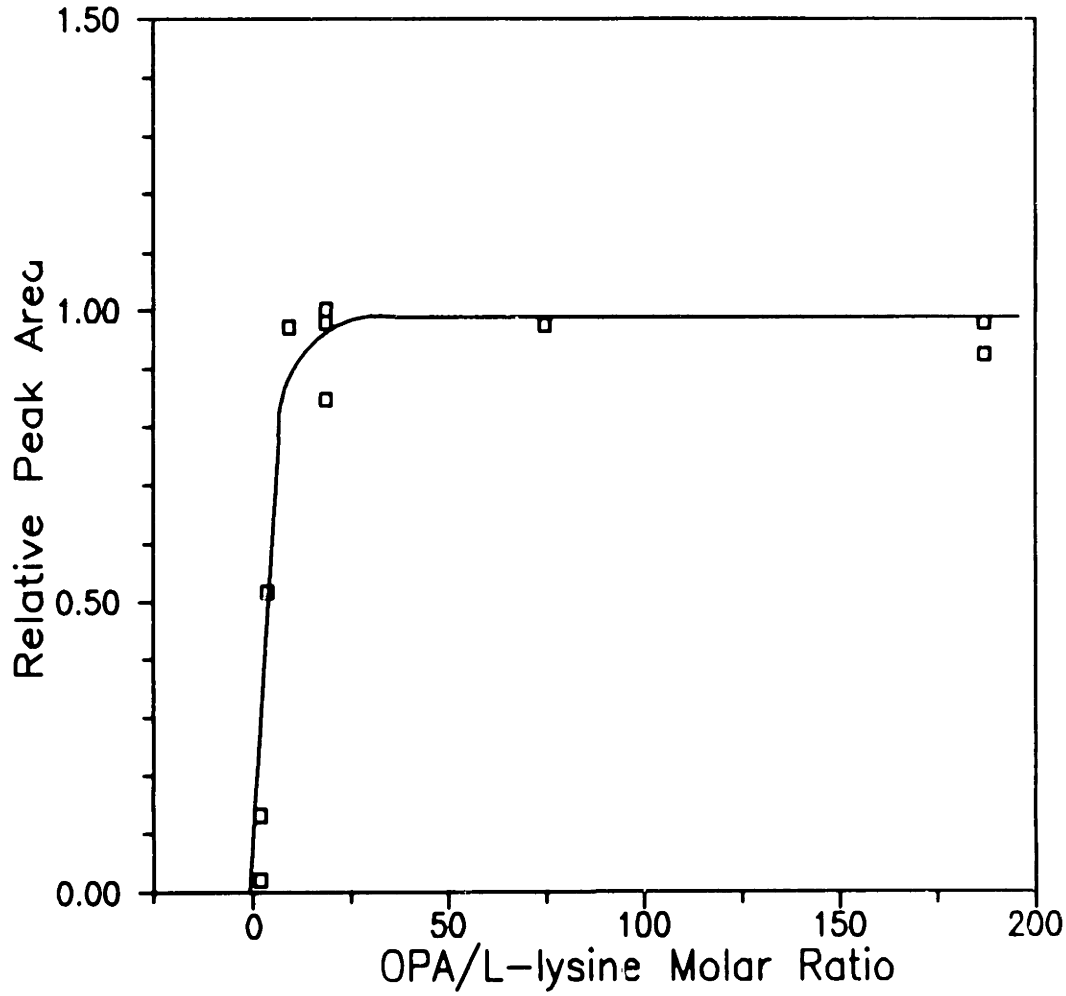

Figure B.2. Effect of OPA to L-lysine ratio on measured peak area.

assay was developed which relies upon the fact that L-threonine specifically inhibits the activity of homoserine dehydrogenase.

Unfortunately, homoserine dehydrogenase is not commercially available. However, Dr. M. Follettie was able to provide us with a strain of *C. glutamicum* harboring a recombinant plasmid coding for a number of genes, including the gene for homoserine dehydrogenase. The enzyme catalyzes the following reaction:

$$\text{ASA} + \text{NADPH} \rightarrow \text{L-homoserine} + \text{NADP} \qquad \textbf{B.1}$$

where ASA is aspartic semialdehyde. Since ASA is also not commercially available, it had to be synthesized. This was done by ozonolysis of DL-allylglycine. The specific details of the ASA synthesis as well as the preparation of the enzyme extracts and the assay protocol can be found elsewhere [Kiss *et al.*, 1990].

A sample calibration curve for this assay is shown in Figure B.3. By measuring the homoserine dehydrogenase activity in the presence of a fermentation broth sample, the concentration of L-threonine in the broth sample can be estimated. This assay has a minimum sensitivity of about 5 mg/l of L-threonine.

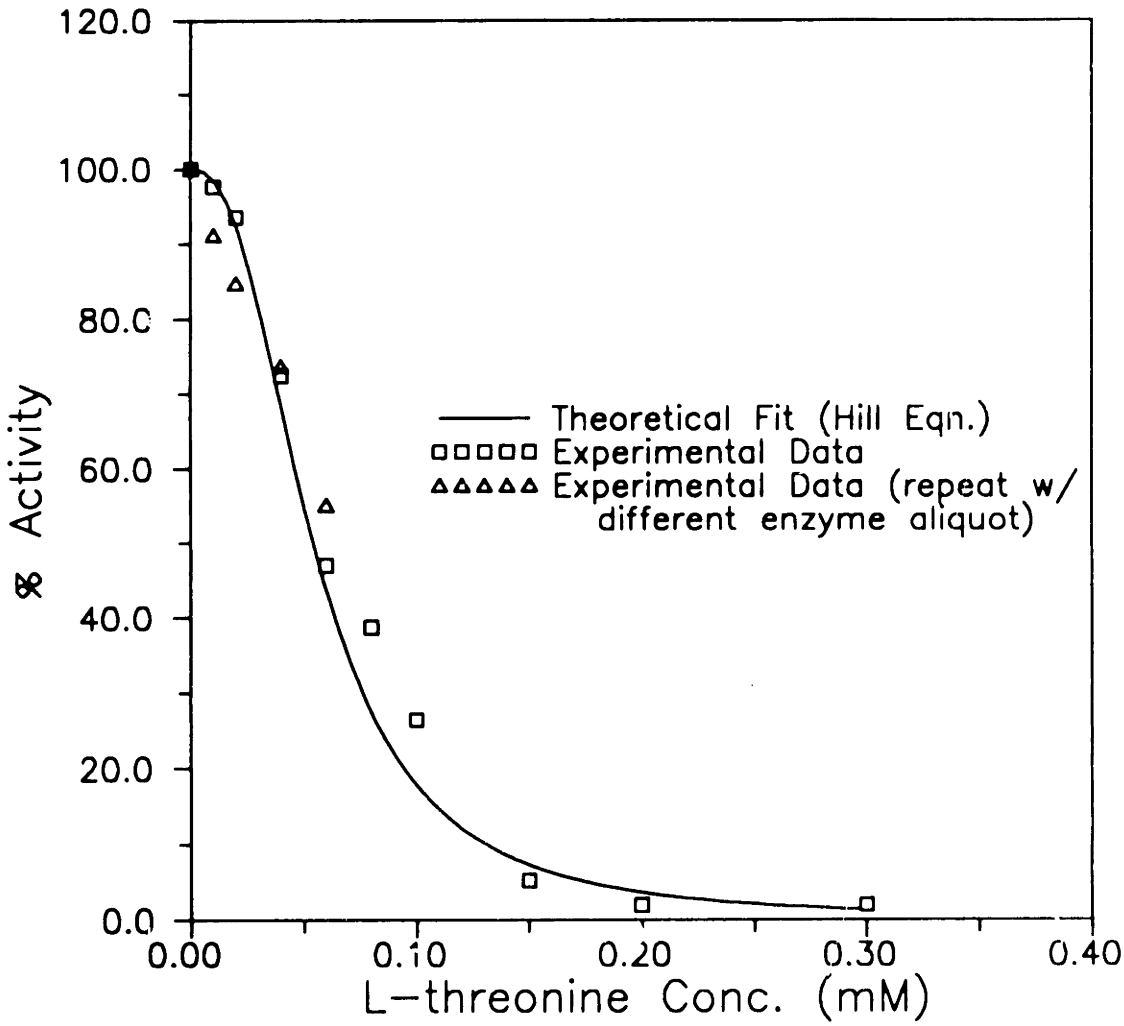

Figure B.3. Standard curve for the L-threonine enzymatic assay using homoserine dehydrogenase.

C. Continuous Culture Data

This appendix contains the steady state data collected in the continuous culture experiments (shown in Table C.1). Note that specific consumption or production rates are given for most metabolites. Since the dilution rate and steady state biomass concentration are given, all of the specific rates can easily be transformed to volumetric rates (the metabolite fluxes used in the intracellular flux estimation of Section 5.3.4 were volumetric fluxes). All continuous culture parameters discussed in Section 5.3 can thus be generated from the data of Table C.1.

Table C.1 - Continuous culture data.

D (hr^{-1})	Biomass DCW (g/l)	L-lysine·HCl (g/l)	Specific L-threonine Uptake Rate (mg/g DCW·hr)	Specific Glucose Uptake Rate (g/g DCW·hr)
0.0333	3.20	4.02	1.04	0.154
0.0538	2.99	2.85	1.80	0.203
0.0750	2.69	2.59	2.79	0.332
0.0950	2.75	2.06	3.46	0.301
0.121	3.03	1.90	3.99	0.697
0.158	2.62	1.11	6.03	0.382
0.180	2.34	0.851	7.69	0.349
0.201	2.53	0.902	7.95	0.440
0.256	2.26	0.396	11.3	0.509
0.301	2.19	0.308	13.7	0.511

D (hr^{-1})	Specific Ammonia Uptake Rate (g/g DCW·hr)	Specific Oxygen Uptake Rate (mmol/g DCW·hr)	Specific Carbon Dioxide Production Rate (mmol/g DCW·hr)	Respiratory Quotient
0.0333	0.0127	1.84	2.63	1.42
0.0538	-	-	-	-
0.0750	0.0267	2.88	3.82	1.33
0.0950	-	-	-	-
0.121	0.0311	-	-	-
0.158	-	-	-	-
0.180	0.0364	3.21	4.14	1.29
0.201	-	-	-	-
0.256	0.0377	-	4.60	-
0.301	0.0421	4.79	5.66	1.18